An investigation into the structural behaviour of thin-walled aluminium alloy welded battened struts

John Henry Howlett

AN INVESTIGATION INTO THE STRUCTURAL BEHAVIOUR OF THIN-WALLED ALUMINIUM ALLOY WELDED BATTENED STRUTS

JOHN HENRY HOWLETT CEng,FIStructE,FFB

Senior Lecturer in Civil and Structural Engineering

Teesside Polytechnic

Middlesbrough

Teesside

A Thesis presented to the University of Durham for the Degree of Master of Science

July, 1972

ABSTRACT

The buckling strength problem for battened struts is largely unsolved. Design recommendations given in both CP 118 "The Structural Use of Aluminium" and BS 449 "The Use of Structural Steel in Building" are therefore far from exact.

This thesis endeavours to verify and extend the knowledge upon which the present design rules for battened struts are based. Full scale testing has been employed and particular attention given to eccentric end loading, producing bending in the plane of the battens.

Thin-walled material is now being increasingly used and calls for more precise design information. The problems of local buckling and torsion therefore assume greater importance.

Battened struts have in the past presented problems of rigidity and this was particularly true before the use of welding. Economically designed aluminium alloy structures are at present largely restricted to bolted and rivetted construction, because of the reduction in strength when welding is used. An Al-Zn-Mg alloy, which is still under development in the U.K., has been used for this work. Its behaviour was excellent and its efficiency after welding has done much to solve the rigidity problem.

The following investigation deals with both axial and eccentric load conditions, using thin walled beaded channels. Axially loaded struts failed by lateral instability of the most heavily loaded channel. The eccentrically loaded struts failed by local buckling of the same channel. Indications are that battens need to be reinforced to combat lateral movement. Their spacing can however be increased if a small reduction in ultimate load is accepted.

The interaction method of analysis, suitably factored, would be ideal for practical use. Further research is needed to establish an upper limit of plasticity for the battened strut configuration. Deflection will however control design.

PREFACE

The investigation presented in this dissertation was undertaken in the Civil and Structural Engineering Department at Teesside Polytechnic, Middlesbrough.

My thanks are due to Professor Higginson of Durham University for his interest and encouragement.

I am indebted to the Faculty of Engineering at Teesside Polytechnic and in particular to Dr. Jenkins - Head of Department of Civil and Structural Engineering and Building, for making available, technician staff, equipment and laboratory space.

Mr. Woodward - Head of Engineering Research, Alcan Research and Development Ltd., is gratefully thanked for arranging the supply of experimental Al-Zn-Mg Alloy under difficult circumstances.

Welding in controlled laboratory conditions was undertaken by the Welding Institute with the kind help of Mr. Young and his staff.

The help of the Departmental Technician Staff is also gratefully acknowledged, particularly that of Mr. K. Sell during the difficult periods covering the manufacture of the testing rig and the meticulous fixing and wiring of so many strain gauges.

Finally the willing help of the Polytechnic Library Staff in locating, so promptly, the reference works involved, was much appreciated.

CONTENTS

LIST OF CHAPTERS

LIST OF FIGURES

LIST OF PLATES

Chapter 1

Statement of the Problem

1.1 Introduction

The problem of buckling strength of battened struts is largely unsolved. The design method is therefore far from exact and extreme accuracy in the calculations is pointless.

Verification and improvement of the relatively simple rules forming the basis of strut design is still needed. This is particularly true for thin walled beaded and lipped sections.

Members formed of more than one main component often require an analytical treatment which is complex. Struts of this type, involving the use of thin walled and beaded aluminium alloy sections, present a problem of some considerable magnitude.

The need to allow for the various types of buckling and the greater complexity of sections makes aluminium strut design rather laborious compared with steel.

1.2 Buckling Considerations

The modes of failure which form the basis of thin walled strut design are:-

(a) Column (flexural) buckling

(b) Local buckling

(c) Torsional buckling.

Column buckling consists of a sudden bowing of the member when the critical load is reached (Plate 1).

Local buckling will appear as a series of waves in the component parts making up the section, whilst the strut as a whole remains straight (Plate 2). It is virtually independent of member length.

Torsional buckling is best envisaged as the central part of the member rotating bodily relative to its ends. This will occur even if the ends are free to rotate (Plate 3).

It must be appreciated that the modes of failure do not necessarily occur separately and interaction frequently exists. Column and torsional buckling are often inter-related whilst column and local buckling interact in the post-buckling situation.

1.3 The Battened Strut

The battened strut may be defined as a compression member, formed by two or more longitudinal components held a fixed distance apart, at intervals, by transverse members known as battens. Components of this

Column Buckling
Test 4

Column Buckling
Test 2

PLATE 1

Local Buckling

PLATE 2

TWO VIEWS OF 3½ 2" BULB L.

Torsional Buckling

PLATE 3

configuration undoubtedly stem from the desire to achieve an optimum mechanical performance with a given amount of material. At any time when material forms the major part of production costs, which may well be suggested as true for aluminium products today, this type of component is a frequent choice.

Steel section rolling processes have, in the past, largely dictated the types of composite profiles developed. For battened struts the usual choice has been double channels. These were positioned a given distance apart with their webs parallel.

Aluminium alloy sections are extruded and can be formed into almost any desired shape. This removes the limitations present with steel sections. What then should be the profile of the struts to be tested?

In contemplating the strut in its basic form one initially selects the theoretically ideal round tube. When cost and practical difficulties are however considered, the closed square box, having equal flexural stiffness on both major axes, is the next best choice. The thinnest permissible material would be used to enable the strut to have the best possible material disposition and stiffness for a given length. The extent to which the flexural stiffness can be safely increased, for a given weight of material is entirely governed by the secondary effects classified as Torsional and Local buckling. Closed box sections

are particularly suitable to combat secondary buckling as their sides behave as webs and are inherently stable.

Further consideration would lead to the concept that the original square box could be replaced by two channels or four angle members, which if thin walled, would have reinforcing beads at their toes. If these components were now moved apart and tied together at intervals by battens or lacing a much improved strut performance would be achieved with a given amount of material. The configuration of the original square box could also be modified to a rectangle and thus provide enhanced stiffness in one direction to combat, say, an externally applied bending moment. Battens could be formed from either flat plate, channel or angle.

The design of battened struts is complex. A large number of parameters exist when normal plain sections are involved and this is further aggravated by the introduction of thin walled and beaded sections.

The ultimate load and the form of the buckling at failure will be influenced by the following variables.

(a) Properties and spacing of main members.

(b) Properties and spacing of the battens.

(c) The effects of thrust, shear and bending moment resulting from the type of loading system applied.

(d) Initial lack of straightness. This may well be minimal with extruded aluminium sections but the effects of welding will produce lack of straightness however well it is controlled.

(e) Type and degree of end fixity.

The problem is non-linear in nature and the lateral displacements will increase at a faster rate than the load. Young's Modulus for aluminium alloy is only one third that of steel and the need to keep slenderness ratios down and working stresses up is particularly important if lateral displacement is to be economically controlled.

Because of the effect of distortions resulting from shear, struts of this type will have deflections in excess of those that would occur with a single member of the same cross sectional area and slenderness ratio. The elastic critical load must therefore also be less and will depend upon the general properties of the main members and on the batten spacing.

Aluminium structural alloys behave differently from steel and their yield and ultimate values are quite close together. Once plasticity is however established the deflections will further increase and the strut reach its ultimate load in advance of the elastic critical load.

The foregoing problems highlight the essential requirement that all battens are rigidly connected to the main members. Any rotational slip at the battens will reduce the strut load carrying capacity. With a material having a low coefficient of friction, welding would appear to be the only satisfactory method of batten attachment.

1.4 Present Design Recommendations

The British Standard Code of Practice CP 118 1969 gives recommendations for "The Structural Use of Aluminium". Section 4 covers design, and the general clause 4.1.1 includes a paragraph indicating that design procedure is basically as for steel. Emphasis is however placed on the necessity of closely examining the stability of parts in compression and that due consideration be given to the overall stability of the structure. Particular attention should be paid to deflections.

Reference to the battened strut clauses in both CP 118 and BS 449 "The Use of Structural Steel in Building" reveals a divergence of requirements. Incompatibility of approach also exists in certain specific areas, which is difficult to justify when the design approach is expected to be basically the same.

Much of the information governing battened strut design undoubtedly originates from empirical methods. This must be expected when so many parameters are

involved. It is, however, felt that the member proportions are on the conservative side and that the design approach is in need of reappraisal, irrespective of whether the material used is steel or aluminium.

A comparison of both codes, together with comments are given in the following table.

CP 118 - Aluminium	BS 449 - Steel	Comments
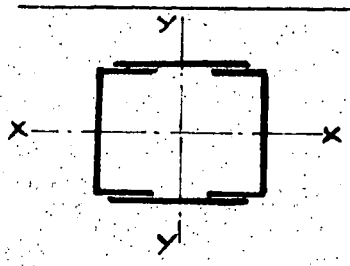	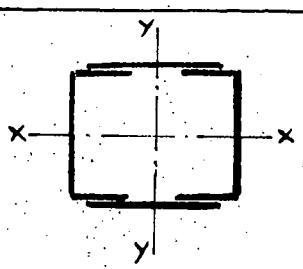	
General Clause 4.3.4.1 Slenderness ratio for axis perpendicular to battens not more than 0.8 times that for axis parallel to battens.	Clause 36b Slenderness ratio about y-y (axis perpendicular to battens) not more than 0.8 times slenderness ratio about x-x.	Agree
Batten Spacing Clause 4.3.4.2 Spacing between CENTRES of battens not to exceed 50 or 0.7 times slenderness ratio of complete strut with respect to axis PERPENDICULAR to battens.	Clause 36b Spacing Centre-to-Centre of END FASTENINGS such that $\frac{\ell}{r}$ of lesser main component over that distance shall not be greater than 50 or greater than 0.7 times ratio of slenderness of members as a whole about its x-x axis (PARALLEL to battens).	Two marked disagreements. 1. Alloy gives centres of battens. Steel gives centres of end fastenings. 2. Slenderness ratio taken on different axes which would give large difference if channels are well spaced out.

CP 118 - Aluminium	BS 449 - Steel	Comments
No Instructions	Where slenderness ratio about y-y exceeds 0.8 times slenderness ratio about x-x spacing of battens centres to centres of end fastenings shall be such that ratio of slenderness, $\frac{\ell}{r}$, of the lesser main component over that distance shall not be greater than 40 or 0.6 times slenderness ratio of the member about its weak axis	3. Steel covers situation not mentioned in the alloy code.
Batten Length Clause 4.3.4.3 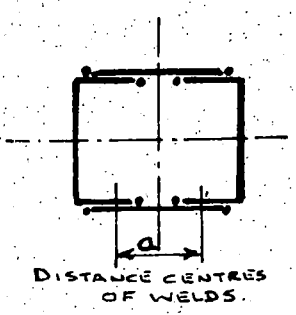 Effective length not less than $\frac{3}{4}$ a - which is distance CENTRES of welds or rivets	Clause 36(e) & (f) For ends and stayed points batten length not less than distance between centroids of main members with intermediate battens not less than $\frac{3}{4}$ that distance. BUT in no case shall length be less than TWICE width of one member in the plane of the battens.	For members placed fairly close together alloy code will give a batten of much less length. This does not seem reasonable with a more flexible material
Batten Thickness Clause 4.3.4.4 Not less than $\frac{a}{36}$ or 0.10" (2.5 mm) which ever is larger. "a" is given above. Rules also given for plates with turned over edges.	Clause 36(g) Not less than $\frac{1}{50}$ of the minimum distance between innermost lines of rivets or GROUPS of welds, unless edges are stiffened.	Alloy code will generally provide thicker battens. Reasonable with a flexible material.

CP 118 - Aluminium	BS 449 - Steel	Comments
Further Comments Clause 4.3.4.5 Additional data limited to a short note on fastenings.	Clauses 36(c) (d) (h) (j) & (k) Several other requirements are set down. Most important of which is that for struts with eccentricity in PLANE of BATTENS, THE EXACT THEORY OF ELASTIC INSTABILITY MUST BE APPLIED OR TESTS USED FOR VERIFICATION. Load factor not to be less than 1.7.	No mention in alloy code of bending in plane of battens. This is a very important ommission.

1.5 Proposed Investigations

There appears to be a clear case for further research into battened strut behaviour. The incompatibility between alloy and steel codes, lack of information in the alloy code and conditions not covered by either codes, provide ample justification for further work.

This research is believed to be the first extended investigation involving aluminium alloy battened struts. The development of thin walled and beaded sections and the limitations of size imposed by the extrusion process, inevitably necessitates the use of combined sections for larger components. This presents problems of special interest.

Whilst the experimental Al-Zn-Mg alloys are not covered by the present CP 118 code, their international acceptance as an ideal material for welding (without appreciable loss of strength) now opens up the whole approach to composite member design. Lack of connection rigidity in battened members has always been a weakness. Welding eliminates this problem.

It will not, in this one work, be possible to find solutions to more than a few of the problems involved. Thin walled and beaded channels, suitably battened, will be used to try to improve the present state of knowledge on the following important design considerations.

1. The stability of the member as a whole.
2. Comparison between concentric and eccentric loading in the plane of the battens.
3. Spacing of battens. Giving due consideration to their location relative to the position of maximum bending moment.
4. Effect of batten plates on overall column stability.

Chapter 2

Historical Background

2.1 Column Buckling

In 1757 Euler published his famous treatise on the strength of columns which included the following statement. "To begin with I should indicate that this moment is not limited to elastic bodies, amongst which we have good reason to doubt that columns should be included. It concerns in essence, a force by which any body resists a change in curvature, and it is totally immaterial whether such a body after flexure is endowed with a force to re-establish its original shape or not. For this reason we might preferably designate this moment as stiffness moment because it occurs in all bodies that resist flexure whether they are elastic or not".

The stiffness moment Euler refers to was designated E_{KK} by him and given as the product of the modulus of elasticity and the square of the shape parameter. In the present Euler formula E_{KK} is replaced by the product of E (Young's Modulus) and I (second moment of area). Both Young's Modulus and the tangent modulus were unknown to Euler and since E is only constant up to a certain stress the basic Euler formula is restricted to use within the elastic range of the material.

A paper published by Engesser[1] in 1899 suggested that E be considered as the slope of the compressive stress-strain diagram. This is now expressed in the tangent modulus formula which is simply a generalised form of the Euler equation. E is replaced by the tangent modulus E_t to give an expression for the buckling stress f.

$$f = \frac{\pi^2 E_t}{\left(\frac{L}{r}\right)^2}$$

where E_t is the slope of the compression stress-strain curve at stress f.

Since Shanley's[2] classic paper in 1947 this formula has been supported by Bleich[3] and is accepted as the correct theoretical explanation of column buckling for materials which have a smooth stress-strain curve.

Other methods of dealing with the inelastic behaviour of struts, at the lower slenderness ratios involve the use of the Perry-Robertson and Secant formulae. These are based on assumed initial strut inaccuracies and must be regarded as empirical.

The Perry-Robertson formula includes an expression to cater for a sinusoidal bow resulting from a bending moment produced by these initial inaccuracies. Assumption is also made that failure will occur when the point of highest stress reaches yield. The formula for

an average stress f at failure is given by

$$(P_E - f)(f_y - f) = \eta \, P_E f$$

where P_E = Euler critical value

f_y = yield stress

η = a non-dimensional "knee" factor, and is a measure of initial deflection Δ . η is defined by $\frac{y_c \Delta}{r^2}$ when y_c is extreme fibre distance.

In practice a constant c is used and η put equal to $c(\frac{L}{r})$.

The steel code BS 449 - 1969 uses the Perry-Robertson formula for strut failure. This is due to the configuration of the stress strain curve and the difficulty of establishing its exact shape, which must be known in order to apply the tangent modulus formula. It is now postulated that if due consideration is given to locked up rolling stresses, the tangent modulus formula does agree with experimental results for steel struts.

Before concluding the strut theory background, mention should be made of the "Straight Line" formula, where a straight line is used to replace the inelastic part of the strut curve. This is the simplest solution of all, but may well offend the perfectionist who

would argue for the theoretically correct solution provided by the tangent modulus approach.

2.2 Local Buckling

This type of local failure is not influenced by conditions resulting from the varying degree of strut end fixity. The mathematical computations are laborious, particularly with complex shaped sections, but the absence of the end fixity problem makes local buckling easier to handle theoretically than either column or torsional buckling.

The first mention of the local instability problem comes from the work of Bryan[4] in 1891 when he discussed the elastic buckling of rectangular plates, simply supported on all four edges and subjected to uniform endlong compression. He indicated that the critical stress was virtually independant of plate length and that when a long plate did buckle this occurred in waves. The length of each wave was approximately equal to the width of the plate. Little other published work appears on the subject until Timoshenko's[5] contribution in 1936 when flat plates were subjected to various degrees of support and restraint along their longitudinal edges. It has subsequently been shown that the effect on the critical stress of restraining the two loaded edges of a plate decreases rapidly as the plate is lengthened. The boundary conditions along the loaded edges have little

effect upon the critical stress when the plate buckles into four or more half waves.

It can be shown that the elastic buckling stress p is given by $p = \frac{kE}{(\frac{B}{t})}$ where B = Plate width where t = Plate thickness.

The factor k is dependant upon the length/breadth ratio, Poisson's ratio and the degree of edge restraint. Graphs and tables are now available giving k values for a variety of conditions. As would be expected, with short plates (less than four half wave lengths) appreciable variation in k will occur. When L/B exceeds four it becomes virtually constant.

Local buckling in sections is a complicated problem. Basically all structural sections consist of a number of rigidly connected plates which all buckle together and with a common half wave length, when the critical load is reached. The edge restraint conditions of the component plates are very complex as one part of the section will want to buckle first but will be restrained, to some extent, by the rest of the section, which is still more stable.

If we consider an alloy channel section strut, the exact solution is difficult. Taking a web to flange width ratio of 3:1 then the simply supported buckling load would be the same for the web and flanges, which

means they would all buckle at the same load IF they were individual plates, simply supported at their junctions. There will, however, in practice, still be some degree of restraint existing at the junctions due to the difference in preferred half wave length of the component parts. With a battened strut this will be further complicated by the effect of the battens and the interaction of the two channels forming the composite member.

The first successful treatment of local buckling involving a complete section and taking account of the interaction between the component "plates" forming I, Z and channel sections was given by Lundquist and Stowell[6] in 1939 using an energy method. In 1945 the same authors[7] confirmed their earlier work on Z sections using the principles of moment distribution, applied to the stability of plate assemblies. Also about this time Baker & Roderick[8] were examining the local buckling of T and I alloy sections using a "coefficient of fixity" concept. The theoretical work of Lundquist and Stowell was subjected to an extensive test programme by HEIMERL[9] in 1947, culminating in a paper to the A.S.C.E. in 1951, which included a useful set of charts to establish k values for I, Z and channel sections and rectangular tubes. Finally a comprehensive and exact solution was put forward by Chilver[10][11] with contributions in 1951 and 1953.

To summarise the position on local buckling, within the elastic range, the following approach is valid.

1. Members such as angles and tees are best dealt with in terms of torsional buckling.

2. For I, Z and channel sections and rectangular tubes, use the N.A.C.A. charts.

3. For other types of section, the best approach would be to use one of the methods devised by Lundquist and Stowell or Chilver. Considerable work will however be involved.

   An approximate, but much easier method of dealing with complex sections is to ignore any interaction and assume the section is composed of a series of plates. Each plate is considered as simply supported at the junction with its adjacent plate. The critical stresses are then calculated for each plate, separately, and the lowest value used to govern the design of the whole section. Results, using this approach, will obviously be on the safe side.

Once the elastic range of the material has been exceeded, the expression $p = \frac{kE}{(\frac{B}{t})}$ given earlier will yield results which are too high, as it does not allow for the inelastic behaviour of the metal. If E is replaced by E_t and the tangent modulus approach involving the

work of Engesser[1] and von Kärmän[12] is adopted the results would be on the conservative side but satisfactory for design purposes.

Since 1936 and the rapid expansion of the aircraft industry a considerable amount of theoretical and experimental research has been undertaken involving inelastic local buckling. This has resulted in precise treatments being developed by Bijlaard[13] and later presented as a general plate theory by Ilyushin[14]. Shanley[1][15] similarly modified the earlier work of von Kärmän. All the solutions however, like those in the elastic range, are for single plates. The problem for structural sections therefore still exists and the tedious mathematical involvement for plate assemblies remains.

The empirical approach offered by Gerard[16], which suggests the introduction of a reduced modulus E_{sec} into the elastic formula, may sometimes tend to over estimate the buckling stress, but in general will give good results.

2.3 Torsional Buckling

The first notable recorded work for torsional buckling of struts would appear to be that by Wagner[17] in 1929. When considering an axially loaded, pin ended, strut, where the ends were free to warp, but restrained from twisting, he derived the following expression for the

elastic critical stress p_T

$$p_T = \frac{GJ}{Ip} + \frac{\pi^2 EH}{IpL^2}$$

where Ip = Polar second moment of area about the shear centre.

G = Shear Modulus

J = St Venant torsion factor

H = Warping factor.

The value of J can be found for any structural shape by methods such as that submitted by Palmer[18] which involves the use of an electrical potential analyser. The establishment of H, which is a measure of the increase in torsional stiffness when warping is resisted, is much more difficult. Sections which have bulbs and fillets become particularly complex and no practical method of providing a really accurate solution appears to exist.

In 1937, both Lundquist[19] and Kappus[20], working independently, concluded that the basic expression developed by Wagner, whilst suitable for doubly-symmetrical and point-symmetrical sections, should not be applied, in its present form, to sections with no or only one axis of symmetry. They suggested that Ip and H values should be referred to the axis of rotation, which would not, as was thought earlier, be coincident with the shear centre.

The findings of Goodier[21] in 1941 and Timoshenko[22] in 1945 did not however fully support this thinking but postulated that any movement of the axis of rotation, away from the shear centre, was the result of interaction between pure column buckling and pure torsional buckling about the shear centre.

From this reasoning, it is now accepted, that in general, with unsymmetrical sections, strut failure will occur as a result of interaction between three basic forms of instability.

1. Column buckling on x-x axis
2. Column buckling on y-y axis
3. Torsional buckling resulting from rotation about the shear centre.

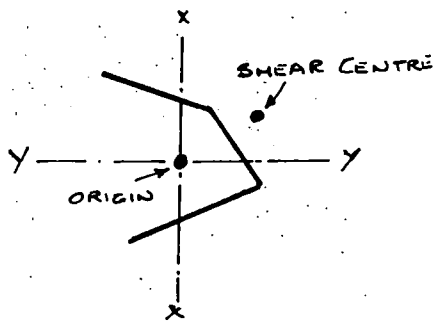

The degree of interaction will of course be apportioned in accordance with the relative weakness of the section to the above forms of buckling.

As with column buckling the effective length of the strut will have an effect upon results and influence both bending and warping.

The work of Goodier and Timoshenko has subsequently been confirmed, by numerous testing programmes, as a satisfactory method for establishing buckling loads resulting from torsion. The testing virtually all relates to

axially loaded struts and is contained in the Aluminium Development Association research reports by Baker and Roderick[8], Bentley[23] and Smith[24] which together with the research conducted by Ramberg and Levy[25] now provides data for sections ranging from angles to "top-hats".

Inelastic torsional buckling still remains a formidable problem and any theoretical work involving the use of the stress-strain curve is extremely difficult to apply in practice. Acceptable theoretical agreement with their test results appears to have been achieved by Ramberg and Levy[25] by adopting an expression E_r for the reduced modulus. E_r is given as a function of E and the tangent modulus E_t to produce a ratio $\frac{E_r}{E}$ by which the critical elastic stress may be factored. Bentley[23] also deals with the inelastic situation by replacing E by E_t and G by $\frac{E_s}{E}$ in Wagner's basic formula.

To summarise on torsional instability, which became apparent in members with reduced wall thickness, it must be accepted that torsional problems were not contemplated until much later than either column or local buckling. Much work has been done during the last few years, but more research is needed, particularly in the inelastic range, and with complex open sections. The brilliant and remarkable work by Vlasov[26] in 1941, dealing with the elastic warping of thin walled beams was not translated into English until 1964, and is

still virtually unknown by practising engineers in the U.K. This is regrettable as it throws new light on the effect of elastic warping in thin walled beams which cannot be explained by the classic thick walled beam theory. Strut problems involving torsion have an analogy with warping in thin walled beams. Vlasov's work indicated that the "sacred" theory of St. Venant and his universally accepted formula are only valid for a beam of circular cross section if additional stresses caused by warping are ignored. He submits that warping causes some longitudinal strains and stresses and infers that work done in twisting is partly used up in developing these stresses, leaving only the remainder of the work to develop the shear stresses attributed to the "St. Venant Twist". It is argued that deflection caused by twisting sets up "a pair" of bending moments which is called a "Bimoment" by Vlasov and represents a mathematical function similar in its applications to a bending moment. Hence it can be said that the total twisting moment is a sum of pure St. Venant twist PLUS some additional torsion which causes a section to bend (restrained warping) and sometimes called "bending twist". It should be noted that this latter twisting component can produce deflections several times larger than the rotational component of St. Venant.

A monograph by Zbirohowski-Koscia[27] endeavours to put the work of scientist Vlasov into a form that will be more readily understood by practising structural engineers.

There does not appear to be any recorded study of interaction between local and torsional buckling in the post buckling situation similar to the work of Bulson[28] covered by A.D.A. report No. 28 for combined local and column buckling.

2.4 Conclusions - Buckling

Not withstanding the complex problems which still remain to be solved for single structural sections it is the aim of this thesis to provide data for the design of compound members such as the battened strut. An approach will therefore need to be used which will endeavour to take account of knowledge as it at present exists. It is accepted that interaction between the three basic forms of buckling is not fully understood and any recommendations will therefore need to be based on test results.

2.5 Compound Members-General

The size limitation placed on extrusions produced in the U.K., by the requirement that dies must fit into an 18 in diameter circle, has enforced the use of fabrication techniques for larger components.

Rockey's admirable works, published in A.D.A. Research Reports[29] to [34] incl. provide comprehensive data for plate girders suitable for the larger beam requirements. Unfortunately the research generally deals with rivetted construction.

Data for strut design is not so far advanced and research appears to be limited to pairs of angles or channels back to back, suitable for such items as truss rafters. Work by Cullimore[35] deals with pairs of angles placed back to back. A useful contribution by Dwight[36] provides data for reinforcement lips and bulbs to combat local and torsional buckling.

The development of the weldable Al-Zn-Mg alloys should result in larger solid fabrications. It would, however, appear that components of the battened strut configuration will still be extensively used purely on the grounds of economic use of an expensive material.

2.6 Alloy Battened Struts

A literature search indicates that no serious work has been undertaken for battened struts in aluminium alloy. This is understandable as prior to the last war the aluminium alloys were little used for main building structure members.

"Structural Aluminium"[37], a handbook published in 1959 offers a broad solution to the problem using an approach

comparable with what would be adopted for thicker steel sections. The recommendations do not include torsional considerations and are obviously mainly applicable to thicker walled plain sections. Where eccentricity of loading is present the use of battened struts is not recommended. The member configuration indicated is also most suitable for rivetted construction.

Reference to the German Standards DIN.4113 and DIN.4114 give some guidance on multi-part compression members. The design requirements are however applicable to both steel and aluminium with adjustment factors for the two materials. This would not appear to be satisfactory when thin walled beaded sections, with complex modes of failure are involved.

2.7 Steel Battened Struts

By comparison a good deal of research has been undertaken for steel battened struts and earlier work will be briefly discussed as a background to the useful contributions made during the last 25 years. Unfortunately most researchers dealt with concentrically loaded members. All references prior to 1913 have been condensed from Dr. Ng's dissertation on the "Behaviour and Design of Battened Structural Members" which is in the University of Cambridge Library.

The first recorded work appears to be that of Engesser[38] in 1891. It concerned concentrically

loaded struts where each of the two main components carried half the load and all the batten connections were considered as completely rigid. Both these assumptions were erroneous as malformation in manufacture causes unequal loading of the main components and the rivetted batten connections are not completely rigid and lead to early failure. Engesser did however make adjustments for E beyond the elastic limit.

Work by Emperger[39] in 1908 involved a series of experiments for angle, channel and I sections. He used "flat ends" for the test pieces which introduced end fixing moments difficult to analyse in theory. The adoption of Tetmajer's[45] empirical straight line formula was not really suitable for comparison with the test results because of its limitations for slenderness ratios in excess of about 105. Some of the struts tested were formed from four corner angles with battens parallel to both major axes which appears to be over ambitious when the batten fixing problem had not been satisfactorily resolved.

In 1909 and 1911 Engesser[40][41] modified his original work to take into account member deformation between the battens and to suggest a variation to the true slenderness ratio by a method involving reduction coefficients. As the coefficients were dependent upon experimental results the method had limited practical application.

A theoretical analysis offered by Krohn[42] in 1908, for double channel columns was, by comparison, simple to apply. A pair of channels were considered to deflect in the plane of the battens and expressions based on Tetmajer's[45] straight line formula and an analogy were employed to find what proportion of the total load was carried by the most heavily loaded member.

Papers by Muller-Breslau[43][44] appear to be the first contributions for eccentrically loaded "built-up" columns and involved the use of a deflection expression based on the sinusoidal curve. Tetmajer's[45] straight line formula was again used although the struts tested did not fail elastically. Account was however taken of panel deformation, due to shear, bending moments at the batten positions, and the distortion of the batten plates themselves. An expression for crippling due to elastic bending was also derived. Muller-Breslau's findings for shear and bending were not satisfactory and his conclusion that eccentricity had no great influence on the crippling load was of course totally incorrect.

From about 1912 the world requirement for large bridges resulting from heavier rail traffic involved the use of the laced and battened type "built-up" members in girder construction. During the period 1922 to 1933 committees were set up by the American Railway Engineering Association and later by the American Society of Civil

Engineers to investigate the design and application of "built-up" struts. Early work by the A.R.E.A. indicated that lacing was to be preferred to battens because of the sudden buckling of the batten plates thermselves. The committee report postulated that batten plates should not be used if the full strength of the strut was to be attained but comments made on batten plate spacing shows these to be too large for good strength development.

Much of the subsequent work contained in the A.S.C.E. reports,[46][47][48] (which contain some 250 pages) involved the collection and summarising of earlier research work on columns. This was a useful service and provided a good background to the problem. The actual testing[47] undertaken was however very limited, being restricted to four columns, three with eccentric end loading which was applied on opposite sides of the main column axis, to induce a specific amount of shear, and one with normal eccentric end loading arranged to induce bending on the strong axis of the column. The end bearing blocks for all tests were so arranged to provide a "pivot end condition" and adjustable eccentricity. It was recognised that the question of shearing stress and shearing strength of columns was important and initial testing was done using the columns as beams with a central point load, by which means it was observed that deflections gave reasonable agreement with calculated values, providing shear

distortion was allowed for. Comment was made on the fact that deflection due to shear exceeded by many times that due to bending moment alone.

In commenting upon the A.S.C.E. testing, the opposed end eccentricities resulted in a shearing force at the ends of the columns of about 5% of the axial load. This is excessive and unlikely to occur in practice except with very short columns. The member proportions adopted for the testing provide a slenderness ratio of only 22 which is particularly low for practical purposes. Although the committee's final report[48] stated that the battened column was only suitable if very small eccentricity existed, it would appear that its use can be economically justified in many instances, where the loading conditions are what could be regarded as normal.

The death of Muller-Breslau resulted in his unfinished works being published by Petermann[49][50] in 1926 and 1931. The first publication gave data for tests carried out on twenty-three columns, all concentrically loaded, and using three different sections of channel with six varying column cross sections. Batten spacing and the number of battens was also varied. Knife edge loading was applied allowing for bending about one axis. Comparisons between the test results and the buckling loads were calculated using the Euler, Tetmajer, Krohn and earlier Muller-Breslau formulae and showed considerable variation. The test specimens were

so varied however that it was unreasonable to try and draw accurate conclusions, but Petermann did suggest that Muller-Breslau's accurate formula $P = \frac{\pi^2 E I_2^1}{L^2}$, involving the complex expression for the derivation of the reduced moment of Inertia I_2^1, should be adopted for evaluation of the buckling load. He also indicated that the slenderness ratio of the individual main components should be limited to 40 between the lateral ties.

Continuing with Muller-Breslau's work, Petermann conducted further experiments using the German mild steel designated "St 48". The same procedure and testing equipment used for the earlier tests was adopted to investigate ten columns, involving five different types of assembly. All columns were of the same length and cross sectional profile but the number of battens was varied, for each of the five types tested. Battens were spaced at equal increments for each type. This work was undertaken mainly to investigate the behaviour of "St 48" mild steel. Petermann concluded that his test results could be favourably compared with those of Muller-Breslau and that the German State Railway formula for columns was acceptable for use with "St 48" steel. He also suggested that the slenderness ratio for individual members between battens be reduced to 30.

Mention of battened columns also occurs in the writings of Ratzersdorf[51] and Timoshenko[5]. A brief comment of their work applicable to this dissertation is as follows.

In 1936 Ratzersdorf issued a rather confused and limited work on test columns which failed by elastic buckling, to his calculated values. Using the straight line formula and a reduced slenderness ratio, which was established by the use of a parameter controlled by the number of battens, he offered a formula for the inelastic buckling load. His results were not favourable when compared with earlier work and he suggested this was due to "movement of the joints". He did not however investigate further.

Timoshenko's contribution, in the same year, assumed that there would be no batten rotation as the column deflected and that the points of contraflexure would occur at the mid-panel position. He derived critical load expressions for the column as a whole and for local failure between the battens. His tests however showed that the overall deflection resulted in batten rotation which moved the point of contraflexure from the mid-panel location assumed.

No other important work appears to have been undertaken on the composite strut problem until 1947 when Wah Hing Ng[52] submitted a Ph.D. dissertation to the

University of Cambridge. This work was an extensive investigation into battened structural members which extended over a three year period.

Ng tested over seventy struts, all with a nominal length of 6 ft and formed from two pressed steel channel sections each with a $2\frac{1}{2}$ in x $\frac{1}{2}$ in x $\frac{1}{8}$ in thick cross-sectional profile. The number of "pairs of battens" per strut ranged from five to nine. Each end of the struts was located onto a "roller and knife edge" arrangement which was adjustable to facilitate both axial and eccentric end loading. The first twenty-five tests were carried out using a single knife edge which was subsequently modified to include two knife edges at right-angles. This latter arrangement permitted the struts to rotate freely about the point in the block precisely at the intersection of the two knife edges and deflect in any desired direction.

Whilst accepting the 10 ton load limitations of the rig one is led to wonder if $2\frac{1}{2}$ in x $\frac{1}{2}$ in x $\frac{1}{8}$ in pressed steel channel section was a suitable selection. The narrow width and general configuration of the flanges are such that the lateral stiffness of the individual channels between battens would be poor and directly influence the frequency requirement of the battens. With a thin pressed steel section one would have expected a flange width of about half the width of the web. Lateral stiffness could also have been further

increased by the provision of pressed lips at the flange toes. With welded struts better overall buckling performance would have been obtained if the channels had been "toed in" bringing the bulk of the metal a further distance from the centroid of the strut.

The end block "rotational and pivot" arrangement appears to be unduly complex by present day standards. It is argued that a single ball seating, with the seat slightly enlarged relative to the ball diameter, and used in conjunction with a high load, slow speed, anti-seize type P.T.F.E. silicon grease, such as the I.C.I. experimental product EP 6225 should now be used. This would appear to give enhanced freedom of movement over previous methods in this "difficult pin end" problem.

The foregoing comments do not detract from the excellent contribution submitted by Ng. Contrary to many earlier investigators he tested a large number of struts involving five different types of specimen (varied batten spacing) with each type loaded axially, and with $\frac{1}{4}$ in, $\frac{1}{2}$ in and $\frac{3}{4}$ in eccentric end loading in the plane of the battens. In addition five specimens were tested under a $\frac{1}{2}$ in eccentric-oblique loading, where the top and bottom eccentricities were positioned on opposing sides of the strut centre line, giving a $1\frac{1}{2}\%$ shear, (much more akin to practice than the 5% given by the A.S.C.E. mentioned earlier). Ng reports that in every

case the oblique loading condition gave larger collapse loads than those for comparable struts with the $\frac{1}{2}$ in top and bottom eccentricity on the same side of the centre-line, giving no end shear. He concluded that struts subjected to end bending moment are weaker when end shear is NOT present. The work was accordingly concentrated on axial and pure eccentrically loaded members, (both eccentricities on same side of axis).

Resulting from his tests Ng found that, in general, the struts collapsed as a result of plastic hinges forming in one of the end panels, when using the loading system as designed. On controlling the descent rate of the load container, thus slowing the strain rate, collapse could be made to occur in one of the mid-height panels. This latter mode of collapse is generally what would be expected in a strut of practical balanced proportions. Ng investigates the end panel failures and goes to some length in his explanation of the situation. In considering the matter further, one is led to the very narrow ($\frac{1}{2}$ in) flange width chosen, which is little more than edge reinforcement of a flat plate. The lateral stiffness of the individual channels is therefore small and it is probable that the moments induced in the individual members of the end panel from eccentric end loading, and any "hold up" at the end bearings, had been just too much for the narrow flanged channels.

The main findings of the work can be summarised as follows:-

(a) None of the specimens failed elastically, but generally by plastic collapse of the channels in the end panel, both channels bending in double curvature. If, however, the strain rate was controlled, plastic collapse occurred with one channel in the centre panel, giving a single curvature configuration.

(b) The most severe loading system is with end loadings equally eccentric on the same side of the strut axis. This is a no-shear condition.

(c) It is uneconomical to save on batten material. Battens should be spaced to give a maximum slenderness ratio of 50 and their depth should be at least equal to the clear distance between the main members for optimum load carrying capacity. The welding for battens to main members is virtually nominal, slightly more being necessary when loading is eccentric.

(d) Ideally, the strut proportions would give a minimum value of slenderness ratio between 70 and 100 overall.

(e) The virtual prohibition of battened struts for main members intimated by the design codes is

unjustified. When properly designed they should be permitted in important structures.

In 1952 Jones[53] in a purely analytical paper submitted "A Theory for Struts with Lattice or Batten Bracing". He assumed that the shear stiffness of a panel can be taken as distributed uniformly along the strut and postulated formulae for the crippling load of a strut with light shear bracing and with equal eccentricities of end loading. Further expressions deal with the condition of different end eccentricities and a uniform transerve loading. The formulae are comparable with those for struts with heavy shear bracing but an extra term has been included for shear stiffness. Jones provides a complete analytical argument to deal with the shear stiffness of the usual forms of light shear bracing and for struts which are batten braced and having both equal and unequal chords. This work is a useful contribution with parts that will have application when investigating the test results of this dissertation.

Research carried out jointly by Koenigsberger and Mohsen[54] in 1956 set out to establish a simple design formula for welded battened struts. They felt that some means of finding the economic design proportions for struts, consistant with a maximum load minimum weight concept, was desirable.

To check the validity of any such formula they conducted a series of tests for battened struts, all designed in accordance with the rules and specifications existing at that time. The purpose of the tests was:-

(a) To establish a load factor for the working to collapse load relationship.

(b) By the use of strain gauges determine surface stresses resulting from axial and eccentric end load and shear, at the positions assumed to be maxima.

The factors controlling the shear coefficient C_b given by Timoshenko's formula were examined for battened struts at $(P_{cr})_b = C_b P_E$

when P_E = Euler expression $\frac{\pi^2 EI}{L^2}$

when $(P_{cr})_b$ = Critical concentric load on the battened strut.

C_b is shown to be a function of $\frac{\lambda c}{\lambda}$

where λ_c = slenderness ratio of main members between battens

where λ = slenderness ratio of strut as a whole. Buckling in plane of battens.

Koenisberger and Mohsin then investigated the breadth to depth proportions for battens and submitted a $\frac{b}{d}$ ratio

where b was the distance, centre to centre of the main member neutral axes and d the depth of the battens along the strut axis. A relationship was also established between the batten bending stress f_b and the ratio of lateral shear force to axial load $\frac{s}{p}$ given by θ and expressed as $\frac{f_b}{\theta}$.

It was now possible to vary C_b with $\frac{\lambda c}{\lambda}$, $\frac{b}{d}$ and $\frac{f_b}{\theta}$ to obtain optimum values for the variables to give a maximum shear coefficient value C_b for welded struts.

These were $\frac{\lambda c}{\lambda} = 0.47$

$\frac{f_b}{\theta} = 400$

$\frac{b}{d} = 1$

Using Timoshenko's formula as a basis, an expression designated as formula (12) was developed and a resulting value for C_b of .085 obtained.

The failure loads from some nineteen concentrically loaded strut tests are given and compared with the work of Engesser, Muller-Breslau, Timoshenko, Bleich and Pippard. Good agreement was obtained when Timoshenko's formula was used as a basis and an effective length of .85 of the length between the battens adopted. When struts with small eccentricities were considered the formula gave good agreement with Ng's work.

In commenting on the practical applications of the struts tested it is a pity that Koenisberger and Mohsin, in company with some earlier welded battened strut researchers chose to toe the main channels "outwards". This reduces the overall strut performance as compared with those which are toed "inwards" and can be properly welded. It is also noted that only two runs of weld have been provided per batten, leaving the inner member edges to battens unwelded. This will reduce the stiffness of the batten-to-member connection and offer a weakness, should one channel try to move laterally relative to its partner. The ball seated end fittings, with the seatings slightly enlarged relative to the ball diameter is undoubtedly as "free" an arrangement as possible.

Finally in 1960 Jenkins[55] tested seven battened columns formed from channels, toed inwards, with seven pairs of battens equally spaced and welded on. All the struts were alike except for the amount of eccentricity applied to the end loading which was transmitted through well greased ball seats. In all cases the eccentricity promoted bending in the plane of the battens.

Strain measurements were restricted to one column and involved the use of $\frac{1}{2}$ in electrical resistance strain gauges located in the bottom end panel where the expected maximum bending moment in the individual

channel members would occur from the eccentric end loading. For a symmetry check these gauge positions were duplicated in the top panel. Batten rotations where measured with the aid of a theodolite, mirrors (attached to the battens) and a vertical board equipped with squared paper. The columns were restrained laterally, at right angles to the battens, at mid-height, by a lateral support device which included balls to ensure virtually unrestricted displacement in the direction of the plane of the battens only. This displacement was measured at mid-height and at batten positions.

In his theoretical comparisons, Jenkins developed expressions for the prediction of maximum load carrying capacity and using elastic theory presented two methods of arriving at the deflected form. The first was based upon the continuous web medium concept with the battens considered as replaced by a hypothetical continuous medium similar to the methods of Chitty[56] and Pippard[57]. The second involved the use of modified normal slope-deflection equations to include for the axial thrust. In the second method he postulated certain simplifying assumptions, which enabled the problem to be reduced to the solution of a set of "n" non-linear simultaneous equations, (n = number of panels in the column) permitting evaluations of slopes and lateral deflections. This followed the work of Ng.

Using "Collapse Theory" Jenkins next considered the ultimate load carrying capacity of the battened column. Accepting that a large number of variables exist, the problem was restricted to the required plane of buckling, by the lateral support device previously mentioned which eliminated the weak axis buckling. This dictated that buckling would take place in the plane of the battens on the strong axis of the section, to which condition two calculation methods were applied.

Method 1 involved a plastic collapse mechanism and the establishment of the intersection point between the elastic response and plastic collapse curves as described by Murray[58]. The actual collapse load for a given strut could then be found from the intersection point of the plastic collapse line and the deflection cruve, derived from the elastic theory.

Method 2 made use of the interaction type of expression as discussed generally by Massonnet[59] which is of the form

$$\frac{P}{P_{cr}} + \frac{M}{M_{cr}} = 1$$

when P = applied load

M = applied end bending moment

P_{cr} = Critical axial load with NO moment

M_{cr} = Ultimate moment with NO axial load.

The value for P_{cr} was derived from the basic Timoshenko expression modified in accordance with the proposals of

Koenigsberger and Mohsin[54] and a value for M_o (considering M_o as the fully plastic Moment of Resistance of the column cross section) was established. This resulted in the basic equation

$$\frac{P}{P_{cr}} + \frac{M}{M_o\left(1 - \frac{P}{P_{cr}}\right)} = 1 \text{ becoming } P^2 - P\left(35 + \frac{228e}{f_y}\right) + 306 = 0$$

where e was the eccentricity (including initial lack of straightness) and f_y was the yield stress of the material.

The curve showing the relationship between P and e derived from this equation was then plotted with the test collapse loads for different values of f_y.

Jenkins found that the continuous medium theory showed good results in predicting column deflections but was in serious error for end batten rotations and bending moments. The lengthy slope deflection method gave fairly accurate data on the state of the column in the elastic range. The methods of arriving at collapse loads were both encouraging, with the intersection of the plastic collapse and elastic response curves giving values 5 to 15% low when compared with the continuous medium theory. Using the slope-deflection curve gave even better agreement. His comments on the calculation work involved and the need to enlist the electronic computer for the production of design tables or formulae are interesting, particularly as the number of

parameters was controlled in this work by the mid-height restraint.

It is of particular interest that in commentry upon the low results obtained when using the interaction formula, he felt these were due to lack of refinement. It was suggested that the formula was in need of further study and that it offered an approach which was easy to apply to practical design.

In conclusion it was noted that Jenkins only used strain gauges on one strut and that these were located in the top and bottom end panels. It is assumed that this was done under the supposition that the highest stresses in the individual members could well exist at this location. Ultimate failure did however occur at the mid-height of the strut and not in the end panels as with the tests conducted by Ng.

2.8 Summary

In summing up the background information available on the battened strut, it is clear that much more work is still needed, even when orthodox thicker steel sections are used. The work of Ng and Jenkins highlights the requirement of some ruling on the minimum lateral stiffness of the individual members in the end panels, particularly if end moments exist in the plane of the battens.

The increasing use of thin walled, cold formed steel members means that investigation will be necessary, exactly along the same lines as is accepted practice for light alloy design. Torsion and local buckling cannot be "glossed over" or the test rigs so arranged as to eliminate certain tendencies if realistic solutions are to be found. The interaction between the various modes of failure is extremely complex and much research is needed.

Because of the difficulties of the interaction problem, and the gaps in knowledge which exist at present, this dissertation will endeavour to develop rules for the design of battened struts. Using the results of the testing programme and Shanley's[60] "Interaction Method" it is hoped to provide a theoretical method of determining allowable loads for battened struts subjected to combined loading.

It is anticipated, that by this approach a "covering" design concept can be established and the areas where further research is needed indicated.

Chapter 3

Aluminium as a Structural Material

3.1 Aluminium Described

The use of aluminium alloy structural frameworks now appears to be limited to specialised applications. This is purely because of material production costs and it can only be hoped that modern technology will develop processes enabling one of the most plentiful materials on the earth's crust to be put to fuller use.

For many years the author has been involved with its application to large specialised structures such as radar and aerial towers, walking dragline and crane jobs, opening bridges and E.O.T. cranes. Experience has established that the potential of this remarkable light-weight material has never been in doubt.

Amongst structural engineers there is a disturbing lack of knowledge of the materials they use. This is regrettable and with the increasing use of thin walled steel sections many engineers will begin to realise how limited is their knowledge of the mechanical behaviour of metals. Alloy sections with their thin walls, beaded or lipped extremities and low modulus have always presented design problems which can only be described as fascinating.

As many structural engineers will not be familiar with aluminium a brief description is included.

Commercially pure aluminium is a ductile metal too soft and low in strength for a structural medium.

When limited amounts of specified elements are added, striking property changes occur, giving increased strength and susceptibility to heat treatment and work hardening.

Many alloying elements are used, the most important being copper, magnesium, silicon, manganese, zinc, nickel and chromium. Which of these are included in any specific alloy and in what quantity is decided by:-

(a) Mechanical properties.
(b) Resistance to corrosion.
(c) Required standard of finish.
(d) Methods of fabrication used.

Structural material is usually formed from wrought alloys whose crystalline structures have been radically changed and mechanical properties much improved by rolling, extruding, forging and drawing processes.

3.2 Treatment

Wrought alloys may be sub-divided into two groups

(a) Heat-treatable alloys.
(b) Non-heat-treatable or work hardening alloys.

Cast alloys are not generally used in structural work. Where they are used the composition is largely decided by the requirements of manufacturing methods. This material is very different in composition from the wrought alloys but can be heat or non-heat treated as required.

(a) Heat Treatment

The term "heat treatment" applied to aluminium alloys denotes "solution treatment" followed by an "ageing" process. This method enables suitable alloys to be considerably hardened and strengthened.

Solution treatment involves heating the alloy to a particular temperature, in the region of 500°C and quenching in water. This will increase the strength of the material whilst allowing it to retain a fair degree of ductility. Forming can be conveniently undertaken at this point before it "age hardens" with time.

With double-heat treatment alloys the age-hardening effect is only slight unless "precipitation treatment" or "artificial ageing" is carried out. This second process is accomplished by re-heating to a temperature of about 170°C for a specified period and has the effect of raising the ultimate

strength still further, particularly the proof stress (yield strength) which is often almost doubled. Precipitation treatment does however reduce ductility and cold forming cannot readily be performed on fully heat-treated materials.

Annealing is carried out extensively during manufacture of rolled or drawn material at a temperature about 350°C. This removes effects of work hardening and is NOT classified as heat-treatment.

(b) Non-heat Treatment

Non-heat treatable alloys do not gain strength from heat treatment but from the amount of cold work applied during manufacture. They rarely prove attractive to the structural engineer because of their relatively low strength in the as-extruded form. Occasional use is justified where improved formability or higher weld strength is desirable.

3.3 Material Designation

The British Standards Institution specify the designation of all material and the relevant data is contained in BS 1470 - 1477 inclusive. Applicable standards for this project are BS 1476, 1477 and 1475.

Complete nomenclature of any product consists of a series of symbols occurring in the following sequence

(a) First prefix letter denotes if material is heat-treatable. H signifies alloy is strengthened by heat-treatment and N denotes it is non-heat treatable. Cast alloys are prefixed LM.

(b) Second prefix defines the form of product. For example E would indicate an extruded section and P would identify plate. When an alloy is referred to in general terms the second prefix is omitted.

(c) Grading of aluminium and its alloys is made by identification numbers. The same number is used in whatever wrought form it may be obtainable. Aluminium of 99.99% purity is given classification 1, whilst the other grades of pure aluminium are identified by suffixes A, B and C.

Alloy numbers range from 3 to 30. Numbers 3 to 8 inclusive are non-heat treatable and 9 onwards refer to heat-treatable material.

(d) Suffix letters are used to denote temper and condition of heat treatment.

The temper designation applies to non-heat-treatable alloys where strength has been increased by strain

hardening. This may be deliberate, as with sheet rolled to a specified degree of hardness, or incidental, as would occur during the stretch straightening of extrusions. Forming or other cold working of a finished product will also affect the temper.

Suffixes adopted for pure aluminium, non-heat-treatable and the heat-treatable alloys are given in Appendix "A" of CP 118, 1969. Reference to this data would show that a WP suffix indicates that solution and precipitation treatments have both been carried out. This treatment is usual for the bulk of structural sections.

A typical structural alloy designated HE30WP should now be fully understood.

3.4 Recommended Structural Alloys

Code of Practice CP 118 lists nine alloys for structural use. Principal alloys are H30, N8 and H9 and supplementary alloys, listed in Appendix C, are H20, H15, N3 to N6 inclusive.

It is regrettable that Al-Zn-Mg alloys with their greatly enhanced weld strength, do not appear in the present Code of Practice. They have not yet found favour in the UK whilst elsewhere, and in particular on the continent of Europe, they are well-established and in demand for a variety of applications.

At present the recognised alloy for structural work in the U.K. is H30 which has inferior permissible stresses and suffers from considerable reduction in strength at the heat affected zones adjacent to the welds. Thus the inefficient and uneconomic method of rivetting is still widely used.

Acceptance of the new Al-Zn-Mg alloys would provide a material of good strength suitable for welding; exactly what the design engineer has needed for a long time with a material where H.S.F.G. bolts give no real advantage.

General Comparison Table for Currently used Alloys		
Alloy	Description	Comments
H30WP (Principal) H20WP (Supp)	General Purpose	Almost as strong as steel. Weldable but with reduced strength adjacent to welds. Painting not required except in severe industrial environment
H9WP (Principal)	Lower strength alloy. Used extensively for curtain walling and window frames	About $\frac{2}{3}$ strength of H30WP. Used where deflection not stress governs design. Painting as above. Suitable for complex extruded shapes.
N8-M (Principal)	Durability excellent. Particularly suitable for marine environment. Weldable.	Principal material for welded structures. No significant loss in properties by welding. Strength much as H9. Not easily extruded, confine to simple structural shapes. No painting unless in abnormal corrosive area.
H15WP (Supp)	Strength high. Low corrosion resistance.	Was most used alloy but is subject to corrosion. Use now confined to specialist applications such as aircraft. Strength greater than any other alloy. Less easily extruded than H30 or H9. Must be protected by metal spraying or painting. Not to be in contact with steel.
Al-Zn-Mg Experimental Ref. No's 40025 40026.	Good strength. Weldability excellent.	Stronger than H30 but not H15. Would be principal alloy for all structures as reduction in strength due to welding is nominal. No other data officially available, it is still subject of research.

3.5 The Test Material

The Al-Zn-Mg alloy material used in this research was cast in the "Alcan Research and Development Limited" research foundry at Banbury and extruded at the Alcan Rogerstone Works in June 1970.

Particulars of the experimental material were supplied by "Alcan R & D" and are given below.

Composition of Experimental Casts

Cast No	Content %										Strut No
	CU	Fe	Mg	Mn	S_1	T_1	Zn	Cr	B	Zr	
320D	.006	.25	1.85	.01	.12	.015	4.32	.01	.0015	.16	2 at S1 2 at S2 2 at S3
321D	.008	.25	1.15	.01	.11	.012	4.66	.01	.0015	.16	*
322D	.01	.27	1.74	.01	.13	.015	4.26	.01	.0016	.16	2 at S4 2 at S5
323D	.01	.26	1.17	.01	.15	.016	4.71	.01	.0013	.16	*

Density 2.8 g/cm^3

Tensile Test Readings - Alcan

Cast No	0.1% P.S.		0.2% P.S.		U.T.S.		Elong-ation %	Strut No
	N/mm^2	Ton/in^2	N/mm^2	Ton/in^2	N/mm^2	Ton/in^2		
320D	304	19.7	338	21.9	400	25.9	11	2 at S1 2 at S2 2 at S3
321D	324	21.0	341	22.1	395	25.6	12	*
322D	329	21.3	340	21.95	394	25.5	11	2 at S4 2 at S5
323D	300	19.5	317	20.5	369	23.9	12	*

% Elongation on $5.65\sqrt{\text{area}}$

Modulus of Elasticity = 7000 kg/mm^2 = 68,700 N/mm^2 (4450 ton/in^2)

*Reserved for future research

No information for Al-Zn-Mg alloys is published in the Code CP118 1969. A comparison between the above figures and those for H.E.30WP, the most used structural alloy at present, indicates that the Al-Zn-Mg alloys have a 11/12% increase in strength.

Tests to confirm the mechanical properties of the material were undertaken at the Polytechnic. Particulars of the tensile tests are given below.

Test specimens were to B.S.18 1962 and the following selected sizes.

Diameter	7.17 mm (.282 in)
Gauge Length	35.62 mm (1.4 in)
Cross sectional area	40.32 mm^2 ($\frac{1}{16}$ in^2)

All specimens were cut from the bulbs or roots of the extruded 5 in x $2\frac{1}{2}$ in channel section.

Test No's 1, 2 and 3 were from material not affected by loading. Test No's 4, 5 and 6 were from material taken from the least compressed side of a tested strut,which had carried load, but not to such an extent that the material would have been stressed beyond the limit of proportionality.

Tensile Test Readings - Polytechnic

Test No	Failure load		Increased Gauge Length		Reduced Dia		
	kN	Ton	mm	in	mm	in	
1	16.75	1.68	40.07	1.575	5.42	.213	
2	16.6	1.66	40.07	1.575	5.37	.211	
3	16.6	1.66	40.07	1.575	5.44	.214	
4	17.5	1.75	40.07	1.575	5.55	.218	Material which had been well stressed in compression
5	17.5	1.75	40.07	1.575	5.39	.212	
6	17.7	1.77	40.07	1.575	5.29	.208	

U.T.S. $= \frac{16.6 \times 10^3}{40.32} = 412$ N/mm^2 (26.6 Ton/in^2) (Tests 2 & 3)

This compares with 394 and 400 N/mm^2 given by Alcan.

% Elongation $\frac{4.45}{35.62} \times 100 = \underline{12.5\%}$

This compares with 11/12% given by Alcan.

It is therefore confirmed that the material supplied conforms to the test data submitted by "Alcan R & D".

The figures obtained for the failure load in Tests 4, 5 and 6 give an enhanced U.T.S. of 434 N/mm^2 (28 ton/in^2). It can be concluded that the additional strength has been derived from working the material.

In the absence of published data for Al-Zn-Mg alloys it was now necessary to develop the compressive stress curves for column and local buckling before work on the initial strut design given in Chapter 6 could proceed.

3.6 Al-Zn-Mg Alloy Compressive Stress Curves

Reference to the Design Panel documents from the Code Drafting Committee for CP 118, 1969 enabled the basic theory behind the published strut and thin plate curves to be resolved. The contributions of Mr. J.B. Dwight proved particularly useful.

This investigation was necessary to provide comparable curves for the Al-Zn-Mg alloy being used in this research. The following reasoning is applicable.

1. Column Buckling - Theoretical Basis

It is accepted that the tangent modulus formula predicts accurately the column buckling strength of pin-ended aluminium struts. This formula depends upon the shape of the compressive stress-strain curve up to the 0.2% proof stress (f_2), which varies considerably.

The profile of the stress-strain curve is dependent upon a "Knee Factor" n. This is confirmed by the fact that if we consider the constant n as defined by the ratio of the 0.2% (f_2) to the 0.1% (f_1) proof stress, various tangent modulus curves, corresponding

to the values of $\frac{f_2}{f_1}$ may be drawn.

To know the sharpness of the knee of the stress-strain curve for any given alloy is therefore important, and must somehow be defined. In this region the stresses recommended for tension, compression and bending will be affected by the shape of the curve adopted.

Material suppliers usually give the 0.2% Proof Stress (f_2); U.T.S. (f_u) and % Elongation (e_u) for any material requested. A simple method for obtaining the "Standard Minimum Stress-Strain Curve" from these properties is therefore required.

An approach attributed to Hill & Clarke[61] suggests a suitable method, which can be adopted as the basis. It is however necessary to know precisely the $\frac{f_2}{f_1}$ ratio, to establish the stress-strain curve. This ratio is unfortunately variable and extremely difficult to obtain from the material suppliers, even for standard alloys.

It was therefore desirable that the method used should be based entirely on tensile properties guaranteed by the suppliers. The following approach satisfies this requirement for new alloys and also caters for the variation of existing alloys.

An empirical expression which may be used to represent the stress-strain curve is given by:-

$$e = \frac{f}{E} + 0.002 \left(\frac{f}{f_2}\right)^n \quad \ldots (1)$$

where e = strain

f = stress

f_2 = 0.2% proof stress

E = Young's Modulus.

Within the elastic range this expression gives the correct slope. The strain is correct at $f = f_2$. By varying n, its shape elsewhere can be adjusted, with the higher n values giving the sharper knee. For the aluminium alloys, values for n range between 5 and 40.

Consideration of expression (1) over the whole range of standard alloys showed it was not completely satisfactory. Where a high ratio of $\frac{\text{U.T.S.}}{\text{0.2\% proof stress}} = \frac{f_u}{f_2}$ existed, a "too rounded" knee occurred which resulted in a pessimistic strut curve.

The required adjustment is given by the following f - e expression:-

$$e = \frac{f}{E} + \frac{1}{500} \left(\frac{f - f_o}{f_2 - f_o}\right)^n \quad \ldots (2)$$

To solve this expression the knee factor n and proportional limit f_o needed to be established.

(a) Finding n

This was found using an empirical formula based entirely on properties given by the material suppliers at $n = \frac{\log (500\ e_u)}{\log (f_u/f_2)}$

The resulting curve agrees with the true tensile stress-strain curve exactly at stress f_2 and very nearly at stress f_u. It was found that the ratio f_u to f_2 is the main controller of n. Variations in e_u have little effect. A simplified expression can therefore be given by

$$n = 10 \frac{f_2}{f_u} - 1.5 \qquad \ldots (3)$$

The quantities f_2, f_u and e are specified minimum tensile properties accepted in lieu of the compressive values. The latter are seldom available and never given in practice.

(b) Finding f_o

The value of f_o correctly locates the failure point (limit of proportionality) on the curve. It is given by

$$f_o = f_2 - \frac{f_u - f_2}{(500\ e_u)^{1/n} - 1} \qquad \ldots (4)$$

Expression (2) can now be solved.

Fixing the stress-strain relationship by solving expression (2) enables the curve relating the buckling stress f_{cr} and the slenderness ratio λ to be obtained, using the tangent modulus strut formula:-

$$f_{cr} = \frac{\pi^2 E_T}{\lambda^2} \qquad \ldots(5)$$

Where E_T = Slope of f-e curve at stress f_{cr}

Then from (2) $\frac{1}{E_T} = \frac{de}{df} = \frac{1}{E} + \frac{n}{500} \frac{(f - f_o)^{n-1}}{(f_2 - f_o)^n}$ $\ldots(6)$

The true column curve expression (5) may however be approximated by an inclined straight line, Fig. 1, defined at the left hand end by λ_A. This location is arbitarily taken as the value of λ on the tangent modulus column curve (5) corresponding to $f_{cr} = f_5$ where f_5 = 0.5% proof stress.

From (2) it can be seen that

$$f_5 = f_o + 2.5^{\frac{1}{n}} (f_2 - f_o) \qquad \ldots(7)$$

Equations (5) (6) and (7) enabled an expression for λ_A to be evolved. This fixed the point of the horizontal cut-off O-A and is given by

$$\lambda_A = \frac{\pi}{\sqrt{\frac{f_5}{E} + \frac{nf_5}{200\ (f_5 - f_o)}}} \qquad \ldots(8)$$

The point λ_B at the right hand (lower) end of the inclined straight line, Fig. 1 is similarly defined by relating the limit of proportionality f_o and the slenderness ratio λ on the tangent modulus (failure) curve and the Euler curve. Points B′ and B are at the same stress level such that $\lambda_B - \lambda_{B'} = 1$, where

$\lambda_B - \lambda_{B'} = 1$, where $\lambda_{B'}$ and λ_B are the respective value of λ at B' and B. λ_B when so defined, locates point B on the stress curve and is given by:-

$$\lambda_B = 210 \left(\frac{100^n}{f_2^{\,n}} \right)^{\frac{1}{(2n-3)}} \qquad \ldots(9)$$

Simplified and expressed in terms of f_o, equation (9) becomes:-

$$\left.\begin{aligned} \lambda_B &= \sqrt{\frac{6.8 \times 10^5}{f_o}} \quad \text{Metric Units} \\ &\text{or} \\ \lambda_B &= \sqrt{\frac{44{,}000}{f_o}} \quad \text{Imperial Units} \end{aligned}\right\} \qquad \ldots(10)$$

The complete strut curve is now defined.

By replacing the true tangent-modulus failure curve by the straight line A B, and applying a load factor, the strut curve giving the permissible compressive stresses could now be calculated and drawn. See Fig. 1.

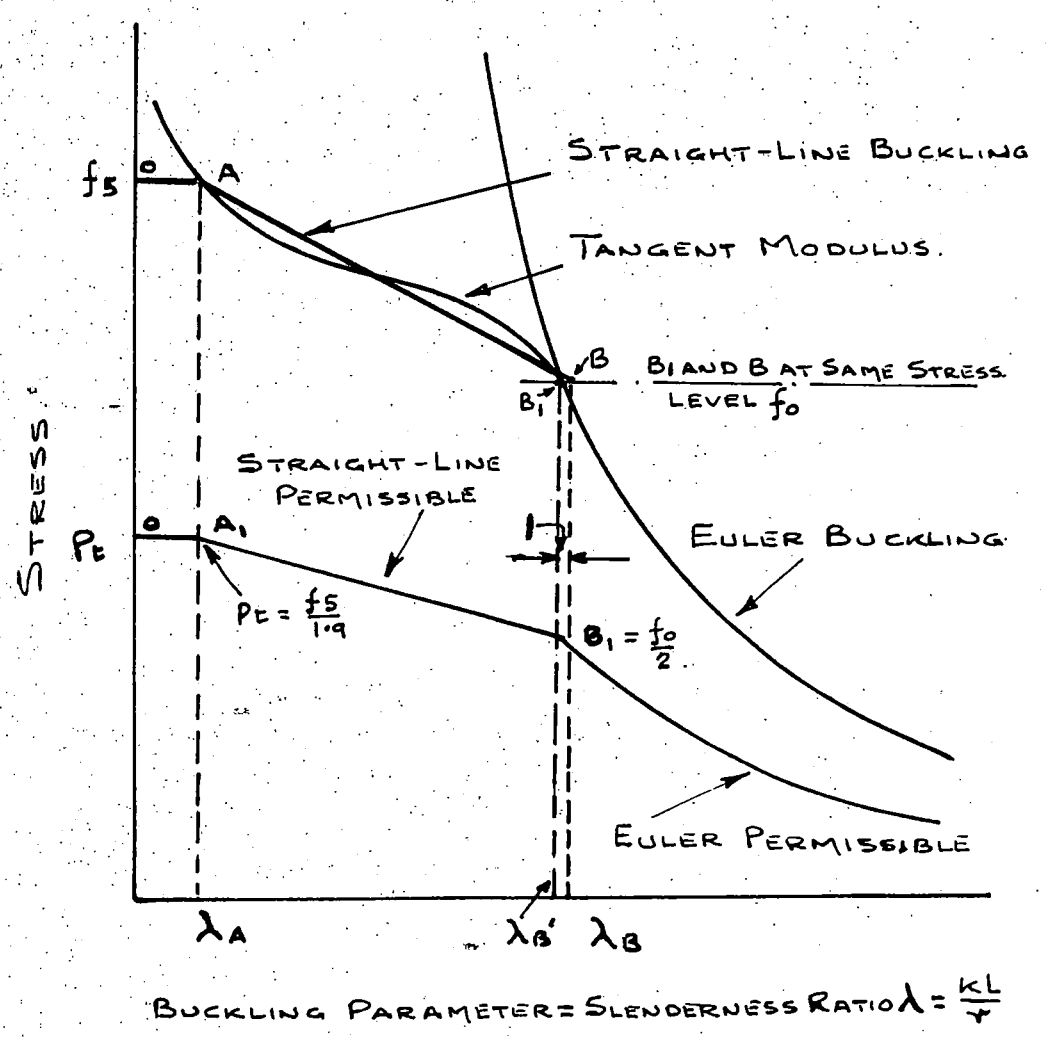

Fig:- 1

It must be remembered when constructing the permissible stress curve that the load factor will be 1.9 at A_1 and 2.0 at B_1. The factor of 2 will look after the wrongly guessed effective lengths on the Euler part of the curve.

2. Column Buckling - Strut Curve Calculations

The foregoing theory was then applied to the Al-Zn-Mg alloy being used for this work and the necessary curve for the compressive stress in struts produced.

Data supplied by Alcan Research and Development Ltd., in June 1970 gave particulars of all casts supplied, (see page 55). The tests conducted at the Polytechnic (see page 57) confirmed the data supplied was satisfactory.

The material for Tests No's 1 to 10 involving struts $M^{k}_{\sim}$ S1 to S5 inclusive was all from Casts 320D and 322D.

Taking an average of the figures for these casts (which were very close) provides the following data for adoption in the calculations.

f_1 = 0.1% proof stress = 317 N/mm^2 (20.5 ton/in^2)

f_2 = 0.2% proof stress = 340 N/mm^2 (22.0 ton/in^2)

f_u = U.T.S. = 400 N/mm^2 (25.75 ton/in^2)

e_u = % elongation = $5.65\sqrt{\text{area}}$ = 11%

E = Young's modulus = 7000 Kg/mm^2 = 68,700 N/mm^2 (4450 ton/in^2)

(a) Finding n (Knee Factor)

Using expression (3) $n = 10\left(\frac{f_2}{f_u}\right) - 1.5$

$= 10\left(\frac{340}{400}\right) - 1.5$

$n = 7$

(b) Finding f_o (Limit of Proportionality)

Using expression (4) $f_o = f_2 - \dfrac{f_u - f_2}{(500\, e_u)^{\frac{1}{n}} - 1}$

$$= 340 - \frac{400 - 340}{(500 \times \frac{11}{100})^{\frac{1}{7}} - 1}$$

$$= 340 - \frac{60}{1.9 - 1}$$

$$f_o = \underline{273\ N/mm^2}\ (17.62\ ton/in^2)$$

(c) Finding f_5 (0.5% Proof Stress)

Using expression (7) $f_5 = f_o + 2.5^{\frac{1}{n}} (f_2 - f_o)$

$$= 273 + 2.5^{\frac{1}{7}} (340 - 273)$$

$$= 273 + 1.140\ (67)$$

$$f_5 = \underline{349\ N/mm^2}\ (22.6\ ton/in^2)$$

Note that the IQS Committee for units and symbols recommends multiples in numerator, e.g.MN/mm^2, but the aluminium and steel standards both adopt N/mm^2.

(d) Finding λ_A

Using expression (8) $\lambda_A = \dfrac{\pi}{\sqrt{\dfrac{f_5}{E} + \dfrac{nf_5}{200\,(f_5 - f_o)}}}$

$$= \frac{\pi}{\sqrt{\frac{349}{68,700} + \frac{7 \times 349}{200(349-273)}}}$$

$$= \frac{\pi}{\sqrt{.005 + .160}}$$

$$\lambda_A = 7.75 \text{ Say } \underline{8}$$

Note Code Appendix D simplifies and standardises at 8 for all alloys. This is not completely satisfactory for alloys with values below 8 such as N.8 m. It will also tend to be conservative for alloys with values much in excess of 8.

(e) Finding λ_B

Using expression (10) $\lambda_B = \sqrt{\dfrac{6.8 \times 10^5}{f_o}}$

$$= \sqrt{\frac{6.8 \times 10^5}{273}}$$

$$= \sqrt{2500}$$

$$\lambda_B = \underline{50}$$

Note Code CP 118 Appendix D (D.2.1) gives an expression for λ_s on the permissible stress curve (Code Fig. 24) which compares at 52.

(f) Finding Pt

$$Pt = \frac{f_5}{\text{Load Factor } 1.9} = \frac{349}{1.9} = 184 \text{ N/mm}^2 (11.9 \text{ ton/in}^2)$$

The strut curves giving compressive stresses are now shown in Fig. 2.

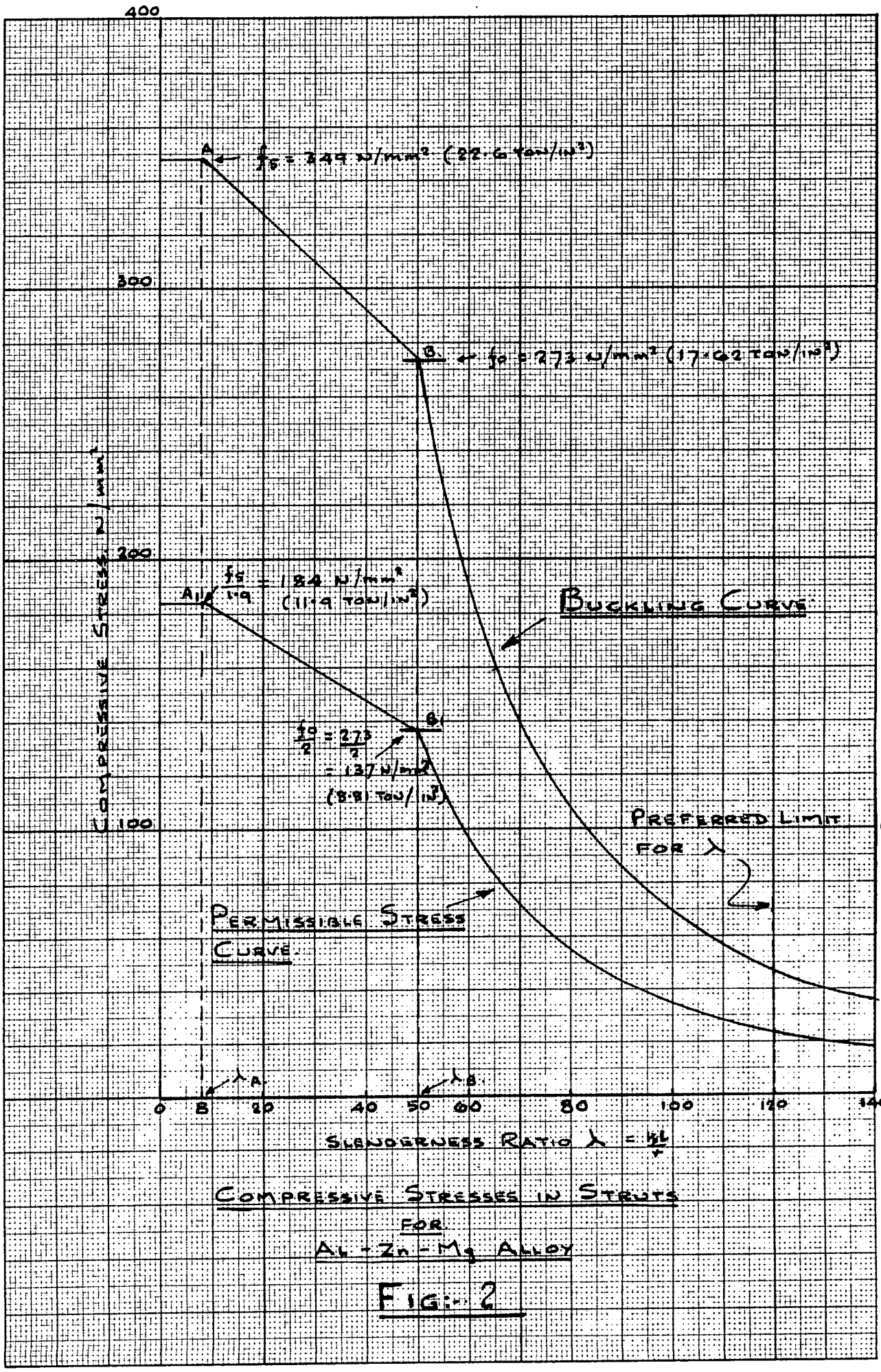

COMPRESSIVE STRESSES IN STRUTS
FOR
Al - Zn - Mg ALLOY

FIG:- 2

3. Local Buckling - Theoretical Basis

All structural members are considered as being built up from a series of plates forming the webs, flanges and reinforcements. In many cases these will be thin plates liable to buckle locally under a compressive load.

C.P. 118, 1969 provides permissible compressive stress curves for beams and thin plates in the most commonly used alloys which include the requirements for local buckling. A comparable curve was required for the Al-Zn-Mg alloy under test.

Local buckling curves are constructed by adopting an approach comparable to that used for strut curves. The secant-modulus curve however replaces the tangent-modulus at the lower buckling parameters. λ is again used to define the buckling parameter which for local-buckling is given by $\frac{mb}{t}$ where:-

m = local buckling coefficient

b = breadth of component plate

t = thickness of component plate.

The curve is constructed in the manner shown in Fig. 3. It is defined by the quantities f_{bcr}, λ_A, and λ_B. The crippling bending stress f_{bcr} has been determined from the expression $f_{bcr} = \frac{Mcr}{z}$ where M_{cr} is the bending stress reached when the extreme fibre stress equals the 1% proof stress. In other words

a 90% over-load will produce 1% plastic strain in the extreme fibres. Z is the ELASTIC section modulus.

The ratio f_{bcr} to f_5 varies with the alloy. It is higher when the alloy has a steeply rising stress-strain curve. This ratio is designated s and has a value which varies from 1.1 for normal sections to 1.5 for solid bar. A value of 1.1 will be adopted.

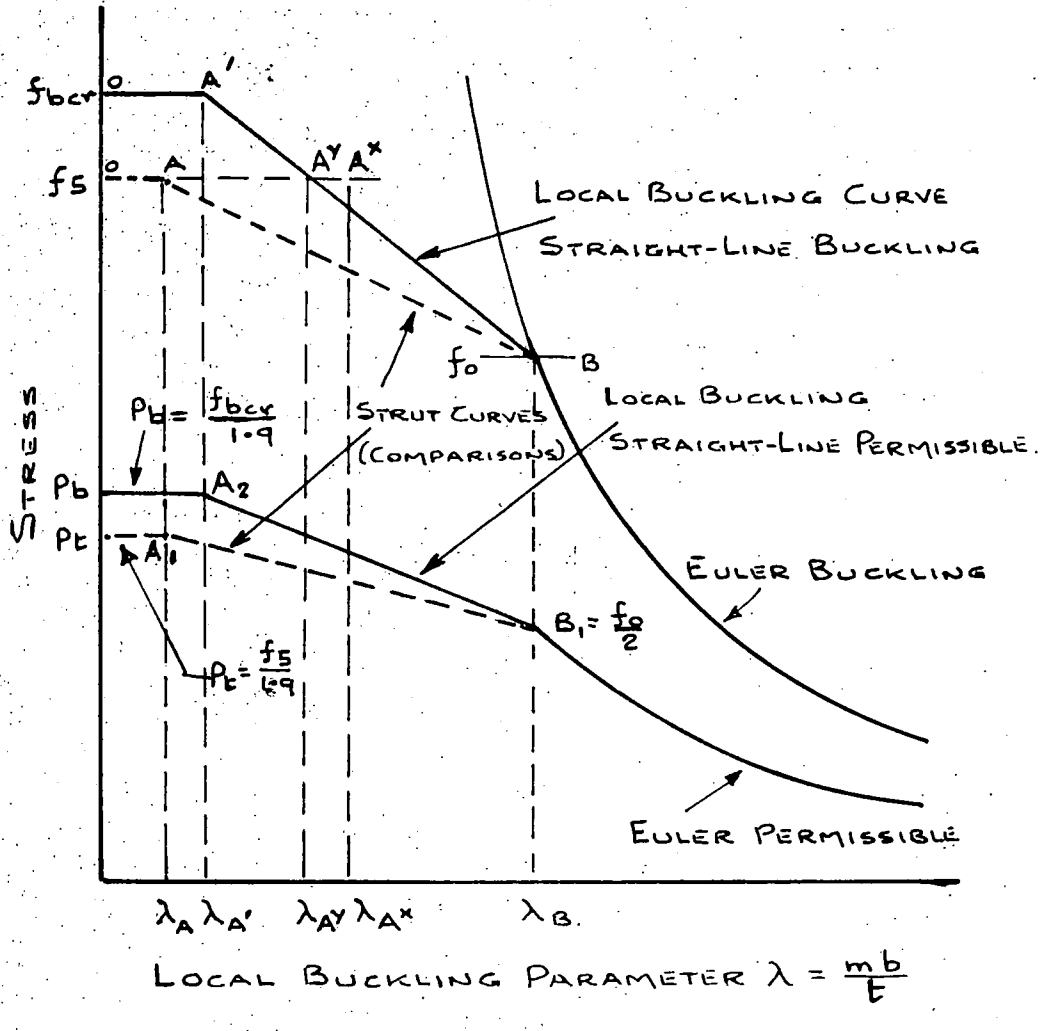

Fig:- 3

A simplified expression involving the use of s for obtaining f_{bcr} is given by

$$f_{bcr} = sf_2 + (5^{\frac{1}{n}} - 1)(1.2 - 0.25)(f_2 - f_o) \quad \ldots(11)$$

The permissible stress Pb is then $\frac{f_{bcr}}{\text{Load factor } 1.9}$

As with column buckling it is required to establish the cut-off points λ_A' and λ_B. The value for λ_B will be the same as already established for column buckling.

Referring to Fig. 3, the inclined straight line A B is that already fixed for column buckling. A similar line A′ B is now necessary for local buckling and is found as follows.

First find $\lambda_A{}^x$ which locates the point at which $f = f_{5(crit)}$ on the secants modulus failure curve. It will be recalled the λ_A for column buckling was similarly defined, but based on the tangent modulus curve.

Using a comparable approach $\lambda_A{}^x$ is given by

$$\lambda_A{}^x = \frac{\pi}{\sqrt{(2.5)^{\frac{1}{n}} \frac{f_2}{E} + 0.005}} \quad \ldots(12)$$

Next position point A^Y along the stress level f_5 by making $\lambda_A Y = \frac{1}{2}(\lambda_A + \lambda_A x)$ ...(13)

or possibly, if $\lambda_{A'}$ is to be maintained at about 8 as with column buckling $\lambda_A{}^Y = \frac{\lambda_A}{3} + \frac{2\lambda_A{}^Y}{3}$ ...(14)

Finally point A' can be located by producing BA^Y up to the stress level of f_{bcr}. The profile of the buckling curve is now complete and the permissible stress curve for local buckling may be constructed as shown in the figure. The curve is applicable for the local buckling of beam compression flanges as well as struts.

4. Local Buckling - Curve Calculations

Materials properties as for column buckling

(a) Finding f_{bcr}

Make s = 1.1

Using expression (11)

$$f_{bcr} = sf_2 + (5^{\frac{1}{n}} - 1)(1.2 - 0.2s)(f_2 - f_o)$$

$$= 1.1 \times 340 + (5^{\frac{1}{7}} - 1)(1.2 - 0.2\times1.1)(340-273)$$

$$= 374 + (.259)(\ .98)(67)$$

$$f_{bcr} = \underline{391\ N/mm^2}\ (25.3\ ton/in^2)$$

Thus permissible stress

$$Pb = \frac{f_{cbr}}{1.9} = \underline{206\ N/mm^2}\ (13.3\ ton/in^2)$$

Note: Code CP 118 Appendix D gives a generalised expression P_{bc} which compares at 205.6 N/mm^2.

(b) Finding $\lambda_A x$

Using expression (12) $\lambda_A x = \sqrt{\frac{\pi}{(2.5)^{\frac{1}{n}} \frac{f_2}{E} + 0.005}}$

$$= \sqrt{\frac{\pi}{(2.5)^{\frac{1}{7}} \frac{340}{68700} + .005}}$$

$$= \sqrt{\frac{\pi}{.0106}}$$

$$\lambda_A x = \underline{30.5}$$

(c) Finding $\lambda_A Y$

Using expression (13) $\lambda_A Y = \frac{1}{2} (\lambda_A + \lambda_A x)$

$$= \tfrac{1}{2} (8 + 30.5)$$

$$\lambda_A Y = \underline{19.25}$$

OR alternatively

Using expression (14) $\lambda_A Y = \frac{\lambda_A}{3} + \frac{2 \lambda_A x}{3}$

$$= \frac{8}{3} + \frac{61}{3}$$

$$\lambda_A Y = \underline{22.96}$$

(d) Finding A′

The Code C.P. 118 standardises on $\lambda_{A'}$ at 8 thus the value of $\lambda_{A}{}^{Y}$ = 22.96 will be adopted. Stress values thus derived may be optimistic for this alloy in which case $\lambda_{A}{}^{Y}$ = 19.25 will need to be used. When $\lambda_{A}{}^{Y}$ = 23 BA^{Y} projected to A′ gives $\lambda_{A'}$ of approx. 8.

The completed local buckling stress curves are shown in Fig. 4.

5. Post Buckling

Mention was made in Chapter 1 of the interrelation of column and local buckling in the post buckling situation.

The compressive stress curve for local buckling developed so far and shown in Fig.4 is simply based on INITIAL buckling. Values of $\lambda = {}^{mb}/t$ which fall to the left of point B will be satisfactory as buckling will virtually cause collapse almost immediately. Where however the value of $\lambda = {}^{mb}/t$ falls to the right of point B the approach is conservative because the MAXIMUM stress is then greater than the INITIAL buckling stress. This value will progressively increase as λ increases and provide a reserve of post buckling strength.

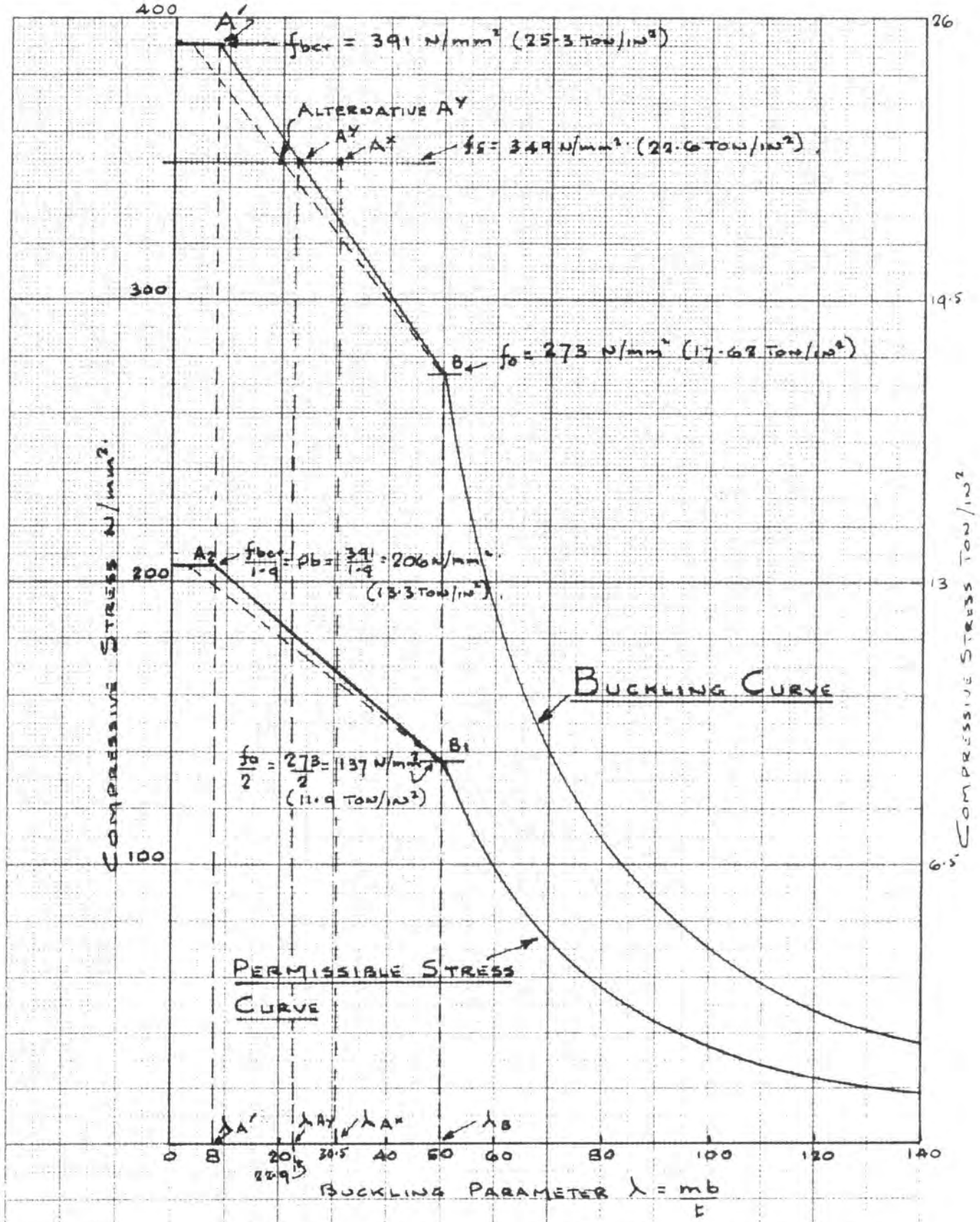

COMPRESSIVE STRESSES IN THIN PLATES - LOCAL BUCKLING

FOR

AL - Zn - Mg ALLOY

(ALSO APPLICABLE FOR LATERAL BUCKLING OF BEAMS WHEN $\lambda = \lambda_{lat}$).

FIG:- 4

In certain circumstances this may be used to advantage.

In general, a post buckling investigation is only worthwhile when the breadth/thickness ratio for webs exceeds 35 and that for flanges exceeds 12. The value of $\lambda = {}^{mb}/t$ should also fall a reasonable distance to the right of B to justify further investigation. A method of dealing with post buckling is given below and shown in Fig. 5.

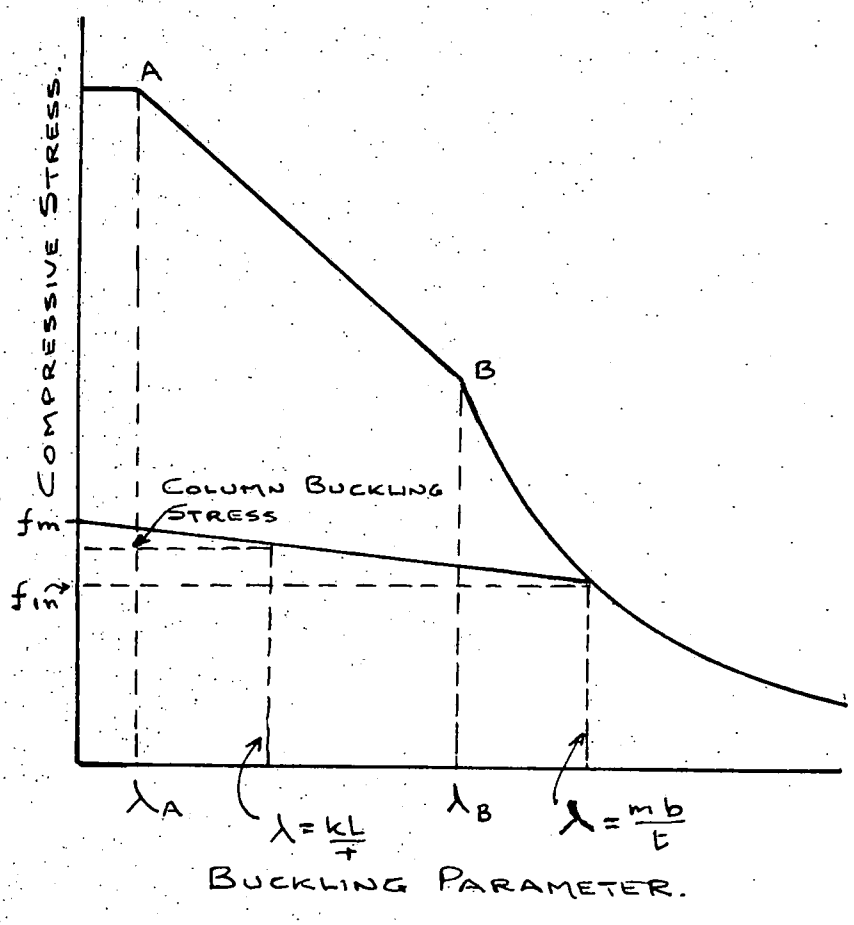

Fig:- 5

(a) Find the value for $\lambda = \frac{mb}{t}$ (say this exceeds $\lambda_B = 50$ by a reasonable amount).

(b) Read off the somewhat conservative INITIAL buckling stress f_{in} from the buckling curve.

(c) Next find the value of the buckling stress f_m based on the MAXIMUM stress for a very short strut given by $fm = \frac{C}{\left(\frac{mb}{t}\right)^{\frac{2}{3}}}$ where C is a constant given by

$$C = \frac{44000}{\lambda_B^{4/3}} \quad \text{Imperial Units}$$

OR

$$C = \frac{6.8 \times 10^5}{\lambda_B^{4/3}} \quad \text{Metric Units}$$

This approach will be found to be similar to Chilver's empirical relationship but with an adjustment to make $f_m = f_{in}$ at B.

Thus for a strut having a column buckling slenderness ratio $\lambda = \frac{KL}{r}$ less than λ_B (dictating the consideration of local buckling) the buckling stress using the post buckling reserve strength is given by

$$f_{cr} = f_{in} + (f_m - P_{in})\left(1 - \frac{\frac{KL}{r}}{\frac{mb}{t}}\right).$$

This expression may be subsequently used if tests indicate this is necessary.

6. Torsional Buckling

Single channel struts need to be checked for torsional buckling using the "Compressive Stresses in Struts" curve FIG 1 with $\lambda = k\lambda_t$. As the section only has one axis of symmetry an interaction will frequently exist between torsional and column buckling in the plane normal to that axis. This will result in a lower buckling stress than that associated with either form of buckling when considered alone, and an interaction coefficient K must be included.

Work by Smith[24] gave immunity curves for channel section where $(L/ry)/(\frac{b}{t})$ was plotted against $\frac{d}{b}$ where d is web depth and b is flange depth. Fig. 6 indicates Smith's proposals and it is suggested that in practice the stress be restricted to that given

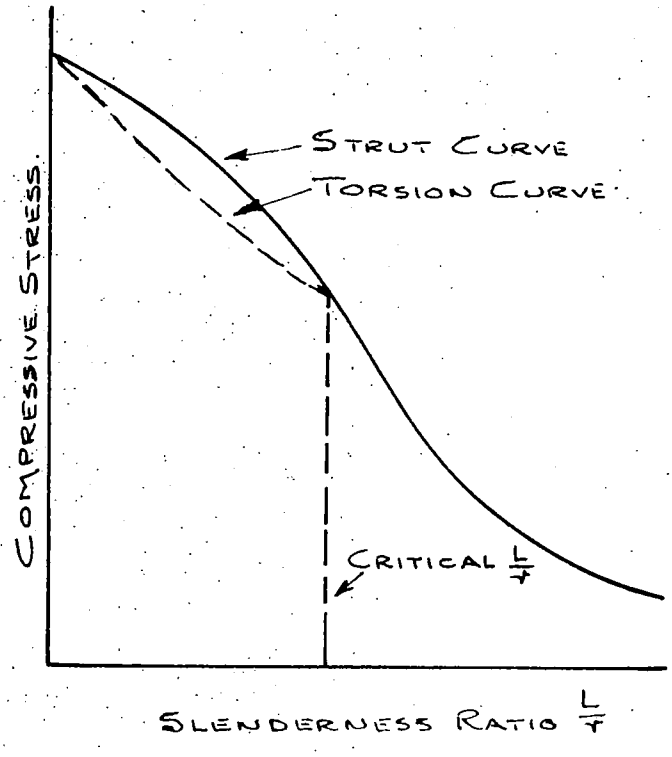

Fig:- 6

by the critical $\frac{L}{ry}$, unless calculations are made to establish and involve the inter-action coefficient K.

Double channel battened struts present a complex torsional problem, particularly if eccentric end loading exists in the plane of the battens. Under this condition a load differential and consequent variable torsional characteristics will exist between the main channel legs. The situation will be still further complicated by the location and individual stiffness of the batten plates.

The battened strut has a profile which cannot be classed as either an "open" or "closed" section and its torsional resistance will fall SOMEWHERE between that expected for these two configurations.

It is therefore not expedient to try and predict the torsional behaviour of the battened strut for the initial design. Consideration will however be given to the problem once the test results have been analysed.

Chapter 4

Theoretical Approach

4.1 General

The design engineer involved with the use of thin walled sections is confronted with a complex problem resulting from the combined stress situation. The various forms of buckling and their interactions may manifest themselves in the individual components as well as the composite member. This makes the problem of stress apportionment particularly arduous.

Even today, practising engineers may follow the ways of their ancestors and endeavour to solve a complex stress situation by breaking the problem down into isolated units. They may well find it is then "justifiable" to apply formulae extracted from some dusty text book, conduct a few tests, and "logically" superimpose their findings to produce a covering solution. This "ostrich" method of approach undoubtedly stems from the use of thicker sections and higher load factors used in the past decade. It may be a great time saver and readily appeal to the gambling instinct but can scarcely be regarded as acceptable now that highly stressed, thin walled, components are commonplace.

With static structures, it can be argued that the only justification for abstruse calculation is the enforced

economics of weight saving. However, with moving structures the economy of material is much more pressing. The fact therefore remains that, for one reason or another, problems exist which must be solved and the further investigation of stress interaction is inevitable.

4.2 The Interaction Method

As previously intimated any investigation into the interaction of stresses resulting from externally applied forces and from member deformation under a simple loading condition gives rise to analysis difficulties.

A method attributed to Shanley[60][62], known as the "Interaction Method", provides a means of determining allowable loads under a combined loading condition. It also has the added attraction of being amenable to intuitive reasoning and common sense. The stress ratio basis makes it compatible with the combined stress approach recommended in both C.P. 118 and B.S. 449. Its suitability for dealing with the complexity of parameters likely to exist with battened strut problems could not be bettered and confirmed its selection for this dissertation.

In briefly discussing the method, it can be said to be non-dimensional and deals only with ratios which are stresses of the same character. It can be demonstrated in its simplest form by assuming a case involving two different types of load and a utilisation factor R,

which for a simple loading condition represents the ratio of an applied simple stress f to a permissible stress p or a failure stress f_{cr}. R_1 and R_2 could therefore represent two conditions.

The effect of these two conditions, one on the other, can be shown by an interaction curve, the shape of which will be dependent upon the nature of the loading under consideration. The curve is usually expressed by a simple stress ratio equation which is derived from either test data or theory.

Once the curve has been established it is possible to directly predict the effect of one loading condition on the other. Any given value of R_1 plotted on the curve will directly indicate what is available to be utilised by R_2 - Fig. 7. It is usual for the effect of one loading condition to reduce the utilisation factor to less than 1.0 but certain conditions may exist which result in the second load increasing the factor to more than 1.0.

Before proceeding to the critical particular cases of combined loading applicable to this work, a consideration of the basis upon which the interaction concept is founded will reveal the following generalised form. For cases involving two types of loading designated R_1^a and R_2^b and knowing that $R_1^a + R_2^b = 1$ the variation of

the exponents "a" and "b" will produce interaction curves above the straight line given by $R_1 = R_2 = 1$. Making one exponent equal to 2 will yield a parabola and with both exponents equal to 2, a circular arc. As the exponents are further increased the curves will approach the boundaries given by $R_1 = R_2 = 1$. Fig. 7.

Thus with infinite exponents complete freedom, indicating zero interaction, would be attained, suggesting that the basic equation should be $R_1^{1/a} + R_2^{1/b} = 1$, where a and b represent the degree of interaction. The expression $R_1^{a} + R_2^{b} = 1$ is however preferred on grounds of simplicity.

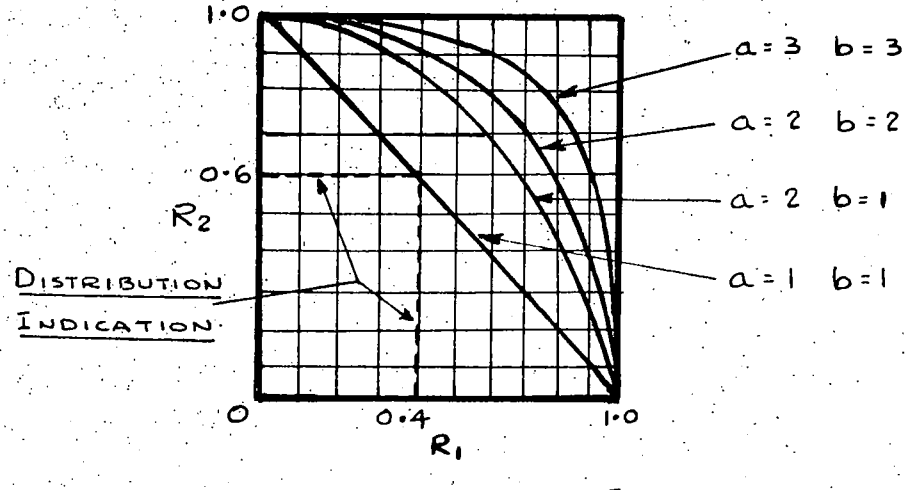

TYPICAL INTERACTION CURVES

FIG:- 7

For any given problem the degree of interaction will need to be sensibly predicted. One would assume that two loading conditions of a similar nature cause effects which are directly additive and give a straight line

interaction curve. If however the two conditions were bending and torsion the resulting critical stresses would not act at the same point or at the same angle and less interaction will therefore take place. Further thought reveals that the normal stress due to torsion acts at 45^{o} to that due to bending, which results in an interaction curve in the form of a circular arc.

Careful consideration of the type of loading condition is therefore essential. Whilst the approach may be regarded as somewhat empirical it must be appreciated that the end points of the interaction curve are correct, at least in so far as they accurately represent the state of knowledge for failure, under simple loading conditions. This must considerably reduce the probable error involved when one type of loading predominates.

Finally, even different materials with varying mechanical properties, can often be represented by a single interaction curve. This feature is particularly useful when dealing with the heat-treatable aluminium alloys.

4.3 Interaction Method Applied to the Battened Strut

No strut theoretically argued as axially loaded, will ever exist in practice. Any theoretical approach, to be useful, must therefore accept that practical inadequacies exist and should, wherever possible, be catered for.

The general list of variables given in Chapter 1 must therefore now be more specifically defined in an effort to optimise the theoretical approach.

Data collected from the battened struts under test will indicate the cumulative effect of a number of interacting stresses and deformations, resulting from the following major contributory factors.

1. Axial load component.
2. Bending moment due to initial intended eccentricity.
3. Bending moment due to deflection under load.
4. Bending moments resulting from initial lack of straightness. These may well produce moments on both major axes.
5. The inducement and redistribution of bending moments resulting from the longitudinal twist of the strut. This manufacturing fault is mainly attributed to welding. With eccentric end loading the twist will affect the relative positions of the top and bottom ball seats and promote additional bending on the major axis at right angles to that initially intended. It will also set up a small amount of horizontal shear.
6. Any inbevel of the individual channel flanges or bowing of the web, which does occur with extruded sections, but is generally only slight, may well affect the ultimate load carrying capacity of the

strut and influence its behaviour to column, torsional and local buckling.

7. Restraining effects of the battens. Their location and number.

8. The effects of friction at the ball seatings. This will tend to reduce the struts effective length and improve its load carrying capacity.

9. The collective influence of the foregoing loads, moments, deflections, malformations and restraints will influence the failure load for column buckling. The location of any local buckling failure and the magnitude of the crippling stress in local buckling will be influenced likewise.

10. The comments for column and local buckling indicated in 9 also apply to torsional buckling.

The foregoing list of contributory factors, all of which interact on each other, highlights the complexity of the situation. Collectively they will influence the ultimate mode of failure and the failure stress. It must of course be appreciated that some of the individual factors controlling the failure stress will vary with each strut manufactured.

Any theoretical approach to the problem must of necessity be operated on a reduced number of parameters to those

listed. The possibility of grouping was therefore considered. It is accepted that a load factor exists to cover for contingencies in design and manufacture, but this does not detract from the desirability of including as many of the variables as possible in the theoretical approach.

Before an examination of the test results can be made, an analysis procedure must be established.

The problem resolves itself into two major factors, namely the effects of axial load and bending moment, which will interact. Problems relating to the battens themselves and any torsional effects on the struts as a whole, will be subsequently considered. Bending will create the major problem as the final bending moments will be made up from a number of the contributory factors listed earlier.

Shanley submits that for combined bending and compression the postulate of the linearity of the interaction curve may be deduced by writing the familiar elastic theory combined stress equation

$$f_{max} = f_c + f_b = \frac{P}{A} + \frac{My}{I} \qquad \ldots\ldots(1)$$

where

f_{max} = maximum normal stress

f_c = average axial compressive stress

f_b = maximum bending stress

A = cross-sectional area

M = bending moment

I = Moments of Intertia with respect to the N.A. about which bending M occurs

y = distance from N.A. to outer fibre

P = applied end load.

This expression is only applicable to relatively short columns in which secondary bending effects are negligible.

Taking the value of f max at failure as a constant fo and normalising expression (1) gives

$$\frac{f\ max}{f_o} = \frac{f_c}{f_o} + \frac{f_b}{f_o} \qquad .....(2)$$

At failure f max = f_o thus the interaction expression at failure is given by

$$\frac{f_c}{f_o} + \frac{f_b}{f_o} = 1 \qquad .....(3)$$

Expression (3) represents a linear interaction curve between intercepts (1,0) and (0,1).

The normal stress at failure is probably not the same for PURE axial load and PURE bending thus expression (1) needs to be generalised by replacing f_o by f_{co} for compression and f_b by f_{bo} for bending.

Where the interaction curve remained straight the interaction expression would be $R_c + R_b = 1$. Fig. 8.

Then $R_c = \frac{f_c}{f_{co}} = \frac{P}{P_o}$ .....(4)

and $R_b = \frac{f_b}{f_{bo}} = \frac{M}{M_o}$ .....(5)

where all suffixes o (i.e. f_{bo}, M_o etc) represent a base value of stress, moment etc.

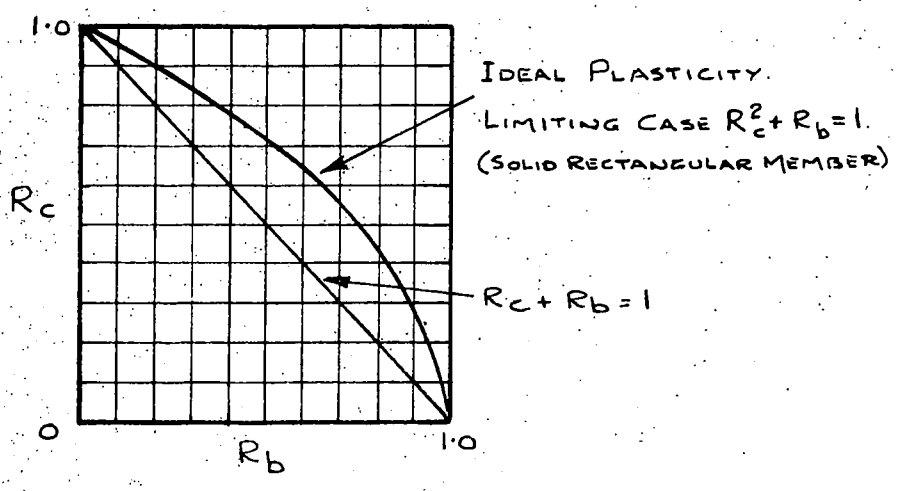

FIG: 8

However, the linearity of the interaction curve is influenced by the "plastic effect", and with ductile materials the bending stress distribution does not remain linear up to failure, as assumed by expression (1). The limiting case for ideal plasticity (i.e. when f max = f yield = constant), as given by a rectangular member is $R^2_c + R_b = 1$. Fig. 8. This type of section would seldom be used to resist bending and for efficiently designed standard sections the plastic effect is small in PURE bending. The effect on the bending stress distribution is generally negligible.

To understand and operate the "Interaction Method" satisfactorily the effects of lateral displacement under load and the influence this displacement has on the moment arm of the load, must be fully appreciated. Both axial and eccentric end loading will therefore be considered in some detail.

Axial Loading

In the case of the axial end loading condition, with pin ends, any lateral displacement (which may also include initial lack of straightness) can be simply determined by considering half the length of the strut shown in Fig. 9.

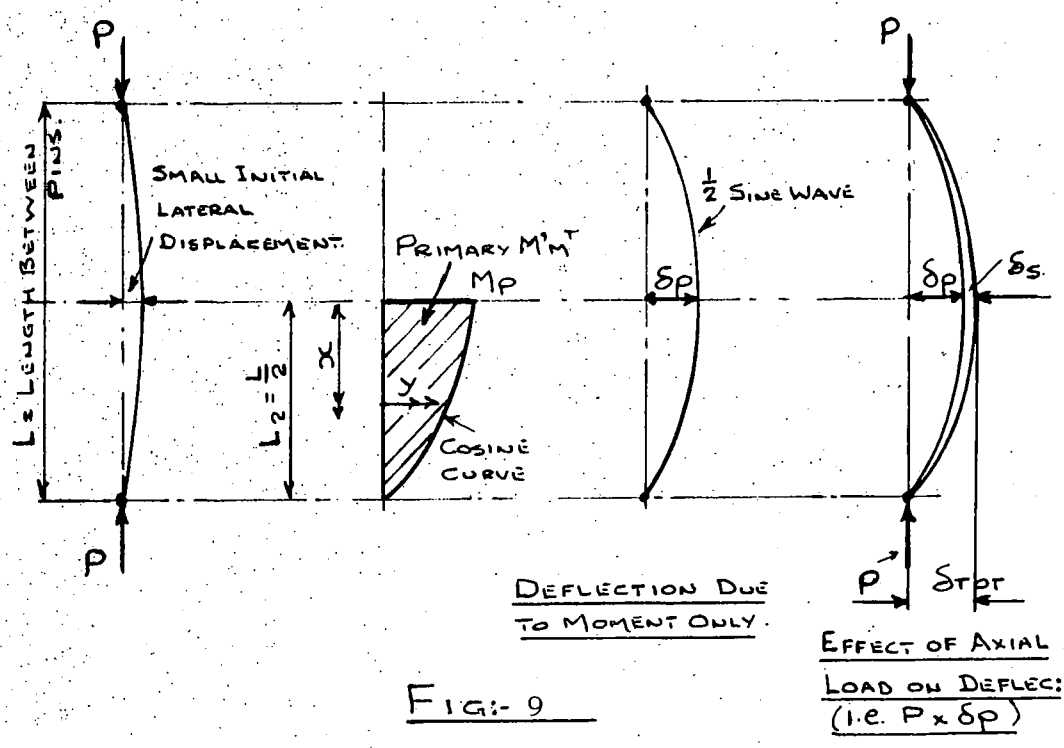

Fig:- 9

Assume the strut to be axially loaded through pin ends and that a small amount of initial lateral displacement exists. The displacement would provide a lever arm for the load and promote a bending moment of sinusoidal distribution over the length of the strut.

An analogy therefore exists between the loading conditions of the strut and a weightless "beam-column" which is transmitting both a compressive axial load P and simultaneously being subjected to a bending moment M_p. Where the bending moment has a sinusoidal distribution over the length of the beam the loading conditions will be identical.

Accepting this identity enables the loading to be considered as producing two additive increments of bending moment and deflection, a PRIMARY moment M_p causing deflection δ_p (when the axial load is absent), PLUS a SECONDARY moment M_s causing further deflection δ_s. The moment M_s and deflection δ_s are produced solely from the inclusion of the axial load P which is now acting through the lever arm provided by the deflection δ_p.

The effect of the secondary moment $M_s = P\delta_p$ is to produce additional deflections which produce additional moment, and so on. This action will be convergent and result in a final value for the maximum total bending moment M_{TOT} which is the sum of all the primary and secondary moments. At the mid-height of the strut this will give a maximum deflection value δ_{TOT} for an axially loaded strut.

It is therefore necessary to establish initially a value for the lateral displacement due to primary bending with

with a maximum value M_p. For a carefully aligned strut, with virtually no lack of straightness, the practical value of M_p could be negligible and the failure and critical values almost coincident.

Taking half the strut (See Fig. 9) as a cantilever of length L_2

$$M = M_p \cos \left(\frac{x}{L_2} \cdot \frac{\pi}{2}\right)$$

where x = distance from mid-height and $L_2 = \frac{L}{2}$

$$\text{Slope } \phi = \int \frac{M}{EI}\, dx = \frac{M_p}{EI} \frac{2L_2}{\pi} \sin \left(\frac{x}{L_2} \frac{\pi}{2}\right)$$

$$\text{Deflection } y = \int \phi\, dx = -\frac{M_p}{EI} \left[\frac{4L_2^2}{\pi^2} \cos \left(\frac{x}{L_2} \frac{\pi}{2}\right)\right]_o^x$$

$$= -\frac{M_p}{EI} \left[\frac{4L_2^2}{2} \cos \left(\frac{x}{L_2} \frac{\pi}{2}\right) - \frac{4L_2^2}{\pi^2}\right]$$

Moment M_p will give the maximum value of y when $x = L_2$

$$\text{Then y max} = \delta_p = \frac{4M_p L_2^2}{\pi^2 EI}$$

Also by replacing L_2 with $\frac{L}{2}$, its actual value

$$\underline{\text{PRIMARY}} \text{ deflection} = \delta_p = \frac{M_p L^2}{\pi^2 EI} \qquad \ldots\ldots(6)$$

and knowing Euler load PE $= \frac{\pi^2 EI}{L^2}$

$$\delta_p = \frac{M_p}{PE}$$

But from earlier reasoning the total maximum deflection δ_{TOT} for axial load will need to include the effects of secondary bending which must be added to (6).

$$\text{then } M_{TOT} = M_p + M_s$$

$$\delta_{TOT} = \frac{M_{TOT}}{P_E} \qquad \ldots\ldots(7)$$

$$\text{But } M_{TOT} = M_p + P\delta_{TOT}$$

$$\text{Then } M_{TOT} = M_p + \frac{P\, M_{TOT}}{P_E} \qquad \ldots\ldots(8)$$

To cover for the convergent effects of the secondary moment it is necessary to include for the amplification of the initial eccentricity which produces primary bending. An elastic amplification factor K_a therefore needs to be included and its value will depend upon the ratio of $\frac{P}{P_E}$. If the load $P = P_E$ the factor becomes infinite and instability exists. A slight eccentricity e of the load P would thus cause instability at a value of $P < P_E$.

$$\text{Let } \frac{M_{TOT}}{M_p} \equiv K_a$$

$$\text{Dividing (8) by } M_p \text{ gives } K_a = 1 + \frac{P}{P_E}\ \frac{M_{TOT}}{M_p} = 1 + (\frac{P}{P_E})K_a$$

$$\text{From which } K_a = \frac{1}{1 - \frac{P}{P_E}} \qquad \ldots\ldots(9)$$

Expression (9) allows for the increase in bending moment due to column deflections. It is only suitable for sinusoidal bending such as would result from axial load. In such cases it may be used to determine the lateral deflection which will be maximum at mid-height. It may be expressed in the dimensionless form

$$\frac{\delta}{e} = \frac{1}{1 - \frac{P}{P_E}}$$

where e is the amplitude of any initial sinusoidal eccentricity, such as lack of straightness.

Expression (9) is therefore applicable to the axially loaded struts covered by Tests 5 and 6 and can be applied in the dimensionless form where known lack of straightness exists.

Eccentric loading

For Tests 1 to 4 and 7 to 11 inclusive the end loading will be 25.4 mm (1 in) eccentric, along the axis parallel to the battens. This eccentricity will produce a PRIMARY bending moment M_p which is constant throughout the length of the strut for any given load P. See Fig. 10

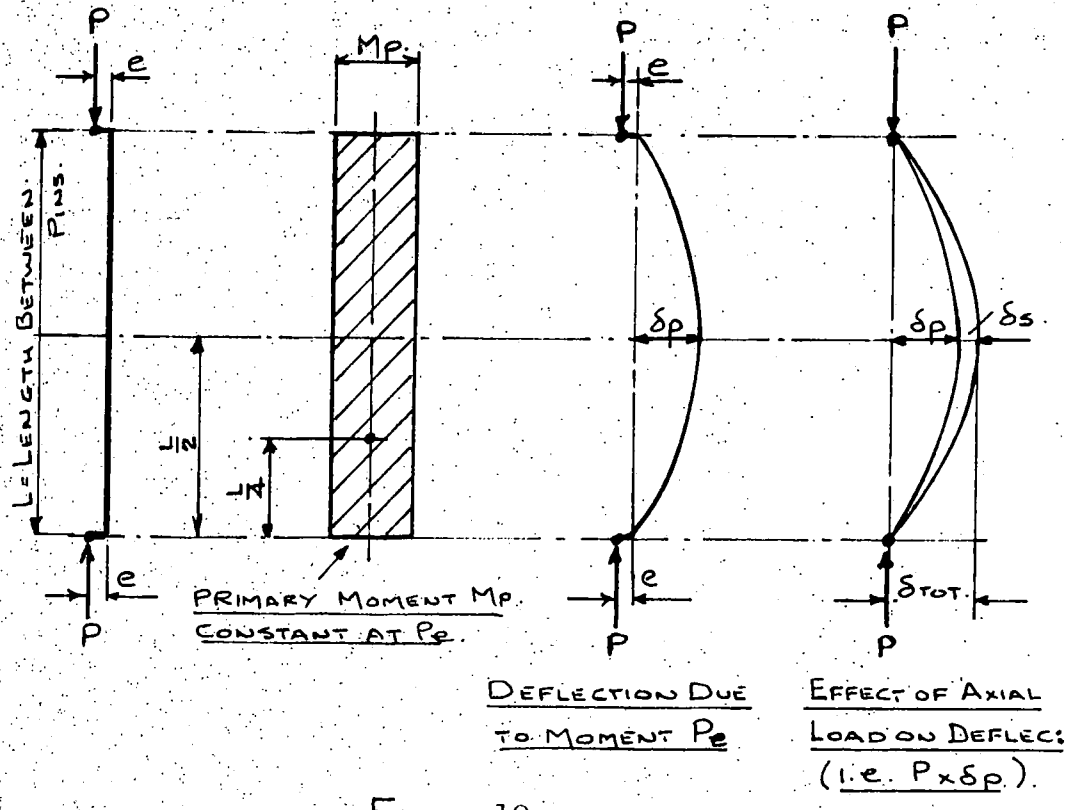

FIG:- 10

∴ PRIMARY deflection from constant PRIMARY moment M_p is given by $EI\,\delta_p = Pe \times \frac{L}{2} \times \frac{L}{4}$.

$$\therefore \delta_p = \frac{PeL^2}{8EI} = \frac{M_p L^2}{8EI} \qquad \ldots\ldots(10)$$

It will again be necessary to provide for the additional deflections resulting from the effects of the SECONDARY moment M_s and an amplification factor Ke will be needed. This will differ slightly from that adopted for the axially loaded strut due to the primary moment now being constant. It may be derived by adding to the differential equation a term representing a constant eccentricity e and given by $\frac{d^2y}{dx^2} + p^2y = -p^2e$.

This equation was solved by Thomas Young in 1807 and letting K_e represent the amplification factor for constant eccentricity its value becomes:-

$$K_e = \frac{1}{\cos\left(\frac{\pi}{2}\sqrt{\frac{P}{P_E}}\right)} \qquad \ldots\ldots(11)$$

For general purposes the simple formula (9) is frequently used as numerically (9) and (11) will give approximately the same results. This may be confirmed by taking the reciprocal of the two amplification factors and considering them as a reduction factor of the effective bending stiffness. Then for sinusoidal bending the stiffness reduction factor is

$$\frac{(EI)_R}{EI} = \frac{1}{K_a} = 1 - \frac{P}{P_E} \qquad \ldots\ldots(12)$$

and for constant primary bending it becomes

$$\frac{(EI)_R}{EI} = \cos\left(\frac{\pi}{2}\sqrt{\frac{P}{P_E}}\right) \qquad \ldots\ldots(13)$$

$(EI)_R$ = reduced bending stiffness.

If the reduction factors (12) and (13) are plotted against $\frac{P}{P_E}$ the sinusoidal bending expression (12) will give a straight line, and that for constant primary bending (13) a curve falling a small amount below the straight line given by (12).

For this dissertation the theoretical approach needs to be as precise as possible. Thus for the eccentrically loaded columns, eccentric loading at distance "e" and any lack of straightness (initial sinusoidal curvature of amplitude "a") need to be combined. This may be done by using the principle of superposition, then

$$\delta_{TOT} = K_a a + K_e e$$

In subsequent calculations δ_{TOT} will be called e_{TOT}. This will infer total eccentricity (for both theoretical and test) for the applied load. It will be applicable to both axial and eccentrically loaded struts.

With the axially loaded columns deflection will all be of sinusoidal curvature and any initial malalignment can be directly included in $K_a a$.

The maximum compressive stress in a column which is subjected to combined compression and bending, (whether the bending is the result of initial deflection or initial eccentricity, or a combination) may therefore be expressed more precisely by the inclusion of a suitable amplification factor K in expression (1) giving

$$f \text{ max} = -f_c - Kfb = -\frac{P}{A} - K\frac{MY}{I} \qquad .....(14)$$

where K is the amplification factor calculated from (9) or (11).

Now consider a relatively short length of column with axial end loading through pin ends, and a small initial deflection. The behaviour at maximum total bending moment will be as if the axial load P and the bending moment M_{TOT}, which actually exists at the point of maximum bending were acting independently. The total bending moment is given by KM.

Assuming the failure of the strut is therefore controlled by the linear interaction equation

$$\frac{P}{P_o} + K\frac{M}{M_o} = 1$$

or

from (4) and (5)

$$R_c + KR_b = 1$$

and substituting for K from expressions (9) and (11) gives

For sinusoidal eccentricity (axial load)

$$R_c + \frac{R_b}{1 - \frac{P}{P_E}} = 1 \qquad \text{.....(15)}$$

For constant eccentricity (eccentric load)

$$R_c + \frac{R_b}{\text{Cos}\,\frac{\pi}{2}\sqrt{\frac{P}{P_E}}} = 1 \qquad \text{.....(16)}$$

In his earlier work Shanley used the slenderness ratio $\frac{L}{r}$ as a parameter for establishing interaction curves. This had limitations and did not seem to be correct as a

normalising basis, which resulted in the parameter $= \frac{P_o}{P_E} = \frac{f_o}{f_E}$ being introduced in 1954. This "buckling ratio" is defined for a column as the ratio between the actual column failing load and the theoretical Euler load. It provides for inelastic effects and local buckling.

Substitute $P_E = \frac{P_o}{\eta}$ in expression (15)

This gives $R_C + \frac{1}{1 - \eta \left(\frac{P}{P_o}\right)} R_b = 1.$

Solving for R_b and replacing $\frac{P}{P_o}$ by R_c gives the following interaction expression for sinusoidal primary bending moment.

$$R_b = (1 - R_c)(1 - \eta R_c) \qquad .....(17)$$

Similarly, when the primary bending moment is constant, substitution in expression (16) gives

$$R_b = (1 - R_c) \operatorname{Cos} \left(\frac{\pi}{2} \sqrt{\eta R_c}\right) \qquad .....(18)$$

Expressions (17) and (18) enable the appropriate interaction curves for both axial and eccentric end loaded struts to be plotted.

If required for the cases of eccentric loading, provision can also be made on the interaction curve charts for varying degrees of eccentricity. Because M = Pe a

straight line running through the origin of a dimensional interaction curve would represent a certain eccentricity e. This can be represented on the normalised interaction curve charts by an "eccentricity ratio" which is established as follows:

$$R_e \equiv \frac{R_b}{R_c} \equiv \frac{\frac{M}{M_o}}{\frac{P}{P_o}}$$

as $M = P_e \qquad e = \frac{M}{P}$

$$\therefore R_e = \frac{e}{\frac{M_o}{P_o}} \quad \text{or} \quad R_e = \frac{e}{e_o} \qquad \text{.....(19)}$$

where e = eccentricity of END load with respect to N.A. of Cross Section

e_o = base value of eccentricity $\frac{M_o}{P_o}$

By replacing M_o by $f_{bo}Z$ and P_o by $f_{ao}A$

Then base eccentricity $e_o = \frac{f_{bo}}{f_{co}} \frac{Z}{A} = \frac{f_{bo}}{f_{co}} r_c$

$$\therefore R_e = \frac{e}{r_c} \frac{f_{co}}{f_{bo}}$$

where f_{co} and f_{bo} are the failure stresses in pure compression and pure bending respectively.

When $f_{co} = f_{bo}$ the base eccentricity will be the core radius and $R_e = \frac{e}{r_c}$.

Note:- The core is defined as that part of the cross section within which an axial force can be applied WITHOUT causing a stress of opposite sign at any point.

The core radius is that value of eccentricity, along a principal axis at which the stress on the opposite edge becomes zero.

We know that $f_{min} = \frac{P}{A} - \frac{Pe}{Z} = \frac{P}{A}\left(1 - \frac{eA}{Z}\right)$ .....(20)

By definition the core radius at fmin must be zero. Making this substitution in (20) and solving for e gives $r_c = \frac{Z}{A}$.

The calculation of the necessary theoretical values for the construction of charts can now proceed.

4.4 Theoretical Calculations

Having described the "Interaction Method" and established the theory for the basic interaction charts it is now necessary to calculate the base or critical values for axial load and bending moment. Local and torsional buckling will also be considered. The theory used will be that generally recognised as the most accurate available for battened struts at this time.

(a) Axial Load

The Euler expression for buckling $PE = \frac{\pi^2 EI}{L^2}$ forms the basis of much of the existing knowledge. Values

for Euler crippling will therefore first be established.

Referring to the section properties given in Chapter 3 and Fig. 18 Chapter 6, the buckling figures are -

For buckling on the x-x axis (weaker axis, parallel to battens)

$$P_E = \frac{\pi^2 EIx}{L^2} = \frac{\pi^2 \times 68\ 700 \times 609.36 \times 10^4}{3657.6^2 \times 10^3} = 309 \text{ kN}$$

(30.9 ton)

For buckling on the y-y axis (stronger axis, at $R^T\angle^S$ to battens)

$$P_E = \frac{\pi^2 EIy}{L^2} = \frac{\pi^2 \times 68\ 700 \times 1179.6 \times 10^4}{3657.6^2 \times 10^3} = 598 \text{ kN}$$

(59.8 ton)

In both cases length L is to the centres of ball seatings.

The foregoing calculations are based upon the assumption that the strut is homogeneous. With battened struts the batten rigidity is vitally important and where this is small the actual critical load will be much lower than that predicted by Euler's expression.

Timoshenko[63] offers an expression for overall column buckling which is based upon Euler and takes into account the bending of the battens themselves. It assumes the battens are rigidly attached, which can only be achieved by welding, and there is no adjustment of the effective to actual lengths between the batten centres. The expression is

$$P_{crit} = \frac{\pi^2 EI}{L^2} \cdot \frac{1}{1 + \frac{\pi^2 EI}{L^2}\left(\frac{ab}{12EI_b} + \frac{a^2}{24EI_c} + \frac{na}{bA_bG}\right)} \quad ..(1)$$

where a = distance, centres of battens

b = distance, between centoids of main members

A_b = cross sectional area of two opposite battens

n = numerical factor, depending on cross sectional shape. Take as 1.2 for a rectangular cross section

G = shear modulus (modulus of rigidity)

I = relevant second moment of column section

I_b = second moment of area of two opposite battens in the direction of the axis of the strut and about an axis perpendicular to the strut axis.

I_c = second moment of area of one main member about the y-y axis

Euler symbols as previously.

The possibility of the channels buckling between the battens was also considered by Timoshenko. He assumed the batten rigidity to be large and submitted that the critical value of the compression force for buckling between batten centres was $\frac{2\pi^2 EI_c}{a^2}$ giving P_{crit} per main member at $\frac{\pi^2 EI_c}{a^2}$.

$$\therefore P_{crit\ (\text{per main member})} = \frac{\pi^2 \times 68{,}700 \times 59.20 \times 10^4}{a^2 \times 10^3} \quad \ldots(2)$$

$$= \text{See table for various values of "a".}$$

Koenigsberger and Mohsin[54] found Timoshenko's expressions in good agreement with their test results, when the batten centre distance was modified to 0.85a.

The P_{crit} values for a single member between battens, assuming the struts were <u>axially</u> loaded, will need to be established for the various batten spacings adopted in the tests. This is necessary to ascertain the base or critical value for an axial load acting on its own. The following Fig.11 indicates the critical values for this type of failure in the tests planned. Comparisons have been given between the Timoshenko and the Koenigsberger & Mohsin predictions using the batten spacings which will exist at, or adjacent to, the mid height of the struts.

FIG. 11

Column Buckling of Individual Main Member between Battens for Axial Load only								
Test No's	Strut Mk	Ultimate Type of Loading	1 Timoshenko."a" as actual distance centres of battens	2 Konigsberger,Mohsin. "a" as 0.85 distance centres of battens	P_{crit} for 1		P_{crit} for 2	
					kN	Ton	kN	Ton
1 and 2	S1	Eccentric	863.5 mm	734 mm	537	53.7	746	74.6
3 and 4	S3	Eccentric	1218.5	1036	270	27	374	37.4
5 and 6	S2	Axial	1041.5	885	370	37	512	51.2
7 and 10	S5	Eccentric	1218.5	1036	270	27	374	37.4
8 and 9	S4	Eccentric	863.5	734	537	53.7	746	74.6

NOTE For Tests 1 to 6 incl. Battens occur at mid-height of strut)
For Tests 7 to 10 incl. Battens straddle mid-height location)

See Figs. 29 and 30 also 39 and 43 inclusive

It will be observed that all critical loads, except those for Tests 3, 4, 7 and 10, using Timoshenko's expression, exceed the local buckling test failure load of 342 kN (34.2 ton) and 310 kN (31 ton) overall column buckling given in Chapter 6.

Theoretical failure loads for overall column buckling, under axial load, assuming buckling in the plane of the battens still needs to be established in accordance with Timoshenko's expression (1) modified to account for buckling between the battens and with the adjusted effective batten centres argued by Konigsberger and Mohsin.

The expressions then become,

For Timoshenko -

$$P_{crit} = \frac{\pi^2 EI}{L^2} \cdot \frac{1}{1 + \frac{2EI}{L^2}\frac{ab}{12EI_b} + \frac{a^2}{24EI_c}\cdot\frac{1}{(1-\alpha)} + \frac{n_a}{bAbG}} \quad \ldots (3)$$

For Konigsberger & Mohsin

$$P_{crit} = \frac{\pi^2 EI}{L^2} \cdot \frac{1}{1 + \frac{\pi^2 EI}{L^2}\frac{0.85ab}{12EI_b} + \frac{(0.85a)^2}{24EI_c(1-\alpha)} + \frac{n(0.85a)}{bA_bG}} \quad \ldots (4)$$

where $\alpha = \dfrac{P_{crit}}{\dfrac{2\pi^2 EI_c}{a^2}}$

$n = 1.2$

$$\text{and } G = \frac{E}{2(1+\gamma)} \qquad \gamma = \text{Poisson's ratio}$$

$$= .33 \text{ (for Al-Zn-Mg)}$$

$$\therefore G = \frac{68,700}{2(1+.33)} \qquad = 25,750 \text{ N/mm}^2.$$

It will be noticed that the expression for α contains P_{crit}. Equations (3) and (4) can therefore only be solved by a trial and error method.

Fig. 12 gives P_{crit} values for overall column buckling using expressions (3) and (4) for the Test numbers and batten spacings as given previously.

It will be observed that none of the critical loads reach the local buckling loads or the loads for column buckling of an individual channel calculated earlier. Those calculated using Konigsberger and Mohsin's expression, approach the local buckling figure when the battens are spaced at the code maximum of 863.5 x 0.85 = 734 mm. Indications therefore are that with axial load only the struts being tested, will fail by overall column buckling in all cases where the batten spacing has been increased beyond this figure but local buckling could be critical for the struts Mk S1 and S4.

The reduction in load carrying capacity at the enlarged batten spacings is much more than the author would have expected. It remains for the

FIG. 12

Column Buckling of Complete Strut between Ball Seats for Axial Load Only.
Assuming Buckling in the Plain of the Battens.

Test No's	Strut Mk	Ultimate type of loading	1 Timoshenko. "a" as actual distance centres of battens	2 Konigsberger, Mohsin. "a" as 0.85 distance centres of battens	P_{crit} for 1		P_{crit} for 2	
					kN	Ton	kN	Ton
1 and 2	S1	Eccentric	863.5 mm	734 mm	267	26.7	310	31.0
3 and 4	S3	Eccentric	1218.5	1036	154	15.4	214	21.4
5 and 6	S2	Axial	1041.5	885	212	21.2	273	27.3
7 and 10	S5	Eccentric	1218.5	1036	154	15.4	214	21.4
8 and 9	S4	Eccentric	863.5	734	267	26.7	310	31.0

tests to confirm or dispute this view.

(b) Bending Moment

The critical pure bending moment $M_{crit} = M_o$ was required as a base value for the interaction expressions. This will be established theoretically in what follows, using data from Chapter 3.

The author would have preferred to confirm any theoretical solutions for M_{crit} by practical testing. This, alas, was not possible, due to the extreme difficulties of simulating the ball end arrangement for a beam, and providing a suitable method of end moment application. Any arrangement developed to perform this duty satisfactorily, is difficult to visualise, particularly with a battened member. To be effective, the moment must be applied at the ends by equipment which would provide no end thrust, have a ball seat freedom and adjust laterally as the beam deflects.

Theoretical values for M_o will therefore be calculated, and a value chosen after all the factors involved have been considered.

Knowing that $M_{crit} = M_o = fb_{crit} \frac{I}{y}$ .....(4)

Then from sectional properties - Fig. 18 (Chapter 6)

$$M_o = \frac{fb_{crit} \times 1179.6 \times 10^4}{89} \quad .....(5)$$

The problem is to establish a realistic value for f_{bcr}. If the strut, working as a beam only, had adequate lateral restraint f_{bcr} would be either the maximum value of 391 N/mm^2 (25.3 ton/in^2), or, as could happen in this case, probably be controlled by local buckling as explained and applied in Chapters 3 and 6 respectively.

Reference forward to Chapter 6 will show the average local buckling failure stress to be between 283 N/mm^2 and 292 N/mm^2 (18.3 to 18.8 ton/in^2). It should however probably be argued that as the strut is, at this stage, being considered in pure bending, the extreme fibres at the back of the web of the channel in compression would be the most highly stressed. If this is accepted, the value adopted should be that calculated for the web element alone (Chapter 6) at a maximum local buckling stress of 318 N/mm^2 (20.5 ton/in^2).

However, the lateral instability of the strut, working purely as a beam and unrestrained between its theoretical ball ends, has yet to be considered. This may well be the criterion and dictate the stress to be adopted for the evaluation of $M_{crit} = M_o$.

For a member of the battened strut configuration the lateral instability problem is particularly difficult and the precision of the solution

questionable. The difficulty lies in assessing how much lateral restraint the channel in TENSION will provide to the channel in compression and wanting to buckle laterally. Any restraining influence would need to be transmitted VIA THE BATTENS which are generally weak in this direction and would bend relatively easily. Battens are also only an intermittent restraint.

As a first calculation the battens are considered as "stiff" and the composite section assumed as a homogeneous unit.

For a doubly symmetrical section CP 118 provides a suitable expression for λ lat given in Clause 4.4.4.2 by

$$\lambda \text{ lat} = 2.3 \left[\frac{I_y (I_y - I_x)}{JI_x}\right]^{\frac{1}{4}} \left(\frac{\ell_f}{y}\right)^{\frac{1}{2}} \quad ..(6)$$

where I_y and I_x = second moments of area about the major and minor axes.

J = torsion factor

ℓ_f = effective length between lateral restraints

y = distance from N.A. to extreme compression fibres

(NOTE I_y and I_x reversed to suit earlier configuration.)

It will be observed that the expression (6) includes for a torsional factor J. This is because a long slender beam may well fail by a combination of torsion and lateral bending.

Calculating J

This will be established in the usual way, by dividing the cross sectional profile into component parts.

The general approach is given in CP 118 (1969) Appendix F; and Fig. 26 of this appendix dictates the extent of the fillet regions to be added to the remaining thin walled, rectangular parts.

The sketch below gives the dimensions of the parts for a given thickness t. For the profile given, the factor N = 2

$\therefore$ when t = 3.97 mm:

Nt = 7.94 mm (N+2)t = 15.88 mm (N+1)t = 11.91 mm

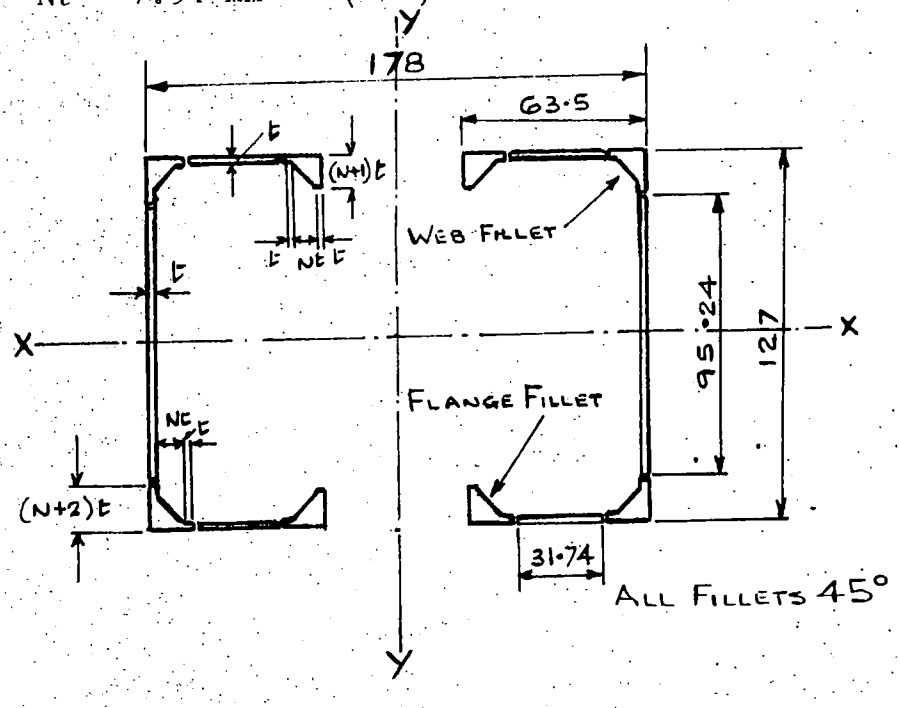

Flange Fillets (4)

$J_1 = \left((p + qn)t\right)^4$ where p and q are empirical constants.

From Fig. 26 p = 0.83 q = 0.39.

$\therefore J_1 = \left((0.83 + 0.39 \times 2)3.97\right)^4$

$= 1670 \times 4$ fillets $= \underline{6680\ mm^4}$

Web Fillets (4)

From Code Fig. 26 p = 0.86 q = 0.39

$J_2 = \left((0.86 + 0.39 \times 2)3.97\right)^4$

$= 1790 \times 4$ fillets $= \underline{7160\ mm^4}$

Flats forming Webs and Flanges

$J_3 = \sum \frac{bt^3}{3} = (2 \times 95.24 + 4 \times 31.74)\ \frac{3.97^3}{3} = \underline{6620\ mm^4}$

Establishing f_{bcr} (for lateral instability)

From expression (6)

$$\lambda \text{ lat} = 2.3 \left[\frac{1179.6\ (1179.6 - 609.36)}{2.04 \times 609.36}\right]^{\frac{1}{4}} \left(\frac{\ell f}{8.9}\right)^{\frac{1}{2}}$$

The value of ℓf is given by $\ell f = k_1 k_2 L$ with values for k_1 and k_2 taken from CP 118, Tables 9 and 10.

Then $k_1 = 1.2$. $k_2 = (0.6 + 0.4) = 1$

and $\ell f = 1.2 \times 1.0 \times 3657.0 = 4390$ mm (440 cm)

NOTE:- k_1 has been taken at 1.2, but this value is possibly suspect, as the ball ends give negligible restraint against twisting. The code also accepts that battens are spaced equally.

Then $\lambda_{lat} = 2.3 \left[\frac{1179.6\ (570.24)}{1243}\right]^{\frac{1}{4}} \left(\frac{440}{8.9}\right)^{\frac{1}{2}}$

$= 2.3 \times 4.82 \times 7.02$

$= \underline{78}$

From Fig. 4 (Chapter 3) $f_{bcr} = \underline{112\ N/mm^2}$ ($7.25\ ^T/in^2$)

Then from expression (5)

$M_{crit} = M_o = \frac{112 \times 1179.6 \times 10^4}{89} = \underline{1490 \times 10^4\ Nmm}$ (59ton in)

As a check, an approach discussed by Venkatraman and Patel[64] was then used, involving the expression

$$M_{crit} = \frac{\pi}{L}\sqrt{EI_xGJ} \qquad \ldots\ldots(7)$$

where I_x is the second moment of area about the weaker laterally unstable axis, at right angles to the plane of bending.

Expression (7) was developed for a pin ended beam subjected to equal end moments. The selected cross section was described as a solid, narrow rectangle, but the degree of narrowness was not defined.

However, the test struts are at present being considered as "stiff homogeneous" units. It therefore appears acceptable to use this expression as a check.

Then from expression (7)

$$M_{crit} = \frac{\pi}{3657}\sqrt{68{,}700 \times (609.36 \times 10^4) \times 25750 \times 20460}$$

$$M_{crit} = M_o = \underline{1263 \times 10^4 \text{ Nmm}} \quad (49.9 \text{ Ton in})$$

Then the crippling stress f_{bc} given by expressions (5) and (7) is

$$f_{bc} r = \frac{M_y}{I}$$

$$= \frac{1263 \times 10^4 \times 89}{1179.6 \times 10^4} = 96 \text{ N/mm}^2 \text{ for (5)}$$

$$(6.25 \text{ Ton/in}^2)$$

A rough interaction curve check, using the foregoing values, immediately indicated that the approach was not suitable. For the struts to be tested, lateral instability of the channel carrying the most compression still seemed a possibility. (See Note Page 118)

It was therefore assumed that the battens had virtually no lateral stiffness and that failure in pure bending would result from the lateral instability of the compression channel with <u>NO</u> lateral restraint. This would give a condition of <u>no torsion</u> as the channels

would move sideways relative to one another causing the battens to buckle or even fail thus:-

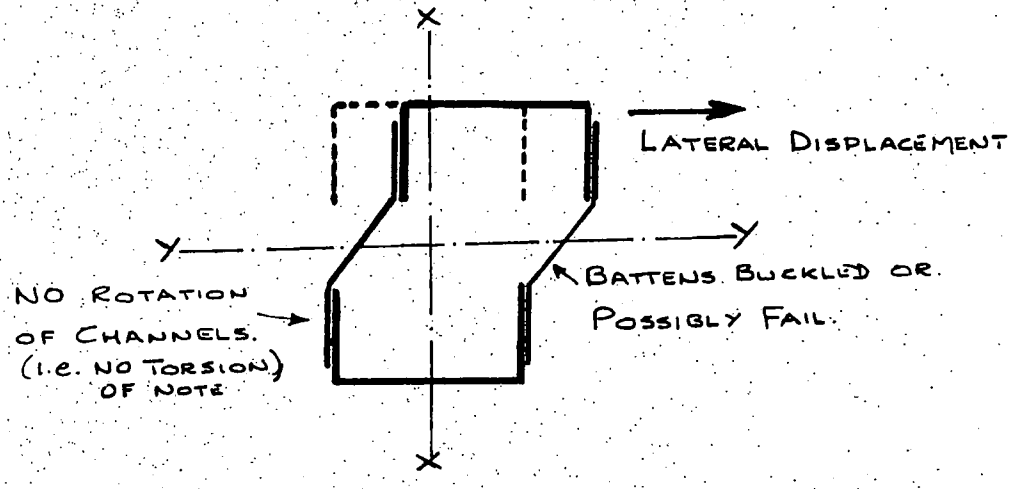

Assuming that the critical value of M_o would exist at onset of plasticity and considering the channel on the "compression" side of the strut to yield as a unit

$$M_o = f_y A_c d \qquad \ldots(8)$$

where f_y = stress at the appropriate slenderness ratio (Fig. 4 Chapter 3).

A_c = area of ONE channel

d = distance between centroids of the pair of channels

$$\frac{L}{ry} = \frac{3657}{5.13 \times 10} = 71.5 \quad \therefore \quad \text{lat} f_y = 136.0 \text{ N/mm}^2.$$

$$\therefore M_o = 136 \times 11.67 \times 10^2 \times 134.4$$

$$= \underline{2133 \times 10^4 \text{ Nmm}}$$

This occurs at f_{bcr} values of 136 N/mm^2. (8.6 ton/in^2).

NOTE:

Comparison between solutions to expressions (6) (7) and (8) highlights an anomaly. It is not reasonable that a "stiff" homogeneous section would carry less moment. Beyond proportionality limit the moment arm of the couple will approximate to the centroids of the channels. If an adjustment is made for this and the value for K_1 is now taken as 1.0 the solution to expression (6) is satisfactory. Expression (7) only has limited analogy and will not be pursued. Knowing the values of actual strain readings expression (9) appears to be correct. The reasoning is logical. M_o will therefore be taken at 21330×10^4 Nmm in all subsequent calculations.

All theoretical values necessary for the establishment of the deflection and interaction curves have now been resolved. Tables giving the results to the lengthy computations involved are included in Chapter 8, covering the "Testing and Comparison of Theoretical and Test Results". An appraisal of the strain gauge readingswill also be dealt with in the same chapter.

Chapter 5

The Testing Rig

5.1 General Considerations

Ideally struts should be tested vertically using a robust rig located over a pit. Such an arrangement enables members being tested to be longer than the legs of the testing frame, and thus reduces any tendency for the frame to move laterally, under load. This ideal was unfortunately not possible for this work.

No strut testing of note had previously been undertaken at Teesside Polytechnic and the first requirement was to develop, and construct, a suitable rig. Space limitation dictated the basic requirement of portability. The work would need to be carried out on a limited budget and careful consideration given to providing a versatile piece of equipment, which would not only be suitable for this research programme, but capable of testing struts of varying type and length, in the future. Any suitable existing equipment would need to be adapted and incorporated wherever possible. The optimum aims would therefore be, an arrangement enabling struts ranging in length from the very minimum to the maximum permitted by the laboratory headroom to be tested, at the maximum permitted load.

5.2 Existing Equipment

The level floor of the heavy structures laboratory has

built-in loading sockets located at 18 in centres on an equalateral triangle pattern. Each socket is capable of sustaining a 15 ton pull through $1\frac{3}{8}$ in diameter studs.

A series of Samual Dennison hydraulic jacks existed as standard laboratory equipment. These are capable of exerting maximum thrusts ranging from 10 ton to 100 ton, when coupled to the complementary control console and pump unit. The loading control of the system is delicate and the console is fitted with a loading dial graduated in increments of 0.02 ton. The 50 ton jack was chosen as the most suitable for the universal testing envisaged and its comparatively delicate control was quite satisfactory. If the jack were to be faulted, it would be on account of its heavy construction and consequent size, which will directly affect the length available for the test specimens. This will need to be accepted. Some form of "Guide Box" was required to prevent the jack from "kicking" sideways under load, as the load transmitting flanges at both ends of the jack are ball seated.

A survey of the laboratory's heavy framework equipment indicated that the existing "Straining Frame" legs together with the heavy double channel cross beam would, if suitably developed, be ideal to form the basic items of the main rig framework. The legs are of exceptionally robust, welded box construction, and

provided with holes for large diameter shear pins, at 12 in intervals, along the major part of their length. Each leg is capable of sustaining a working tensile pull of 30 tons through studs located in the floor loading sockets. The top cross beam, being attached to the legs through a single centrally located shear pin at each end, would not promote end moments and sway under load would be unlikely.

By utilising the existing equipment described and developing a "Guide Box" with "Guide Channels" and a "Thrust Box", all of which are subsequently described, a rig was produced capable of exerting thrusts of up to 50 tons on strut specimens of any desired cross sectional profile. Full use was made of the laboratory headroom available and struts ranging in length from 12 in to 12 ft in increments of 12 in can now be tested. A very versatile strut testing rig as shown in Fig. 13 Plate 4 is now available as standard laboratory equipment. The fact that the assembly is portable is an added attraction.

5.3 New Components - Design and Fabrication

The function, design and fabrication of the new components, necessary to the rig, are now described. All work was undertaken in the Polytechnic workshops.

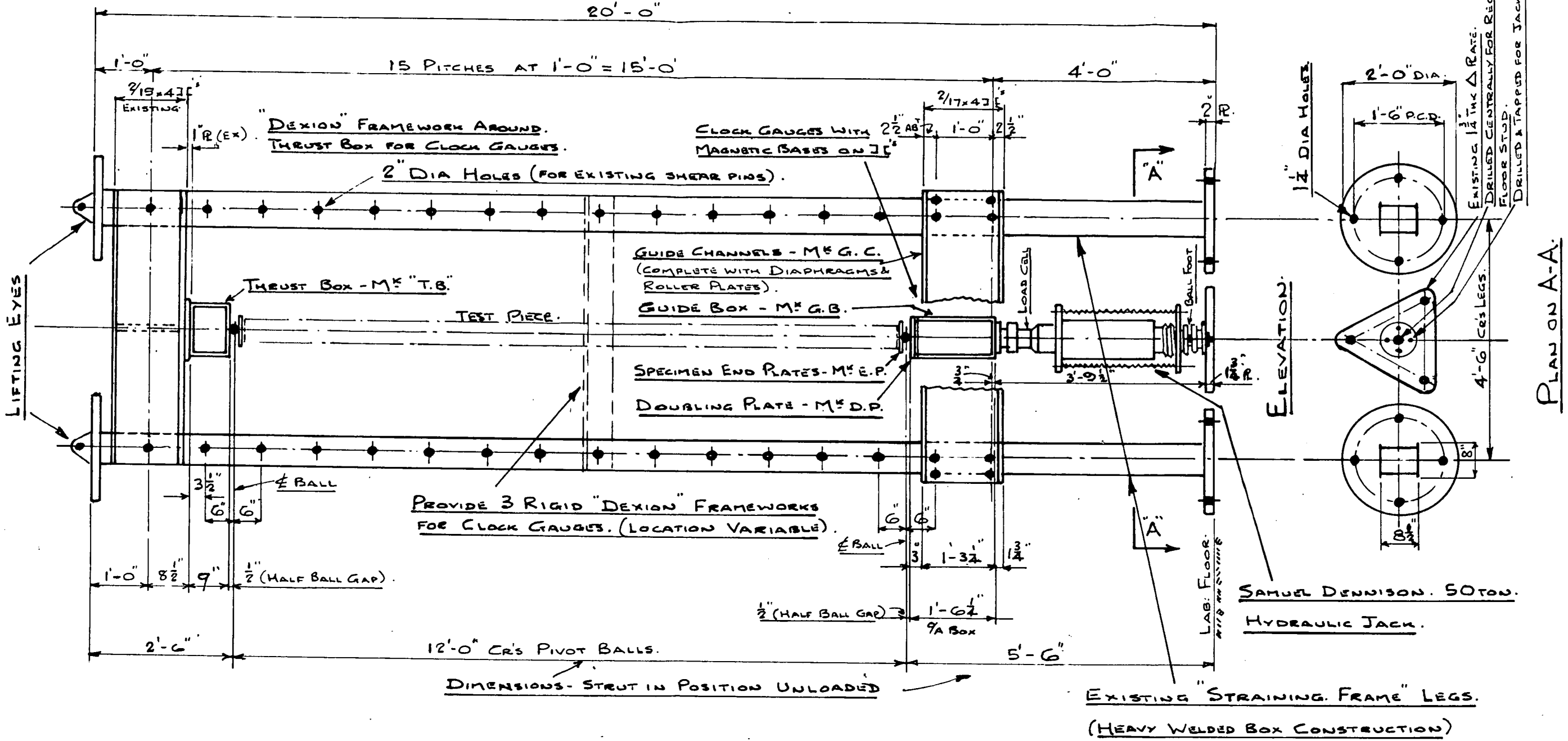

—GENERAL ARRANGEMENT OF TEST RIG.—

FIG:- 13

SCALE: ½" = 1 FT

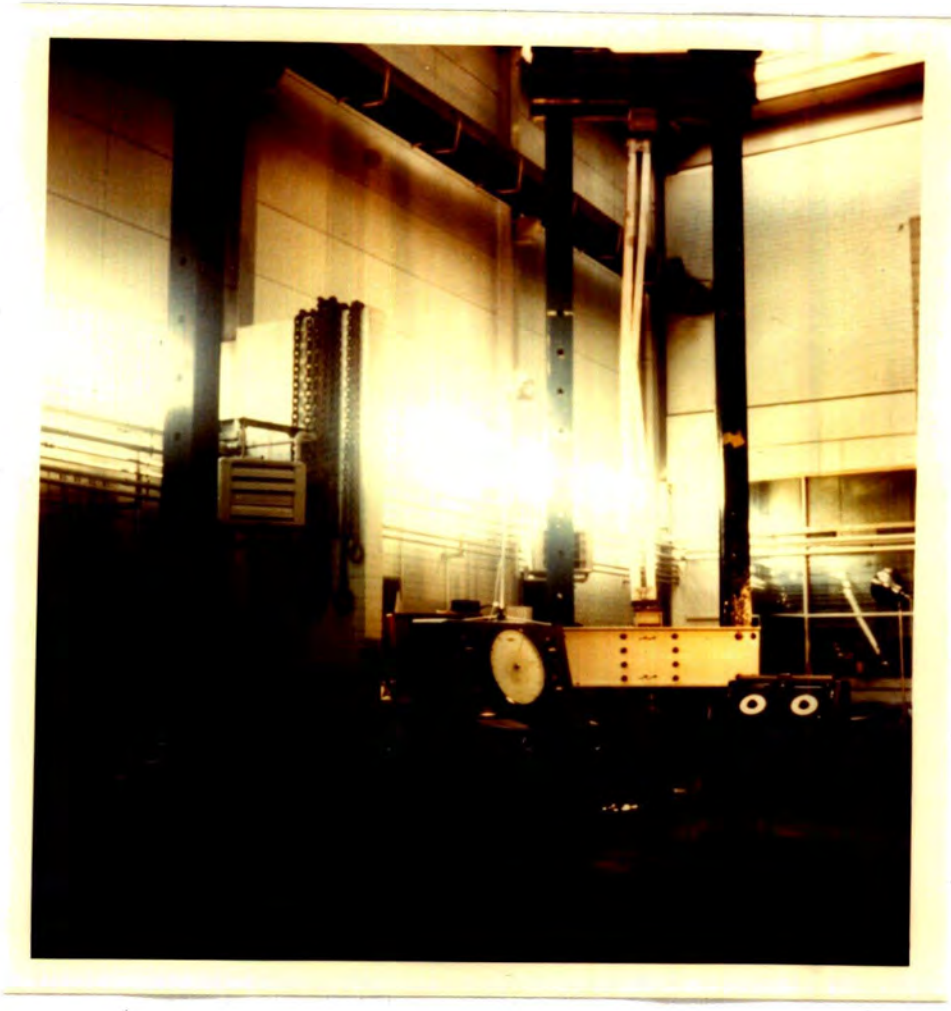

The Testing Rig

PLATE 4

(a) Guide Box Fig. 14 Plate 5

The basic requirement for this unit was to transmit longitudinal thrusts of up to 50 tons from the hydraulic jack, through a ball seating to the test specimen.

In performing this duty the box must hold the ball ended jack in a precisely vertical position throughout the length of its travel. As the test strut bows and shortens under load the ball seating between the strut and the top of the guide box must move in a precisely vertical plane throughout the whole vertical travel of the box. This must all be achieved with the absolute minimum of frictional drag at the guide wheels if the recorded thrust is to be transmitted fully to the strut under test.

The concept of the guide box was developed in conjunction with that of the guide channels, later described, and resulted in the provision of a rigidly constructed box housing ten guide wheels as shown in Fig. 14 . The idea of three wheels on opposing sides of the box was implemented so that the two upper wheels could be located in the same horizontal plane. This ensured the box remained precisely square within the adjustable roller plates. One further wheel only, at a lower level, was used on these two sides, thus ensuring even

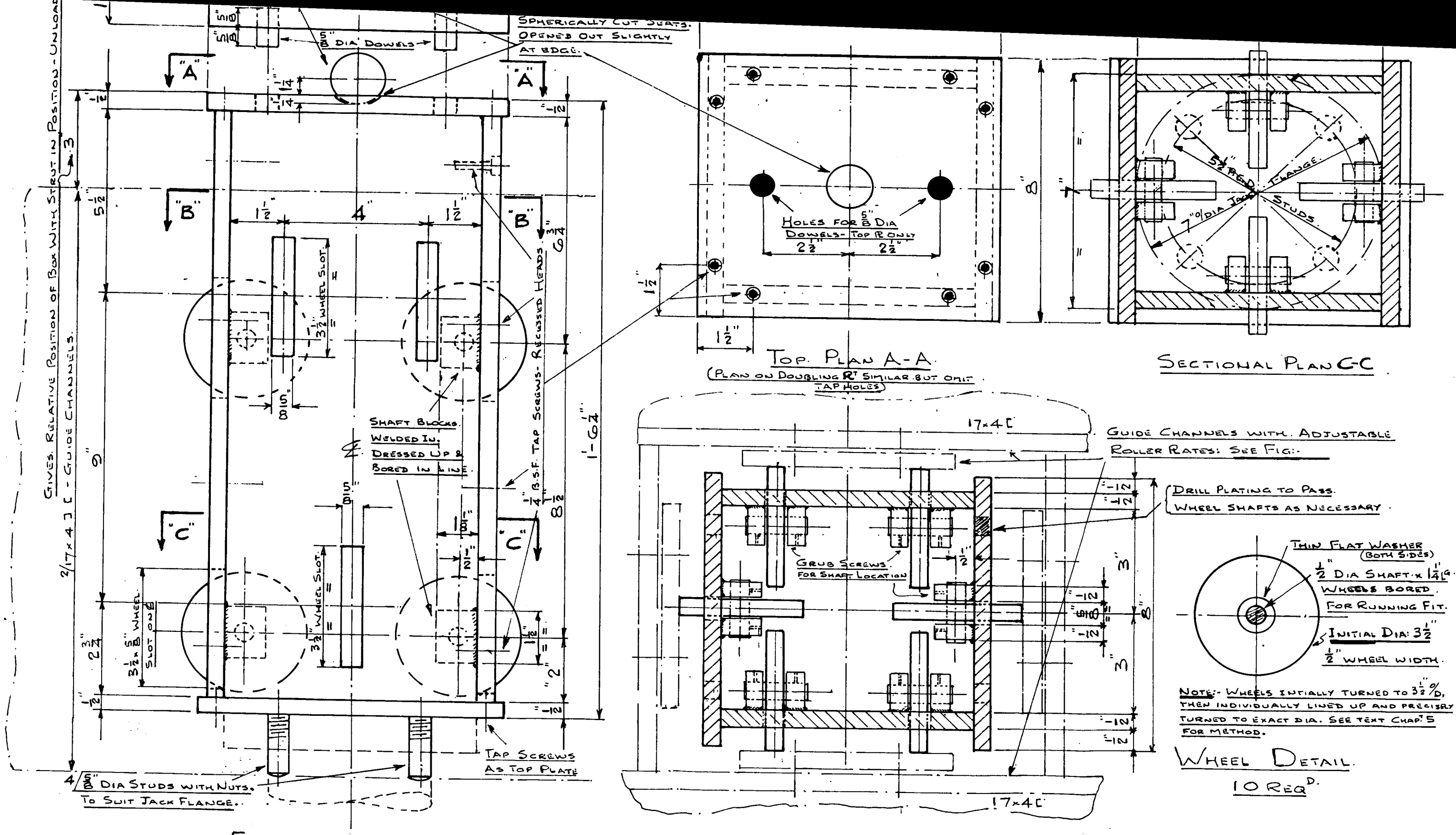
GIVES RELATIVE POSITION OF BOX WITH STRUT IN POSITION - UNLOADED
2 [17 x 42 C - GUIDE CHANNELS.
4 5/8" DIA STUDS WITH NUTS. TO SUIT JACK FLANGE.
5/8" DIA DOWELS
SPHERICALLY CUT SEATS. OPENED OUT SLIGHTLY AT EDGE.
SHAFT BLOCKS WELDED IN. DRESSED UP & BORED IN LINE.
1/4" B.S.F. TAP SCREWS - RECESSED HEADS
TAP SCREWS AS TOP PLATE
3 1/2" WHEEL SLOT
3 1/2" x 5" WHEEL SLOT OVAL
HOLES FOR 5/8" DIA DOWELS - TOP R ONLY
5 1/2" PCD
7" DIA JACK STUDS
FLANGE
TOP PLAN A-A
(PLAN ON DOUBLING R^T SIMILAR BUT OMIT TAP HOLES)
SECTIONAL PLAN C-C
17 x 42 C
GRUB SCREWS FOR SHAFT LOCATION
GUIDE CHANNELS WITH ADJUSTABLE ROLLER RATES: SEE FIG:-
DRILL PLATING TO PASS WHEEL SHAFTS AS NECESSARY
THIN FLAT WASHER (BOTH SIDES)
1/2" DIA SHAFT x 1 1/4" LG
WHEELS BORED FOR RUNNING FIT.
INITIAL DIA: 3 1/2"
1/2" WHEEL WIDTH.
NOTE:- WHEELS INITIALLY TURNED TO 3 1/2" % D, THEN INDIVIDUALLY LINED UP AND PRECISELY TURNED TO EXACT DIA. SEE TEXT CHAP^T 5 FOR METHOD.
WHEEL DETAIL
10 REQ^D.

Guide Box
without
Doubling Plate

Doubling Plate

PLATE 5

wheel seating on the roller plates which would not have been possible had four wheels been adopted. The remaining sides were furnished with two wheels each, located on the vertical centre line towards the ends of the box.

The height of the box was made as large as possible consistent with the guide channel and roller plate depth, the vertical movement of the box when testing, and the practical difficulty of fitting the wheels onto their respective shafts. All wheels were spaced as far apart as practicable to minimise, however slight, any tendency for the box to "tilt" under load. A condition brought about by the fact that the jack was ball jointed and that horizontal force would exist at the ball seating under the strut.

Deformation of the box under load could not be tolerated if the guide wheel system was to operate satisfactorily. Rigidity therefore controlled the design and $\frac{1}{2}$ in thick mild steel plate was adopted throughout. All side plates were milled true and square on all edges, and mating surfaces. End plates were similarly milled, before their faces were surface ground. After the cutting of the guide wheel slots and the fitting, boring, and tapping of the wheel

shaft blocks, the plates were carefully assembled using accurately positioned, Allan key headed tap screws. This ensured tight fitting of the mating surfaces. Internal tie/strut bolts were then positioned to minimise any possible deflection of the box sides under load. By exercising extreme care throughout all stages of manufacture, the technique adopted produced a box into which the guide wheels could be precisely fitted.

The assembly, with top plate removed, was now set up on a plane table. This provided a datum for the exact alignment of the guide wheels and ensured their complete squareness with the end plates. Each wheel was turned and fitted individually to override any irregularities in the mild steel box sides. By this means accuracy to within 0.002 to 0.003 in was achieved for the wheel locations.

Except for small test loads, the $\frac{1}{2}$ in thick box top would need to be reinforced. This was necessary to combat deflection, punching shear at the ball seating and to distribute the load properly to the box sides. It was not possible to reinforce internally due to guide wheels etc., and a doubling plate was therefore needed. This was made $1\frac{1}{2}$ in thick and surface ground, thus

ensuring even load distribution, minimal deflection and an acceptable bearing stress at the ball seat. Both the guide box top plate and the doubling plate were provided with centrally located, spherically cut, ball seats suitable for a $1\frac{1}{2}$ in diameter bright steel ball. The seatings were slightly enlarged at their periphery, to minimise any frictional grip on the ball, but not to such an extent that its central location was affected. Lubrication of the ball seatings is described later. Locating dowels attach the doubling plate to the box top plate.

A 50 ton test load was applied to the completed box in an Avery compression testing machine. Deflections and distortions were checked and the results assessed as completely satisfactory.

(b) Guide Channels Fig:- 15 Plate 4

A positive yet finely adjustable location for the guide box at its working position in the rig defined the requirement. This was achieved using heavy bridging channels, suitably diaphragmed, between the main legs of the rig. The important "rigid" connection to the rig legs being made using large machined ferrules and long bolts with plannished, recessed, washers. Two bolt positions were used on each main leg, using the holes provided for the large shear pins. This

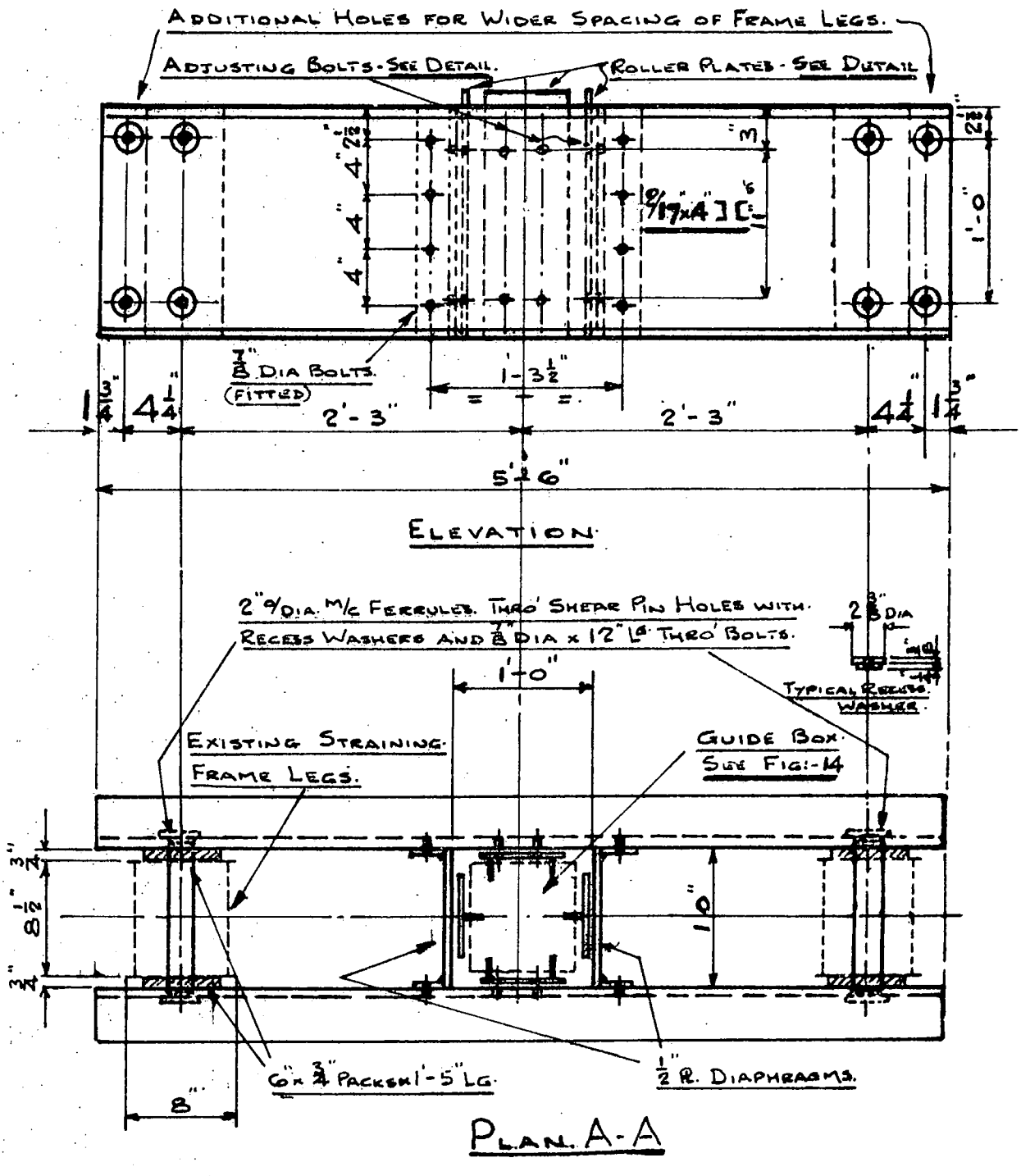

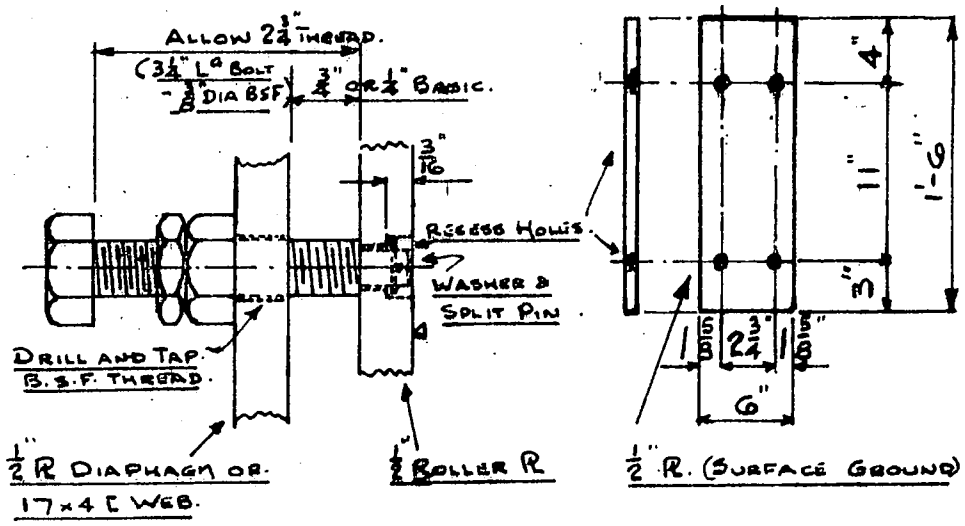

16 BOLTS THUS
(WITH NUTS)

4 ROLLER PLATES THUS.

1 SET OF GUIDE CHANNELS COMPLETE - Mk G.C.

FIG:- 15

system provided a completely rigid assembly into which the guide box could be positioned.

The fine adjustment, in any direction, necessary for the guide box was accomplished by using surface ground roller plates to mate with the guide box wheels. These were attached to the main guide channels and their diaphragms with finely threaded, adjustable, lock-nutted, studs. By this method it was easy to locate the guide box ball seat in its precise working position and ensure that the box was vertical throughout its length of travel with all the guide wheels just in contact with the roller plates.

All parts were investigated for strength and stiffness against lateral movement which could result from the horizontal thrust induced by the deflected strut under load.

(c) Thrust Box Fig:- 16 Plate 6

The function of the thrust box was to provide a positive location for the upper ball seat and act as a "make-up" piece to the existing double-channel cross beam. The depth of the box was fixed so that strut lengths could always be an exact number of feet, centre to centre of end balls, whichever shear pin holes were selected in the main legs.

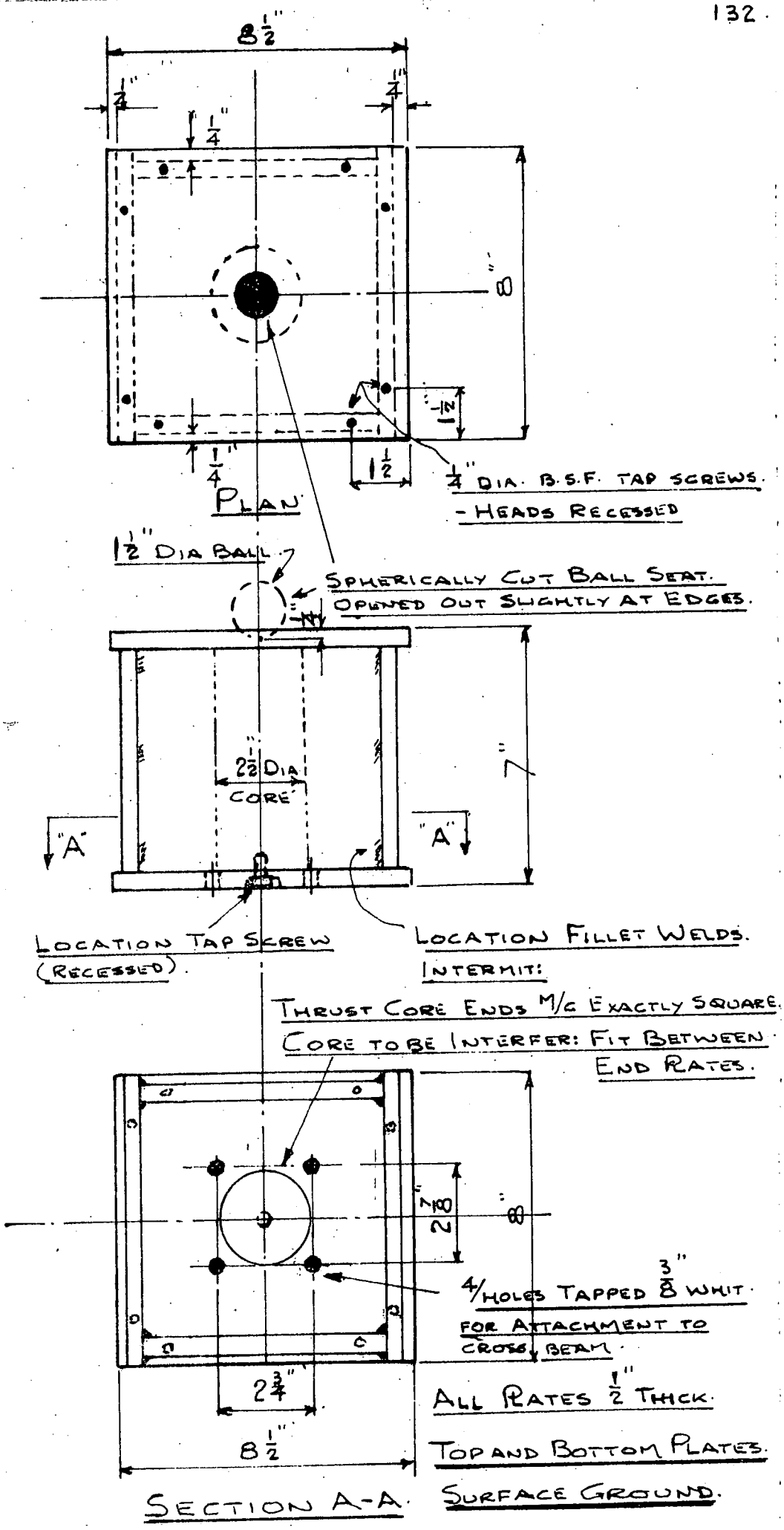

1 THRUST BOX REQ^D MK T.B.

FIG:- 16

Thrust Box

PLATE 6

Design and fabrication techniques employed for the side and end plates were precisely as for the guide box. The absence of guide wheels did however enable an internal thrust core to be inserted, obviating the need to use a $1\frac{1}{2}$ in thick doubling plate, as was necessary for the guide box. Mild steel plate $\frac{1}{2}$ in thick again formed the box. The core was a 2 in diameter bar exactly cut to length, and dead square thus ensuring it fitted tightly between the box end plates. It was located on the centre line of the ball seat by means of a tap screw at one end. This core ensured that the load was transmitted direct from the ball seating to the diaphragmed channels of the heavily constructed existing cross beam.

To ensure the exact verticality of the strut under test it was vital that the top and bottom ball seats were exactly in line. This was achieved by drilling and tapping a fine hole at the base of the thrust box ball seat for the suspension of a plumb line.

(d) Spreader Plate

A large $1\frac{3}{4}$ in thick triangular plate existed. This was modified for attachment of the bottom hydraulic jack flange and for positive location to a floor socket. A satisfactory arrangement for

spreading the load from the jack to the laboratory floor was thus provided.

(e) Strut End Plates Fig:- 17 Plate 7

After experimentation with other forms of end connection and ball seating arrangement for the strut specimens, the vital importance of positive location and complete rigidity became abundantly clear.

It was finally decided to provide surface ground steel plates $1\frac{1}{4}$ in thick which could satisfactorily accommodate the spherically cut ball seats at any desired location. These were to be attached to alloy end plates welded to the struts by close toleranced bolts. A central dowel was provided in the steel plates which would mate with a carefully positioned hole in the alloy end plates. The dowel was drilled and tapped on its longitudinal axis for a small eye bolt required to accept a length of spring tensioned nylon thread later described.

(f) Clock Gauge Frameworks

Rigid frames were fabricated from angle section dexian, bolted together. The frames were arranged to span between the main legs of the rig, to which they were attached, at the desired level,

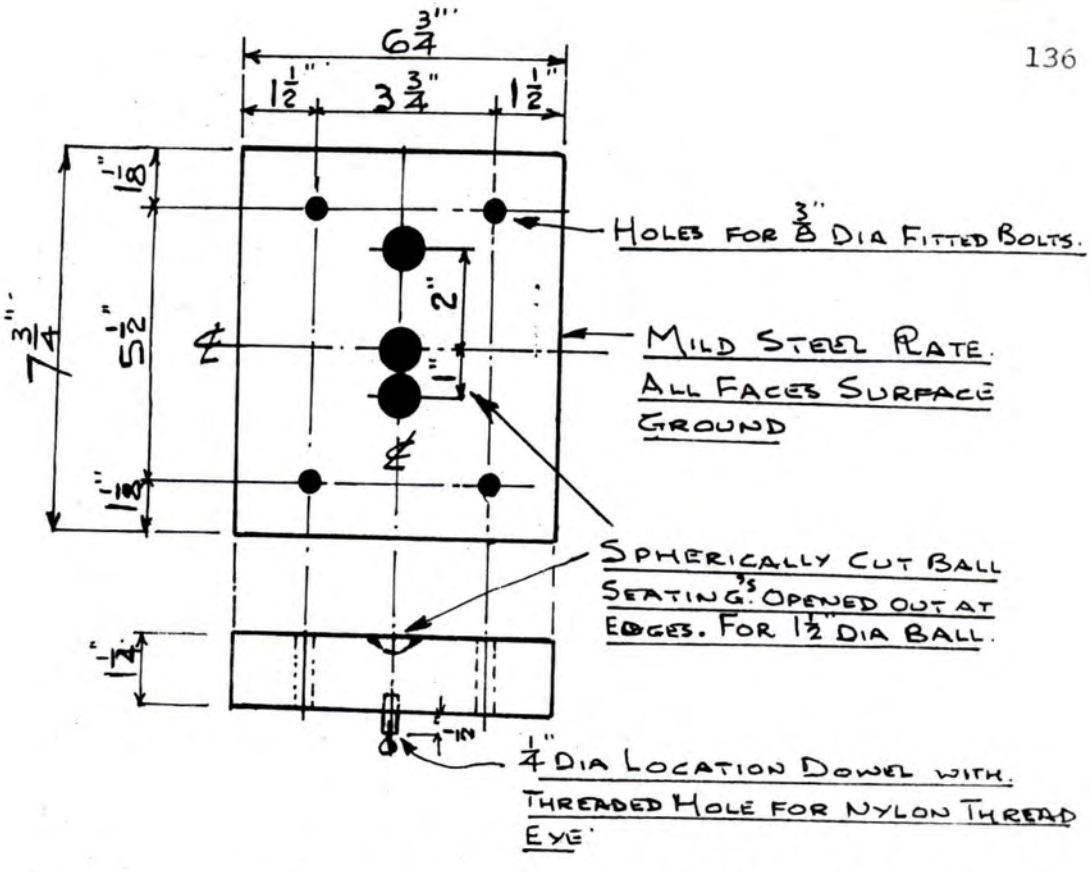

DETAIL OF STRUT END PLATES. MK S.P.-2 REQD.

Fig. 17

Strut End Plates

PLATE 7

by means of long bolts through the existing shear pin holes.

Clock gauge brackets were made from threaded rods, bent to the desired shape for the precise location of the gauges, at selected points on the strut.

5.4 Testing the Rig - (Plate 9)

The completed rig was fully tested under working load using an alloy battened strut similar to those planned for the research programme. All the important features were carefully scrutinised and such items as the guide box checked for freedom of movement and for any signs of lateral displacement or twisting.

The load output from the guide box to the specimen was checked against the input recorded on the jacking console, with the aid of a load cell interposed between the top of the guide box and the specimen. The load cell was coupled electrically to a Boulton & Paul "Transducer Unit". Plate 8

Deflections of the rig were checked with a theodolite and the data analysed in the light of what affect it might have upon the test results. Forward thinking on this problem proved adequate with the displacements occurring virtually as envisaged. The upward deflection

The "Boulton & Paul"
Transducer Unit

PLATE 8

Rig Proved to Strut Failure

PLATE 9

of the top cross beam did not induce movement of the legs and would not affect the data required on strut shortening under load, as this could be established from direct readings on the strut itself.

The function of the rig was assessed as a completely satisfactory alternative to the usually considered ideal, of a framework over a pit. In postulating over any "short comings" of the arrangement it could well be that the major problem still remains that of the degree of fixity existing at the ball seats.

Previous efforts to minimise this effect, whilst often ingenious, and sometimes elaborate, are not convincing. It is therefore argued that the key to the problem lies in the form of lubricant used and not in an elaborate mechanical contrivance.

For this reason ball seats which were spherically cut and then enlarged slightly at the periphery, to minimise the "frictional grip" of the ball in its seating, and yet provide a precise location, was the simple choice. If the new I.C.I. PTFE/silicone grease (Experimental Product 6225) is used in conjunction with this simple concept it may well be that the best solution so far, has been achieved.

E.P. 6225 is a silicone based compound incorporating a new grade of finely divided PTFE powder. It is in

the experimental stage and data are still being accumulated, but indications are that the product is an exceptionally effective lubricant under high load/slow speed conditions. It is an excellent anti-seize compound on metal parts subjected to high loads.

NOTE:- All work on the testing rig has been undertaken using Imperial Units. This was considered advisable where existing equipment required modification and the new components made to function with it.

Also, in the Autumn of 1969, when the rig was being fabricated, very little S.I. Workshop equipment was available.

Chapter 6

Specimen Selection, Design and Fabrication

6.1 Selection

The first requirement when researching into the behaviour of battened struts is that the component parts work as a homogeneous unit. To eliminate joint rotation and consequent early failure, welding was therefore essential.

To satisfy this requirement the choice of a high strength Al-Zn-Mg alloy was inevitable. Whilst still in the experimental stage, and not yet commercially available in the U.K., its exceptional strength properties after welding dictated its selection.

The form to be taken by the test struts was next carefully considered. Factors controlling the supply, design, fabrication techniques and test rig capacity, all contributing to the ultimate choice. The selection of sections likely to be used in practice, and for which dies existed, was also desirable. The profile finally chosen took the following form.

1. Standard 127 mm x 63.5 mm (5 in x $2\frac{1}{2}$ in) beaded channels would be used for the main longitudinal members. Factors dictating this choice being:-
   (a) Their load carrying capacity would make full use of the test rig.

(b) The 2:1 web to flange width ratio, usual with smaller standard channels, would correct a problem encountered by earlier researchers using pressed steel sections. They selected small flange widths which did little more than provide web edge reinforcement. This resulted in local failure between the battens, frequently in the end panel.

(c) The chosen section was thin walled and torsional instability was therefore possible.

(d) The flange beads would give improved performance against all forms of buckling.

2. Batten plates were used in pairs, spaced initially at the maximum distance apart permitted by the Code C.P. 118, 1969. Subsequent test struts had incremental increases in excess of this distance.

In some cases pairs of battens were located at the mid-height of the strut whilst with others this mid-height position was straddled.

Pairs of battens were provided at the ends of the main members ensuring composite action was maintained in the end panels. This is of vital importance.

3. Thin alloy end plates were selected for attachment to the ends of the strut to facilitate the precise location of the steel end plates carrying the ball seatings. Particulars of the alloy plates are given under 6.3 - Fabrication. The steel end plates are described in Chapter 5 and shown in Fig. 17 and Plate 7

4. Much consideration was given to the distance between the channels as the struts were to be subjected to both axial and eccentric end loading in the plane of the battens.

For axial loading the ideal would be to select a distance giving equal radii of gyration on both major axes. Tests with T.I.G. welding equipment, necessary for welding this alloy, did however dictate that a distance of 50 mm (2 in) was the minimum acceptable between the channel toes, to complete all the welding required. The profile ultimately selected was as shown in Fig. 18. This was not theoretically ideal but did provide the best possible arrangement for axial loading. Buckling should occur on the major axis parallel to the battens.

SECTION PROFILE

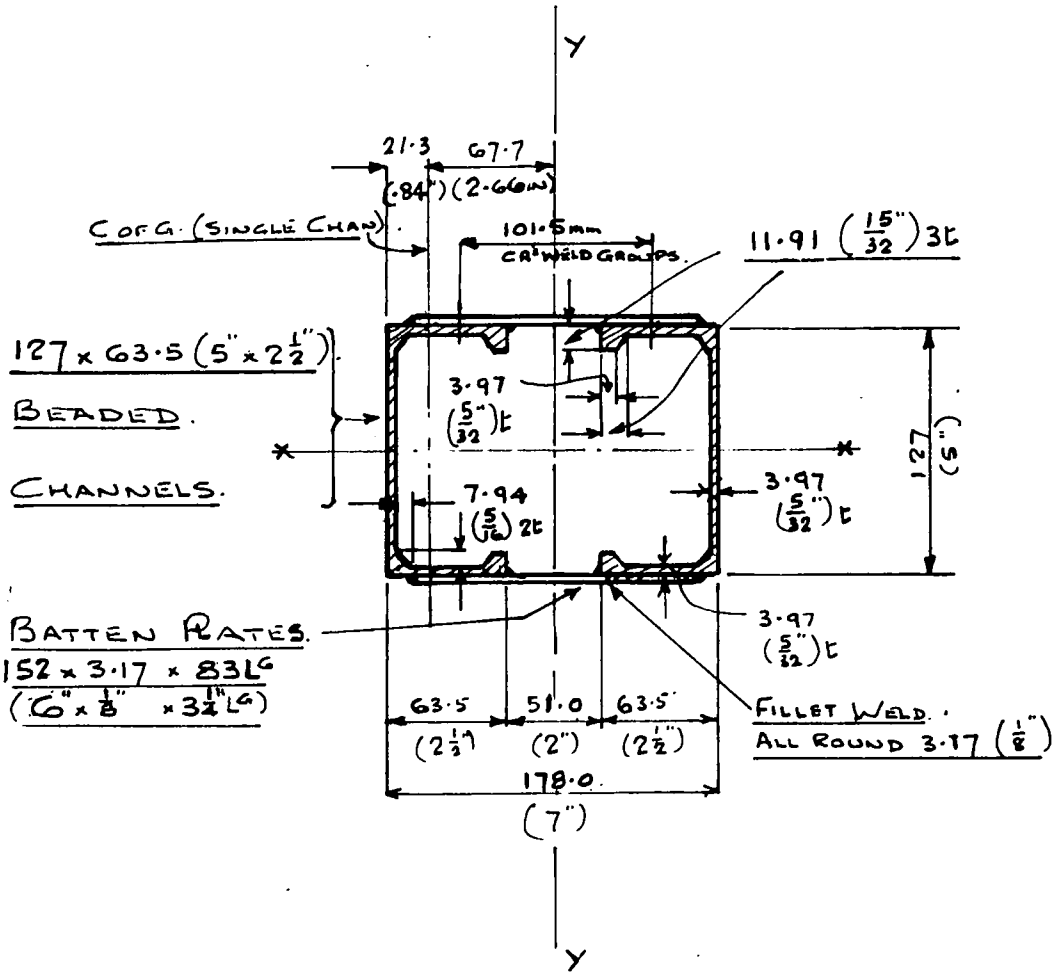

FIG:-18

SECTION PROPERTIES.

AREA. 2 CHANNELS AT 11·67 = 23·34 cm² (3·62 in²).

WEIGHT. 2 " " 3·119 = 6·238 kg/m (4·19 LB/FT)

INERTIA.

I_x - SINGLE CHANNEL. = 304·68 cm⁴ (7·32 in⁴)

I_x - COMPLETE SECTION = 609·36 cm⁴. (14·64 in⁴)

I_y - SINGLE CHANNEL = 59·20 cm⁴ (1·42 in⁴)

I_y - COMPLETE SECTION = 1179·60 cm⁴ (28·34 in⁴)

RAD: GYRATION r_x - SINGLE CHANNEL. = } 5·13 cm
r_x - COMPLETE SECTION = } (2·02 in)

r_y - SINGLE CHANNEL = 2·26 cm (0·89 in)

r_y - COMPLETE SECTION. = 7·11 cm (2·80 in)

The arrangement was however ideally suited to eccentric end loading on the major axis parallel to the battens. An eccentricity of 25 mm (1 in) was chosen, enabling an investigation to be carried out into a type of loading (causing buckling in the plane of the battens) not encouraged by the present Code recommendations.

Figs. 29, 30 and 39 to 43 provide details and identification marks for all axial and eccentrically loaded struts tested.

6.2 Design

At this stage initial designs were undertaken for axial and eccentrically loaded struts to establish the order of the failure loads. The designs were carried out in strict accordance with the requirements of CP 118 (1969) Clause 4.3.4. - "Battened Struts". The cross sectional profile selected for the struts is as Fig. 18 with properties as listed.

The first requirement was to establish the proportions and spacing of the battens.

Spacing was fixed in accordance with Clause 4.3.4.2. It must be reiterated that an anomaly exists between the alloy and steel code recommendations on batten spacing as recorded in the table included in Chapter 1. This is further aggravated by the ambiguity of Clause 4.3.4.2. which refers to "spacing between battens" and

"measurement between centres of battens". In view of this situation the problem was considered as follows:-

Initially four equal batten spaces as indicated for Strut S1 were chosen. Fig. 39 and 40.

Then Spacing, centres of battens = 863.5 mm (2'-10") ..(1)

Spacing, between battens = 781 mm (2'-6¾") ..(2)

Least slenderness ratio $\frac{d}{r_y}$ - single channel is given by:-

For (1) $\frac{d}{r_y} = \frac{86.35}{2.26} = 38.2$; For (2) $\frac{d}{r_y} = \frac{78.1}{2.26} = 34.5$

Code requires that this value should not exceed the lesser of $0.7 \times \frac{\ell}{r_x}$ of strut as a whole OR 50

$$= 0.7 \times \frac{365.76}{5.13}$$

$$= 0.7 \times 51.4 = \underline{36.0} \text{ OR } \underline{50}$$

The value of 38.2 slightly exceeds 36.0 but was accepted as it referred to the more conservative location of batten centres. Thus accept spacing is at permitted maximum.

Length of battens was established by Clause 4.3.4.3

Centres of weld groups were taken at a = 101.5 mm (Code Fig 5).

$\therefore \frac{3}{4} a = .75 \times 101.5 = 76.1$ mm minimum

Batten length fixed at 83 mm ($3\frac{1}{4}$ in). For welded battens effective length taken as <u>total</u> length.

<u>Thickness</u> of battens was given by Clause 4.3.4.4.

Minimum = $\frac{a}{36}$ OR 2.5 mm (0.10 in)

$$\frac{a}{36} = \frac{101.5}{36} = \underline{2.82} \text{ mm}$$

Use <u>3.17 mm</u> ($\frac{1}{8}$ in) thick plate.

<u>Fastening</u> - requirements are dictated by Clause 4.3.4.5. This requires the simultaneous resistance of:-

(a) Longitudinal Shearing Force $\frac{sd}{2a}$
(b) Moment of $\frac{sd}{4}$
(c) Any other forces due to bending of the struts

) See Code for symbols

In view of the complexity of the eccentric loading situation, (eccentricity on the axis parallel to the battens) which will give large variation of load between the main channel legs, plus the stresses induced by deflection, the minimum fastening requirements are difficult to predict at this stage. It was therefore decided to provide "all round" fillet welds developing the full strength of the batten plates. Proposals for adjustment to this provision can be made after the strain gauge readings for the battens are known.

The profile of the struts was now completely established enabling the calculations for the theoretical failure stresses and loads to be made.

1. Column Buckling

(a) Axial Load

Effective length (centres of ball ends)

= 3.657 m = 365.7 cm (12'-0")

Overall Slenderness Ratios =

$\frac{\ell}{r_x} = \frac{365.7}{5.13} = 71.3$ (Parallel to battens)

$\frac{\ell}{r_y} = \frac{365.7}{7.11} = 51.4$ (Perpendicular to battens)

Clause 4.3.4.1 requires 51.4 NOT to exceed 0.8 x 71.3: $51.4 < 57.04$ O.K.

Slenderness ratio (single channel between centres of battens) =

$\frac{\ell}{r_y} = \frac{86.35}{2.26} = 38.2$ IF pin-ended will be reduced by end fixity depending on batten stiffness.

Criterion for Column Buckling $\lambda = \frac{\ell}{r_x} = 71.3$.

From Chapter 3 - Fig. 2 Crippling Stress = 133 N/mm^2 (8.6 ton/in^2).

$\therefore$ Crippling load = area x stress

$$= \frac{2334 \times 133}{10^3} = \underline{310.4 \text{ kN}} \text{ (31.04 Ton)}$$

(Note:- Tests 5 and 6 with battens spaced at 1041.5 mm centres failed at 371 kN (37.1 ton) and 331 kN (33.1 ton) respectively).

(b) Eccentric Loading

The eccentric loading will promote bending in the plane of the battens and their spacing becomes important. Calculations will therefore be made to predict the failure load when the battens are spaced at 863.5 mm (2'-10") centres, which is the maximum permitted by the code. Prediction will also be made for the failure load when the batten spacing is opened out to 1218.5 mm (4'-0") centres. Tests will also be conducted at this latter dimension.

Code Clause 4.1.4.2. provides the expression for combined bending and axial compression by

$$\frac{f_c}{p_c} + \frac{f_{bc}}{p_{bc}\left(1 - \frac{f_c}{p_E}\right)} \leqslant 1$$

This may be expressed in terms of the yield stress by

$$f_c + \frac{f_{bc}}{1 - \frac{f_c}{P_E}} \leqslant P_y \qquad \ldots(1)$$

where f_c = mean axial stress

$f_{bc} = \frac{P_e}{Z}$ where P is applied load, e the eccentricity and Z the section modulus

P_E = Euler stress for flexural buckling in the plane of the eccentricity $\frac{\pi^2 E}{\lambda^2}$

P_y = 0.1% proof stress.

An Alcan handbook which deals with battened struts suggests that when bending in the plane of the battens exists, the equivalent slenderness ratio to be employed is given by

$$\lambda = \sqrt{\lambda^2_y + \lambda^2_c}$$

where λ_y = slenderness ratio for the major axis about which bending occurs.

λ_c = slenderness ratio of one channel about its weaker axis.

Employing this method of approach gives the following calculations for the failure loads.

Battens at 863.5 mm (2'-10") Centres

$$f_c = \frac{\text{load}}{\text{area}} = \frac{P \times 10^3}{2334} = .43P \text{ N/mm}^2$$

P_y = 0.1% Proof - (average as given in Chapter 3) = 317 N/mm^2 (20.5 Ton/in^2)

$$f_{bc} = \frac{Pe}{Z} \text{ and } e = 25.4 \text{ mm (1 in)}$$

$$Z = \frac{I}{y} = \frac{1179.6 \times 10^4}{89} = 132100 \text{ mm}^3$$

$$\therefore f_{bc} = \frac{P \times 25.4 \times 10^3}{132100} = .192 \text{ P N/mm}^2$$

$$P_E = \frac{\pi^2 E}{\lambda^2} \quad \text{where} \quad \lambda = \sqrt{\lambda_y^2 + \lambda_c^2}$$

and λ_y = 51.4)) See Axial

λ_c = 38.2)) Loaded Strut

Thus $\lambda = \sqrt{51.4^2 + 38.2^2}$

$= \underline{64}$

$$\therefore P_E = \frac{\pi^2 \times 68700}{64^2} = 165 \text{ N/mm}^2.$$

Substituting values in (1) gives

$$.43P + \frac{.192P}{1 - \frac{.43P}{165}} = 317.$$

$P_{crit.}$ = $\underline{280}$ kN (28.0 ton)

(NOTE: Test 1 with battens at this spacing failed at 277 kN (27.7^T)

Test 2 with battens at this spacing failed at 265 kN (26.5^T)

Tests 8 and 9 with battens at this spacing failed at 280 kN (28^T) and 282 kN (28.2^T) respectively. Here the battens straddled the mid height location.

Battens at 1218.5 mm (4'-0") Centres

Then $\lambda_y = 51.4$ (as before)

$$\lambda_c = \frac{121.85}{2.26} = 53.8$$

Thus $\lambda = 51.4^2 + 53.8^2$

$= 74.3.$

$$\therefore P_E = \frac{\pi^2 \times 68700}{74.3^2} = 122 \text{ N/mm}^2$$

Substituting in (1) gives

$$.43P + \frac{.192P}{1 - \frac{.43P}{122}} = 317$$

P_{crit} = 227 kN (22.7 Ton)

(NOTE: Tests 3 & 4 with battens at this spacing failed at 245 kN (24.5 ton), and 265 kN (26.5 ton) respectively. Tests 9 & 10 with battens at this spacing but straddling the mid height failed at 251 kN (25.1 ton) and 259 kN (25.9 ton) respectively).

2. Local Buckling

Buckling of this type appears as deformation in a series of waves. It may occur in one or more of the component elements making up a section. As a first investigation into this problem, the code approach as given by CP118 (1969) Clause 4.5.1 was used to establish if local buckling was likely to be critical when considering ultimate failure. Interaction between column and local buckling was ignored at this stage.

The critical buckling stress for simple local buckling may be obtained from Chapter 3 - Fig 4 at $\lambda = \frac{mb}{t}$

where λ = the buckling parameter

m = local buckling coefficient - See Code Table 11 and Appendix K

b = breadth of elemental part - See Code Table 11 and Appendix K

t = thickness of elemental part - See Code Table 11 and Appendix K

The value of λ was calculated in accordance with Code Clauses 4.5.1.3 and 4.5.1.4 thus:-

Find the buckling parameter for all component "plates" making up a section and take highest value. The value for m needs careful consideration. To fit in with the present code the beads of the channel being used will need to be

approximated to the circular bulb or rectangular lip.

Refer to Fig. 18 and Code Table 11.

(a) Web Element

Using Code Clause 4.5.1.3 web element is taken with b = distance between flanges

b = 127 - 2 (3.97) = 119.06 mm. t = 3.97 mm

$\therefore$ Web element $\lambda = \frac{mb}{t} = \frac{1.6 \times 119.06}{3.97} = 48$ ...(1)

Alternatively if web element is taken with b = distance between the web fillets

b = 127 - 2 (11.91) = 103.18 mm. t = 3.97 mm

Then Web element $\lambda = \frac{mb}{t} = \frac{1.6 \times 103.18}{3.97} = 41.5$..(2)

Note - It is however very unlikely that in practice the stress distribution will be UNIFORM across the web, due to the initial lack of straightness of the strut. Therefore m is more likely to be reducing towards 1.2. Assume a value of m = 1.3 on a web width b = 103.18 mm.

Then Web element $\lambda = \frac{mb}{t} = \frac{1.3 \times 103.18}{3.97} = 33.7$..(3)

$\therefore$ Crippling Stress from Fig. 4 Chapter 3 becomes

For (1) 278 N/mm^2 (18 Ton/in^2)

(2) 296 N/mm^2 (19.2 Ton/in^2)

(3) 318 N/mm^2 (20.5 Ton/in^2)

(b) Flange Element

To examine the buckling resistance of the flange it was necessary to break it down into component "plates" in the following manner.

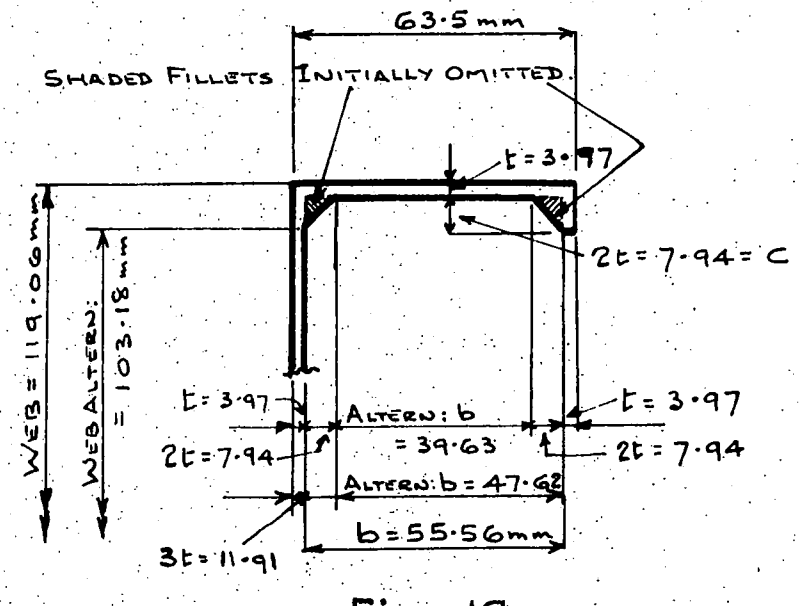

Fig:- 19

(i) Flange as Web Element

Referring to Fig. 19 and omitting the fillets (shaded) to conform with the Code configurations gives b = 55.56 mm. For the parallel portion of flange with both edges supported m = 1.6.

Using Code Clause 4.5.1.3(1)

$$\lambda = \frac{mb}{t} = \frac{1.6 \times 55.56}{3.97} = 22.6 \qquad \ldots(4)$$

If the shaded fillets were included, and it could well be argued that the flange was supported between the springings of the web and bead fillets b = 39.63 mm .

Then $\lambda = \frac{mb}{t} = \frac{1.6 \times 39.63}{3.97} = 16.0$ ...(5)

Comparing either solutions (4) or (5) with Web element values (1) (2) or (3) indicated that the "web element" of the flange was not critical.

(ii) Lip as Flange Element

Again omitting shaded fillet to suit Code configuration Code Clause 4.5.1.3(2) was used. Lip has one edge supported and one free thus m = 5.1.

$\therefore \lambda = \frac{mc}{t} = \frac{5.1 \times 7.94}{3.97} = 10.2$ ...(6)

The effect of the fillet would be to considerably reinforce the lip and reduce $\lambda = 10.2$. Therefore lip is not critical.

(iii) Flange-Lip Combination

No provision is made in the code for beaded lips. For an initial check approximations were therefore made and in the first instance the shaded fillets omitted. This enabled Code Clause 4.5.1.3(3) to be applied to establish the order of λ.

m is given by $5.1\left(1 - \frac{c^2}{80t^2}\right)$ where

c = lip width

t = lip thickness

$\therefore$ Referring to Fig. $m = 5.1\left(1 - \frac{7.94^2}{80 \times 3.92^2}\right)$

$$\therefore m = \underline{4.6}$$

Considering initially b = 55.56 (max. between web and lip)

$$\lambda = \frac{mb}{t} = \frac{4.6 \times 55.56}{3.97} = 65 \qquad \ldots(7)$$

If however b is taken at 39.63 (distance between fillets).

$$\lambda = \frac{mb}{t} = \frac{4.6 \times 39.63}{3.97} = 45.8 \qquad \ldots(8)$$

From physical manipulation of a short length of the actual section indications are that any lateral displacement of the "flange-lip combination" would tend to "hinge" from the springing of the web fillet.

A second alternative was therefore calculated in which b at 47.62 was taken as the distance between the web fillet springing and the inside of the lip.

Then $\lambda = \frac{mb}{t} = \frac{4.6 \times 47.62}{3.97} = 55.2 \qquad \ldots(9)$

This figure will be somewhat reduced by the inclusion of the lip fillet tending to reduce b to less than 47.62.

From Fig. 4 Chapter 3 the Crippling Stresses become:-

For (7) 160 N/mm^2 (10.3 Ton/in^2)

(8) 284 N/mm^2 (18.4 Ton/in^2)

(9) 222 N/mm^2 (14.3 Ton/in^2)

(c) Comparisons

The web buckling solutions to (1) (2) and (3) were then compared with those for the "flange lip combination" (7) (8) and (9). It was apparent that a CRITICAL situation could well exist.

On face value the solution to (7) at 160 N/mm^2 (10.3 Ton/in^2) was the criterion for local buckling. This indicated failure of the component covered by the "flange lip combination." Consideration of the degree of end fixity offered by the fillets at the web and lip, which would reduce the buckling length b, suggested that the solution to (2) web, at 296 N/mm^2 (19.2 Ton/in^2) and to (8) - flange, at 284 N/mm^2 (18.4 Ton/in^2) should be compared. This again indicated that failure of the flange lip combination was just possible before the web; a situation difficult

to accept. It was therefore necessary to refer to the Code Appendix K for more exact treatment.

(d) Local Buckling of Entire Section

Code Appendix K provides a more accurate method of determining local buckling stress. The calculated value of m is for the entire section. The method covers for uniform axial compression only and unfortunately plain and lipped channels are the only types catered for. Approximation will therefore again be necessary.

Using Appendix K (2), referring to Fig. 19 and omitting shaded fillets

$$\frac{t_1}{t_2} = \frac{3.97}{3.97} = 1 \qquad \frac{b}{a} = \frac{59.53}{119.06} = 0.5$$

Radius of gyration of lip about axis through its centroid parallel to parent flange = $r = \sqrt{\frac{I}{A}}$

$$I = \frac{bd^3}{12} = \frac{3.97 \times 7.94^3}{12} = 166 \text{ mm}^4$$

$$A = 3.97 \times 7.94 = 31.5 \text{ mm}^2$$

$$\therefore r = \sqrt{\frac{166}{31.5}} = 2.29 \text{ mm}$$

$$\text{Then } \frac{r}{t_2} = \frac{2.29}{3.97} = .562$$

Referring to Fig. 32 (Code Appendix K) and interpolating between "plain" and $\frac{r}{t_2} = 1$ $m = 1.9$

$$\lambda = \frac{ma}{t_1} = \frac{1.9 \times 119.06}{3.97} = 57 \qquad \ldots(10)$$

Thus Crippling Stress (Fig. 4 Chapter 3) =

$\underline{210\ N/mm^2}$ (13.6 Ton/in^2.)

With an alternative $\frac{b}{a}$, taking b from the springing of the web fillet at 51.59 mm

$\frac{b}{a} = \frac{51.59}{119.06} = .43$ and $m = 1.8$

$$\lambda = \frac{ma}{t_1} = \frac{1.8 \times 119.06}{3.97} = 54 \text{ (very little improvement)} \qquad \ldots(11)$$

Giving Crippling Stress = 232 N/mm^2 (15 Ton/in^2)

The application of the Appendix K method, whilst of necessity not precise due to the neglect of the fillets (not catered for by the Code), gives crippling stresses for (10) (11) lower than the most likely solutions to (2) and (8). It was not considered satisfactory to accept figures with so much variation and axial compression tests on short lengths of channel were therefore undertaken.

(e) Details of the Tests (carried out on a "Dennison" machine)

TEST 1

Length of channel test piece 480 mm (15 in) - ends milled true and square.

Loading - axial.

Failure load 342 kN (34.2 Ton).

Average failure stress = $\frac{\text{load}}{\text{area}} = \frac{342 \times 10^3}{1167}$

$= 292 \text{ N/mm}^2 \ (18.8 \text{ Ton/in}^2)$ ...(12)

Observations and measurements taken between the insides of the flange toes established that deformation in a series of waves, as discussed by Bryan[4], commenced in the flanges at about 280 kN (28 Ton). This deformation increased in steps with each 10 kN (1 Ton) increment of load. The test piece was however still capable of sustaining the applied load until the onset of failure at 342 kN (34.2 Ton). At this point the specimen commenced and continued to buckle in all component parts and failed to sustain the load.

Average stress at onset of deformation =

$\frac{280 \times 10^3}{1167} = 240 \text{ N/mm}^2 \ (15.25 \text{ Ton/in}^2)$ ...(13)

TEST 2

Length of channel test piece 610 mm (24 in) - ends milled true and square.

Loading - axial

Failure load 330 kN (33 Ton)

$$\text{Average failure stress} = \frac{\text{load}}{\text{area}} = \frac{330 \times 10^3}{1167}$$

$$= 283 \text{ N/mm}^2 \ (18.3 \text{ Ton/in}^2) \qquad \ldots(14)$$

Observations and measurements were again taken. Deformation followed the same pattern as in Test 1 but commenced at a load of 270 kN (27 Ton).

Average stress at onset of deformation =

$$\frac{270 \times 10^3}{1167} = 230 \text{ N/mm}^2 \ (14.95 \text{ Ton/in}^2) \qquad \ldots(15)$$

(f) Conclusions - Local Buckling

Comparison of the calculated values with the test results suggests that the theoretical predictions that flange buckling initiates any local buckling failure are true when the compression is uniform.

Flange deformation appeared to commence at the stresses given by test solutions (13) and (15). These compare favourably with the calculated "flange lip combination" stress given by (9) and the entire section stress given by (11). At this stage no apparent web buckling was present, suggesting that the web element was sustaining

Local Buckling - 15" Length
Test 1

See Plate 2 for Buckled 24" length
for Test 2

PLATE 10

the section and could accept further load.

This was confirmed when further increments of load were added until the onset of web buckling and complete local buckling failure occurred at the average test failure stresses given by (12) and (14). These figures were in very close agreement with the calculated solution given by (8).

It was therefore concluded that when the flanges deformed at about 230 N/mm^2 (15 Ton/in^2) the web was still in a position to accept more load and did in fact sustain the section until web buckling commenced at 285 N/mm^2 (18.5 Ton/in^2) bringing about complete section failure in local buckling.

3. Post-Buckling

In general the values of $\lambda = \frac{mb}{t}$ fall below λ_B at 50 and further investigation was not necessary. The odd value that exceeds 50 was not much in excess of this value and post buckling investigation was not justified at this stage.

4. Mode of Failure

The foregoing initial design was based entirely on Code Recommendations which would normally be used by

a design engineer plus a simple UNIFORM compression test.

The calculations predicted that for the axially loaded struts failure would be by overall column buckling at 310.4 kN (31.04 Ton) giving an average stress of 133 N/mm^2 (8.6 Ton/in^2). This, of course, was with batten proportions and spacings at the Code recommendations.

Indications were that local buckling would not become a controlling factor until the flanges of the individual channels were stressed to 230 N/mm^2 (15 Ton/in^2) and the webs to 285 N/mm^2 (18.5 Ton/in^2). It was however felt that just before ultimate failure occurred the lateral deformation could be such that the redistribution of stress across the section (at maximum displacement) might result in the web of the channel carrying most compression, becoming critical to local buckling. This situation would also be further aggravated where the end loading was eccentric.

Sufficient basic design work had now been completed to justify the chosen profile for the test struts. The order of load carrying capacity was known together with failure stresses likely to occur. It was now possible to decide the best positions for electrical strain gauges and mechanical gauges

necessary to record displacement.

The testing programme could now proceed with varied batten spacings and eccentric end loading to obtain the required research data investigated and discussed in Chapter 8.

6.3 Fabrication

All fabrication work on the test struts was undertaken at the Welding Institute Research Laboratories, Abington Hall, near Cambridge.

The pairs of main channels for each strut were initially cut to a length somewhat in excess of their finished length. Batten plates and end plates were accurately cut to the required size.

Each pair of channels were then jigged and marked off for the welding on of the batten plates. Welding was accomplished under controlled laboratory conditions using "Tungsten Inert Gas Equipment". The procedure adopted kept the distortion to a practical minimum.

Each strut (complete with battens) was then carefully marked off to length. The ends were milled true and square to give the exact length.

Finally the end plates were positioned and welded to give struts as detailed and marked in Figs 29,30 & 39 to 43.

The marking, drilling and reamering to exact size of the holes to receive the detachable steel end plates carrying the ball seatings was undertaken at the Polytechnic. Each steel end plate is attached to the strut by four bright steel bolts which are an interference fit in the holes. Great care was exercised in fitting the plates as it precisely locates the position of the ball seatings.

Chapter 7

Instrumentation

7.1 Initial Distortions

Before the commencement of instrumentation work the struts were checked for initial distortions. These could have occurred during the extrusion of the individual channels and/or during the welding of the composite section. All important deformations were measured, marked and recorded.

Lack of straightness was first investigated. This was accomplished with the aid of a finely divided rule and a tensioned nylon line, positioned along the full length of the strut. All faces of the struts were checked and the amount of "bow" established at intervals along their length. The likely direction of lateral displacement became apparent from this exercise, enabling the planned eccentricity to be arranged so as to give additive displacement to any initial bow on that axis.

Some degree of longitudinal twist existed on all struts. This was mainly due to welding and the amounts were fortunately small. To establish the degree of twist the units were "set up" across straight edges on a plane table, measurements then being taken using feeler gauges. It was appreciated that the twist would offset

the 25 mm (1 in) eccentric ball seatings (in the strut end plates) from their planned positions and produce an additional bending moment. This would occur on the axis at right angles to that for the planned bending moment and would need to be included in the analysis of test results.

Any in-bevel of the channel flanges resulting from the extrusion process was only slight and sensibly uniform for all flanges. It was therefore decided that this would have little effect upon the test results and was disregarded.

7.2 Electrical Instrumentation

Surface strain readings were to be taken using a "Savage and Parsons 50 Way Strain Recorder" - Type No. SS33/50.

Up to fifty $\frac{1}{4}$ in foil gauges were used on each strut and their locations were thoroughly cleaned before the gauges and their tabs were cemented on. The exact locations varied throughout the testing programme and are indicated on the figures included with the experimental results for each test.

After the meticulous soldering of all the wiring connections, and circuit testing, the gauges were sprayed with a suitable laquer to exclude all dust and moisture. It was considered necessary to provide a

Lay-out for Dummy Gauges

PLATE 11

dummy gauge to each active gauge to achieve the best possible results. The usual procedures for balancing the gauges and taking strain readings were applied.

Perusal of the gauge locations indicates that eight gauges were frequently used, around the strut, at a given level. These were positioned in such a way that variation of stress, resulting from the combined action of direct load and bending moment, could be established. As the gauges were located at, or near, the extremities of the webs and flanges, calculations could be made to establish the stress levels across the strut as a whole, or on individual channels. The gauge arrangement allowed readings to be related to both major axes or read diagonally if so desired.

In considering the detailed location of the gauges the eccentric and axially loaded struts will be reported separately.

(a) Eccentrically Loaded Struts

For Tests 1 and 2 the struts were eccentrically loaded. Pairs of battens were spaced equally throughout the length of the strut at slightly more than the maximum distance permitted by C.P.118.

It was rationally estimated that ultimate failure was likely to commence at mid-height, in the channel carrying the most compressive load. Gauges were accordingly grouped around the central

battens just outside the heat affected weld zones.

The possible, though less likely, failure by buckling of the same channel in one or other of the panels adjacent to the mid-height location was appreciated. These panels were therefore gauged to give readings at possible buckling positions and enable stresses at these locations to be compared with those at the assumed mid-height failure position.

Further gauges were used at points of possible local web buckling. These were selected after consideration of initial deformations likely to promote failure in highly stressed areas. Gauges were also located at levels where the strain could be mainly attributed to direct loading.

Similar rational reasoning was applied to the gauge positioning on all subsequent struts tested. Gauges were moved to positions of anticipated high strain as suggested by the variation of the batten spacing. In some cases battens straddled the mid-height location adopted for Tests 1 and 2 resulting in the necessity of extensively gauging the three middle panels on the more heavily loaded channel.

(b) Axially Loaded Struts

For axially loaded struts the legs theoretically carry equal loading and buckling should occur at mid-height on the major axis parallel to the battens. The gauge positioning was accordingly arranged to cover both main legs.

Additional gauges to cater for local buckling at the possible positions where ultimate failure would commence were also included. This was done after due consideration of the likely effects of initial distortions.

(c) General

Some tests included gauges on selected batten plates. In all cases these were positioned near the plate edges and adjacent to the main members in an effort to obtain the type and magnitude of the stresses existing across the plates. Batten function can be particularly complex if torsion is present.

A check was made on the effects of welding by the inclusion of gauges within the heat affected zones.

As a matter of interest, in one test, the surface strain on the 25 mm dia. ball at the lower strut mounting was recorded. The gauge was located along the horizontal axis.

7.3 Mechanical Instrumentation

After placing each strut in the testing rig mechanical instrumentation was carried out in the following sequence.

(a) Verticality Check

Although the precise vertical travel of the "guide box" was checked during the rig proving test, it was felt that "spot verticality" checks were adviseable.

To provide for this requirement and to facilitate the initial vertical positioning of the strut in the rig, a theodolite and nylon line were used. The line was located between eyes positioned on the centroids of the steel end plate dowels. It was spring tensioned. This provided a vertical datum line for the full height of the strut exactly on its centroid. The theodolite could then be used to check initial verticality and any deviation during testing, at any position up the strut.

(b) Strut Shortening

With the strut now accurately positioned in the rig a plumb line was suspended from the top of the strut in line with the ball seatings. The plumb bob was sighted against a finely divided rule attached to the strut at its bottom end. The side selected for the rule was at right angles

to the axis on which the major bending would occur. This ensured that the readings were not substantially affected by the change in slope at the end of the strut. Amounts of strut shortening could now be read for each increment of load.

(c) Mid-Height Lateral Displacement

In addition to clock gauges, which would give precise readings for lateral and rotational displacement, a method of quickly reading the mid-height deflection, in the plane of major bending, was instituted.

This took the form of a finely divided rule positioned horizontally at the mid-height of the strut, on one face. A theodolite sighted on the rule enabled incremental readings of the displacement, in the plane of bending, to be made.

(d) Clock Gauges

The main requirement for clock gauges was to give readings of lateral and rotational displacement, at selected positions on the strut.

To obtain the required information gauges were arranged around the strut in groups of eight at each selected level. Each group was sub-divided to give two gauges on each side of the strut. All gauges in the groups were positioned as close

to the strut edges as practicable consistent with the estimated deflections.

For the earlier tests groups of eight gauges were located at the top, bottom and mid-height of the strut. This approach gave data for the lateral displacement on both major axes and indicated any twisting together with what stage in the loading it took place.

In later tests gauges at the top and bottom of the strut were omitted. Also when the battens straddled the mid-height location, groups of gauges were positioned at the mid-height and at the level of the lower mid battens.

Additional gauges were also used on some struts in an effort to establish the change in slope of the end plates as the struts deflected under load.

Data collected from all the instrumentation is discussed in Chapter 8 covering the analysis of the test results. Tabulated readings from the tests are given in a separate Appendix.

As a result of the research being undertaken during the transitional period for changing to S.I. units much of the instrumentation had to be done using instruments graduated in Imperial Units. Figures have been converted to conform with S.I. requirements.

Chapter 8

Experimental Results and Theoretical Comparisons

8.1 Planning of Tests

In the past much has been written upon the effect of batten spacing. Frequently the batten moments, shears, and slopes resulting from bending in the plane of the battens have been investigated. Some of the work was by mathematical paper exercise on "ideal" struts, ignoring lateral instability of the member as a whole. Where tests were conducted the components were often so proportioned, or restrained, that the co-existence of bending and lateral instability was not a problem.

Reference to both the alloy and steel Codes (See Chapter 1) clearly indicates that knowledge of the problem is limited. The alloy code makes no mention and the steel code, whilst giving restrictive conditions, really evades the issue of bending in the plane of the battens.

It therefore appeared reasonable to test struts which would simulate practical conditions and be free to buckle, on their entire length, on both major axes.

Careful consideration of the problem seemed to indicate that the Code limit on batten spacing would probably result in eccentrically loaded struts (in the plane of the battens) failing by lateral movement.

If however the batten spacing was increased, in increments, a situation could ultimately be reached when buckling of the channel carrying the most compressive load plus bending, would fail on its own weak axis, between the battens, or buckle locally.

The battens therefore play a very important role. Whilst it was accepted that the proportions given by the respective Codes could be satisfactory for dealing with individual channel buckling, between battens, any lateral movement must surely present problems. It seemed very unlikely that thin, unreinforced, batten plates, even with a gap between channel toes of only 50 mm (2 in), would satisfactorily ensure that the strut worked as a homogeneous unit.

If the batten plates had been adequately reinforced a torsional failure would be the probable outcome. With the type of thin plate invariably used at present, in practice, there seemed little doubt that whilst a small amount of torsion must exist, the ultimate failure (at the smaller batten spacings) could be by the "lateral instability" of one channel.

It is appreciated that lateral instability cannot exist without some torsional effect; but the following test results intimate that where thin batten plates are used,

NO REAL TORSIONAL PROBLEM exists. However, the batten plates will enable the least loaded channel to "hold up" the lateral failure of its more heavily loaded partner. This presents a complex problem for subsequent research, into the reinforcement of batten plates.

The following test results will show what happens to struts eccentrically loaded in the plane of the battens. The battens themselves are at the present recommended minimum sizes but the spacings have been incrementally increased. No axially loaded strut can ever exist in practice as manufacturing malformations are bound to produce eccentricities. The author sees no justification for the Codes tending to isolate battened struts which have bending in the plane of the battens. Bending could almost always be present even with "axial" load.

8.2 Testing Programme

A total of twelve struts were tested. One, fabricated locally in H.E.30 material, was used to prove the rig, and ancillary components. The remaining eleven, having been fabricated under ideal laboratory conditions, in Al-Zn-Mg alloy, were used for the main testing.

Little needs to be said about the proving strut, except to state that the intermediate battens were welded and that steel end brackets were bolted on. Care was taken with the end bracket fixing which was accomplished with fitted bolts in carefully drilled holes.

Under test the usual type of rigidity weakness was still manifest at the bolted joints. Ultimate failure occurred by buckling in the lower end panel, in a way encountered by earlier researchers using rivetted connections. Design engineers must realise that this type of assembly is not now acceptable with composite members. Plate 12 .

To obviate the weakness described the main test struts had pairs of battens, welded on, at their extreme ends. End brackets were discarded and replaced by thin alloy end plates welded to the strut. These plates facilitated the attachment of the thick steel end plates described earlier. As subsequent tests proved, this method was entirely satisfactory and changed completely the location of ultimate failure, to the anticipated mid-height or mid-panel positions.

For the main testing programme the eleven struts tested were divided into five "identical" pairs and one special. The single strut was included for general interest as it had only one pair of intermediate battens, at mid-height. It was appreciated that ideally,three "identical" struts should be tested at each selected batten spacing. This was not possible for reasons of time and expense. Limiting each type to two, enabled the fullest use to be made of the available material.

The Proving Strut Buckled
in
Bottom Panel

PLATE 12

Two "identical" struts were loaded axially and four pairs, plus the special, were subjected to eccentric loading. The degree of eccentricity was made constant at 25.4 mm (1 in) and located along the major axis parallel to the battens.

After careful positioning and final checking, and with all recording systems at "GO" each strut was loaded incrementally. Readings were taken at each load increment up to failure and careful visual inspection was carried out at the higher load levels.

For some tests, cine cameras, including an ultra-high-speed unit were directed at the areas of anticipated failure. By this means, an effort was made to record such deformations as would be difficult for the eye sensibly to observe.

A complete appendix of test results, which includes all recorded readings of both displacements and strains has also been compiled. This extensive file of data together with films and photographs provides a bank of information for future research.

It may well be that the amount of recording undertaken will be considered excessive. It was however felt that with a new material, which was both expensive and difficult to obtain, as much data as possible should be collected in the hope that it may prove useful in subsequent work.

Before embarking upon the consideration of the actual tests some mention must be made of the importance of welding.

Much has been said about batten rotation causing early failure and the need for battens to be welded. Subsequent test data will show that other considerations, not mentioned by previous researchers, are equally important.

The battens must be welded, at the channel toes, for the full depth of the batten plate. Where lateral instability of one channel proves critical the effective "lever arm" of the battens resisting lateral movement will be greatly influenced by these welds. They will play an important role in fixing the level of the ultimate failure load.

The use of rivets (still widespread with aluminium alloy) is surely not justified. They are already known to permit joint movement and under lateral displacement of one channel the "lever arm" will increase to the centres of the rivet holes. This will provide a further reduction to the resistance of lateral movement. In addition, the most likely location of batten bending failure would be at the rivet holes, which condition would be preceeded by a situation inducing tension in the rivets. Aggravation of the batten rotation problem would therefore be inevitable.

TEST Nº 4.

LOAD KN	TSN	Gauge Location 1.	2	3	4.	5.	6	7
20	2	·456	·170	·233				
	4	·800	·426	·527				
	6	·215	·135	·155				
	8	·274	·195	·212				
	10	·324	·255	·268				
	12	·377	·319	·325				
	14	·425	·384	·380				
	15	·450	·420	·410				
	16	·470	·450	·436				
	17	·496	·491	·466				
	18	·518	·530	·496				
	19	·540	·568	·520				
200	20	·562	·608	·548				
	21	·584	·65	·574				
	22	·303	·35	·302				
	23	·310	·369	·310				
	24	·322	·400	·325				
250	25	·330	·434	·340				
260	26	·340	·478	·350				
	27							
	28							
	29							
	30							

Fig:- 20.

THEODOLITE READINGS.

LATERAL DISPLACEMENT OF STRUT AT MID-HEIGHT (ON Y-Y AXIS)

INITIAL SETTING. 5"

LOAD KN	LOAD TON	READINGS mm	READINGS IN	LAT. DISPLACEMENT mm	LAT. DISPLACEMENT IN
20	2		5·062		·062
	4		5·125		·125
	6		5·187		·187
	8		5·250		·250
	10		5·312		·312
	12		5·375		·375
	14		5·484		·484
	15		5·531		·531
	16		5·578		·578
	17		5·656		·656
	18		5·718		·718
	19		5·781		·781
200	20		5·859		·859
	21		5·937		·937
	22		6·062		1·062
	23		6·140		1·140
	24		6·312		1·312
250	25		6·484		1·484
260	26		6·781	43·24	1·781
	27				
	28				
	29				
	30				

FIG:- 21

FAILURE LOAD 265 KN (26·5 TON)

TEST Nº 4

VERTICAL DISPLACEMENT

(ON ℄ BALL SEATS)

MEASUREMENT BY PLUMB-LINE AND RULE.

INITIAL SETTING 2·375"

LOAD		READINGS		VERT DISPLACE:	
KN	TON	mm	IN	mm	IN.
20	2		2·375		·000
	4		2·343		·032
	6		2·312		·063
	8		2·312		·063
	10		2·281		·094
	12		2·250		·125
	14		2·218		·157
	15		2·218		·157
	16		2·187		·188
	17		2·187		·188
	18		2·156		·219
	19		2·156		·219
200	20		2·125		·250
	21		2·125		·250
	22		2·093		·282
	23		2·093		·282
240	24		2·062		·313
	25				
	26				
	27				
	28				
	29				
	30				

FIG·22

FAILURE LOAD 265 KN. (26·5 TON)

TEST Nº 4.

CLOCK-GAUGE READINGS.

LATERAL DISPLACEMENT.

POSITION - TOP OF STRUT.

GAUGE GRADUATIONS .0001"

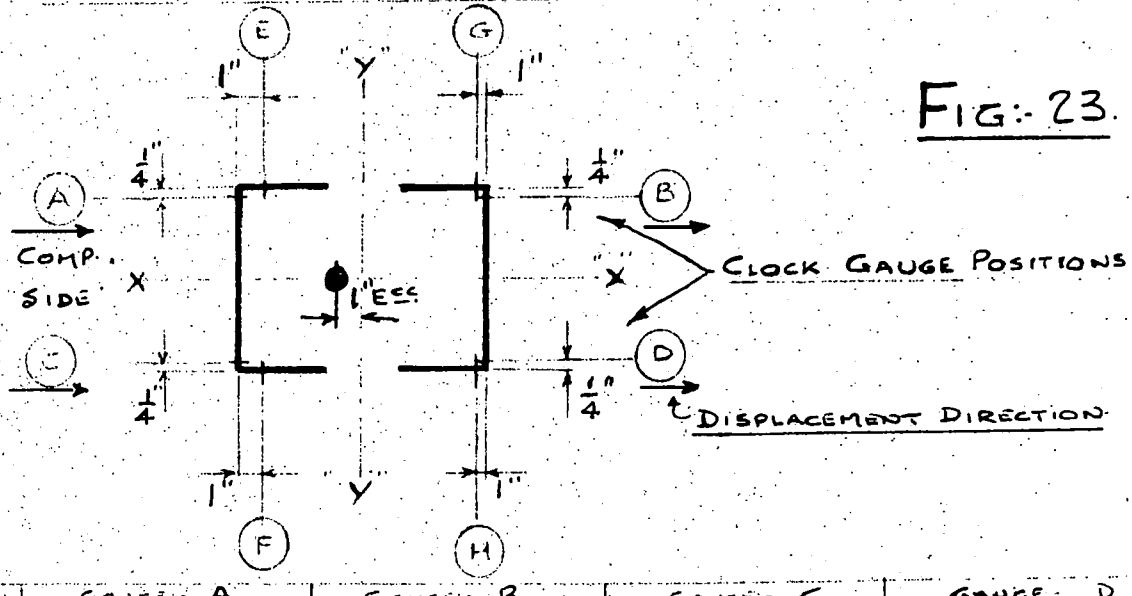

FIG:- 23.

LOAD		GAUGE A			GAUGE B			GAUGE C			GAUGE D		
			DISPLACEMENT			DISPLACEMENT			DISPLACEMENT			DISPLACEMENT	
KN	TON	READING	mm	IN	READING	mm	IN	READING	mm	IN	READING	mm	IN
	0	.0758		—	.0075		—	.1285		—	.1455		—
	2	.0746		.0010	.0087		.0012	.1274		.0011	.2465		.0010
	4	.0698	.147	.0058	.0129		.0057	.1231		.0054	.2497		.0042
	6	.0651		.0105	.0192		.0117	.1155		.0150	.2612		.0157
	8	.0582	.442	.0174	.0280		.0205	.1075		.0210	.2627		.0172
100	10	.0542		.0214	.0369		.0294	.0962		.0325	.2697		.0242
	12	.0482	.696	.0274	.0431		.0356	.0912		.0375	.2753		.0298
	14	.0412		.0344	.0522		.0447	.0885		.0400	.2840		.0385
	15	.0385		.0371	.0566		.0491	.0862		.0423	.2876		.0421
	16	.0355	1.019	.0401	.0607		.0532	.0833		.0452	.2913		.0458
	17	.0318		.0438	.0648		.0573	.0793		.0492	.2950		.0495
	18	.0279		.0477	.0695		.0620	.0753		.0532	.2995		.0540
	19	.0232		.0524	.0745		.0670	.0702		.0583	.3045		.0590
200	20	.0189	1.440	.0567	.0801		.0726	.0658		.0627	.3093		.0638
	21	.0133		.0623	.0866		.0791	.0603		.0682	.3155		.0700
	22	.0082		.0674	.0930		.0855	.0551		.0734	.3210		.0755
	23	.0036		.0721	.0990		.0915	.0494		.0791	.3260		.0805
240	24	.0077	2.116	.0833	.1075		.1000	.0415		.0870	.3345		.0890
	25												
	26												
	27												
	28												
	29												
	30												

FAILURE LOAD 260 KN (26.5 TON)

TEST Nº 4

CLOCK-GAUGE READINGS

LATERAL DISPLACEMENT

POSITION TOP OF STRUT.

GAUGE GRADUATIONS ·0001"

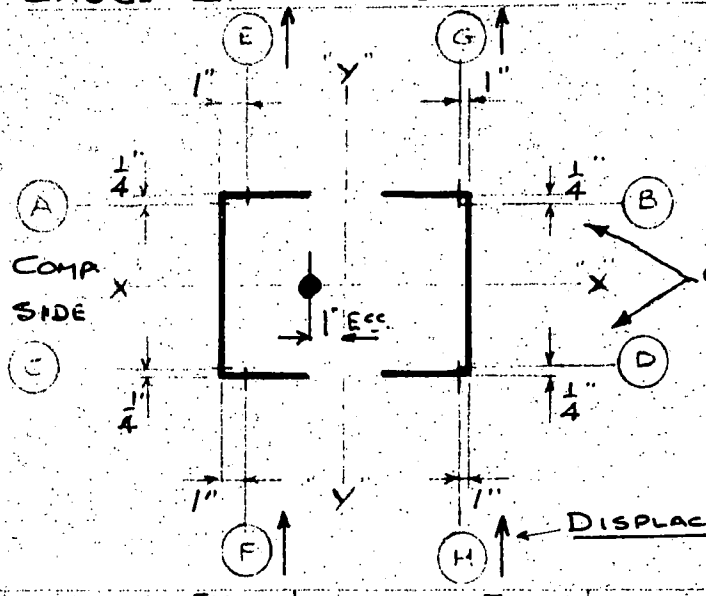

FIG 24

LOAD		GAUGE E			GAUGE F			GAUGE G			GAUGE H		
		READING	DISPLACEMENT		READING	DISPLACEMENT		READING	DISPLACEMENT		READING	DISPLACEMENT	
KN	TON		mm	IN		mm	IN		mm	IN		mm	IN
	0	·4930		—	·0883		—	·1095		—	·4137		—
	2	·4931		·0001	·0852		·0031	·1096		·0001	·4121		·0016
	4	·4932		·0002	·0824		·0059	·1096		·0001	·4121		·0016
	6	·4936		·0004	·0824		·0059	·1096		·0001	·4120		·0017
	8	·4969		·0039	·0812		·0071	·1099		·0004	·4077		·0060
100	10	·4965		·0035	·0812		·0071	·1099		·0004	·4077		·0060
	12	·4967		·0037	·0812		·0071	·1099		·0004	·4077		·0060
	14	·4983		·0053	·0808		·0075	·1101		·0006	·4100		·0037
	15	·4983		·0053	·0808		·0075	·1101		·0006	·4100		·0037
	16	·4985		·0055	·0808		·0075	·1100		·0005	·4100		·0037
	17	·4986		·0055	·0803		·0080	·1100		·0005	·4097		·0040
	18	·4988		·0058	·0801		·0082	·1101		·0006	·4092		·0045
	19	·4994		·0064	·0795		·0088	·1101		·0006	·4090		·0047
200	20	·4996		·0066	·0790		·0093	·1101		·0006	·4083		·0054
	21	·5007		·0077	·0782		·0101	·1101		·0006	·4080		·0057
	22	·5150		·0220	·0778		·0105	·1101		·0006	·4072		·0065
	23	·5090		·0160	·0770		·0113	·1102		·0007	·4061		·0076
240	24	·5050		·0120	·0756		·0127	·1106		·0011	·4051		·0086
	25												
	26												
	27												
	28												
	29												
	30												

FAILURE LOAD 265 KN. (26·5 TON)

TEST Nº 4

CLOCK-GAUGE READINGS

LATERAL DISPLACEMENT.

POSITION - MID HEIGHT STRUT.

GAUGE GRADUATIONS .001"

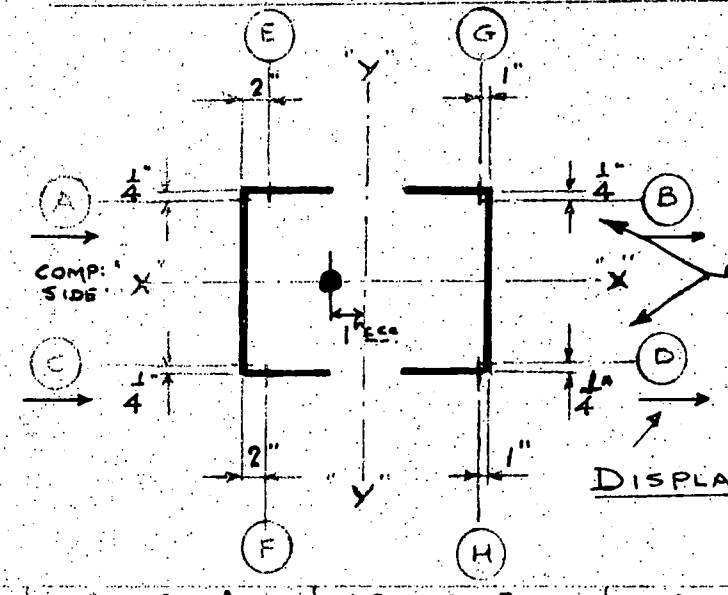

FIG 25

LOAD		GAUGE A			GAUGE B			GAUGE C			GAUGE D		
		READING	DISPLACEMENT		READING	DISPLACEMENT		READING	DISPLACEMENT		READING	DISPLACEMENT	
KN.	TONS		mm	IN.		mm	IN		mm	IN.		mm	IN
	0	1·983		—	·001		—	1·759		—	·147		—
	2	1·934	1·24	·049	·049		·048	1·710		·049	·191		·044
	4	1·881	2·58	·102	·101		·100	1·658		·101	·244		·097
	6	1·828	3·93	·155	·156		·155	1·605		·154	·295		·148
	8	1·766	5·50	·217	·220		·219	1·543		·216	·360		·213
100	10	1·700	7·19	·283	·286		·285	1·478		·281	·427		·280
	12	1·624	9·10	·359	·364		·363	1·402		·357	·502		·355
	14	1·535	11·40	·448	·455		·454	1·314		·445	·592		·445
	15	1·488	12·59	·495	·503		·502	1·263		·496	·642		·495
	16	1·438	13·85	·545	·554		·553	1·208		·551	·691		·544
	17	1·378		·605	·613		·612	1·136		·623	·751		·604
	18	1·312	17·20	·671	·679		·678	1·069		·690	·815		·668
	19	1·250		·733	·745		·744	1·008		·751	·879		·732
200	20	1·173	20·51	·810	·821		·820	·928		·831	·953		·806
	21	1·090		·893	·906		·905	·846		·913	1·041		·894
	22	·986	25·30	·997	1·012		1·011	·740		1·019	1·142		·995
	23	·899		1·084	1·099		1·098	·653		1·106	1·226		1·079
240	24	·750	31·30	1·233	—			·500		1·259	—		
	25												
	26												
	27												
	28												
	29												
	30												

FAILURE LOAD 265 KN. (26·5 TON)

TEST Nº 4.

CLOCK-GAUGE READINGS

LATERAL DISPLACEMENT

POSITION - MID HEIGHT STRUT.

GAUGE GRADUATIONS .001"

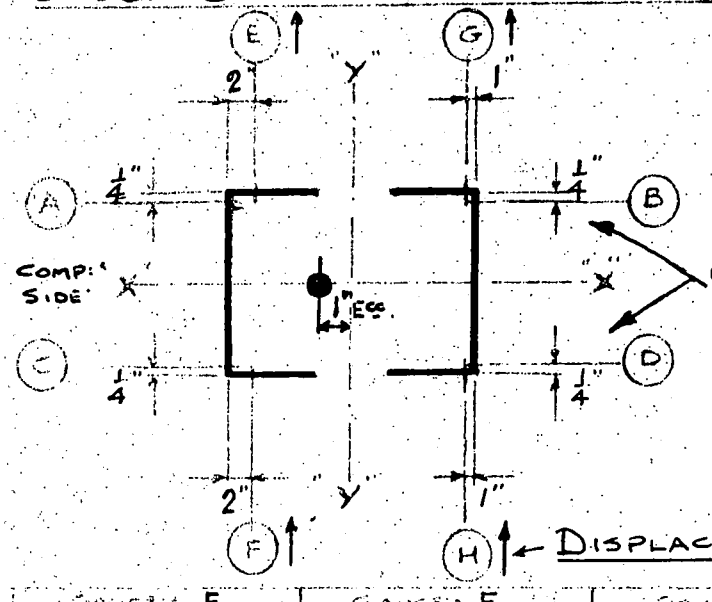

FIG 26

LOAD kN	LOAD TON	GAUGE E READING	GAUGE E DISPLACEMENT mm	GAUGE E DISPLACEMENT IN	GAUGE F READING	GAUGE F DISPLACEMENT mm	GAUGE F DISPLACEMENT IN	GAUGE G READING	GAUGE G DISPLACEMENT mm	GAUGE G DISPLACEMENT IN	GAUGE H READING	GAUGE H DISPLACEMENT mm	GAUGE H DISPLACEMENT IN
	0	·677		—	·476		—	·645		—	·396		—
	2	·684		·007	·472		·004	·647		·002	·393		·003
	4	·687		·010	·470		·006	·648		·003	·388		·008
	6	·693		·016	·469		·007	·649		·004	·385		·011
	8	·701		·024	·465		·011	·650		·005	·380		·016
100	10	·709		·032	·462		·014	·653		·008	·374		·022
	12	·718		·041	·458		·018	·656		·011	·367		·029
	14	·727		·050	·451		·025	·661		·016	·359		·037
	15	·733		·056	·450		·026	·663		·018	·356		·040
	16	·739		·062	·446		·030	·664		·019	·350		·046
	17	·746		·069	·443		·033	·667		·022	·345		·051
	18	·757		·080	·436		·040	·673		·028	·340		·056
	19	·765		·088	·430		·046	·677		·032	·333		·063
200	20	·775		·098	·425		·051	·682		·037	·326		·070
	22	·788		·111	·418		·059	·686		·041	·316		·080
	24	·804		·127	·408		·068	·696		·051	·308		·088
230	23	·820		·143	·396		·080	·707		·062	·295		·101
	24												
	25												
	26												
	27												
	28												
	29												
	30												

FAILURE LOAD 265 KN. (26·5TON)

TEST Nº 4

CLOCK-GAUGE READINGS

LATERAL DISPLACEMENT

POSITION BOTTOM OF STRUT

GAUGE GRADUATIONS ·001"

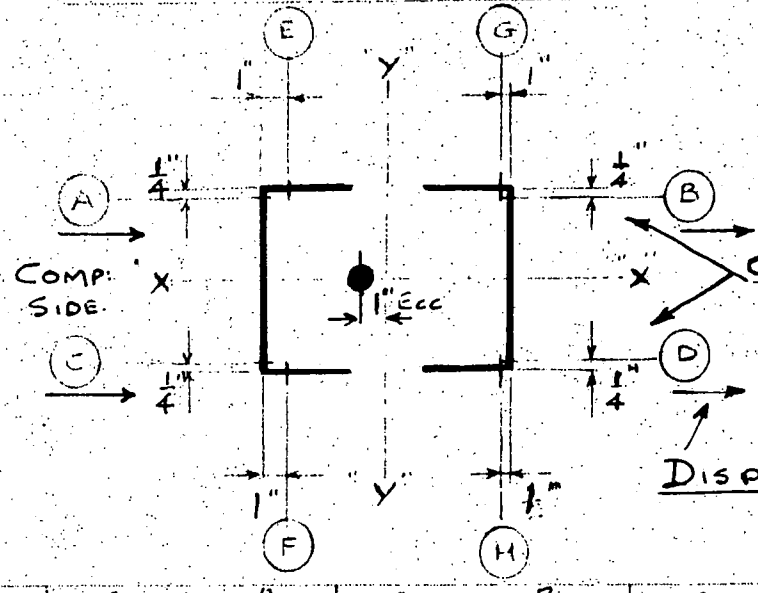

FIG 27

LOAD		GAUGE A			GAUGE B			GAUGE C			GAUGE D		
		READING	DISPLACEMENT		READING	DISPLACEMENT		READING	DISPLACEMENT		READING	DISPLACEMENT	
KN	TON		mm	IN		mm	IN		mm	IN		mm	IN
	0	·400		—	·109		—	·410		—	·070		—
	2	·395		·005	·113		·004	·402		·008	·077		·007
	4	·388	·305	·012	·118		·009	·394		·016	·086		·016
	6	·383		·017	·124		·015	·387		·023	·093		·023
	8	·376	·610	·024	·130		·021	·380		·030	·100		·030
100	10	·370		·030	·137		·028	·375		·035	·107		·037
	12	·364	·915	·036	·144		·035	·368		·042	·113		·043
	14	·357		·043	·151		·042	·361		·049	·120		·050
	15	·353		·047	·155		·046	·358		·052	·124		·054
	16	·350	1·270	·050	·159		·050	·354		·056	·128		·058
	17	·346		·054	·163		·054	·350		·060	·132		·062
	18	·341		·059	·167		·058	·346		·064	·136		·066
	19	·337		·063	·172		·063	·342		·068	·141		·071
200	20	·332	1·727	·068	·175		·066	·337		·073	·145		·075
	21	·327		·073	·182		·073	·332		·078	·151		·081
	22	·321	2·007	·079	·187		·078	·327		·083	·156		·086
	23	·316		·084	·193		·084	·323		·087	·161		·091
240	24	·308	2·337	·092	·200		·091	·316		·094	·169		·099
	25												
	26												
	27												
	28												
	29												
	30												

FAILURE LOAD 265 KN. (26·5 TON)

TEST Nº 4.

CLOCK-GAUGE READINGS

LATERAL DISPLACEMENT

POSITION BOTTOM OF STRUT.

GAUGE GRADUATIONS .001"

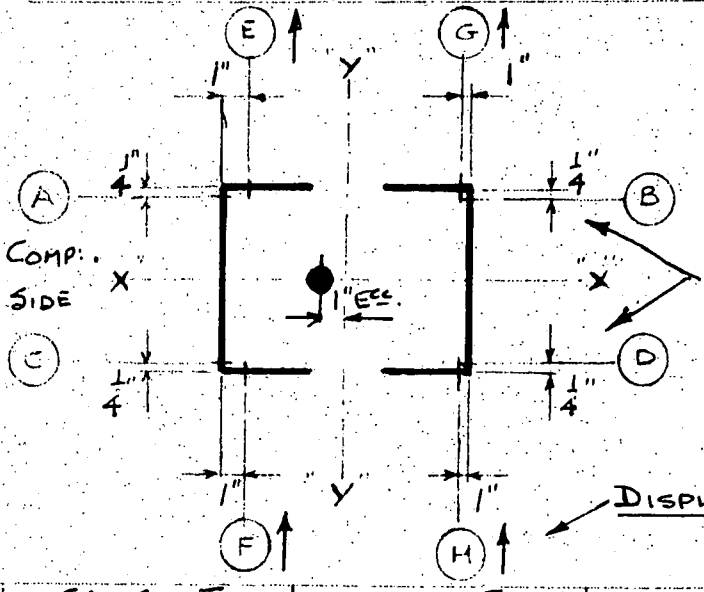

FIG 28

LOAD		GAUGE E			GAUGE F			GAUGE G			GAUGE H		
KN	TON	READING	DISPLACEMENT mm	DISPLACEMENT IN	READING	DISPLACEMENT mm	DISPLACEMENT IN	READING	DISPLACEMENT mm	DISPLACEMENT IN	READING	DISPLACEMENT mm	DISPLACEMENT IN
	0	·236		—	1·003		—	·257		—	1·006		—
	2	·236		·000	1·005		↓ ·002	·258		·001	1·002		·004
	4	·235		↓ ·001	1·005		↓ ·002	·259		·002	1·001		·005
	6	·235		↓ ·001	1·005		↓ ·002	·259		·002	1·000		·006
	8	·236		·000	1·005		↓ ·002	·260		·003	1·000		·006
100	10	·237		·001	1·004		↓ ·001	·260		·003	·999		·007
	12	·238		·002	1·004		↓ ·001	·260		·003	·999		·007
	14	·239		·003	1·003		·000	·260		·003	·998		·008
	15	·239		·003	1·002		·001	·260		·003	·998		·008
	16	·240		·004	1·002		·001	·261		·004	·997		·009
	17	·241		·005	1·001		·002	·261		·004	·997		·009
	18	·241		·005	1·001		·002	·261		·004	·997		·009
	19	·240		·004	1·000		·003	·261		·004	·996		·010
200	20	·243		·007	1·000		·003	·262		·005	·996		·010
	21	·244		·008	0·999		·004	·262		·005	·995		·011
	22	·245		·009	·998		·005	·263		·006	·994		·012
	23	·247		·011	·998		·005	·264		·007	·993		·013
240	24	·249		·013	·996		·007	·265		·008	·991		·015
	25												
	26	DISPLACEMENT AS			DISPLACEMENT AS								
	27	DIAGRAM ARROWS.			DIAGRAM ARROWS.								
	28	EXCEPT AT 4 & 6 TON			EXCEPT AT 2 TO 12 TON								
	29	LOAD.			LOADS INCLUSIVE.								
	30												

FAILURE LOAD 265 KN. (26·5 TON)

Consideration of the experimental findings will be divided into two sections. Axial and eccentrically loaded members will be considered separately.

Figs 20 to 28 inclusive have been included as a typical example of the main test readings taken for all struts tested. They serve as an indication of the type of data now available. Read in conjunction with Fig. 41.

8.3 Axially Loaded Struts - Tests Nos. 5 and 6

To provide confirmation for the theory already presented in Chapter 4 two struts were tested under axial load. Some bending, due to "lack of straightness", will certainly exist with any axially loaded member.

With this thought in mind; struts $M\frac{k}{-}$ S2 were selected. These exhibited rather more "lack of straightness" than the remainder and represented a condition likely to occur frequently in practice. The "bow" in the struts was confined mainly to the axis which would cause bending in the plane of the battens. This will have resulted chiefly from welding.

Reference to Chapter 4 will indicate that if the Euler loads only are considered, elastic failure should occur on the weaker x-x axis, in a direction at $R^t\angle's$ to the battens. This is assuming the strut works as a homogeneous unit.

Under these conditions the predicted failure would be by overall column buckling, at the load P_E = 309 kN (30.9 ton). The battens would NOT, in theory, be expected to contribute much to the ultimate strength of the struts, other than ensure that the components worked as a homogeneous unit. Battens were spaced at 1041.5 mm (3'-5") centres, well in excess of the code maximum of 863.5 mm (2'-10"). This was not initially considered important.

Testing however revealed that where "lack of straightness" induced some degree of bending in the plane of the battens earlier thinking was not valid. The bending caused a load differential between the main channels and in both tests deflection in the plane of the battens continued right up to failure. The mode of ultimate collapse was not apparent until the last increment of load. It finally occurred on the x-x axis as the Euler prediction, at loads of 371 kN (37.1 ton) and 331 kN (33.1 ton) for Tests 5 and 6 respectively. Inelastic effects undoubtedly accounted for the load carrying capacity being in excess of the Euler load of 309 kN. Some ball "sticture" seems possible in Test 5 and a vibrator, operated during the application of the load, would have helped.

The important observation however was that the channels did not buckle simultaneously and it became obvious that lateral instability existed in the channel carrying the

most direct load plus bending. Battens bent freely on their weak (thin) axis, rotating about the welds at the junction between the plates and the channel toes.

Reference back to Chapter 4 and Figs 11 and 12 shows that Konigsberger and Mohsin, when considering "lack of straightness", causing bending in the plane of the battens, predicted that buckling of a single channel between the battens would not be a problem, with battens at 1041.5 mm centres. They did however predict that with battens spaced at this dimension overall column buckling in the plane of the battens would occur at 273 kN (27.3 ton). The present tests show this to be incorrect both for magnitude of load and axis of failure as lateral stiffness was not considered by them.

It should however be pointed out that the deflections, (7.75 mm (0.3 in) and 12.9 mm (0.5 in) for Tests 5 and 6 respectively) occurred on the axis parallel to the battens whilst virtually no lateral deflection took place on the axis of final failure until almost the last increment of load. Until the last stages, the predictions of Konigsberger and Mohsin for y-y (strong axis) failure looked highly probable. Referring again to Fig. 12 (Chapter 4) it will be seen that with battens spaced at 836.5 mm (2'-10") centres, and using an effective length of 0.85 a failure of 310 kN (31.0 ton) was predicted. This value is identical to the Euler value for failure on the x-x (weak) axis. Simultaneous failure on both axes would be an ideal solution but batten proportions and

spaces will not support this in practice.

After careful consideration of the test data, inspection of film and the visual inspection of the struts tested, it was considered that ultimate failure occurred on the x-x (weak) axis. It was thought to be an Euler type failure culminating in the channel carrying most load buckling laterally, over the full length of the strut. Thus the theory of Konigsberger & Mohsin (which was developed via Timoshenko) is unlikely to be applicable in practice unless adequate lateral restraint is provided to ensure failure occurs by buckling in the plane of the battens. The "stiffness" of the battens in a lateral direction will not only dictate the ultimate strength of the strut but also the frequency and character of any lateral restraints required.

The tests used the minimum proportioned battens permitted by the code and will investigate the possible loads at the various batten spacings. As has now been resolved, the approach for both axial and eccentrically loaded struts will be compatible as no axially loaded strut will be without some bending.

Figs 29 and 30 give the strut layouts and gauge locations for the axial Tests Nos. 5 and 6. The precise plan locations of the clock gauges will follow the general pattern depicted by the typical test figures shown in Figs. 23 to 28 .

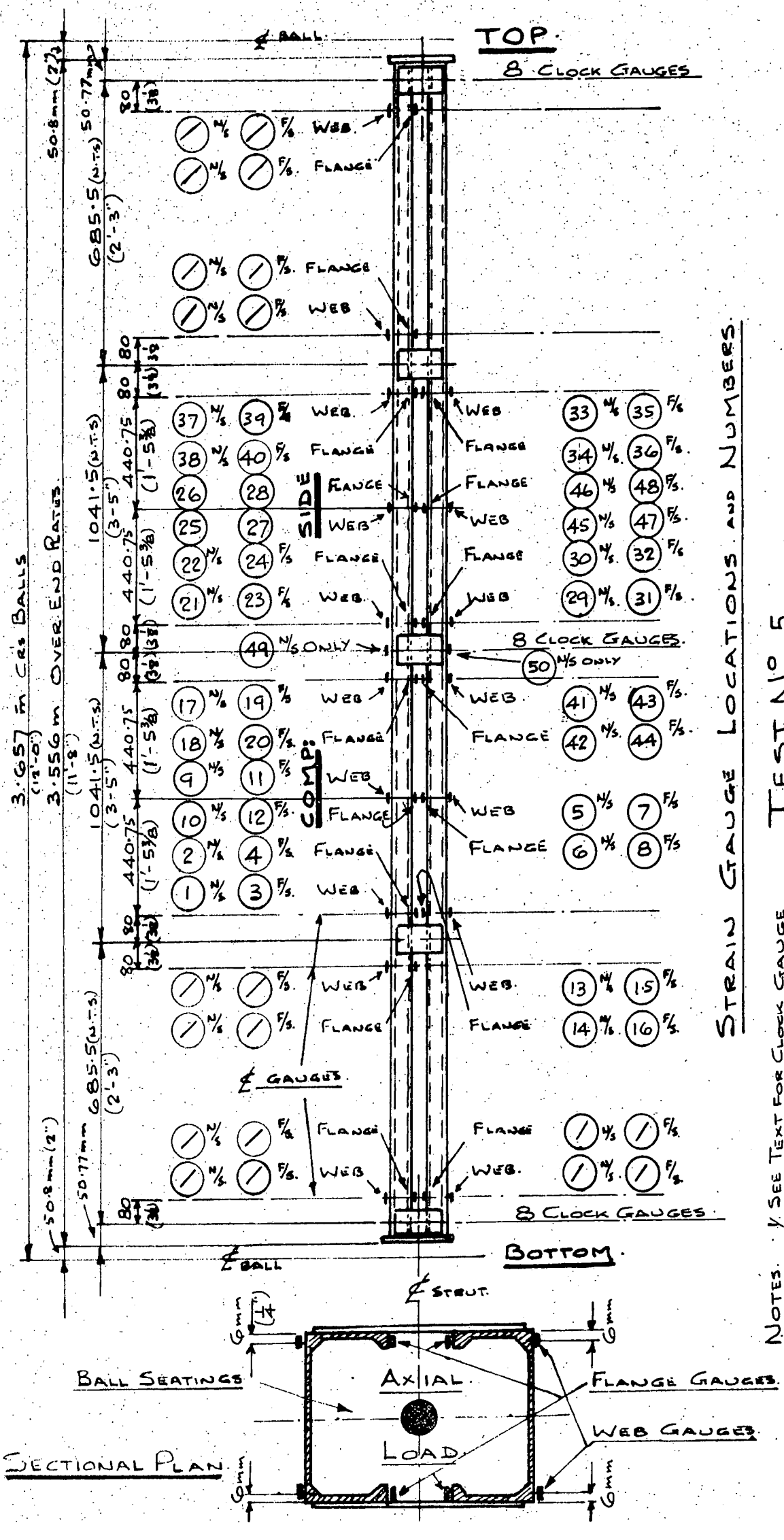
TOP.
8 CLOCK GAUGES
℄ BALL
50.8mm (2")
50.77mm
685.5 (N.T.S) (2'-3")
1041.5 (N.T.S) (3'-5")
440.75 (1'-5⅜")
80 (3⅛")
3.657 m C/c BALLS (12'-0")
3.556m OVER END RATES (11'-8")
WEB.
FLANGE
SIDE
COMP:
8 CLOCK GAUGES.
49 N/S ONLY
50 N/S ONLY
℄ GAUGES.
BOTTOM.
℄ BALL
℄ STRUT.
BALL SEATINGS
AXIAL LOAD
FLANGE GAUGES.
WEB GAUGES.
SECTIONAL PLAN.
N/S DENOTES NEAR SIDE
F/S " FAR "
STRAIN GAUGE LOCATIONS AND NUMBERS.
TEST No 5
USING STRUT MK S2
FIG: 29
NOTES. 1/ SEE TEXT FOR CLOCK GAUGE PLAN LOCATION AND LETTERS.
2/ COMPRESSION SIDE DESIGNATED FROM LACK OF STRAIGHTNESS.

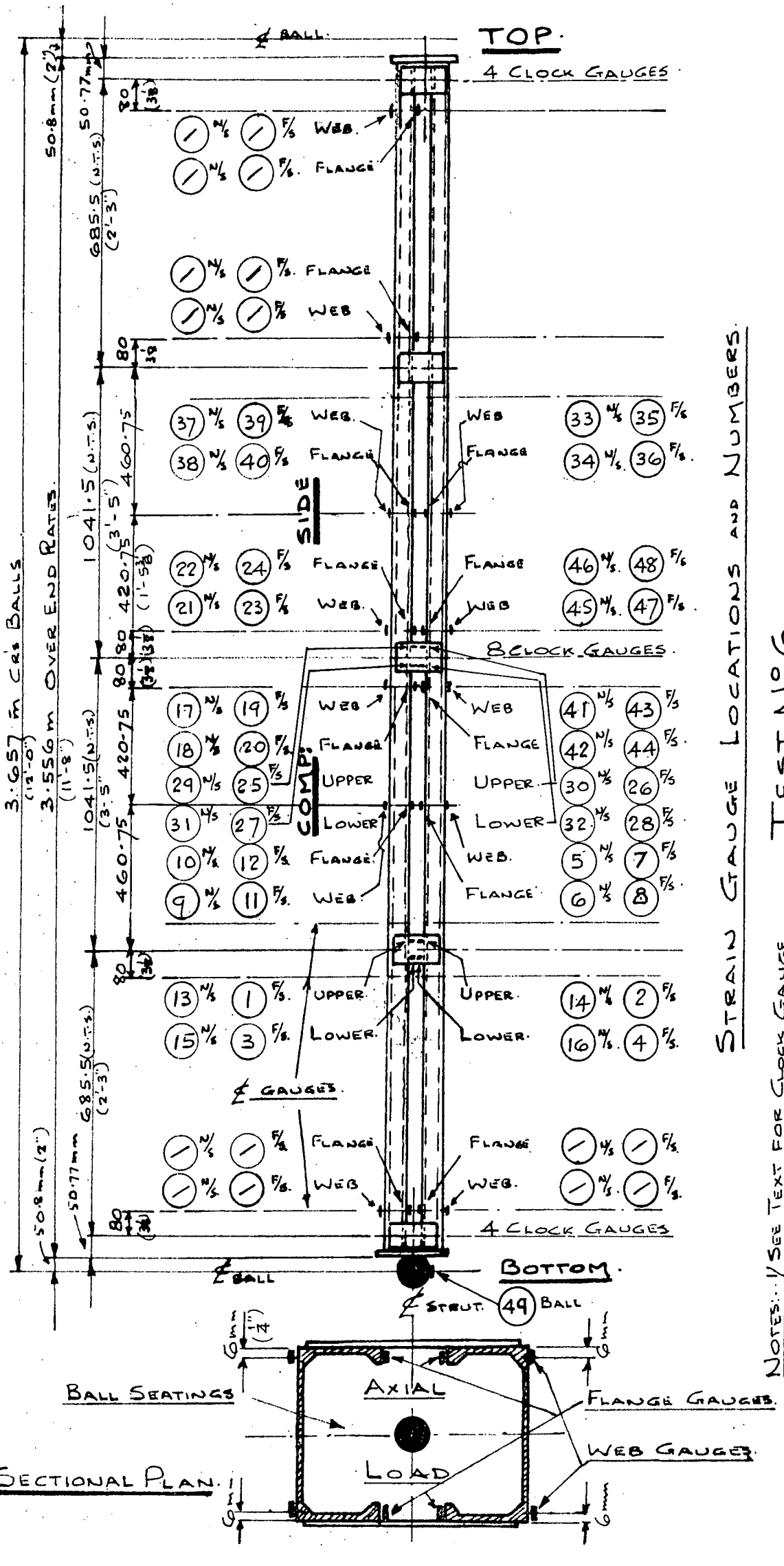

STRAIN GAUGE LOCATIONS AND NUMBERS.

TEST N° 6

USING STRUT MK S2.

FIG: 30

N/S DENOTES NEAR SIDE

F/S " FAR "

NOTES: 1/ SEE TEXT FOR CLOCK GAUGE PLAN LOCATION AND LETTERS.

2/ COMPRESSION SIDE DESIGNATED FROM LACK OF STRAIGHTNESS.

FIG: 31 THEORETICAL DEFLECTION VALUES (DUE TO LACK OF STRAIGHTNESS) FOR AXIAL LOADING.

INCREMENT OF LOAD P KN	DEFLECTION a FROM SINUSOIDAL B.M. $a = \frac{Py L^2}{\pi^2 E I_y}$		AMPLIFICATION FACTOR FOR SINUS B.M. DEFLECTION $a = Ka = \frac{1}{1 - P/P_E}$	TOTAL DEFLECTION $Ka\,a = e_{TOT}$	
	TEST 5	TEST 6	TESTS 5 & 6.	TEST 5	TEST 6
25	0·092	0·104	1·02	0·094	0·106
50	0·18	0·21	1·04	0·19	0·22
75	0·27	0·31	1·15	0·31	0·36
100	0·37	0·42	1·19	0·44	0·50
125	0·46	0·52	1·26	0·58	0·66
150	0·55	0·63	1·33	0·63	0·84
175	0·64	0·73	1·41	0·90	1·03
200	0·74	0·84	1·49	1·10	1·25
225	0·83	0·94	1·62	1·34	1·52
250	0·92	1·04	1·73	1·59	1·80
275	1·01	1·15	1·86	1·88	2·14
300	1·10	1·25	2·01	2·21	2·51

GENERAL DATA.

NOTE:- INITIAL LACK OF STRAIGHTNESS AT MID HEIGHT WAS RATHER MORE FOR STRUTS Mks 52 THAN THE REMAINDER. FOR THIS REASON THEY WERE CHOSEN FOR TESTS 5&6 AS LACK OF STRAIGHTNESS ON THE Y-Y (STRONG) AXIS COULD WELL PROVE INTERESTING WITH AXIALLY LOADED STRUTS. THE REMAINDER OF THE STRUTS - WITH LESS LACK OF STRAIGHTNESS - WOULD ALSO ENABLE AN AVERAGE FIGURE TO BE USED FOR THE ECCENTRICALLY LOADED STRUTS. TO MINIMISE CALCULATION.

LACK OF STRAIGHTNESS ON Y-Y AXIS.

TEST 5 = 2·2mm TEST 6 = 2·5mm.

LACK OF STRAIGHTNESS ON x-x AXIS

NEGLIGIBLE ON BOTH STRUTS.

NOTATION.

P = INCREMENTAL LOAD -(KN)

y = INITIAL (LACK OF STRAIGHTNESS) SINUSOIDAL ECCENTRICITY. SEE ABOVE

a = DEFLECTION DUE TO Py (mm)

Ka = AMPLIFICATION FACTOR.

E = 68,700 N/mm²

I_y = 1179·6 cm⁴ (STRONG AXIS)

L = 3657mm (LENGTH CR's BALL PIVOTS)

NOTE:- THE LACK OF STRAIGHTNESS WILL PROMOTE BENDING IN THE PLANE OF THE BATTENS. I.E. BENDING ON Y-Y AXIS 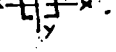

, APPLICABLE VALUE FOR $P_E = \frac{\pi^2 E I_y}{L^2} = 598$ KN.

READ IN CONJUNCTION WITH FIG: 35

FIG:32 THEORETICAL VALUES OF $\frac{P}{P_0}$ AND $\frac{M}{M_0}$ FOR LACK OF STRAIGHTNESS ON AXIALLY LOADED STRUTS.

INCREMENT OF LOAD P KN	$\frac{P}{P_0}$	THEORETICAL DEFLEC: $K_a Q = e_{TOT}$		THEORETICAL MOMENT $P_E = M$.		$\frac{M}{M_0}$	
		TEST 5	TEST 6	TEST 5	TEST 6	TEST 5	TEST 6
25	0·08	0·09	0·11	2·3	2·8		
50	0·16	0·19	0·22	9·5	11·0		
75	0·24	0·31	0·36	23·3	27·0		
100	0·32	0·44	0·50	44·0	50·0		
125	0·40	0·58	0·66	72·5	82·5		
150	0·48	0·63	0·84	94·5	126·0		
175	0·57	0·90	1·03	157·5	180·3		
200	0·65	1·10	1·25	220·0	250·0	·010	·011
225	0·73	1·34	1·52	301·5	342·0	·014	·015
250	0·81	1·59	1·80	397·5	450·0	·018	·021
275	0·89	1·88	2·14	517·0	588·5	·024	·027
300	0·97	2·21	2·51	663·0	753·0	·031	·035

FROM FIG 31.

2 TYPICAL

2 TYPICAL

THEORETICAL VALUES FROM CHAPTER 4.

$P_0 = P_E = \frac{\pi^2 E I_x}{L^2}$

WHERE P_E = EULER CRIPPLING LOAD TAKEN ON THE X-X (WEAK) AXIS OF THE COMPLETE STRUT.

$\therefore P_0 = 309\,KN$ (30·9T)

= AXIAL CRIP: LOAD.

NOTE:- THE KONIGSBERGER MONSIN PREDICTION OF PCRIT AT 273 KN (27·3T) FOR THE AXIALLY LOADED STRUTS, WITH BATTENS SPACED AT 1041·5 mm, AND BUCKLING ON THE Y-Y AXIS (PARALLEL TO BATTENS), HAS BEEN IGNORED AT THIS STAGE. THE LACK OF STRAIGHTNESS CAUSING BENDING IN THIS PLANE, WITH THE AXIAL LOADING, DID NOT CONFIRM THAT THIS WAS TRUE. BUCKLING TOOK PLACE ON THE X-X AXIS

M_0 = CRIPPLING MOMENT (WITH NO END LOAD)

$M_0 = f_y . A_c . d .$

$M_0 = 2133 \times 10^4$ Nmm.

(84·2 TON IN)

NOTATION.

P = INCREMENTAL LOAD - KN.

e_{TOT} = TOTAL THEORETICAL DEFLECTION FROM FIG:- GIVING ECCENTRICITY FOR P.

$M = P e_{TOT}$ - Nm (KNm)

FIG: 33 ACTUAL MID-HEIGHT DEFLECTIONS UNDER AXIAL LOAD.

DATA ABSTRACTED FROM TEST RESULTS. BENDING ON Y-Y AXIS.

INCREMENTS OF LOAD P.	TEST Nº5	TEST Nº6	GENERAL DATA
40	0·31	0·79	CLOCK GAUGE READINGS. THE DEFLECTION FIGURES GIVEN ARE ACTUAL MID-HEIGHT READINGS. THEY HAVE NOT BEEN ADJUSTED TO COVER FOR THE DISPLACEMENT AT THE TOP AND BOTTOM OF STRUT. AS COMPARED WITH ECCENTRIC LOADING THE AXIAL LOADING DISPLACEMENT WAS SO SMALL THE TOP & BOTTOM MOVEMENTS (0·007)mm AT 320KN) WERE NEGLECTED.
80	0·48	1·37	
120	0·74	2·03	
160	1·12	3·02	
200	1·47	4·22	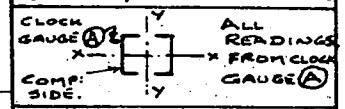
240	1·96	5·89	PAIRING OF STRUTS. TESTS 5 AND 6 HAVE IDENTICAL BATTEN SPACING.
280	2·69	8·43	
300	3·18	10·37	
330	4·29	13·21	
360	7·75		
TEST LOAD AT FAILURE →	371	331	LOAD P – KN.
THEODOLITE READING AT FAIL: →	10·9	15·3	DEFLECTION – mm.

FIG:-34 COMPUTATION OF TEST VALUES TO ESTABLISH $\frac{P}{P_o}$ AND $\frac{M}{M_o}$ FOR AXIAL LOAD.

INCREMENT OF LOAD P	$\frac{P}{P_o}$	TEST Nº5 e_{TOT}	TEST Nº5 $M = Pe_{TOT}$	TEST Nº5 $\frac{M}{M_o}$	TEST Nº6 e_{TOT}	TEST Nº6 $M = Pe_{TOT}$	TEST Nº6 $\frac{M}{M_o}$
40	0·129	0·31	12	0·001	0·79	32	0·002
80	0·26	0·48	38	0·002	1·37	110	0·005
120	0·39	0·74	89	0·004	2·03	244	0·011
160	0·52	1·12	179	0·008	3·02	484	0·022
200	0·65	1·47	294	0·014	4·22	844	0·039
240	0·78	1·96	470	0·022	5·89	1413	0·066
280	0·90	2·69	753	0·035	8·43	2370	0·111
300	0·98	3·18	954	0·045	10·37	3111	0·146
330	1·07	4·29	1416	0·066	15·25	5048	0·236
360	1·16	7·75	2770	0·130			
FAILURE VALUES $e_{TOT.}$		10·9	4053	0·19	15·3	5064	0·23
TEST LOAD AT FAILURE. KN		371			331		
$\frac{P}{P_o}$ AT FAILURE		1·20			1·07		

THEORETICAL VALUES (FROM CHAPTER 4)

$P_o = P_E = \frac{\pi^2 E I_x}{L^2}$

WHERE P_E IS THE EULER CRIPPLING LOAD TAKEN ON THE "X-X" (WEAK) AXIS OF THE COMPLETE STRUT

AXIAL STRUT LOAD.

$P_o = 309$ KN. (30·9 TON)

M_o = CRIPPLING BENDING MOMENT WITH NO END LOAD. AXIS Y-Y

$M_o = f_y . A_c . d .$

$M_o = 2133 \times 10^4$ N mm (84·2 TON IN)

TEST VALUES. (ABSTRACTED FROM TEST DATA APPENDIX).

P = INCREMENTAL TEST LOAD – UP TO FAILURE IN KN.

e_{TOT} = TOTAL LATERAL DEFLECTION AT MID-HEIGHT, UNDER LOAD. DUE TO LACK OF STRAIGHTNESS AND. CAUSING BENDING ON Y-Y AXIS.

TEST LOAD DEFLECTIONS. AT MID-HEIGHT READ FROM CLOCK GAUGE (A)

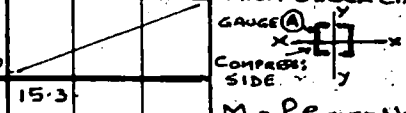

$M = Pe_{TOT} = Nm$ (KN mm)

NOTE:- e_{TOT} VALUES AT FAILURE INCLUDE THEODOLITE READINGS IN LIEU OF CLOCK GAUGES.

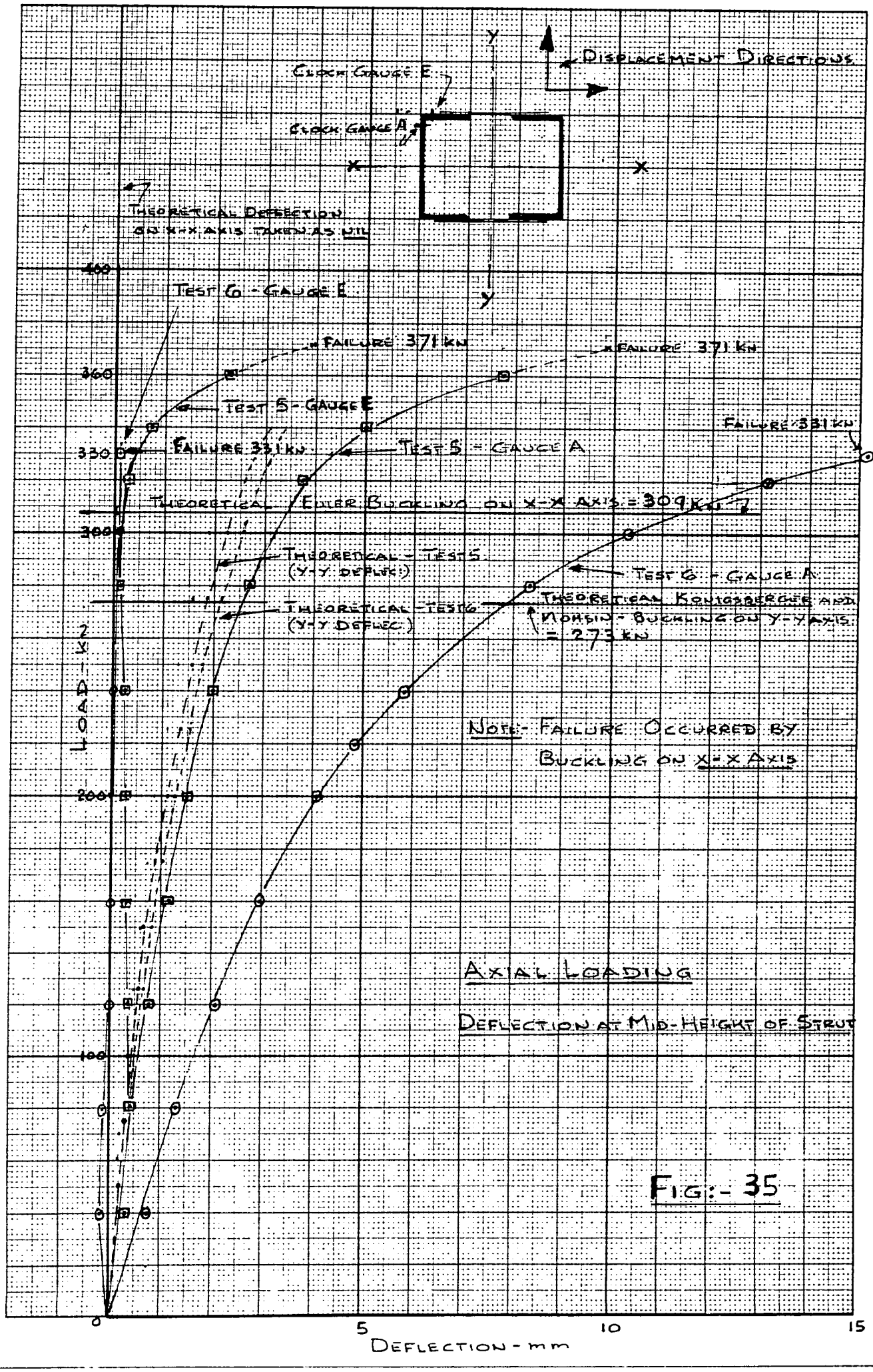

Note:- Failure Occurred by Buckling on X-X Axis

Axial Loading

Deflection at Mid-Height of Strut

Fig:- 35

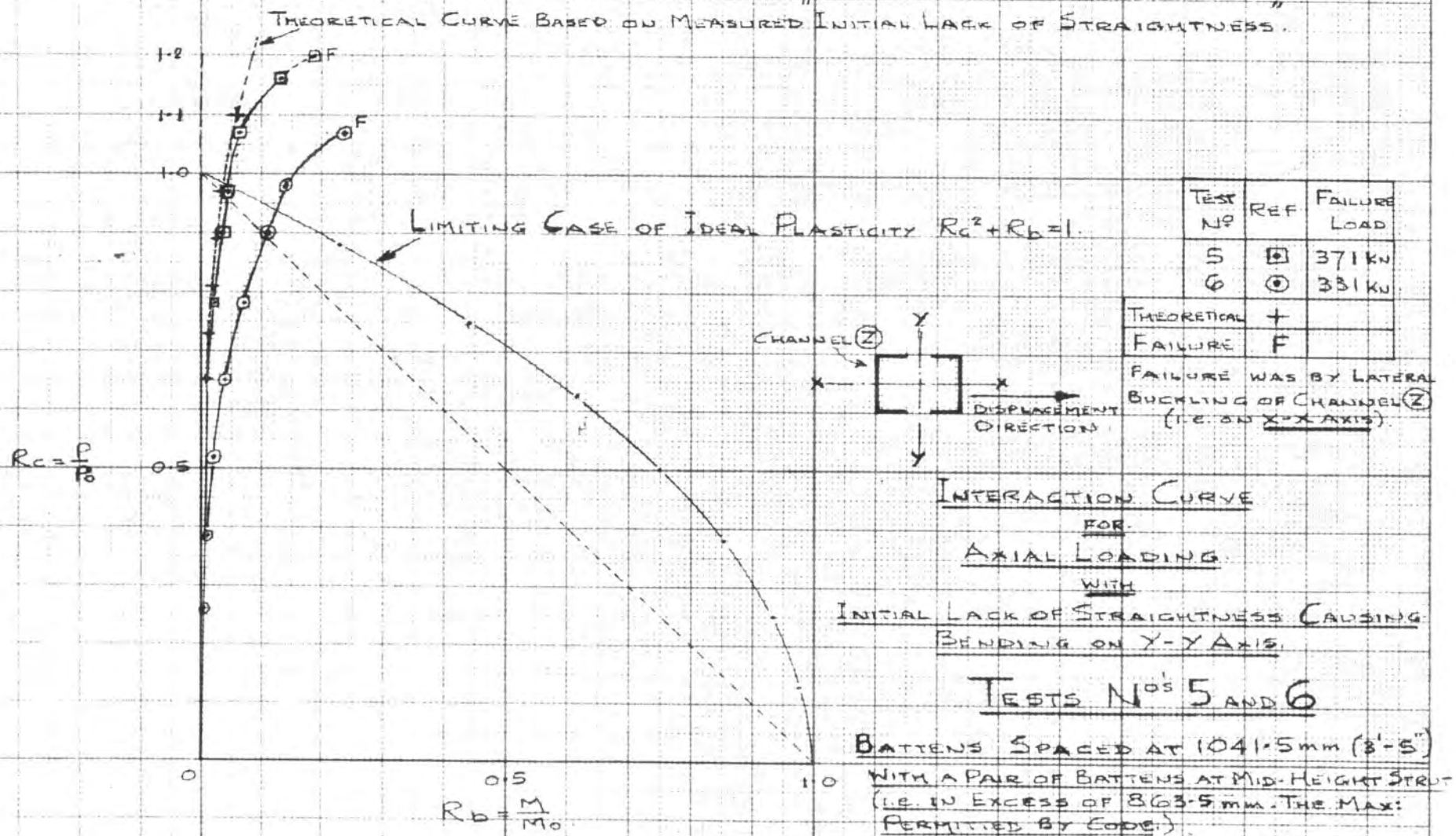

INTERACTION CURVE
FOR
AXIAL LOADING
WITH
INITIAL LACK OF STRAIGHTNESS CAUSING BENDING ON Y-Y AXIS.

TESTS Nº's 5 AND 6

BATTENS SPACED AT 1041·5mm (3'-5")
WITH A PAIR OF BATTENS AT MID-HEIGHT STRUT
(I.E. IN EXCESS OF 863·5mm. THE MAX: PERMITTED BY CODE).

FIG:- 36

Figs. 31 and 33 are self explanatory and give all the calculation method and necessary data for the establishment of the theoretical and actual deflection curves shown in Fig. 35 .

Similarly Figs 32 and 34 give the theoretical and actual load/moment apportionment culminating in these being plotted on the interaction curve shown in Fig. 36 .

In both cases the values have been plotted, in suitable increments, right up to ultimate failure. For axial loading, with only a small amount of bending, the values plotted are naturally in close proximity to the direct load line. Interaction is thus very small in this case. Bending on the x-x axis is also very small and was initially ignored.

Knowing that for several of the tests failure occurred by the ultimate lateral movement at mid-height, an attempt will be made to establish how this was "triggered off". Did local buckling play a part?

IMPORTANT NOTE

Reference to the following Interaction Curves for both axial and eccentric loading will reveal that a curve for "IdealPlasticity" has been included. This was mentioned in Chapter 4 and represents the condition for a solid rectangular member.

A homogeneous section such as an I beam has the bulk of material adjacent to its extreme fibre. It is therefore efficient in bending and the inelastic effect is generally negligible.

With the type of beaded section being used, which has concentrated areas of material (i.e. flange lips) well removed from the extreme web fibres relative to the y-y axis, the inelastic effect is difficult to predict. The situation is further aggravated by the fact that it is only battened at intervals along its length.

Reference to the actual test strain gauge readings in the area of ultimate failure, particularly with eccentric loading, reveal a wide stress variation across the section. This is true not only when comparing the web strains of the two channels, (as would be expected) but also between the back of the web and the tip of the flange of the channel carrying most load. The strain readings referred to were taken just before failure and suggest that even after the web has yielded, some reserve of strength exists in the flange beads. This may well be important when considering the lateral instability of one channel.

To suggest a "Limit of Ideal Plasticity" for a composite section behaving in this fashion is not justified without research into its inelastic behaviour. This should involve tests at various moment arms to establish a suitable interaction curve. Reference will however be made to the plastic limit line indicated to see how the section

compares with a solid rectangle. It will be seen from the graphs that in most tests the theoretical and test readings look compatible at this level. It could provide a factoring datum for future inelastic investigations.

Having stated the problem which exists for inelastic analysis of the test readings, investigations will now proceed using the elastic limit as a basis for calculation.

Overall Stability

Critical overall slenderness $= \frac{L}{r_x} = \frac{3657}{5.13 \times 10} = 71.5$

Critical slenderness of one channel between battens $= \frac{L}{r_y} = \frac{1041.5}{2.26 \times 10} = 46.7$

(or possibly $0.8 \times 4.67 = 37.5$)

Strong axis slenderness of complete section $= \frac{L}{r_y} = \frac{3657}{7.11 \times 10} = 51.4$

Criterion $= \frac{L}{r_x} = 71.5$ giving comp. stress Fig. 2 =

$= \underline{136\ N/mm^2}$ $(8.6 T/in^2)$

Where overall column buckling is the criterion this is the maximum elastic stress value which can be safely worked to.

The Elastic critical load $P_o = \underline{309\ kN\ (30.9\ ton) = P_E}$.

Note:- Konigsberger and Mohsin predicted failure on the other (i.e. strong) axis at 273 kN (27.3 ton). This has been ignored at present.

Criterion for bending laterally (see Chapter 4) =

$= 136\ N/mm^2$ $(8.6\ T/in^2)$

This maximum elastic stress gives M_o = 2133×10^4 N mm

Theoretical Values

At Onset of Plasticity

From Fig. 36 the ratio of $\frac{P}{P_o}$ and $\frac{M}{M_o}$ are 0.97 and 0.0385 respectively.

$\therefore$ Direct Load = $P = P_o \times .97$

$= 309 \times .97 = 303$ kN

Bending $= M = M_o \times 0.035$

$= 21330 \times 0.035 = 748$ Nm

Thus Direct Stress = $\frac{\text{Load}}{\text{Area}} = \frac{303 \times 10^3}{2334} = 130.2\ N/mm^2$

Av. Bending Stress = $\frac{M}{Ac.d} = \frac{748 \times 10^3}{11.67 \times 10^2 \times 135.4} = 4.7\ N/mm^2$

$134.9\ N/mm^2$

This checks with 136 N/mm^2 Overall Stability Criterion.

At Projected Limit of Ideal Plasticity

Again using Fig. 36 the theoretical values at this level are:-

Direct stress = 131 N/mm^2

Av. bending stress = 5.4 N/mm^2

Total = 136.4 N/mm^2

Test Values

Using the same method as for the theoretical values the total average stresses at, onset of plasticity, limit of ideal plasticity, last load increment at which strain readings were taken before failure and at failure, were established. These are given in Fig. 37 and are self explanatory.

Fig. 38 gives strain gauge readings and the resulting stresses for selected gauges at the same locations. The readings given are the highest for each strut, irrespective of their position.

In considering the struts generally, the most highly stressed areas are at mid-height. The gauges at $\frac{1}{4}$ point level gave readings approaching those at mid-height. Batten bending stresses were not high, but it was apparent that both battens at mid-height were in tension, whilst at $\frac{1}{4}$ points bending did exist across the battens. It was interesting to note that at $\frac{1}{4}$ points the highest strains were at the channel flange tips, indicating a "wave" action over the length of the strut. Gauges at the mid-panel positions were somewhat lower in value, but still relatively high.

Gauges No's 19 and 23 both on the web, $^{F}/_{S}$, at about mid-height, (See Figs. 29 and 30) had the highest readings on both struts. Their position also gave an indication of the direction of lateral movement at failure. The gauge ring 80 mm below mid-ht. (Test 6) was analysed for comparisons with average stresses derived from the interaction curves. Figs. 37 & 38. The detailed investigation was carried out at the last reading before failure. (See Page 211).

FIG:37 ESTABLISHMENT OF TOTAL AVERAGE STRESS AT VARIOUS LOCATIONS-FROM INTERACTION CURVES.

LOCATION	TEST Nº.	VALUES FROM FIG 34 AND INTERACTION CURVE FIG 36				DIRECT STRESS. $= \frac{P}{AREA}$	AV. BENDING STRESS $= \frac{M}{Ac.d}$	TOTAL AV. STRESS. (N/mm^2)
		$\frac{P}{P_o}$	$\frac{M}{M_o}$	DIRECT LOAD P. (KN)	BENDING M. (Nm)			
AT ONSET OF PLASTICITY.	5	0·96	0·05	296	952	128	6	134
	6	0·89	0·11	275	2340	118	15	133
AT PROJECTED LIMIT OF IDEAL PLASTICITY.	5	0·98	0·05	303	953	130	6	136
	6	0·94	0·13	290	2775	124	18	142
AT LAST STRAIN READING WHEN P=360 TEST 5 =330 TEST 6.	5	1·16	0·13	360	2770	154	18	172
	6	1·07	0·24	330	5048	142	32	174
AT 371 KN	5	1·20	0·19	371	4053	159	26	175
FAILURE 331 KN	6	1·07	0·23	331	5064	142	32	174

FIG:-38 ESTABLISHMENT OF ACTUAL STRESSES FROM STRAIN GAUGE READINGS AT GIVEN CRITICAL LOCATIONS.

TEST Nº 5 (FAILURE 371 KN).

GAUGE Nº	LOCATION	STRAIN READINGS.-(GAUGE FACTOR 2·08)			CALCULATED STRESSES N/mm²		
		AT ONSET OF PLASTICITY. P AT 295 KN (INTERPOL.)	AT PROJECTED LIMIT OF IDEAL PLASTICITY P AT 300 KN (NEAREST)	AT LAST STRAIN READING WHEN P = 360 KN.	AT ONSET OF PLASTICITY P AT 295 KN (INTERPOL.)	AT PROJECTED LIMIT OF IDEAL PLASTICITY. P AT 300 KN (NEAREST).	AT LAST STRAIN READING WHEN P = 360 KN.
19	WEB - NEXT TO MID HEIGHT	0·719 DIV n = 2	0·732 DIV n = 2	0·510 DIV n = 1	118	121	168
23	WEB - NEXT TO MID HEIGHT	0·699 "	0·713 "	0·504 "	115	118	166
32.	FLGE - NEXT TO MID HEIGHT	0·690 "	0·703 "	0·491 "	114	116	162
44.	FLGE - NEXT TO MID HEIGHT	0·720 "	0·730 "	0·511 "	118	120	169

NOTE: STRESS READINGS DERIVED FROM STRESS = STRAIN × E. STRESS = $\frac{\text{STRAIN}}{\text{G.FAC} \times 100} \times E \times \text{DIV } n$

A.R. = STRAIN.
GAUGE FACTOR = 2·08
E = 68 700 N/mm².
$n = \left(\frac{100\,AR}{R}\right)$.

TEST Nº 6. (FAILURE 331 KN).

GAUGE Nº	LOCATION.	STRAIN READINGS.-(GAUGE FACTOR 2·08)			CALCULATED STRESSES N/mm²		
		AT ONSET OF PLASTICITY P AT 275 KN (INTERPOL.)	AT PROJECTED LIMIT OF IDEAL PLASTICITY P AT 290 KN.	AT LAST STRAIN READING WHEN P = 330 KN	AT ONSET OF PLASTICITY P AT 275 KN (INTERPOL.)	AT PROJECTED LIMIT OF IDEAL PLASTICITY. P AT 290 KN.	AT LAST STRAIN READING WHEN P = 330 KN.
19	WEB - NEXT TO MID-HEIGHT	0·770 DIV n = 2	0·827 DIV n = 2	0·529 DIV n = 1	127	136	174
23	WEB - NEXT TO MID-HEIGHT.	0·783 "	0·842 "	0·540 "	129.	139	178
48 (AS 32 TESTS)	FLGE MID PANEL UPPER.	0·692 "	0·741 "	0·464 "	114	122	151
44	FLGE - NEXT TO MID HEIGHT	0·679 "	0·730 "	0·454 "	112	120	149

TEST No. 6.

LOAD 330KN. LAST STRAIN READINGS BEFORE FAILURE (331KN).

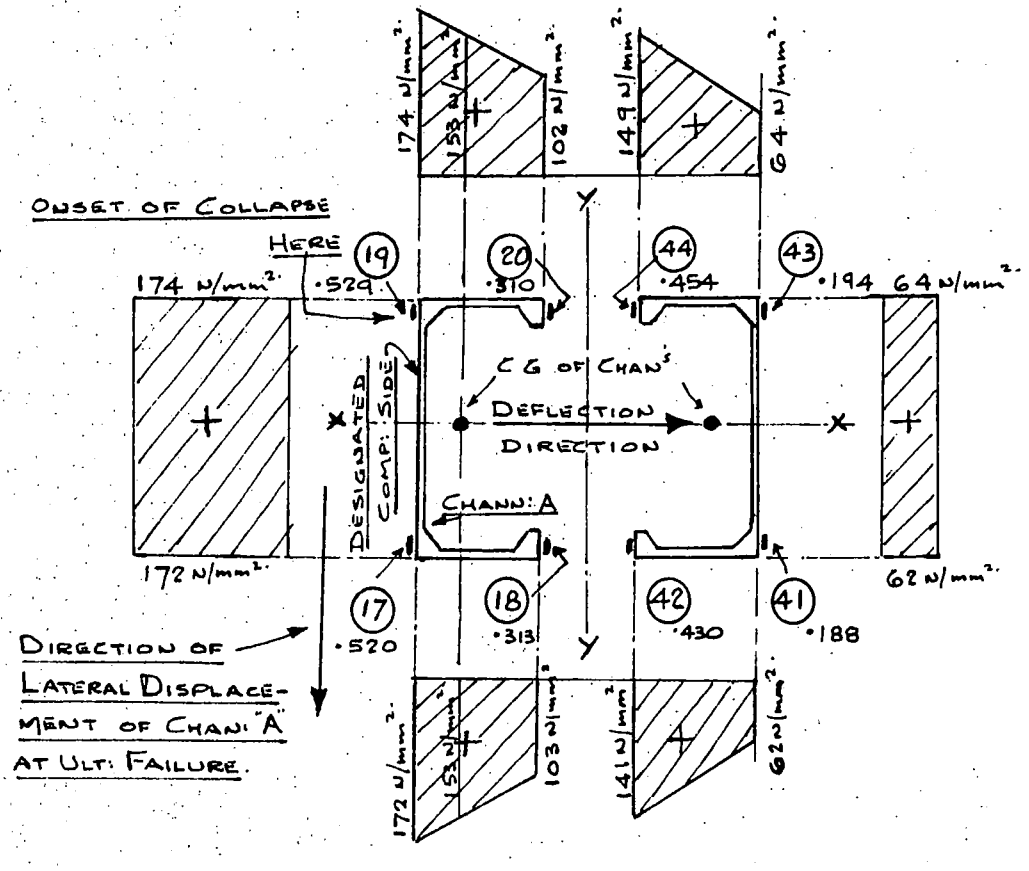

STRESS DISTRIBUTION ACROSS SECTION.

GAUGES 80mm BELOW MID-HEIGHT.

THE ABOVE DIAGRAM ILLUSTRATES THE INTERESTING SITUATION THAT FULL PLASTICITY IS NOT PRESENT IN THE "COMPRESSION SIDE" CHANNEL, EVEN AT THIS VERY HIGH LOAD (WITHIN 1 KN OF FAILURE). IT MAY BE THAT THE WEB AND ROOT FILLETS ARE FULLY PLASTIC BUT THE FLANGE FILLETS OF THE SAME CHANNEL ARE STILL IN THE ELASTIC RANGE. AN ELASTO-PLASTIC CONDITION THEREFORE EXISTS.

NOTE.

THE "PROJECTED INTERACTION CURVE FOR IDEAL PLASTICITY", WHICH WAS PURELY AN INITIAL ASSUMPTION, MUST THEREFORE ONLY BE REGARDED AS A "FACTORING BASE LINE".

WHILST THE ABOVE STRAIN READINGS WERE TAKEN WITHIN 1KN OF ULTIMATE FAILURE IT MUST BE REMEMBERED THAT THE GAUGES WERE SITUATED 80mm FROM MID-HEIGHT. BUCKLING COMMENCED AT EXACTLY THE MID-HEIGHT. GAUGES AT OTHER LOCATIONS ON THE STRUT AND AT OTHER LOAD LEVELS SHOW THE SAME GOOD AGREEMENT WITH RESULTS DERIVED FROM THE INTERACTION CURVES.

In summarising, the first consideration must be to establish what "triggered" failure. Lateral instability of Channel "A" is considered to be the cause. The basis for this view being that the highest web stress is considerably less than the local buckling values given in Chapter 6, and those set up in the eccentrically loaded struts. This precludes local buckling as the trigger.

The stress distribution, (see page 211) shows that the web and its root fillets are in plasticity but the flange lips are not. The predicted "onset of plasticity" is at about 136 N/mm^2, which value has been well exceeded in the web of Channel "A".

Collapse commenced exactly at mid-height, adjacent to gauge 19, at the corner of highest stress, which will be nominally higher than 174 N/mm^2 taken about 80 mm away. The collapse of the corner root fillet immediately raised the stresses in the web and flange which then buckled locally. With the whole web in the plastic range and the flange tips not, lateral movement occurred along the line of the web in the obvious direction as indicated. See Plates 13 and 14.

This confirms that the failure was by lateral instability of one channel. Thus battens will influence failure load, as their spacing and stiffness will control the lateral movement. This will be discussed further with the eccentrically loaded struts.

The interaction curve approach, suitably factored for plasticity, is ideal, as eccentric loading will establish.

CONCLUSIONS therefore are that until lack of straightness reaches such proportions that deflection is large and local buckling of channel "A" web takes places, failure will be by lateral buckling of the same channel. This will occur in an elasto-plastic situation at values in excess of the Euler Load of 309 kN.

8.4 Eccentrically loaded Struts - Test No's. 1 to 4, 7 to 10 and 11 Inclusive

Five pairs of struts and a special were tested with the loading 25.4 mm eccentric along the major axis parallel to the battens. They were all so arranged that any moment due to "lack of straightness" would be additive to that produced by the selected eccentricity.

Struts M^{kd} S1 and S4 had panel spaces on either side or straddling the mid-height position at 863.5 mm (2'-10") centres of battens. They therefore form a group, with spaces fixed at the Code maximum. Tests 1, 2, 8 and 9 cover this group and the results should be comparable.

Similarly struts M^{kd} S3 and S5 were fabricated with panel spaces on either side or straddling the mid-height at 1218.5 mm (4'-0") centres of battens. These also form a group but with the batten spacing now well in excess of what is permitted. The batten centres were opened out to encourage an Euler type buckling failure between the battens in the most heavily loaded channel. Tests 3, 4, 7 and 10 cover this group and the results should again be comparable.

A single strut M^{kd} S7 was included for interest. In this case pairs of battens were only provided at the ends and at mid-height. It is covered by Test 11.

The general considerations already submitted for the axially loaded struts are valid and the following tests embrace the same reasoning, proportions and procedures. The only major variation is that the initial 25.4 mm eccentricity will produce considerably more bending moment in the plane of the battens and affect both channel and batten behaviour. The Interaction Curve approach will also now be put to full use. Lack of straightness on the x-x axis was very small and resulted in minimal deflections which have been generally neglected.

Figs. 39 to 43 give the strut layouts and gauge numbers. Test 11 - special strut - will be investigated later.

Theoretical and actual deflection curves from data established in Figs. 44 and 46 are shown in Fig. 48. Good agreement exists between the tests within the elastic range, but beyond this the effects of batten frequency and stiffness become apparent. They influence the deflection and ultimate load. As expected the highest values were for the smaller batten spacings. There is a suggestion that struts with battens straddling the mid-height perform better than struts with battens at mid-height.

However, the deflection values were used to establish the values for $\frac{P}{P_o}$ and $\frac{M}{M_o}$, see Figs. 45 and 47. From these the relevant interaction curves depicted in Figs. 49 to 53 were established. Note that in addition to Fig. 49, covering all

struts, subsequent diagrams give the load/moment apportionment for each pair of "identical" struts.

An investigation of the test data, including strain readings, is now made, as for the axially loaded struts.

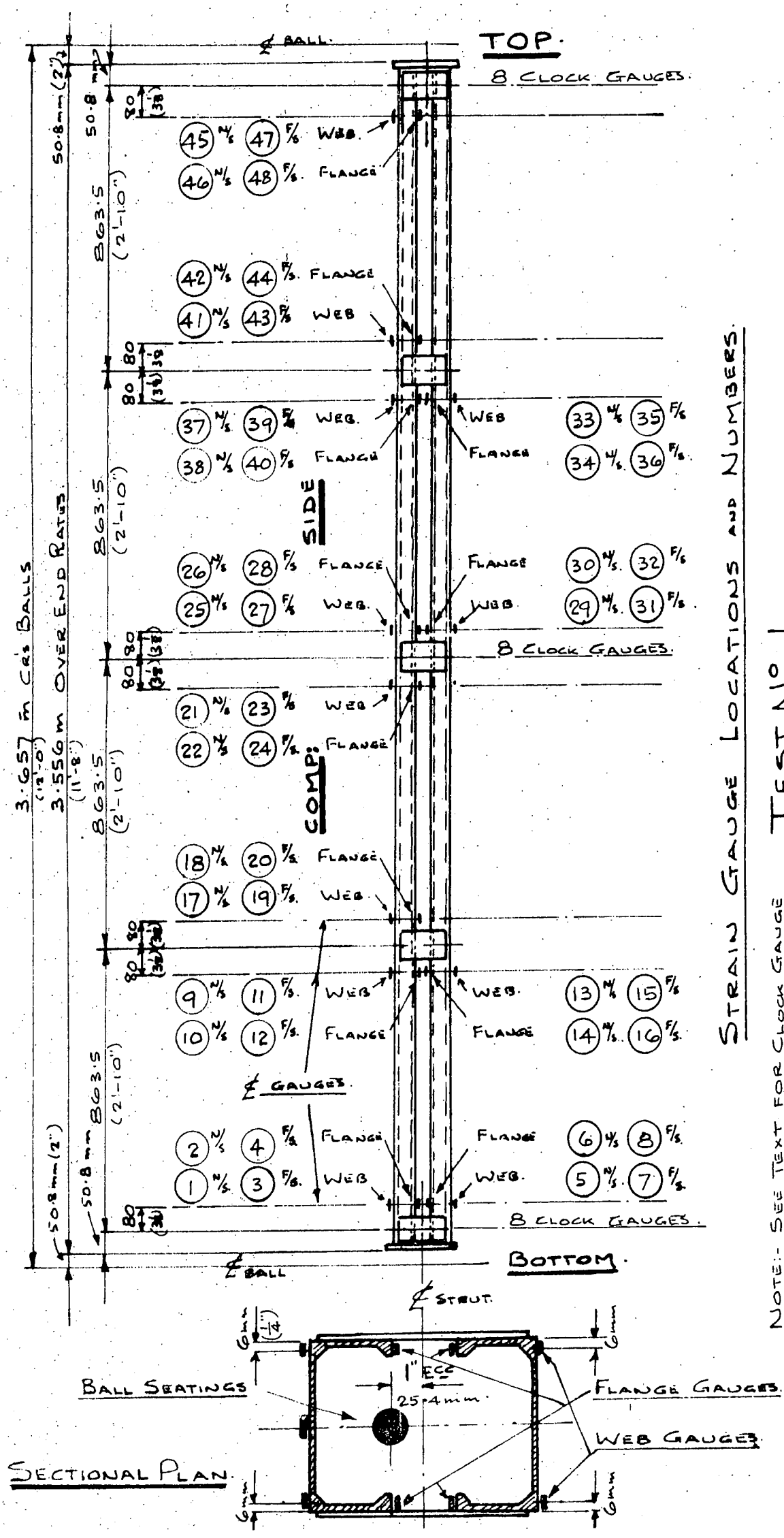

STRAIN GAUGE LOCATIONS AND NUMBERS.

TEST No 1

USING STRUT Mk. S1

FIG: 39

N/S DENOTES NEAR SIDE

F/S " FAR "

NOTE:- SEE TEXT FOR CLOCK GAUGE PLAN LOCATION AND LETTERS.

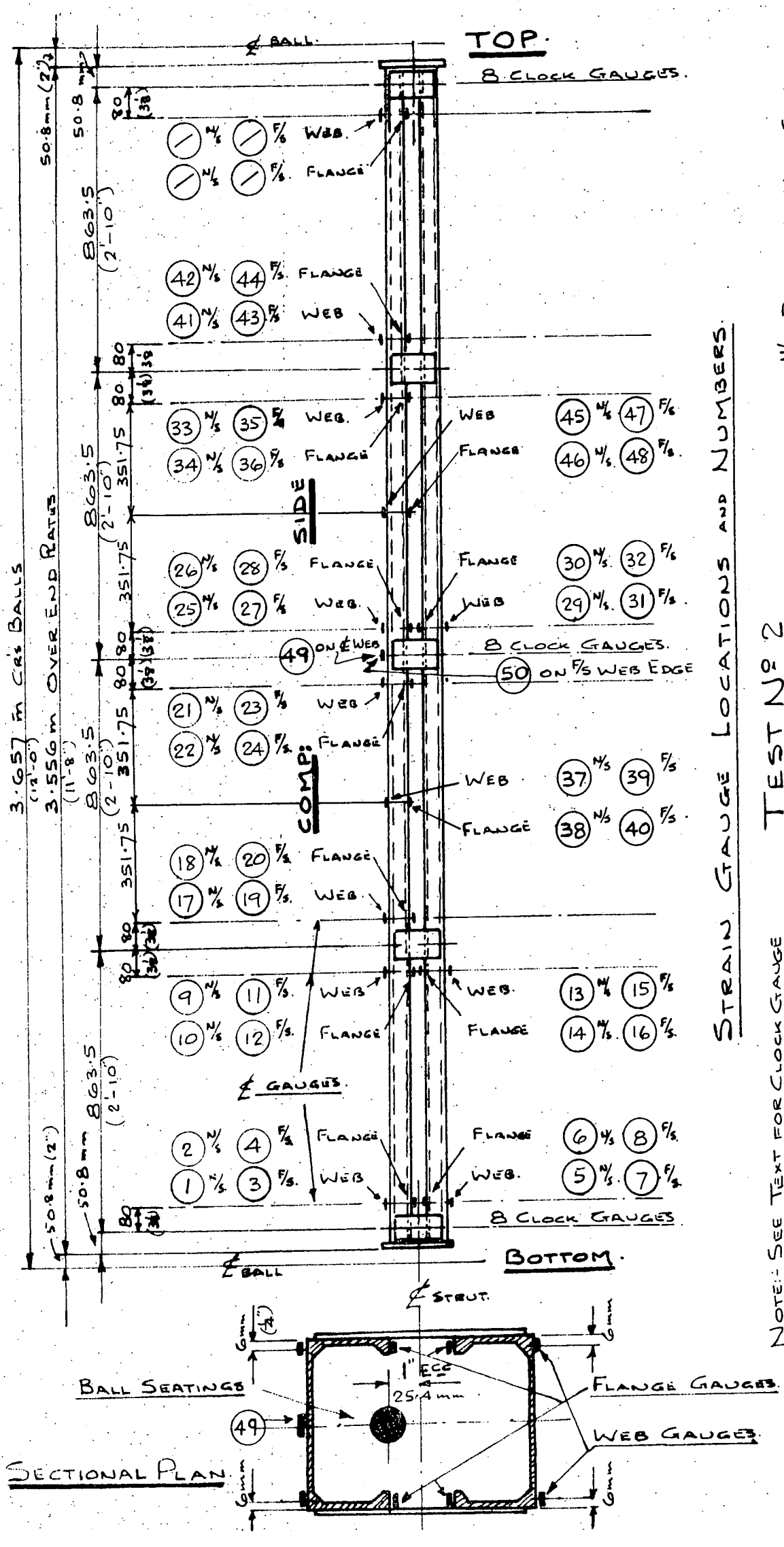
TOP.
8 CLOCK GAUGES.
℄ BALL
50·8 mm (2")
80 (3½")
863·5 (2'-10")
351·75
WEB.
FLANGE.
N/S
F/S
42 44 FLANGE
41 43 WEB
33 35 WEB.
34 36 FLANGE
SIDE
26 28 FLANGE
25 27 WEB.
49 ON ℄ WEB
50 ON F/S WEB EDGE
8 CLOCK GAUGES.
21 23 WEB
22 24 FLANGE
COMP.
18 20 FLANGE
17 19 WEB.
9 11 WEB
10 12 FLANGE
℄ GAUGES.
2 4 FLANGE
1 3 WEB
8 CLOCK GAUGES
BOTTOM.
℄ BALL
3·657 m C/L BALLS (12'-0")
3·556 m OVER END RATES (11'-8")
45 47
46 48
30 32
29 31
37 39
38 40
13 15
14 16
6 8
5 7
STRAIN GAUGE LOCATIONS AND NUMBERS.
TEST No 2
USING STRUT MK S1
FIG: 40
N/S DENOTES NEAR SIDE
F/S " FAR "
NOTE:- SEE TEXT FOR CLOCK GAUGE RAN LOCATION AND LETTERS.
℄ STRUT.
6mm
1" ECC
25·4 mm
BALL SEATINGS
FLANGE GAUGES.
WEB GAUGES.
49
SECTIONAL PLAN.

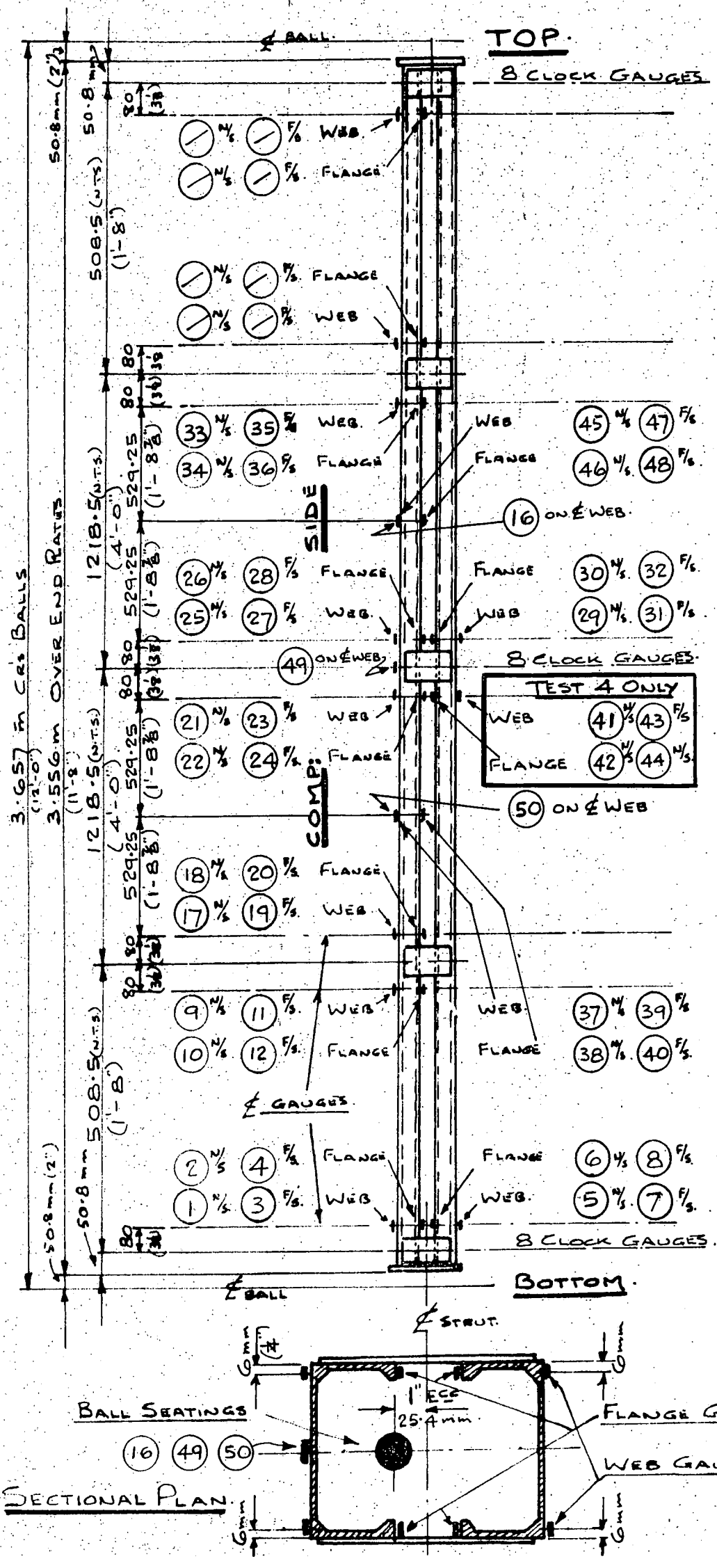

STRAIN GAUGE LOCATIONS AND NUMBERS.

TESTS Nos 3 & 4

USING STRUSM'S3

FIG: 41

N/S DENOTES NEAR SIDE

F/S " FAR "

NOTE:- SEE TEXT FOR CLOCK GAUGE PLAN LOCATION AND LETTERS.

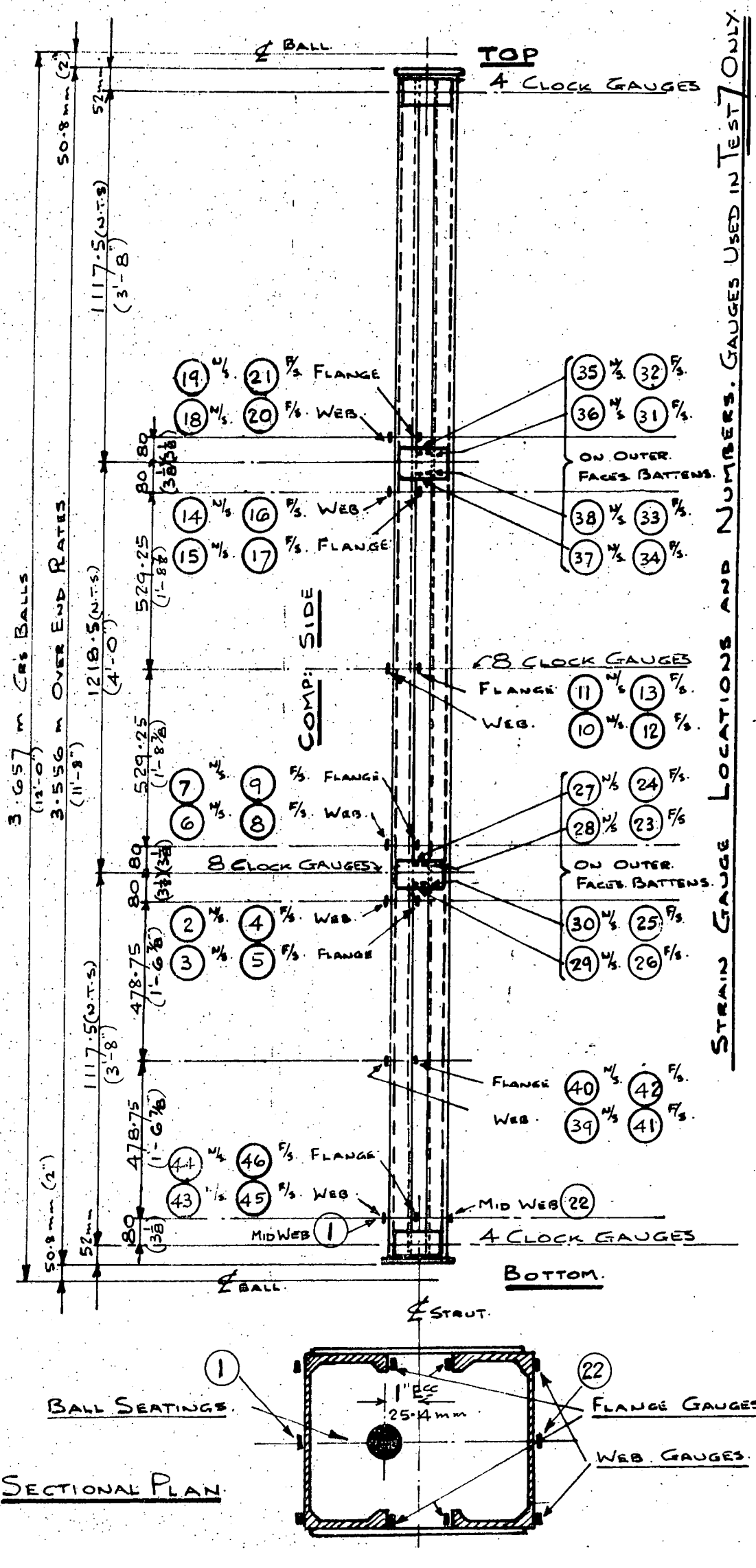
℄ BALL
TOP
4 CLOCK GAUGES
50·8 mm (2")
52mm
1117·5 (N.T.S.) (3'-8")
3·657 m C/L BALLS (12'-0")
3·556 m OVER END RATES (11'-8")
1218·5 (N.T.S.) (4'-0")
19 N/S. 21 F/S. FLANGE
18 N/S. 20 F/S. WEB.
80 80 (3⅛ 3⅛)
14 N/S. 16 F/S. WEB.
15 N/S. 17 F/S. FLANGE
529·25 (1'-8⅝")
COMP: SIDE
℄8 CLOCK GAUGES
FLANGE 11 N/S. 13 F/S.
WEB. 10 N/S. 12 F/S.
529·25 (1'-8⅝")
7 N/S. 9 F/S. FLANGE
6 N/S. 8 F/S. WEB.
8 CLOCK GAUGES
80 80 (3⅛ 3⅛)
2 N/S. 4 F/S. WEB.
3 N/S. 5 F/S. FLANGE
478·75 (1'-6⅞")
1117·5 (N.T.S.) (3'-8")
FLANGE 40 N/S. 42 F/S.
WEB. 39 N/S. 41 F/S.
478·75 (1'-6⅞")
44 N/S. 46 F/S. FLANGE
43 N/S. 45 F/S. WEB.
50·8 mm (2")
52mm
80 (3⅛)
MID WEB 1
MID WEB 22
4 CLOCK GAUGES
BOTTOM.
℄ BALL
℄ STRUT
35 N/S. 32 F/S.
36 N/S. 31 F/S.
ON OUTER FACES BATTENS.
38 N/S. 33 F/S.
37 N/S. 34 F/S.
27 N/S. 24 F/S.
28 N/S. 23 F/S.
ON OUTER FACES BATTENS.
30 N/S. 25 F/S.
29 N/S. 26 F/S.
N/S. DENOTES NEAR-SIDE
F/S " FAR- "
STRAIN GAUGE LOCATIONS AND NUMBERS. GAUGES USED IN TEST 7 ONLY.
TESTS Nos 7 AND 10
USING STRUTS Mk. 5S
FIG: 42
NOTE:- SEE TEXT FOR CLOCK GAUGE PLAN LOCATION AND LETTERS.
1
22
1" ECC
25·4 mm
BALL SEATINGS.
FLANGE GAUGES.
WEB. GAUGES.
SECTIONAL PLAN.

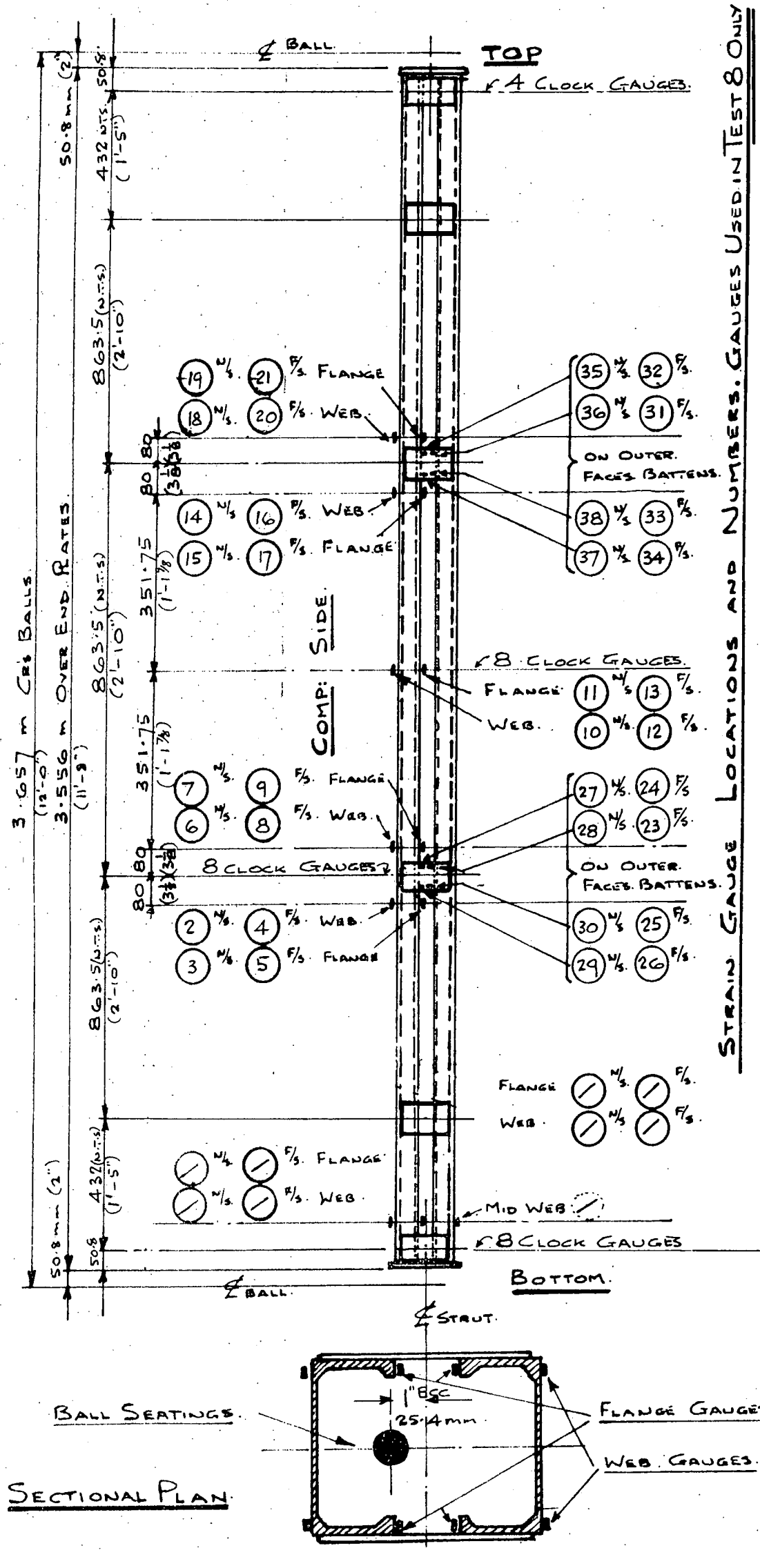
℄ BALL
TOP
4 CLOCK GAUGES.
50·8 mm (2")
432 MTS. (1'-5")
863·5 (M.T.S.) (2'-10")
351·75 (1'-1⅞")
80 (3⅛")
8 CLOCK GAUGES.
3·657 m C/L BALLS (12'-0")
3·556 m OVER END RATES (11'-9")
19 N/S. 21 F/S. FLANGE
18 N/S. 20 F/S. WEB.
14 N/S 16 F/S. WEB.
15 N/S 17 F/S. FLANGE
35 N/S 32 F/S.
36 N/S 31 F/S.
ON OUTER FACES BATTENS.
38 N/S 33 F/S.
37 N/S 34 F/S.
COMP: SIDE
8 CLOCK GAUGES.
FLANGE 11 N/S 13 F/S.
WEB. 10 N/S 12 F/S.
7 N/S. 9 F/S. FLANGE
6 N/S. 8 F/S. WEB.
27 N/S. 24 F/S
28 N/S. 23 F/S.
ON OUTER FACES. BATTENS.
8 CLOCK GAUGES
2 N/S. 4 F/S. WEB.
3 N/S 5 F/S. FLANGE
30 N/S 25 F/S.
29 N/S. 26 F/S.
FLANGE N/S. F/S.
WEB N/S F/S.
N/S F/S. FLANGE
N/S F/S. WEB
MID WEB
8 CLOCK GAUGES
BOTTOM.
℄ STRUT.
℄ BALL
50·8 mm (2")
N/S. DENOTES NEAR-SIDE
F/S " FAR- "
STRAIN GAUGE LOCATIONS AND NUMBERS. GAUGES USED IN TEST 8 ONLY.
TESTS Nº 8 AND 9
USING STRUTS MK. S4
FIG: 43
NOTE:- SEE TEXT FOR CLOCK GAUGE PLAN LOCATION AND LETTERS.
BALL SEATINGS.
1" BCC
25·4mm
FLANGE GAUGES.
WEB GAUGES.
SECTIONAL PLAN.

FIG 44 THEORETICAL DEFLECTION VALUES FOR ECCENTRIC LOADING.

INCREMENT OF LOAD P KN	DEFLECTION e FROM CONSTANT B.M ($e = \frac{PeL^2}{8EI_y}$)	DEFLECTION a FROM SINUSOIDAL B.M. ($a = \frac{P_y L^2}{\pi^2 E I_y}$)	AMPLIFICATION FACTOR FOR CONSTANT B.M. DEFLEC: ($e = Ke = \frac{1}{\cos(\pi/2\sqrt{P/P_E})}$)	AMPLIFICATION FACTOR FOR SINUS: B.M. DEFLEC: ($a = Ka = \frac{1}{1 - P/P_E}$)	TOTAL DEFLECTION $Ke\,e + Ka\,a = e_{TOT}$	GENERAL DATA.
25	1·32	0·075	1·06	1·02	1·40 + 0·08 = 1·48	NOTE:- THE INITIAL LACK OF STRAIGHTNESS AT MID HEIGHT OF STRUTS VARIED BETWEEN 1·4 mm AND 2·2 mm. (I.E. ONLY 0·8 mm VARIATION). THIS WAS CONSIDERED SMALL ENOUGH TO ADOPT AN AVERAGE LACK OF STRAIGHTNESS FOR ALL STRUTS OF 1·8 mm, FOR SIMPLICITY. VALUES FOR "a" WERE CALCULATED ACCORDINGLY AND THE STRUTS SO ARRANGED THAT THE VALUES "WERE ADDATIVE TO DEFLECTION "e" IN ALL CASES.
50	2·64	0·15	1·11	1·04	2·93 + 0·16 = 3·09	
75	3·96	0·225	1·18	1·15	4·65 + 0·26 = 4·91	
100	5·28	0·300	1·27	1·19	6·71 + 0·36 = 7·07	
125	6·60	0·375	1·32	1·26	8·71 + 0·47 = 9·18	NOTATION. P = INCREMENTAL LOAD (KN). e = INITIAL CONSTANT ECCEN: = 25·4 mm. $\mathcal{e}$ = DEFLECTION DUE TO Pe (mm). y = INITIAL (LACK OF STRAIGHTNESS) SINUSOIDAL ECCENTRICITY = 1·8 mm AV. a = DEFLECTION DUE TO Py (mm). Ke, Ka = RESPECTIVE AMPLIFICATION FACTORS. $E = 68{,}700\ N/mm^2$. $I_y = 1179.6\ cm^4$ (STRONG AXIS). L = 3657 mm (LENGTH C'RS BALL PIVOTS)
150	7·92	0·450	1·41	1·33	11·17 + 0·60 = 11·77	
175	9·25	0·525	1·51	1·41	13·97 + 0·74 = 14·71	
200	10·55	0·600	1·61	1·49	16·99 + 0·89 = 17·88	
225	11·88	0·675	1·76	1·62	20·91 + 1·09 = 22·00	NOTE:- THE TOTAL DEFLECTION VALUES GIVEN ARE FOR 25·4 mm ECCENTRIC LOADING IN THE PLANE OF THE BATTENS. I.E. CAUSING BENDING ABOUT THE y-y AXIS. $K = \left[\frac{I_x}{I_y} - x\right]$. THE EULER VALUE OF $P_E = \frac{\pi^2 E I_y}{L^2}$ FOR BENDING ABOUT THE y-y AXIS AT 598 KN MUST THEREFORE BE USED.
250	13·20	0·750	1·90	1·73	25·10 + 1·30 = 26·40	
275	14·50	0·825	2·05	1·86	29·70 + 1·53 = 31·23	READ IN CONJUNCTION WITH FIG: 48
300	15·84	0·905	2·20	2·01	34·85 + 1·82 = 36·67	

FIG: 45 THEORETICAL VALUES OF $\frac{P}{P_o}$ AND $\frac{M}{M_o}$ FOR ECCENTRICALLY LOADED STRUTS.

INCREMENT OF LOAD P KN	$\frac{P}{P_o}$	THEORETICAL DEFLECTION +25·4 mm ECCENTRICITY = e_{TOT}	THEORETICAL MOMENT $Pe_{TOT} = M$.	$\frac{M}{M_o}$	THEORETICAL VALUES FROM CHAPTER 4.
25	0·08	26·88	472	0·03	$P_o = P_E = \frac{\pi^2 E I_x}{L^2}$ WHERE P_E = EULER. CRIPPLING LOAD TAKEN ON THE X-X (WEAK) AXIS OF THE COMPLETE STRUT. ∴ P_o = 309KN (30·9T) = AXIAL CRIP: LOAD. NOTE: THE KONIGSBERGER MOHSIN PREDICTIONS OF P_{CRIT}'S AT 214, 273 & 310 KN AT VARIOUS BATTEN SPACES, FOR BUCKLING ON THE Y-Y AXIS (PARALLEL TO BATTENS), UNDER AXIAL LOAD, HAVE BEEN IGNORED AT THIS STAGE. THE LACK OF STRAIGHTNESS CAUSING BENDING IN THIS PLANE, WITH THE AXIALLY LOADED STRUTS, DID NOT CONFIRM THAT THIS WAS TRUE.
50	0·16	28·49	1425	0·07	
75	0·24	30·11	2258	0·11	
100	0·32	32·47	3247	0·15	
125	0·40	34·58	4281	0·20	
150	0·48	37·17	5575	0·26	
175	0·57	40·31	7054	0·33	M_o = CRIPPLING MOMENT (WITH NO END LOAD) $M_o = f_y \cdot A_c \cdot d$. $M_o = 2133 \times 10^4$ N mm (84·2 TON IN)
200	0·65	43·22	8644	0·42	
225	0·73	47·40	10 665	0·50	
250	0·81	51·80	12 950	0·61	NOTATION. P = INCREMENTAL LOAD - KN. e_{TOT} = TOTAL THEORET: DEFLECTION FROM FIG: 4 + 25·4 mm GIVING TOTAL ECCEN: FOR P. M = Pe_{TOT} NM. (KN mm)
275	0·89	56·65	15 579	0·73	
300	0·97	62·07	18 621	0·88	

FIG:46. COMPUTATION OF ACTUAL DEFLECTIONS AT MID-HEIGHT. DATA ABSTRACTED FROM TEST RESULTS.

INCREMENT OF LOAD P KN	LOCATION ON STRUT	TEST Nº1	TEST Nº2	TEST Nº3	TEST Nº4	TEST Nº7	TEST Nº8	TEST Nº9	TEST Nº10	GENERAL DATA.
40	TOP.	0·08	0·31	0·28	0·15	0·10	0·18	0·16	0·23	CLOCK GAUGE READINGS. THIS TABLE MAKES AN AVERAGED ADJUSTMENT USING THE TOP & BOTTOM GAUGES TO COMPENSATE FOR ANY SMALL RELATIVE MOVEMENT OF THE RIG. GAUGE A. ALL CASES. THIS WILL NOT APPLY TO THEODOLITE READINGS IN GENERAL.
	MID: Hᵀ	1·90	2·45	1·94	2·58	1·98	2·59	2·46	2·86	
	BOTTOM	0·16	0·15	0·25	0·31	0·11	0·22	0·02	0·39	
	ACTUAL	1·78	2·22	1·67	2·25	1·88	2·39	2·37	2·55	
80	T	0·76	0·61	0·52	0·44	0·42	0·39	0·41	0·48	
	M	5·08	5·45	4·10	5·50	4·77	5·14	5·28	5·26	
	B.	0·35	0·39	0·56	0·61	0·37	0·39	0·28	0·63	
	ACTUAL	4·52	4·95	3·55	4·97	4·38	4·75	4·93	4·70	
120	T	1·04	0·95	0·90	0·70	0·71	0·79	0·76	0·79	
	M	8·68	9·18	8·50	9·10	7·68	8·63	8·89	9·02	
	B	0·64	0·69	0·90	0·91	0·57	0·56	0·48	1·03	
	ACTUAL	7·84	8·36	7·61	8·39	7·04	7·95	8·27	8·11	
160	T	1·37	1·34	1·34	1·02	1·12	1·30	1·16	1·18	PAIRING OF TESTS.- WITH IDENTICAL BATTEN SPACING. TESTS 1 AND 2. 3 - 4 7 - 10 8 - 9.
	M	13·10	15·25	14·30	13·85	12·70	13·14	13·16	14·17	
	B	1·02	1·02	1·27	1·27	0·98	1·19	0·92	1·40	
	ACTUAL	11·90	14·07	13·00	12·70	11·65	11·90	12·12	12·88	
200	T	1·78	1·81	1·92	1·44	1·45	1·59	1·63	1·60	
	M	18·40	20·40	22·80	20·51	20·7	18·34	18·39	21·69	
	B	1·40	1·46	1·78	1·73	1·55	1·45	1·49	1·84	
	ACTUAL	16·81	18·76	20·95	18·93	19·20	16·82	16·83	19·97	
240	T	2·36	2·41	3·81	2·12	2·22	2·40	2·31	2·54	NOTE:- BOTH THIS TABLE AND THE DEFLECTION GRAPH FIG:-48 SUGGEST THAT BALL STICTURE WAS PRESENT.- MAINLY AT THE LOWER LOADS. WHEN THE STRUTS. WERE. "MOST STRAIGHT".
	M	27·21	30·50	37·82	31·30	33·30	26·10	26·95	33·19	
	B	1·81	2·10	3·56	2·34	2·24	2·31	1·81	2·44	
	ACTUAL	25·12	27·25	41·5	29·07	30·07	23·75	24·89	31·70	
260	T	2·69	FROM THEODOLITE;				2·70	2·77		
	M	31·50					31·06	33·68		
	B.	2·38					2·01	1·84		
	ACTUAL	28·97	37·7				28·7	31·37		
220	T	2·06	2·14	2·39	2·12	1·85	1·90	1·91	2·07	
	M	22·60	25·2	28·80	25·30	25·85	22·39	22·48	27·43	
	B	1·69	1·76	1·85	2·01	1·95	1·85	1·62	2·14	
	ACTUAL	20·73	23·25	26·7	23·23	23·95	20·51	20·72	25·32	
TEST LOAD AT FAILURE KN		277·5	265	245	265	251	280	282	259	LOAD P - KN DEFLECTION - mm
THEODOLITE READING AT FAILURE.		39·67	41·27	42·87	43·24	40·64	41·40	41·00	42·90	

IMPORTANT NOTE:- THESE DEFLECTION VALUES ARE REQUIRED FOR COMPARISON CALCULATIONS AT INTERACTION CURVE - PLASTIC LINE INTERSECTIONS.

FIG. 47. COMPUTATION OF TEST VALUES TO ESTABLISH $\frac{P}{P_o}$ AND $\frac{M}{M_o}$ FOR ECCENTRIC LOADING.

INCREMENT OF LOAD P	$\frac{P}{P_o}$	TEST Nº1 e_{TOT}	TEST Nº1 $M=Pe_{TOT}$	TEST Nº1 $\frac{M}{M_o}$	TEST Nº2 e_{TOT}	TEST Nº2 $M=Pe_{TOT}$	TEST Nº2 $\frac{M}{M_o}$	TEST Nº3 e_{TOT}	TEST Nº3 $M=Pe_{TOT}$	TEST Nº3 $\frac{M}{M_o}$	TEST Nº4 e_{TOT}	TEST Nº4 $M=Pe_{TOT}$	TEST Nº4 $\frac{M}{M_o}$	TEST Nº7 e_{TOT}	TEST Nº7 $M=Pe_{TOT}$	TEST Nº7 $\frac{M}{M_o}$	TEST Nº8 e_{TOT}	TEST Nº8 $M=Pe_{TOT}$	TEST Nº8 $\frac{M}{M_o}$	TEST Nº9 e_{TOT}	TEST Nº9 $M=Pe_{TOT}$	TEST Nº9 $\frac{M}{M_o}$	TEST Nº10 e_{TOT}	TEST Nº10 $M=Pe_{TOT}$	TEST Nº10 $\frac{M}{M_o}$
40	0·129	27·18	1087	0·051	27·62	1105	0·051	27·07	1083	0·051	27·65	1106	0·051	27·28	1091	0·051	27·79	1112	0·052	27·27	1091	0·051	27·95	1118	0·052
80	0·26	29·92	2394	0·112	30·35	2428	0·113	28·95	2316	0·108	30·37	2430	0·113	29·78	2382	0·111	30·15	2412	0·113	30·33	2426	0·113	30·10	2408	0·112
120	0·39	33·24	3989	0·187	33·76	4051	0·189	33·02	3962	0·185	33·79	4055	0·189	32·44	3893	0·182	33·35	4002	0·187	33·67	4040	0·189	33·51	4021	0·188
160	0·52	37·30	5968	0·279	39·47	6315	0·296	38·40	6144	0·288	38·10	6096	0·285	37·05	5982	0·280	37·30	5968	0·279	37·52	6003	0·281	38·28	6125	0·287
200	0·65	42·21	8442	0·395	44·16	8832	0·414	46·35	9270	0·434	44·33	8866	0·415	44·60	8920	0·418	42·22	8444	0·396	42·23	8446	0·396	45·37	9074	0·425
240	0·78	50·52	12125	0·568	52·65	12636	0·592	66·90	16056	0·753	54·47	13073	0·613	55·47	13313	0·624	49·15	11796	0·553	50·29	12070	0·566	57·1	13704	0·642
260	0·84	54·37	14136	0·662	63·10	16406	0·774										54·10	14066	0·659	56·77	14760	0·692			
220	0·71	46·13	10149	0·476	48·65	10703	0·501	52·1	11460	0·537	48·63	10699	0·501	49·35	10857	0·508	45·91	10100	0·474	46·12	10147	0·476	50·72	11158	0·523
FAILURE VALUES e_{TOT}, M, $\frac{M}{M_o}$		65·07	18057	0·85	66·67	17668	0·83	68·27	16726	0·78	68·64	18190	0·85	66·04	16576	0·78	66·80	18704	0·87	66·40	18725	0·87	68·3	17690	0·83
TEST LOAD AT FAILURE kN		277·5			265			245			265			251			280			282			259		
$\frac{P}{P_o}$ AT FAILURE		0·89			0·86			0·79			0·86			0·82			0·91			0·91			0·84		

THEORETICAL VALUES. (FROM CHAPTER 4)

$P_o = P_E = \frac{\pi^2 E I_x}{L^2}$ WHERE P_E IS THE EULER CRIPPLING LOAD TAKEN ON THE "X–X" (WEAK) AXIS OF THE COMPLETE STRUT

AXIAL STRUT LOAD $P_o = 309$ kN (30·9 TON).

M_o = CRIPPLING BENDING MOMENT WITH NO END LOAD. AXIS Y-Y.

$M_o = f_y \cdot A_c \cdot d$

$M_o = 2133 \times 10^4$ Nmm (84·2 TON IN)

TEST VALUES. (ABSTRACTED FROM TEST DATA APPENDIX)

P = INCREMENTAL TEST LOAD – UP TO FAILURE IN kN.

e_{TOT} = TOTAL ECCENTRICITY PRODUCING MOMENT. I.E. TOTAL DEFLECTION UNDER LOAD + 25·4 mm INITIAL ECCENTRICITY.

TEST LOAD DEFLECTIONS AT MID-HEIGHT READ FROM CLOCK-GAUGES (A) IN GENERAL AND INCLUDE ADJUSTMENT FROM GAUGES AT TOP & BOTT. STRUT.

$M = Pe_{TOT}$ – Nm (kNmm)

NOTE:- e_{TOT} VALUES AT FAILURE INCLUDE THEODOLITE READINGS IN LIEU OF CLOCK GAUGES.

IMPORTANT. NOTE:- WHEN P = 220·008 kN THE THEORETICAL INTERACTION CURVE INTERSECTS THE PLASTIC LIMIT LINE TO GIVE M = 10516 Nm AT $\frac{M}{M_o}$ = 0·493.

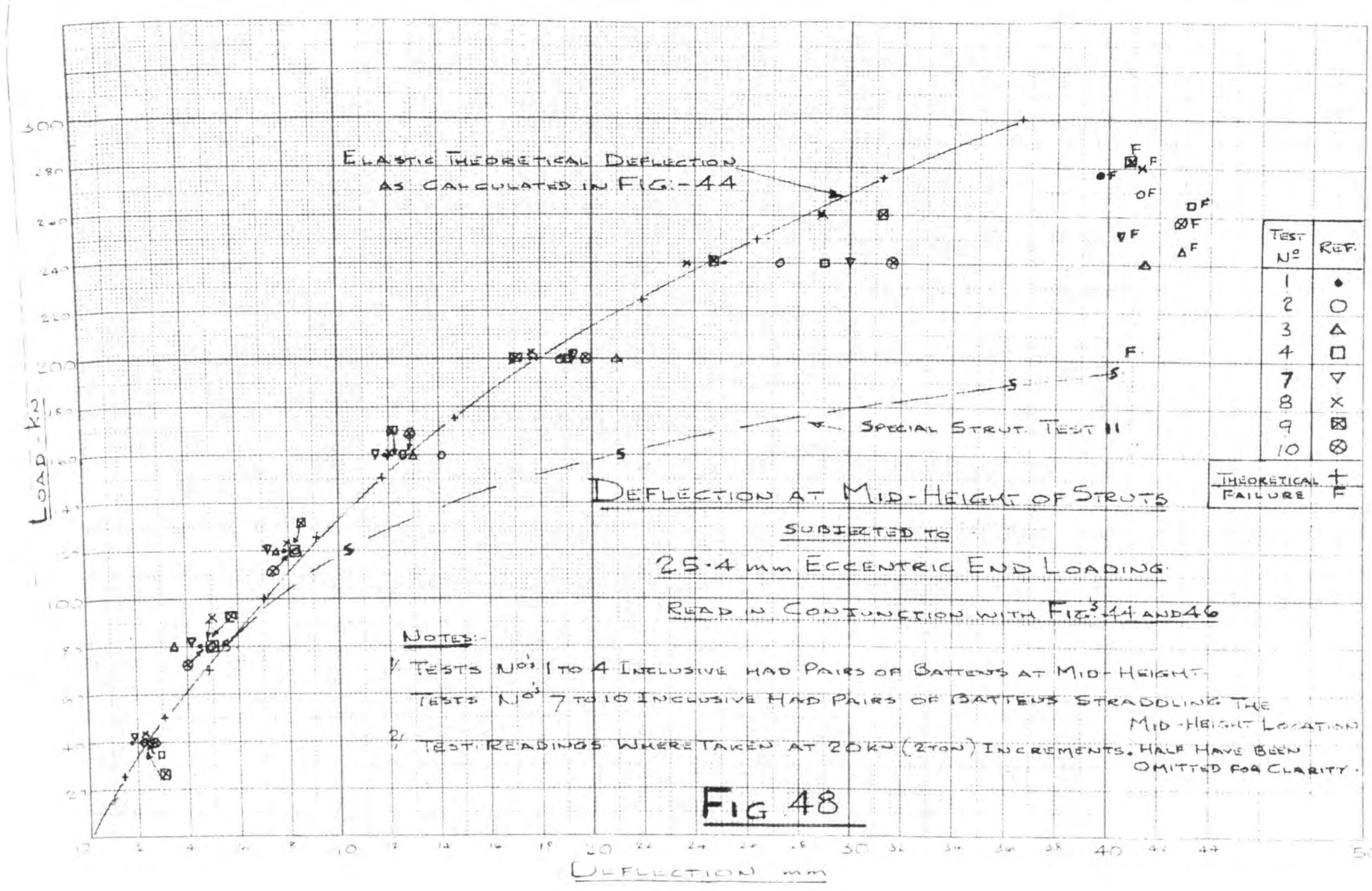

NOTES:-

1/ TESTS Nº 1 TO 4 INCLUSIVE HAD PAIRS OF BATTENS AT MID-HEIGHT. TESTS Nº 7 TO 10 INCLUSIVE HAD PAIRS OF BATTENS STRADDLING THE MID-HEIGHT LOCATION

2/ TEST READINGS WERE TAKEN AT 20KN (2TON) INCREMENTS. HALF HAVE BEEN OMITTED FOR CLARITY.

FIG 48

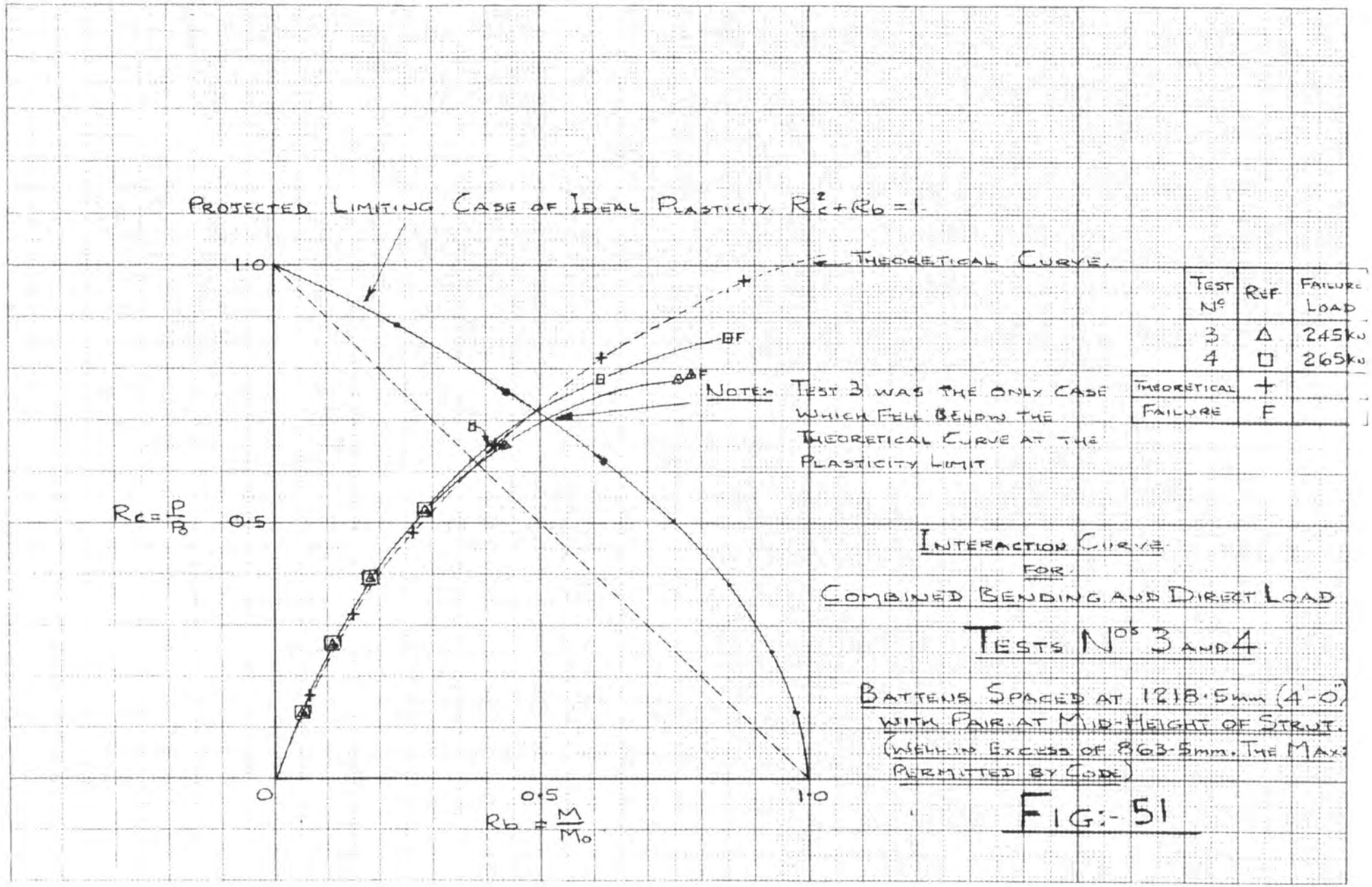
PROJECTED LIMITING CASE OF IDEAL PLASTICITY $R_c^2 + R_b = 1$
THEORETICAL CURVE.
1·0
0·5
0
0·5
1·0
$R_c = \frac{P}{P_o}$
$R_b = \frac{M}{M_o}$
F
F
F
NOTE:- TEST 3 WAS THE ONLY CASE WHICH FELL BELOW THE THEORETICAL CURVE AT THE PLASTICITY LIMIT
TEST Nº | REF | FAILURE LOAD
3 | △ | 245kN
4 | □ | 265kN
THEORETICAL | +
FAILURE | F
INTERACTION CURVE FOR COMBINED BENDING AND DIRECT LOAD
TESTS Nº 3 AND 4
BATTENS SPACED AT 1218·5mm (4'-0") WITH PAIR AT MID-HEIGHT OF STRUT. (WELL IN EXCESS OF 863·5mm. THE MAX: PERMITTED BY CODE)
FIG:- 51

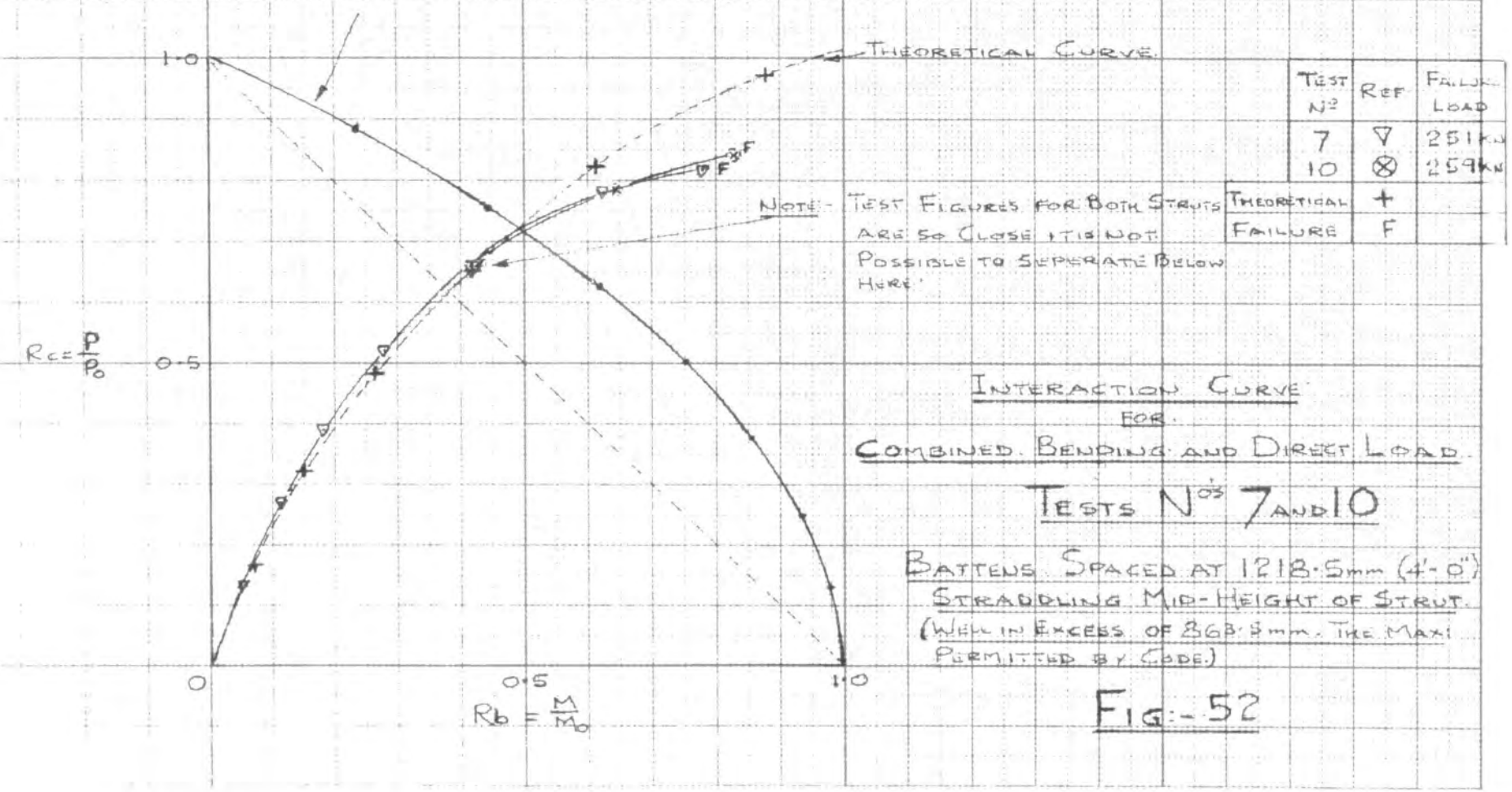

INTERACTION CURVE FOR COMBINED BENDING AND DIRECT LOAD.

TESTS Nº 7 AND 10

BATTENS SPACED AT 1218·5mm (4'-0") STRADDLING MID-HEIGHT OF STRUT. (WELL IN EXCESS OF 868·5mm. THE MAXI PERMITTED BY CODE.)

FIG:- 52

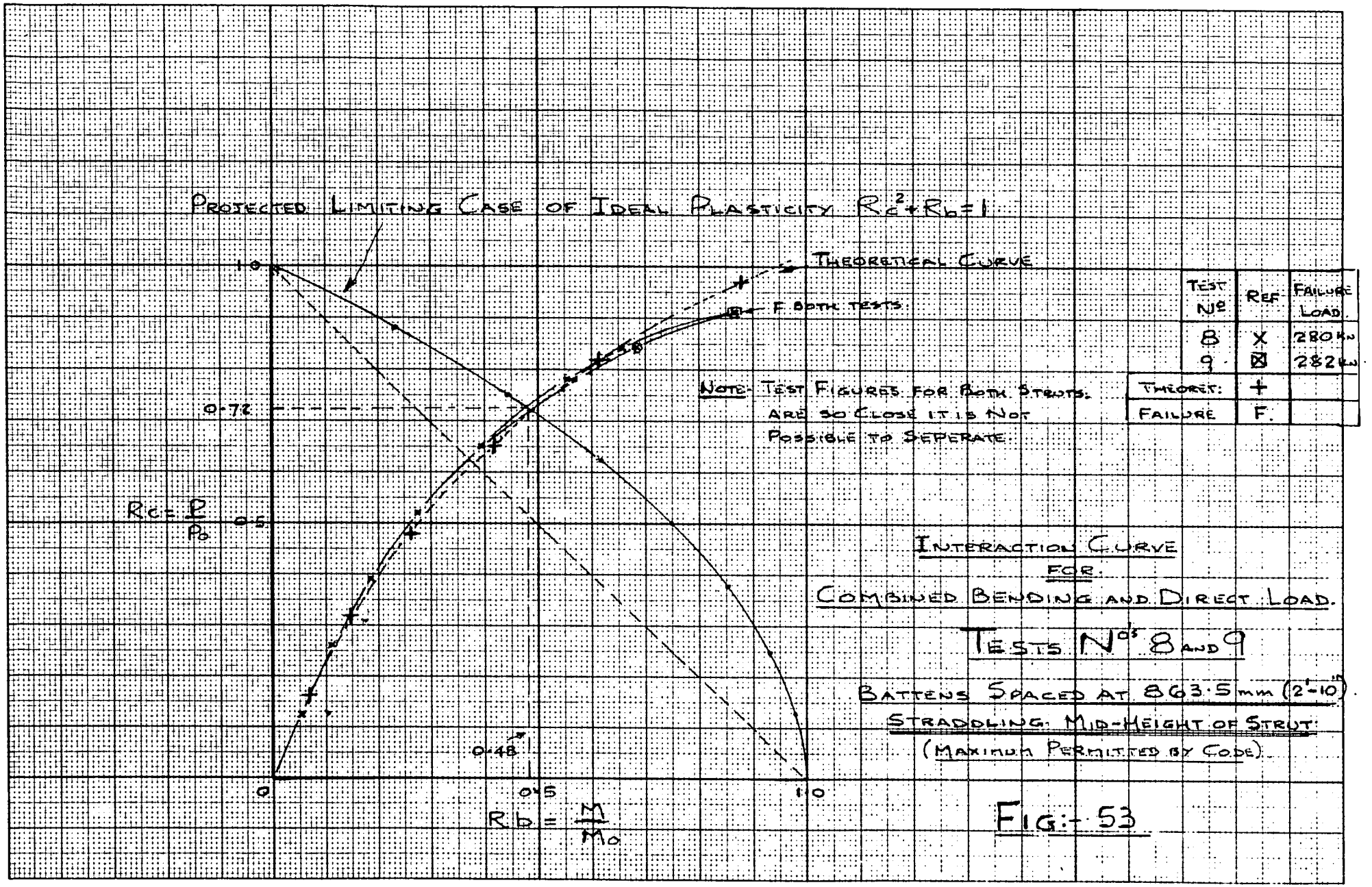

	Test Nº	Ref	Failure Load
	8	X	280 kN
	9	⊠	282 kN
Theoret:		+	
Failure		F.	

NOTE: TEST FIGURES FOR BOTH STRUTS. ARE SO CLOSE IT IS NOT POSSIBLE TO SEPERATE.

INTERACTION CURVE FOR COMBINED BENDING AND DIRECT LOAD.

TESTS Nos 8 AND 9

BATTENS SPACED AT 863·5 mm (2'-10")

STRADDLING MID-HEIGHT OF STRUT

(MAXIMUM PERMITTED BY CODE).

FIG:- 53

Again using the elastic properties of the material the theoretical average stresses due to column buckling will first be established. This will be done at "Onset of Plasticity" and at the "Projected Limit of Ideal Plasticity".

Overall Stability

Critical overall slenderness = $\frac{L}{r_x}$ = 71.5 (as axial struts).

Strong axis slenderness of complete section = $\frac{L}{r_y}$ = 51.4 (as axial struts).

Critical slenderness of one channel between batten centres

- Tests 1, 2, 8 and 9

$$\frac{\ell}{r_y} = \frac{863.5}{22.6} = 38.2 \text{ (possibly x 0.8)}$$

Tests 3, 4, 7 and 10

$$\frac{\ell}{r_y} = \frac{1218.5}{22.6} = 53.5 \text{ (possibly x 0.8)}$$

Accepting that the Code limits batten spacing, and this has now purposely been exceeded in some cases, the criterion (on face value) is $\frac{L}{r} = 71.5$.

From Fig. 2 this gives Max Comp. Stress = 136 N/mm^2 (8.6 Ton/in^2)

This would give an elastic critical load value of P_o = 309 kN (30.9 ton) which we know to be false because bending in the plane of the battens will reduce this, see Chapter 6. However the question is; will a single channel buckle between the battens or will local buckling prevail??. Also $M_o = 2133 \times 10^4$ Nmm (from Chapter 4).

Theoretical Values

Using theoretical values from "Interaction Curves" for all eccentrically loaded struts.

At "Onset of Plasticity"

$$\frac{P}{P_o} = 0.62 \qquad \frac{M}{M_o} = 0.38$$

$\therefore$ Direct load = P = 309 x 0.62 = 192 kN

Bending Moment = M = 21330 x 0.38 = 8,100 Nm

$$\text{Direct Stress} = \frac{P}{\text{area}} = \frac{192 \times 10^3}{2334} = 82.5 \text{ N/mm}^2$$

$$\text{Av. Bending Stress} = \frac{M}{Ac.d} = \frac{8100 \times 10^3}{11.67 \times 10^2 \times 135.4} = 50.9 \text{ N/mm}^2$$

Total Av. Stress = $\underline{133.4}$ N/mm^2

At Projected "Limit of Ideal Plasticity"

$$\frac{P}{P_o} = 0.72 \qquad \frac{M}{M_o} = 0.49$$

$\therefore$ Direct load = P = 309 x 0.7 = 223 kN

Bending Moment = M = 21330 x 0.49 = 10,200 Nm

$$\text{Direct Stress} = \frac{P}{\text{area}} = \frac{223 \times 10^3}{2334} = 96.0 \text{ N/mm}^2$$

$$\text{Av. Bending Stress} = \frac{M}{Ac.d} = \frac{10{,}200 \times 10^3}{11.67 \times 10^2 \times 135.4} = 64.8 \text{ N/mm}^2$$

Total Av. Stress $\underline{160.8}$ N/mm^2

Test Values

Again using the same method as for the theoretical values the total average stresses at onset of plasticity, limit of ideal plasticity, last increment at which strain readings were taken before failure and at failure, were established. These are given in Figs. 54 to 57 and are self explanatory.

It was appreciated that with the increased deflections due to eccentric load the average stress values would not be precise as the moment arm "d" would vary. This is because the stress distribution C.G. across the section would not coincide with the channel C.G.'s. Due to increasing deflection it would also vary with each increment of load and with each test. However after approximate checks the "yield" moment arm was used and at the larger deflections this would tend to give stress values on the high side. For the critical channel "A", its stress distribution C.G. would move towards the back of the channel as the deflection increased. At high load levels direct comparison is justified between the calculated average and strain gauge stresses.

Figs. 58, 59 and 60 give strain gauge readings and the resulting stresses for selected gauges at the load levels previously stated. The readings given are the highest for each strut, irrespective of their position.

In considering the struts generally, the most highly stressed areas were at mid-height with the exception of Tests 3 and 4. Here the battens were spaced at 1218.5 mm (4'-0") centres and failure occurred at approximately mid-panel (lower) adjacent to the mid-height. It must however be emphasised that stresses at other positions were almost equally high and those on the flange lips, next to the end battens, as high as anywhere on the strut. This highlights the absolute necessity that battened struts have completely rigid batten or cheek plate attachment at their ends.

As with the axially loaded struts, rings of gauges at the critical positions on selected struts were analysed at the load at which the last strain recording could be read, before failure.

Reference to pages 242 to 246 will give a detailed investigation of the stresses existing at these critical positions. The stresses given may be compared with those in the tables giving by Figs. 54 to 60 inclusive.

FIG:-54 ESTABLISHMENT OF TOTAL AVERAGE STRESS AT VARIOUS LOCATIONS-FROM INTERACTION CURVES

LOCATION	TEST Nº.	VALUES FROM FIG:47 AND INTERACTION CURVE FIG 50				DIRECT STRESS $= \frac{P}{AREA}$	BENDING STRESS $= \frac{M}{Ac.d}$	TOTAL AV. STRESS (N/mm²)
		$\frac{P}{P_o}$	$\frac{M}{M_o}$	DIRECT LOAD P (KN)	BENDING M (Nm)			
AT ONSET OF PLASTICITY	1	0·63	0·37	195	7892	84	50	134
	2	0·62	0·38	191	8105	82	52	134
AT PROJECTED LIMIT OF IDEAL PLASTICITY	1	0·72	0·48	223	10 220	96	65	161
	2	0·71	0·49	219	10452	94	67	163
AT LAST STRAIN READING WHEN: P = 270 KN TEST 1 = 260KN TEST 2.	1	0·87	0·76	269	16200	116	102	218
	2	0·84	0·77	260	16406	112	104	216
AT 277·5KN FAILURE 265 KN	1	0·89	0·85	277·5	18057	119	114	233
	2	0·86	0·83	245	17668	105	112	217

FIG·55 ESTABLISHMENT OF TOTAL AVERAGE STRESS AT VARIOUS LOCATIONS - FROM INTERACTION CURVES

LOCATION.	TEST Nº	VALUES FROM FIG 47 AND INTERACTION CURVE FIG 51.				DIRECT STRESS $= \frac{P}{\text{AREA}}$	BENDING STRESS $= \frac{M}{Ac.d}$	TOTAL AV. STRESS (N/mm²)
		$\frac{P}{P_o}$	$\frac{M}{M_o}$	DIRECT LOAD P (KN)	BENDING M (Nm)			
AT ONSET OF PLASTICITY.	3	0·61	0·38	188	8105	81	52	133
	4	0·62	0·37	191	7892	82	50	132
AT PROJECTED LIMIT OF IDEAL PLASTICITY	3	0·70	0·51	216	10878	93.	69	162.
	4	0·72	0·49	222	10452	95	66	161
AT LAST STRAIN READING WHEN P = 240 KN TEST 3. = 260 KN TEST 4.	3	0·78	0·75	240	16056	103.	102	205
	4	0·84	0·78	260	16650	112	106	218
AT 245 KN	3	0·79	0·78	245	16726	105	106	211
FAILURE 265 KN	4.	0·86	0·85	265	18190	114	115	229.

FIG-56 ESTABLISHMENT OF TOTAL AVERAGE STRESS AT VARIOUS LOCATIONS - FROM INTERACTION CURVES.

LOCATION	TEST Nº	VALUES FROM FIG 47 AND INTERACTION CURVE FIG 52				DIRECT STRESS $= \frac{P}{AREA}$	BENDING STRESS $= \frac{M}{Ac.d}$	TOTAL AV. STRESS. (N/mm^2)
		$\frac{P}{P_o}$	$\frac{M}{M_o}$	DIRECT LOAD P (kN)	BENDING M (Nm)			
AT ONSET OF PLASTICITY	7	0·63	0·38	195	8105	84	51	135
	10	0·63	0·38	195	8105	84	51	135
AT PROJECTED. LIMIT OF IDEAL PLASTICITY.	7	0·72	0·49	222	10452	95	66	161
	10	0·71	0·50	219	10665	94	68	162
AT LAST STRAIN READING WHEN P=240kN.	7	0·78	0·62	240	13313	103	84	187
	10	0·78	0·64	240	13704	103.	87	190.
AT 251kN FAILURE 259kN	7	0·82	0·78	251	16576	107	105	212
	10	0·84	0·83	259.	17690	111	112	223

FIG:- 57. ESTABLISHMENT OF TOTAL AVERAGE STRESS AT VARIOUS LOCATIONS - FROM INTERACTION CURVES.

LOCATION.	TEST Nº	VALUES FROM FIG 47 AND INTERACTION CURVE FIG:- 53				DIRECT STRESS.	BENDING STRESS.	TOTAL AV: STRESS.
		$\frac{P}{P_o}$	$\frac{M}{M_o}$	DIRECT LOAD P (KN)	BENDING M (Nm)	$= \frac{P}{\text{AREA}}$	$= \frac{M}{Ac.d.}$	(N/mm²)
AT ONSET OF PLASTICITY	8	0·62	0·37	192	7892	82	50	132.
	9	0·62	0·37	192	7892	82	50	132
AT PROJECTED LIMIT OF IDEAL PLASTICITY.	8	0·73	0·48	225	10238	97	65	162
	9	0·72	0·49	223	10452	96	66	162
AT LAST STRAIN READING WHEN P = 270KN.	8	0·88	0·75	270	15998	116	107	223.
	9	0·88	0·77	270	16210	116	115	231
AT 280KN FAILURE 282 KN	8	0·91	0·87	280	18704	120	118	238
	9	0·91.	0·87	282.	18725	121	118	239

FIG. 58 ESTABLISHMENT OF ACTUAL STRESSES FROM STRAIN GAUGE READINGS AT GIVEN CRITICAL LOCATIONS

TEST Nº 1 (FAILURE 277·5 KN)

GAUGE Nº	LOCATION	STRAIN READINGS (GAUGE FAC: 2·08) AT ONSET OF PLASTICITY P AT 195 KN (INTERPOL:)	AT PROJECTED LIMIT OF IDEAL PLASTICITY P AT 220 KN (NEAREST)	AT LAST STRAIN READING WHEN P = 270 KN	CALCULATED STRESSES N/mm² AT ONSET OF PLASTICITY P AT 195 KN (INTERPOL:)	AT PROJECTED LIMIT OF IDEAL PLASTICITY P AT 220 KN (NEAREST)	AT LAST STRAIN READING WHEN P = 270 KN
21	WEB - NEXT TO MIDHEIGHT	0·716 Divn = 2	0·862 Divn = 2	0·607 Divn = 1	117	142	200
23	Do	0·749 "	0·903 "	0·640 "	122	149	210
25	Do	0·704 "	0·845 "	0·595 "	116	138	196
27	Do	0·751 "	0·910 "	0·650 "	124	150	214
46	FLGE - NEXT TO TOP OF STRUT	0·626 "	0·780 "	0·610 "	102	139	200
48	Do	0·609 "	0·760 "	0·575 "	100	126	188

NOTE:- ALL STRESSES FOR TEST 1 ARE LOWER THAN EXPECTED. P.T.F.E. GREASE WAS NOT USED FOR THIS TEST. "STICTURE" AT BALL SEATS IS LIKELY. IN TEST 2 GAUGE (49) AT ℄ WEB - MIDHEIGHT WAS CRITICAL. IT FAILED JUST BEFORE LAST READING.

TEST Nº 2 (FAILURE 265 KN).

GAUGE Nº	LOCATION	STRAIN READINGS (GAUGE FAC 2·08) AT ONSET OF PLASTICITY P AT 190 KN (NEAREST)	AT PROJECTED LIMIT OF IDEAL PLASTICITY P AT 220 KN (NEAREST)	AT LAST STRAIN READING WHEN P = 260 KN	CALCULATED STRESSES N/mm² AT ONSET OF PLASTICITY P AT 190 KN (NEAREST)	AT PROJECTED LIMIT OF IDEAL PLASTICITY P AT 220 KN (NEAREST)	AT LAST STRAIN READING WHEN P = 260 KN
21	WEB - NEXT TO MID HEIGHT	0·786 Divn = 2	0·490 Divn = 1	0·700 Divn = 1	130	161	230
23	Do	0·730 "	0·455 "	0·638 "	120	150	209
25	Do	0·761 "	0·474 "	0·680 "	126	155	223
27	Do	0·742 "	0·460 "	0·640 "	123	152	210
37	WEB - MID LOWER PANEL	0·800 "	0·500 "	0·717 "	132	164	235
39	Do	0·730 "	0·450 "	0·600 "	120	149	197
45	WEB - MID UPPER PANEL	0·820 "	0·515 "	0·747 "	135	170	244
47	Do	0·718 "	0·404 "	0·591 "	118	134	194
50	WEB - EXACTLY ⅝ MIDHEIGHT	0·716 "	0·454	0·757 "	118	150	250

FIG:-59 ESTABLISHMENT OF ACTUAL STRESSES FROM STRAIN GAUGE READINGS AT GIVEN CRITICAL LOCATIONS.

TEST Nº 3 (FAILURE 245KN).

GAUGE Nº	LOCATION	STRAIN READINGS -(GAUGE FAC: 2·08) AT ONSET OF PLASTICITY AT 190KN (NEAREST)	AT PROJECTED LIMIT OF IDEAL PLASTICITY AT 215 KN (INTERPOLATED)	AT LAST STRAIN READING WHEN P=240KN.	CALCULATED STRESSES. N/mm² AT ONSET OF PLASTICITY AT 190KN (NEAREST)	AT PROJECTED LIMIT OF IDEAL PLASTICITY AT 215KN (INTERPOLATED)	AT LAST STRAIN READING WHEN P=240KN.
21	WEB - NEXT TO MID-HEIGHT	0·845 Divn=2	0·514 Divn=1	0·655 Divn=1	139	170	215
23	Do	0·830 "	0·504 "	0·641 "	136	166	210
25	Do	0·840 "	0·514 "	0·660 "	138	169	217
27	Do	0·830 "	0·504 "	0·650 "	136	166	213
34	FLGE - NEXT UPPER INTER. BATT.	0·809 "	0·513 "	0·738 "	133	169	243
35	WEB - Do	0·584 "	0·326 "	0·745 "	96	108	245
45	WEB - MID-PANEL	0·847 "	0·515 "	0·671 "	139	170	221
49	WEB - MID HEIGHT ON ℄	0·962 "	0·585 "	0·897 "	154	193	294
50		0·844	0·511 "	0·660	138	168	217
18		0·840	0·514	0·712	138	169	235

TEST Nº 4 (FAILURE 265KN).

GAUGE Nº	LOCATION	STRAIN READINGS. -(GAUGE FAC: 2·08) AT ONSET OF PLASTICITY AT 190KN (NEAREST)	AT PROJECTED LIMIT OF IDEAL PLASTICITY AT 220KN (NEAREST).	AT LAST STRAIN READING WHEN P=260KN	CALCULATED STRESSES. N/mm². AT ONSET OF PLASTICITY AT 190KN (NEAREST)	AT PROJECTED LIMIT OF IDEAL PLASTICITY AT 220KN (NEAREST).	AT LAST STRAIN READING WHEN P=260KN.
21	WEB - NEXT TO MID HEIGHT	0·774 Divn=2	0·486 Divn=1	0·682 Divn=1	127	160	224
23	Do	0·760 "	0·475 "	0·688 "	125	156	227
25	Do	0·777 "	0·490 "	0·695 "	129	161	230
27	Do	0·760 "	0·478 "	0·670 "	125	158	220
45	WEB - MID PANEL	0·824 "	0·520 "	0·755 "	133	171	249
18	FLGE - NEXT LOWER INTER BATT.	0·744 "	0·485 "	0·810 "	122	160	266
49	WEB ON ℄ AT MID HEIGHT	0·855 "	0·550 "	FAILED BEFORE L.S.R.	140	182	HIGHEST VALUE - SUGGESTS LOCAL BUCK. WEB.
50	WEB ON ℄ AT MID PANEL.	0·793 "	0·497 "	0·710 "	130	164	233

FIG. 60 ESTABLISHMENT OF ACTUAL STRESSES FROM STRAIN GAUGE READINGS AT GIVEN CRITICAL LOCATIONS.

TEST Nº 7 (FAILURE 251 KN)

GAUGE Nº	LOCATION	STRAIN READINGS-(GAUGE FAC: 2·08)			CALCULATED STRESSES. N/mm²		
		AT ONSET OF PLASTICITY P AT 195 KN (INTERPOL)	AT PROJECTED LIMIT OF IDEAL PLASTICITY P AT 220 KN (NEAREST)	AT LAST STRAIN READING WHEN P = 240 KN	AT ONSET OF PLASTICITY P AT 195 KN (INTERPOL)	AT PROJECTED LIMIT OF IDEAL PLASTICITY P AT 220 KN (NEAREST)	AT LAST STRAIN READING WHEN P = 240 KN
2	WEB - LOWER. INTER. BATT.	0·847 Div n=2	0·520 Div n=1	0·619 Div n=1	138	170	203
4	Do.	0·725 "	0·444 "	0·526 "	119	146	172
6	Do	0·735 "	0·439 "	0·503 "	121	144	165
8	Do.	0·630 "	0·369 "	0·418 "	103	147	137
10	WEB - MID HEIGHT.	0·920 "	0·578 "	0·715 "	150	188	235
12	Do.	0·730 "	0·432 "	0·487 "	120	142	160
44	FLGE - BOTTOM OF STRUT.	0·796 "	0·513 "	0·635 "	130	169	208
46	Do.	0·689 "	0·448 "	0·562 "	113	147	182

TEST Nº 8 (FAILURE 280 KN).

GAUGE Nº	LOCATION	STRAIN READINGS-(GAUGE FACTOR 2·08)			CALCULATED STRESSES. N/mm²		
		AT ONSET OF PLASTICITY P AT 190 KN (NEAREST)	AT PROJECTED LIMIT OF IDEAL PLASTICITY P AT 225 KN (INTERP:)	AT LAST STRAIN READING WHEN P = 270 KN.	AT ONSET OF PLASTICITY P AT 190 KN (NEAREST)	AT PROJECTED LIMIT OF IDEAL PLASTICITY P AT 225 KN (INTERP:)	AT LAST STRAIN READING WHEN P = 270 KN.
2	WEB - LOWER. INTER BATT.	0·778 Div n=2	0·498 Div n = 1	0·715 Div n = 1	128	164	235
4	Do	0·690 "	0·436 "	0·594 "	113	144	195
6	Do	0·758 "	0·479 "	0·672 "	124	154	220
8	Do.	0·660 "	0·407 "	0·578 "	108	134	190
10	WEB - MID HEIGHT.	0·820 "	0·523 "	0·785 "	134	172	257
12	Do	0·700 "	0·434 "	0·555 "	115	143	182
14	WEB - UPPER. INTER BATT:	0·735 "	0·466 "	0·670 "	120	154	221
18	Do.	0·754 "	0·485 "	0·699 "	124	160	230

TEST Nº 4.

LOAD 260kN. LAST STRAIN READINGS BEFORE FAILURE (AT 265kN).

NOTE:- FOR TEST 4 ONLY ALL STRAIN GAUGE READINGS ARE AVAILABLE IN THIS TEXT, SEE FIG 20. THEY WILL BE OF USE IN WHAT FOLLOWS.

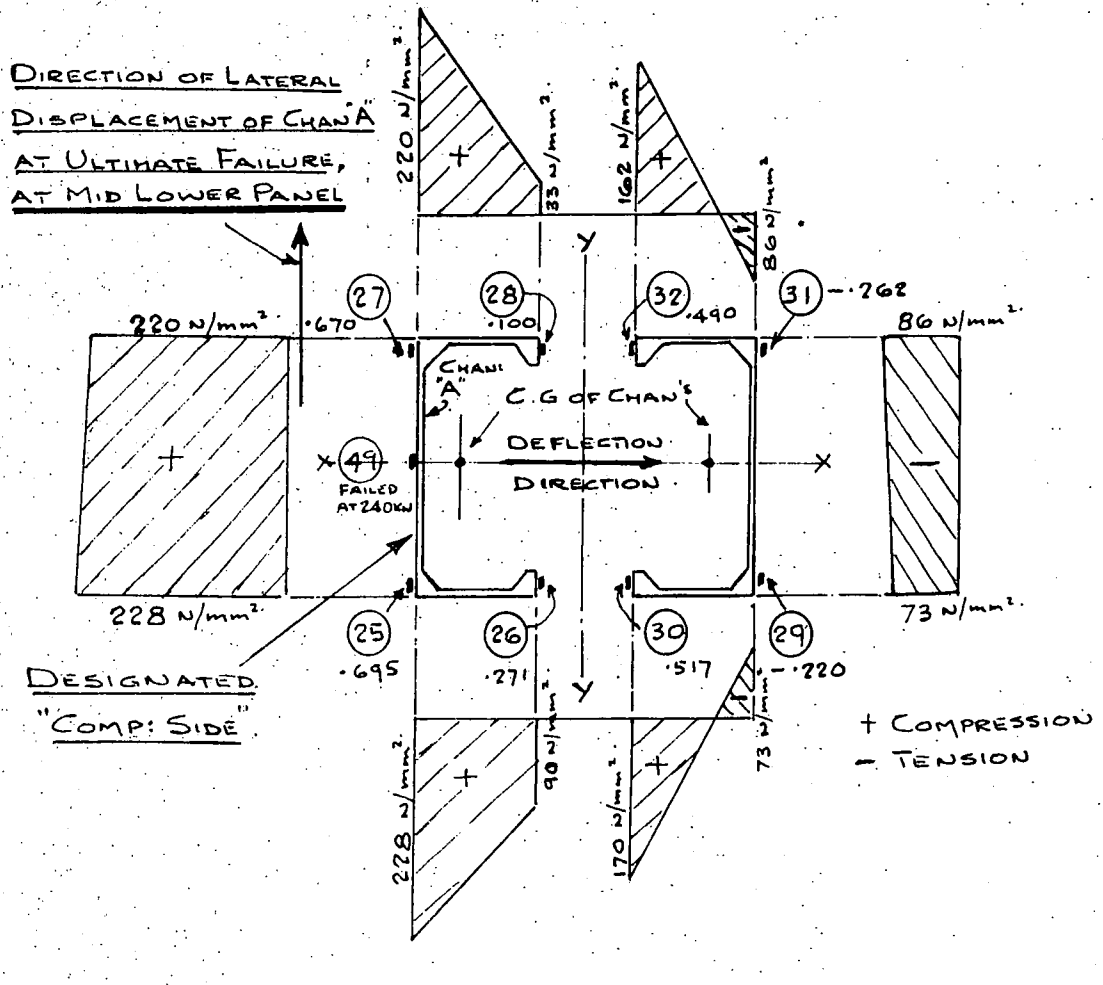

STRESS DISTRIBUTION ACROSS SECTION.

GAUGES 80mm ABOVE MID-HEIGHT. EXCEPT (49) WHICH WAS AT MID-HEIGHT.

THE ABOVE DIAGRAM ILLUSTRATES THE INTERESTING SITUATION THAT FULL PLASTICITY IS NOT PRESENT IN THE "COMPRESSION SIDE" CHANNEL, EVEN AT THIS HIGH LOAD. IT MAY WELL BE THAT THE WEB AND ROOT FILLETS ARE FULLY PLASTIC BUT THE FLANGE FILLETS OF THE SAME CHANNEL ARE STILL IN THE ELASTIC STATE. AN ELASTO-PLASTIC CONDITION THEREFORE EXISTS.

NOTE

THE "PROJECTED INTERATION CURVE FOR IDEAL PLASTICITY", WHICH WAS PURELY AN ASSUMPTION, MUST THEREFORE ONLY BE REGARDED AS A "FACTORING BASE LINE".

TEST Nº 4 IS OF PARTICULAR INTEREST. BUCKLING WAS LIKELY AT SEVERAL LOCATIONS. SEE FIG'S 41 AND 20. FURTHER INVESTIGATION WAS THEREFORE NECESSARY. THE BATTEN SPACING WAS 1218·5mm (4'-0").

TEST Nº4

LOAD 260KN. LAST STRAIN READINGS BEFORE FAILURE (AT 265KN)

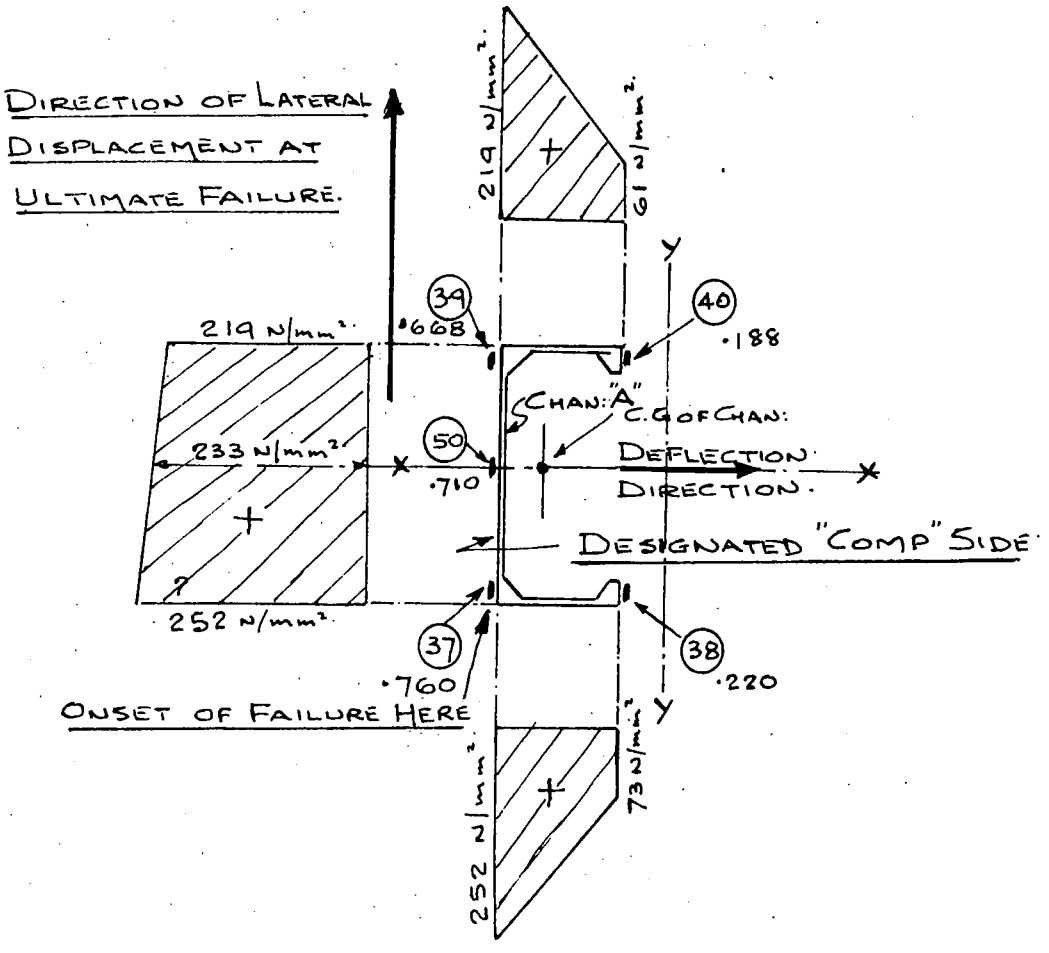

STRESS DISTRIBUTION ACROSS "COMP: SIDE" CHANNEL AT MID-LOWER PANEL LOCATION ADJACENT TO MID HEIGHT. SEE FIG 41.

THIS WAS THE FAILURE POSITION. (APPROX).
SEE PLATE 14

THIS LOCATION ENABLES JUDGEMENT TO BE MADE ON THE "COMP SIDE" CHANNEL AT A LOCATION WELL AWAY FROM THE INFLUENCE OF THE BATTENS AND THEREFORE ANY RESTRAINING EFFECT, LOCALLY, FROM THE OTHER CHANNEL.

TEST Nº 2

LOAD 260KN. LAST STRAIN READINGS BEFORE FAILURE (AT 265KN)

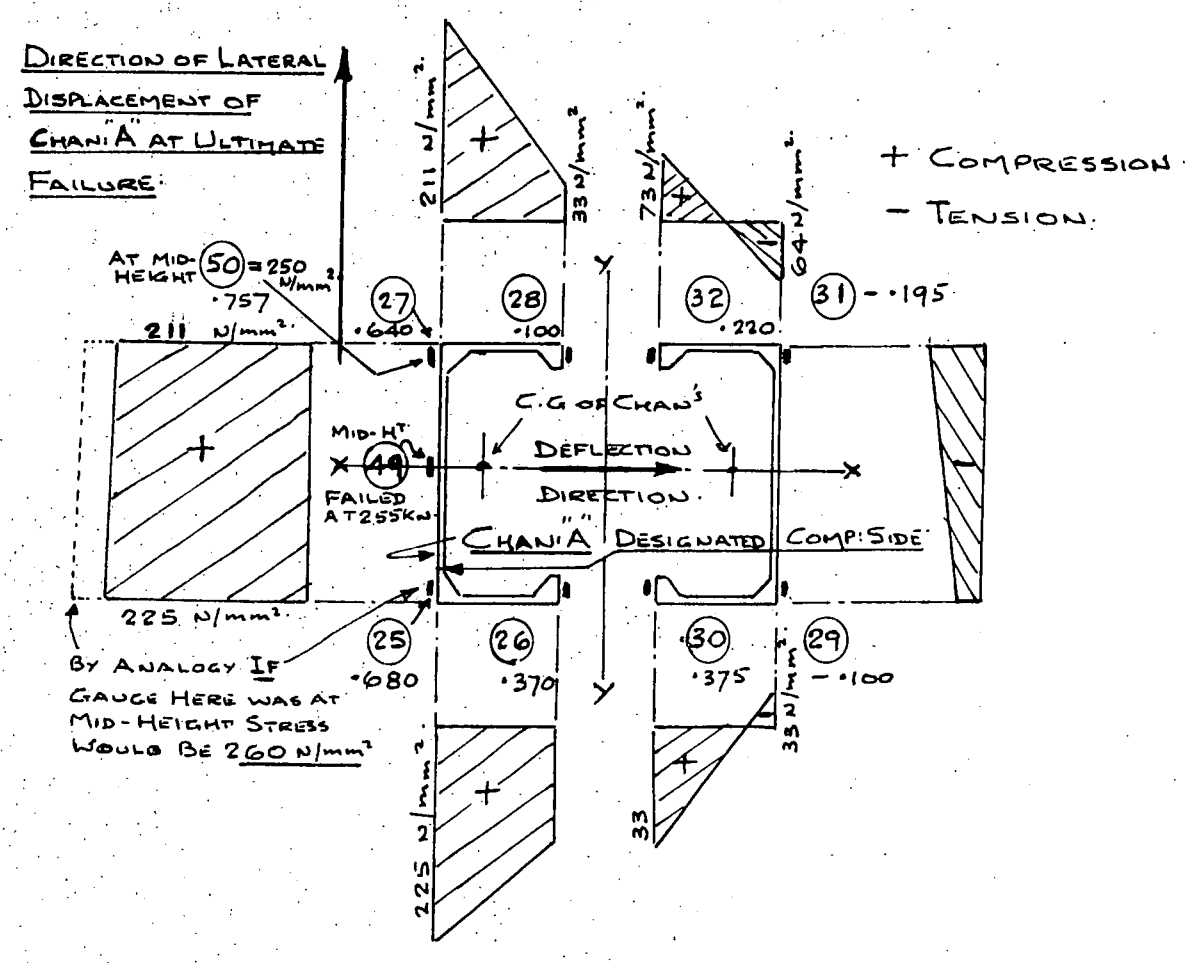

STRESS DISTRIBUTION ACROSS SECTION.

GAUGES 80mm ABOVE MID-HEIGHT EXCEPT FOR (49) AND (50) WHICH ARE AT MID-HEIGHT.

FAILURE AT MID-HEIGHT.

SEE PLATE 14.

NOTES:- GENERALLY AS PAGE 242.

TEST Nº7.

LOAD 240KN. LAST STRAIN READINGS BEFORE FAILURE (AT 265KN).

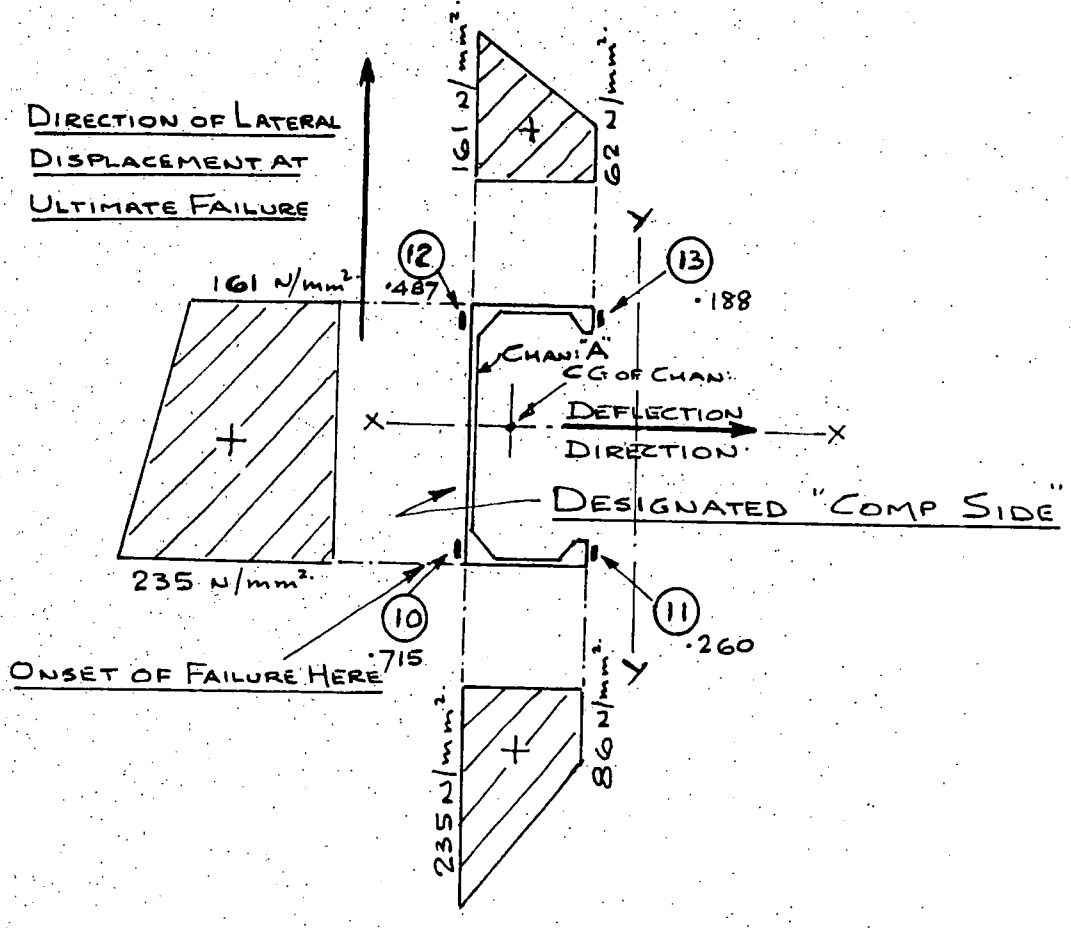

STRESS DISTRIBUTION ACROSS "COMP: SIDE" CHANNEL AT MID-HEIGHT OF STRUT.

THIS WAS THE FAILURE POSITION.

SEE PLATE 14.

NOTES: GENERALLY AS PAGE 246.

TEST Nº 8.

LOAD 270KN. LAST STRAIN READINGS BEFORE FAILURE (AT 280KN).

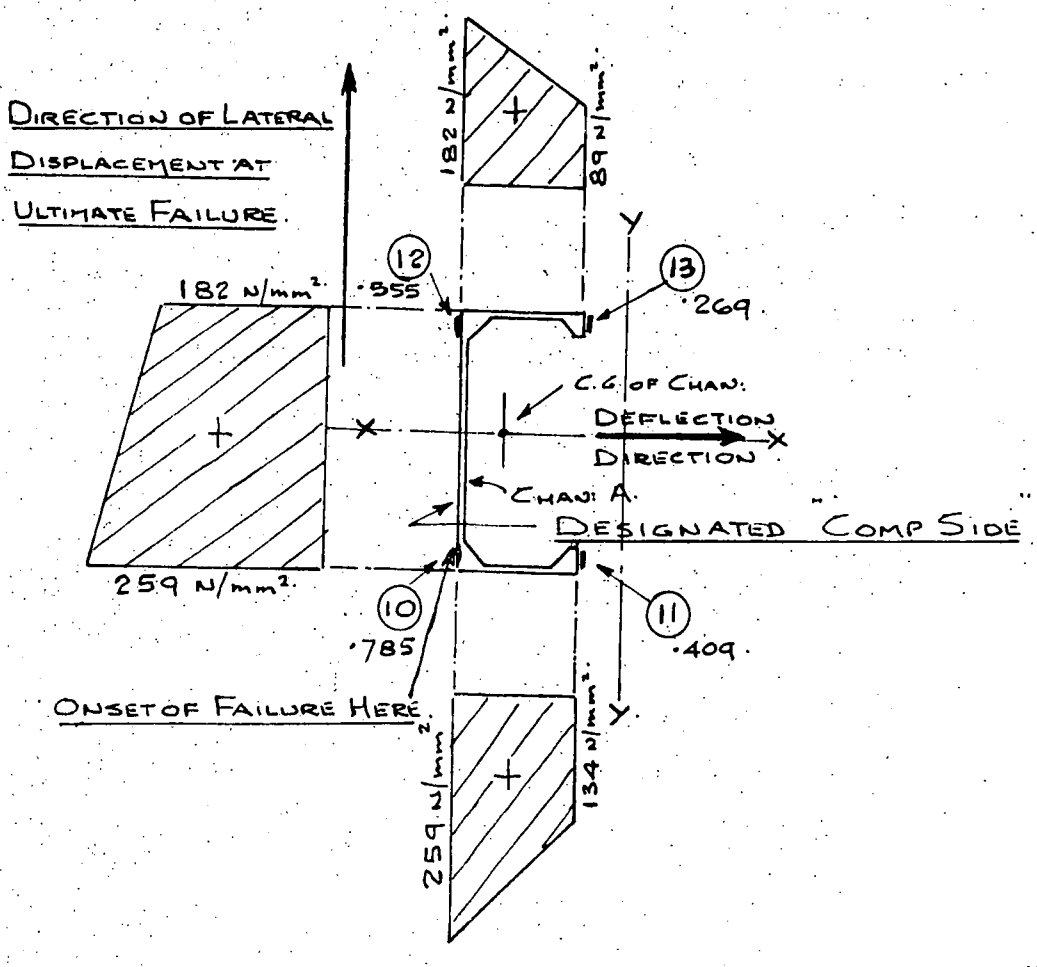

STRESS DISTRIBUTION ACROSS "COMP: SIDE" CHANNEL AT THE MID-HEIGHT LOCATION.

THIS WAS THE FAILURE POSITION.
SEE PLATE. 14.

THIS LOCATION AGAIN ALLOWS JUDGEMENT WHEN BATTENS ARE WELL AWAY FROM THE SEAT OF FAILURE.

NOTE.

STRESSES AT THE BATTENS STRADDLING THE MID-HEIGHT. ARE ONLY SLIGHTLY LOWER. PLATE 14 DOES IN FACT SHOW THAT FOR TEST 9 FAILURE TOOK PLACE AT THE BATTENS ABOVE MID-HEIGHT. FAILURE WAS THEN 282KN.

Consideration of the foregoing stress tables and diagrams for eccentric loading will reveal that as the deflections increased, beyond those encountered with axial load, the load at failure dropped. The stresses at the web of the "comp. side" channel however continued to rise, thus causing more of the material to pass into the plastic range. A situation therefore existed where the load had reduced to such a level that lateral buckling could not occur. The outer fibre stresses however continued to rise as the strut deflected until a local buckling situation was established.

The ultimate failure had exactly the same appearance as with the axial tests. The mode of failure was however different, as the stress level at the web was now of the order established for local buckling - see Chapter 6. Failure in all cases was by local buckling, which, because of a very small amount of bending on the x-x axis "triggered off" from one edge of the web, quickly involving the web root and the thin "web" of the flange. Lateral displacement therefore occurred to provide an overall deformation of the same character as the axially loaded members but at a reduced load.

If the effect of batten plates is now considered, Fig. 47 and the interaction curves will confirm that spacing has an effect upon the strut's load carrying capacity. It is now accepted that with the eccentrically loaded struts the

"comp. side" channel buckles locally and then moves laterally due to the differential of the buckling stress across the web. Battens appear to be quite adequate to deal with the usual bending moments and shear forces in the plane of battens. However, it is suggested that additional lateral stiffness might be advisable, to delay the final lateral movement of the channel. It is accepted that at this point it is already starting to buckle locally, but as batten reinforcement has been proposed where the load is axial, it could be standardised for all conditions.

The present Code recommendations endeavour to control the slenderness ratios on the major axes and between the battens. This ensures that an axially loaded strut will sustain the Euler load, calculated for its weaker axis. Bending in the plane of the battens will reduce this load in ratio with deflection. Batten stiffness and spacing being of course influential in how much deflection occurs for a given load.

The test programme clearly shows this effect. Tests 1, 2, 8 and 9 have spacing at the present Code maximum and the Interact Curves (Figs 50 and 53) show that their load carrying capacity (Fig. 47) is in general, much better than for Tests 3, 4, 7 and 10 (Figs 51 and 52), where the spacing is large at 1218.5 mm (4'-0"). Tests 8 and 9 also suggest that where battens straddle the mid-height, load carrying capacity is at its best for the given spacing.

Tests 1, 2, 8 and 9 all failed at mid-height and confirmed the Code batten spacing to be more than adequate. Tests 3, 4, 7 and 10 failed at a mid-panel and suggested that the batten spacing was too large. This was surprising as the $\frac{\ell}{r}$ for a single channel, between the battens was 54 (or if 0.8ℓ was taken, 43) which accords with the Code requirement of 50. However inspection of the stress levels, derived from strain readings, at several positions on any of the given struts, showed that they were so close that mid-panel failure only just prevailed. A small spacing reduction would have moved the failure location to mid-height. It so happens that for Tests 7 and 10 the mid-panel of failure is also at mid-height.

Reference must now be made to the "Projected Limit of Ideal Plasticity". As previously explained this is for a solid rectangle and represents an UPPER LIMIT FOR THE EFFECTS OF PLASTICITY for combined bending and axial load. Using this interaction curve as a datum, and referring to all the interaction curve diagrams, enables the following statement to be made.

All eccentric load tests with the exception of Test 11 and possibly Test 3 give load/moment distribution curves which compare very closely with the theoretical elastic load/moment distribution curve at its intersection with the "Ideal Plasticity" interaction curve. Even the tests at the largest batten spacing are in reasonable agreement.

Test 11, which will be mentioned later, failed at the intersection of the load/moment and ideal plasticity curves?

Indications therefore are that this interaction curve representing the upper limit of the effects of plasticity would prove a suitable factoring datum. An extensive series of tests should however be conducted on various eccentricities and with the dimension back to back of channels varied. This would provide a "well spread" series of results from which an Interaction curve "IDEAL" for the battened strut could be established.

The Al-Zn-Mg alloy seems an excellent material. Strain gauges were located in the heat affected weld zones and it is interesting to be able to report that no readings were excessively high. From a welding standpoint it has marked superiority over the present high-strength alloys with their considerable loss of strength in welding.

Much more could be said about the smaller happenings and indications noticed during testing. Two further struts are still in stock and more investigation will proceed as time permits.

Before passing to the "Special" strut - Test 11 - reference still has to be made to the comparison between the stresses established from the interaction curves and the strain gauge readings.

The method of approach and tabling is exactly as previously covered for axial load. Figs 54 to 60 again give data for the highest stressed gauges irrespective of position. Pages 242 to 246 give diagrammatic information on stress distribution for "rings" of gauges at, or adjacent to the position of ultimate failure. All stresses are for the last possible strain readings before failure. Tests 2, 4, 7 and 8 were chosen to represent each type of batten spacing. It should perhaps be re-stated that when comparing "Average" stresses from the interaction curves with those from the strain readings it be remembered that the moment arm "d" was used. As this was to the centroids of the channels, comparisons at the lower stresses will give total average stresses on the high side. Once the material has started into the plastic range the interaction curve stresses and strain gauge stresses become more and more comparable.

To summarise on this section of the work, it can be concluded that the ultimate load is controlled by the local buckling of one channel, at stresses in the order of those calculated in Chapter 6. The ultimate mode of failure of the "identical pairs" was as shown in Plates 13 and 14.

The total stress built up in the channels from all causes will be influenced by batten spacings. For the struts tested, and accepting the load reduction which results, battens centres could be opened out to approaching 1218.5 mm (4'-0"). Further research is needed with varying amounts

of eccentricity and varying distances back to back of channels. Battens would be better reinforced.

The welded struts in Al-Zn-Mg alloy helped considerably with the rigidity problem, particularly in the important areas at the ends of the struts and in combating local instability.

The elasto-plastic investigation has proved interesting. Strut deflection is however so large with light alloy that practical application is limited. Deflection will control design at relatively low stresses.

Tests 11 and 2

Tests 6, 5 and 7, 10

Typical Local Buckling Failures

PLATE 13

Failed Struts

in Pairs

PLATE 14

Special Strut - Test 11

As a last contribution, one strut, affectionately referred to as the "Special" was tested with interesting results.

Battens were cut out of a spare strut until only three pairs remained. These were located at each end and in the middle. It was loaded 25.4 mm (1 in) eccentric along the axis in the plane of the battens. Clock gauges were used but no strain gauges.

The distance centres of battens was now 1727 mm (5'-8") which gave a slenderness ratio for one channel between the batten centres of $\frac{172.7}{2.26}$ = 76.5 (or if 0.8 ℓ is taken, 63). This is well in excess of the Code requirement of 50. The $\frac{L}{r_x}$ (weak axis) value for the complete strut was 71.3.

Remembering that Tests 3, 4, 7 and 10, with the spacing at 1218.5 mm (4'-0") buckled at mid-panel of the "comp. side" channel the outcome of this test seemed obvious.

However the strut unexpectedly buckled at mid-height, on the centre-line of the battens, by a perfectly symmetrical local buckle of the "comp. side" channel web. The failure load was 195 kN and the mid-height deflection 40 mm (1.57 in). The parts of the mid-height battens, between the channel toes, "smashed out" completely.

It is not proposed to investigate this test in detail. Its deflection and load/moment distribution curves have however been added to Figs 48 and 49, for comparisons. It will be noted that the later curve intersects with the "Limit of Plasticity" interaction curve at failure.

Plate 4 "Testing Rig" shows this strut in its failed position.

Chapter 9

Discussion

9.1 General

At the outset it should be stated that this research project has involved much more effort and taken up considerably more time than was at first envisaged.

It was known to be rather large to try and accomplish on a part-time basis, additional to a normal work load. Loss in transit of the first batch of specially cast Al-Zn-Mg alloy ingots was a major delaying factor. However, it is hoped that this contribution will justify the effort, add a little to the limited knowledge on battened struts, and stimulate further research.

Answers to a number of basic problems are still needed, particularly for struts which are loaded eccentrically in the plane of the battens.

Two general statements, considered to be supremely important must therefore be made before the final conclusions of this work are enumerated.

1. Basic Concept

   The only justification for the use of battened struts at all is the economics of weight saving. Their proportions must therefore be chosen with this object in mind. Almost all the practical testing

investigated appears to have been undertaken with ill-chosen and/or badly arranged profiles.

The first requirement for any battened strut, which is subjected to eccentric loading, is that the proportions are so arranged that the axis of major stiffness is offered to resist the bending. In practice some bending will always exist and can frequently be visualised from the type of connection to another component. Logic therefore dictates that the best use of material is made when the bending is located on the major axis ~~parallel~~ at R.T.'s to the battens. The main member spacing can be varied to suit the demands of optimum design, based on the cross sectional profile of the main members. It is only after this situation has been reached that the introduction of intermediate lateral ties, between say a series of battened columns, should be considered.

Having presented the basic requirements, it seems remarkable that the bulk of past practical testing has been with members so arranged that the axis ~~at~~ ~~R.T.'s~~ parallel to the battens was the major axis. This of course means that bending in the plane of the battens has taken place on the strut's minor axis.

It is appreciated that the earlier scientific work of Timoshenko presented solutions for bending in the

plane of the battens. The proportions used dictated that overall column buckling was bound to occur in this plane. This was acceptable at that stage and represented an initial scientific statement. Later researchers should however have turned their attentions to the economic proportions and tried to establish rules for a "Practical Economic Strut". It is acknowledged that a strut whose major buckling strength is on the axis parallel to the battens, will considerably reduce the number of unsolved parameters. However, it will do little to resolve the complex problem of optimum strut design.

2. Full Scale Testing

Simulation of structural problems is ideal to establish general trends. It is not however justified when realistic practical solutions are required. This is particularly true when structurally efficient but fanciful shapes, usual with aluminium alloy, are being used.

Far too much research is now undertaken where the mode of failure is controlled by the researcher to prove some particular point, which may, but frequently has not, a use in a real working situation. This is a pity and is doubtful progress.

One is led to wonder if much of the work undertaken is now controlled by its suitability to simulation

techniques. This may well produce some interesting solution just for its own sake. If this is so it must be deprecated.

The author is convinced from years of practical experience that simulation techniques and mathematical processes have an extremely important role to play. It is however vitally important that experience and concept is not overlooked for it is these alone which will enable the researcher to get his priorities correct, as a first step.

At this initial stage full scale testing, in the material to be ultimately used, is essential. Unless the correct main parameters are initially established all abstruse calculation will be meaningless.

9.2 The Testing Rig

This worked extremely well and full justified the time and effort put into its design and manufacture. Its concept may well be regarded as somewhat crude as its construction was on a limited budget.

All particulars, including the proving test, are included in Chapter 5. Little needs to be added now except to confirm that throughout the whole testing programme no apparent weaknesses came to light.

The usual problem of strut end fixity was undoubtedly present to some extent. The use of the P.T.F.E. silicon grease, earlier described, appears to have been very effective. It may well be that the simple ball arrangement, together with the grease, is just as satisfactory, if not better, than some of the more elaborate systems that have been devised.

9.3 The Test Findings and Proposals for Future Research

The detailed findings have been given in Chapter 8 but a general reference summary is now given.

1. When the deflection was small at final load, struts failed by lateral instability of the most heavily loaded channel. Failure was on the x-x (weaker) axis of the complete strut.

2. With the much larger deflections encountered under eccentric load, failure was by local buckling. This occurred in the web/root of the most heavily loaded channel, either at mid-height or mid-panel. The larger the deflection the lower the failure load. Stresses at the back of the "comp. side" channel were of course much higher than with the axial conditions and resulted in local buckling.

It must be stated that the usefulness of any elasto-plastic investigation is doubtful. With aluminium alloys the deflection is by then so large it would

govern design, long before the local buckling situation was reached.

3. Battens play a vital role. Load carrying capacity of the strut depends upon their spacing and stiffness.

   In addition to the design requirements legislating for the usual moments and shears, resulting from deflection in the plane of the battens, further conditions should be imposed. These would relate to the provision of battens with lips or flanges, which are required to cater for lateral movement of one channel.

   Further research, as detailed earlier, is required here.

4. Batten spacing can be increased substantially if some reduction in ultimate load is acceptable. The spacing does not appear to be highly important within the elastic range of the material.

   Further research in the inelastic range is required to establish the true limit of plasticity interaction curve for battened struts. Comprehensive testing at a series of eccentricities and channel spacings is required.

Again, is it justified? As deflections are so large practical application will be limited.

5. End battens and/or fixings are extremely important. Rigidity at these locations are essential if the strut is to perform efficiently.

6. The Al-Zn-Mg alloy and the satisfactory welding of battened struts is a considerable step forward. From a strength standpoint this weldable material is an unqualified success.

7. Because of lateral movement the method of welding battens is important. See Chapter 8.

8. Where battened struts are to be tied against lateral movement the location of the ties is important. They should be positively attached to the member which has the lateral weakness and NOT to the centre of the battens.

9. Finally the Interaction Method of Analysis appears to be very satisfactory. Its simplicity recommends its use for practical problems.

After further research to establish a true plasticity limit, its use when suitably factored, would be ideal within the inelastic range.

Aluminium alloy is an excellent material for research. Its comparatively fine tolerances and thin-walled profiles serve excellently to illustrate the structural behaviour of metals. It highlights many problems with which the design engineer in steel may not be so well acquainted.

As an introduction it was suggested that the battened strut posed problems which were largely unsolved. This statement has now been unquestionably confirmed. It is however hoped that this work will revive interest in this fascinating problem. Much more needs to be done before a comprehensive set of design requirements can be confidently defined.

BIBLIOGRAPHY

	Author	Article/Book	Journal/Publisher
1.	Engesser, F.	"Über die Knick-festigkeit" Gerader Stäbe	"Zeitschrift für Architektur und Augenieurwesen 1889. pp 445-462
2.	Shanley, F.R.	Inelastic Column Theory	Journal of Aeronaut Sciences Vol. 14, p 261, May 1947
3.	Bleich, F.	Buckling Strength of Metal Structures	McGraw-Hill pp 90-207 (1952)
4.	Bryan, G.H.	Proc: London Maths Soc. 1891. 22. p 54	
5.	Timoshenko, S.	Theory of Elastic Stability	Eng. Soc. Monographs. McGraw-Hill 1936
6.	Lundquist, E.E. and Stowell, E.Z.	Technical Note	N.A.C.A. Tech. Note 743: 1939
7.	Lundquist, E.E. and Stowell E.Z. and Schuette, E.H.	Technical Report	N.A.C.A. Report 809: 1945
8.	Baker, J.F. and Roderick, I.W.	The Strength of Light Alloy Struts	A.D.A. Res.Rep. No. 3: 1948
9.	Heimerl, G.J.	Determination of Plate Compression Strength	N.A.C.A. Tech. Note 1480 1947
10.	Chilver, A.H.	Behaviour of Thin Walled Structural Members in Compression	Engineering 1951 172 (4466)
11.	Chilver, A.H.	A Generalised Approach to the Local Instability of Certain Thin Walled Struts	Aeronaut: Quarterly. Vol. 55: August 1953

12.	Von Kärmän, T.	Untersuchungen Über Knickfestigkeit	Forschung-sarbeiten No. 81: 1910
13.	Bijlaard, P.P.	Koninklyde Nederlandsche Akad Wetenschappen 1938 61(7) p 731	
14.	Ilyushin, A.A.	Prikl Mat I Mekh (Moscow) 1944 8(5) p 337	
15.	Shanley, F.R.	The Column Paradox	Journal of Aeronaut Sciences Vol.13 No. 12 Dec. 1946
16.	Gerard, G.	Secant Modulus Method for Determining Plate Instability Above the Proportional Limit	Journal of Aeronaut Sciences Vol. 13 p 38 1946
17.	Wagner, H.	Torsion and Buckling of Open Sections 1929	N.A.C.A. Tech. Mem. 851-1938 Gives Translation
18.	Palmer, P.J.	The Determination of Torsional Constants for Bulbs & Fillets by Means of an Electrical Potential Analyser	A.D.A. Res. Rep. No. 22 1953
19.	Lundquist, E.E.	The Strength of Columns that Fail by Twisting	Journal Aeronaut Sciences Vol. 4: p 249. April 1937
20.	Kappus, R.	Twisting Failure of Centrally Loaded Open Sections in the Elastic Range (German) 1937	N.A.C.A. Tech.Mem. 851 - 1938 Gives Translation
21.	Goodier, J.N.	The Buckling of Compressed Bars by Torsion and Flexure	Cornell University Eng.: Exp: Station Bulletin No. 27 1941

22.	Timoshenko, S.	Theory of Bending, Torsion and Buckling of Thin Walled Members of Open Cross Section	Journal Franklin Inst: March/May 1945
23.	Bentley, K.	Theory and Design of Pin-Joined Struts of Open Section	A.D.A. Tech: Mem: 172 - 1952
24.	Smith, R.E.	Column Tests on some Proposed Aluminium Standard Structural Sections	A.D.A. Res:Rep: 28 1955
25.	Ramberg, W. and Levy, S.	Instability of Extrusions under Compressive Loads	Journal Aeronaut: Sciences Vol. 12 p 485. Oct 1945
26.	Vlasov, V.Z.	Thin Walled Elastic Beams (Russian)	Israel Programme for Scientific Translation - Jerusalem 1961
27.	Zbirohowski-Koscia, K.	Thin-Walled Beams	Crosby-Lockwood 1967
28.	Bulson, P.S.	Local Instability Problems of Light Alloy Struts	A.D.A. Res: Rep: 29 1955
29.	Rockey, K.C.	The Design of Intermediate Vert. Stiffs. on Web Plates subject to Shear	A.D.A. Res: Rep: 31 Dec 1955
30.	Rockey, K.C.	The Design of the Web Plates of Light Alloy Plate Girders	A.D.A. Res: Rep: 32 Jan 1956
31.	Rockey, K.C.	The Behaviour of Web Plates of Rate Girders subject to Pure Bending	A.D.A. Res: Rep: 33 Aug 1957
32.	Rockey, K.C.	Shear Buckling of a Web Reinforced by Vert:Stiffs: and Central Horiz: Stiff.	A.D.A. Res: Rep: 35 Dec 1957

33.	Rockey, K.C.	Web Buckling and the Design of Web Plates	A.D.A. Res. Rep. 36 Sept 1958
34.	Rockey, K.C.	Plate Girder Design	A.D.A. Res. Rep. 37 Jan 1958
35.	Cullimore, M.S.	Aluminium Double Angle Struts	I.S.E. Symposium Alum. in Struct. Eng. Paper 5 June 1963
36.	Dwight, J.B.	Aluminium Sections with Lipped Flanges and Their Resistance to Local Buckling	I.S.E. Symposium Alum. in Struct. Eng. Paper 8 June 1963
37.	-	Structural Aluminium	Alcan Industries (Formerly Northern Alum. Ltd.) Sept 1959
38.	Engesser, F.	Die Knickfestestigkeit Gerader Stäbe (The Buckling Resistance of Straight Columns)	Zentralblatt Der Bauverwaltung Berlin 5-12-1891 p 483
39.	Emperger, F.	Welchen Querverband Bedarf eine Eisensäule (What Cross Connections are necessary in an Iron Column)	Beton und Eisen 19-2-08 etc. pp 71,96,119 and 148
40.	Engesser, F.	Uber die Knickfestigkeit von Rahmenstäben (On the Buckling Resistance of Battened Columns)	Zentralblatt der Bauverwaltung Berlin 10-3-09 p 136
41.	Engesser, F.	Uber Knickfestigkeit und Knicksicherheit (On the Buckling Resistance and Factor of Safety against Buckling)	Der Eisenbau Leipzig Oct 1911, p 385

42.	Krohn, R.	Beitrag zur Untersuchung der Knickfestigkeit Gegliederter Stäbe (Contribution is the Investigation of Buckling Resistance of Built-up Columns)	Zentralblatt der Bauverwaltung Berlin 21-10-08 p 559
43.	Müller-Breslau, H.	Über Exzentrisch Gedrückte Gegliederte Stäbe (On Eccentrically Compressed Built-up Columns)	Sitzungsberichte d.k. Preuss Akad. D.Wissenchaften Berlin 17-2-10 p 166
44.	Müller-Breslau, H.	Über Exzentrisch Gedrückte Stäbe und Über Knickfestigkeit (On Eccentrically Compressed Columns and on Buckling Resistance)	Der Eisenbau Leipzig Sept 1911 pp 339,443,475
45.	Tetmajer, L.	Die Gesetze der Knichungs-und der Zusammengesetzten Druckfestigkeit der Technisch Wichtigsten Baustoffe (The Laws Governing Buckling and the Eccentric Stresses in the Technically Most Important Materials)	1896
46.	A.S.C.E. Committee	Progress Report of Special Committee on Steel Column Research	Trans. A.S.C.E. Vol. 89 1926 pp 1485 - 1549
47.	A.S.C.E. Committee	Second Progress Report of Special Committee on Steel Column Research	Trans. A.S.C.E. Vol. 95 1931 pp 1152 - 1254
48.	A.S.C.E. Committee	Final Report of the Special Committee on Steel Column Research	Trans. A.S.C.E. Vol. 98 1933 pp 1376 - 1462

49.	Petermann	Müller-Breslaus Knickversuche mit Rahmenstaben (Müller Breslau's Buckling Experiments with Battened Columns)	Der Bauingenieur Vol. 7.17 24-12-26 pp 979-981, 1009 - 1016
50.	Petermann	Knickversuche mit Rahmenstaben Aus St 48. (Buckling Experiments with Battened Columns of St 48)	Der Bauingenieur Vol. 12 10-7-31 pp 509 - 515
51.	Ratzersdorfer,J.	Die Knickfestigkeit von Staben und Stabwerken. (Buckling Resistance of Columns and Built-up Columns)	Springer. 1936 pp 218 - 226
52.	Ng. Wah Hing	The Behaviour and Design of Battened Structural Members	PhD Dissertation Dec 1947 Univ. Cambridge Lib.
53.	Jones, B.D.	A Theory for Struts with Lattice or Batten Bracing	The Struct.Eng. May 1952 pp 108 - 113
54.	Koenigsberger,F. and Mohsin, M.E.	Design and Load Carrying Capacity of Welded Battened Struts	The Struct.Eng. June 1956 pp 183 - 203
55.	Jenkins, W.M.	The Welded Battened Column	Thesis to I.C.E. for Part III Examination Ass. Membership Spring 1960
56.	Chitty, L.	On the Cantilever Composed of a number of Parallel Beams Interconnected by "Cross-Bars"	Phil. Mag.XXXVIII Oct 1947 pp 685 - 699
57.	Pippard, A.J.S.	Studies in Elastic Structures	Arnold 1952 Ch. 8

58.	Murray, N.W.	The Determination of the Collapse Loads of Rigidly Jointed Frameworks in which the Axial Forces are Large	Proc. I.C.E. Pt. III Vol. 5 April 1956
59.	Massonnet, C.	Stability Considerations in the Design of Steel Columns	Trans. A.S.C.E. (Struct.Div.) Sept 1959
60.	Shanley, F.R.	Strength of Materials	McGraw-Hill 1957 pp 633 - 670
61.	Hill & Clarke		Alum. Research Labs. Tech. Paper No. 12 1955.
62.	Shanley, F.R.	Optimum Design of Eccentrically Loaded Columns	A.S.C.E. Struct.Div. Journal, Vol. 93, No. ST4, August 1967
63.	Timoshenko, S.	Theory of Elastic Stability	McGraw-Hill 1936 pp 145 and 146.
64.	Venkatraman, B. Sharad, A. Patel	Structural Mechanics with Introductions to Elasticity and Plasticity	McGraw-Hill 1970

Abbreviations

N.A.C.A. - National Advisory Committee for Aeronautics (U.S.A.)
A.S.C.E. - Americian Society of Civil Engineers
A.D.A. - Aluminium Development Association
I.S.E. - Institution of Structural Engineers
I.C.E. - Institution of Civil Engineers

Publications Consulted and Not Mentioned in Text

Moir, C.M.	Factors Influencing Design of Thin Walled Members	The Struct. Eng. Feb 1948
Niles, A.S.	Experimental Study of Torsional Column Failure	Washington Oct 1939
Chilver, A.H.	The Thin Walled Channel Strut	Civil Eng. & P.W. Review Vol. 48 No. 570 Dec 1958
Pumphrey, W.I.	An Examination of Welding and Tensile Properties of some Al-Zn-Mg Alloys	A.D.A. Res. Reps., 16-25 1953-55
Harvey, J.M.	Structural Strength of Thin Walled Channel Sections	Engineering Aug 1951
Rockey, K.C. and Hill, H.V.	Thin Walled Steel Structures	Crosby Lockwood 1969
Chilver, A.H.	Thin Walled Structures	Chatto and Windus 1967
Temple, J.E.	Structural Design in Aluminium Alloys	James Booth & Co. Ltd. Handbook 1947
McLester, R.	Fatigue Strength of Welded and Riveted Joints in Aluminium	I.S.E. Symposium Alum. in Struct. Eng. Paper 1 June 1963
Marshall, W.T. Nelson, H.M. and Smith, I.A.	Experiments on Single Angle Alum. Alloy Struts	I.S.E. Symposium Alum. in Struct. Eng. Paper 3 June 1963
Chilver, A.H. and Britvec, S.J.	Plastic Buckling of Aluminium Columns	I.S.E. Symposium Alum. in Struct. Eng. Paper 4 June 1963
Redshaw, S.C.	Alum. Angles in Tension	I.S.E. Symposium Alum. in Struct. Eng. Paper 6 June 1963

Hartmann & Clark	The U.S. Code	I.S.E. Symposium Alum. in Struct. Eng. Paper II June 1963
"A Discussion"	Comparison of Alum. Codes of Practice and Future Trends (Refers Al-Zn-Mg Alloy)	I.S.E. Symposium Alum. in Struct. Eng. pp 177 - 193 June 1963
Pippard, A.J.S.	Studies in Elastic Structures - also refers - "The Critical Load on Battened Columns"	Phil. Mag. XXXIX Jan 1948 pp 58 - 66
Dobie, W.B.	Accuracy of Determination of the Elastic Torsional Properties of Non Circular Sections using Relaxation Methods and the Membrane Analogy	The Struct. Eng. Sept 1952
Dobie, W.B.	The Torsional Strength of Structural Members	The Struct. Eng. Feb 1952
Godfrey, G.B.	The Allowable Stresses in Axially Loaded Struts. (Deals with Several European Codes)	The Struct. Eng. March 1962
Kuang-Han Chu and Anatole Longinow	Torsion in Sections of Open and Closed Parts	Journal Struct.Div. A.S.C.E. Dec 1967
Shanley, F.R.	Mechanics of Materials	McGraw-Hill
Young, D.H.	Rational Design of Steel Columns	Trans. A.S.C.E. Vol. 10 1936 pp 422 - 500
Young, D.H.	Shearing Stresses in Steel Columns	Memoires Vol. 2 1933 & 1934 pp 408 - 495
Stowell, E.Z. Heimerl, G.J. Libove, C. and Lundquist, E.E.	Buckling Stress of Flat Plates and Sections (This paper is a summary of earlier work together with k value charts for I, Z and C sections)	A.S.C.E. Vol. 77 Proc. Sep. 77 July 1951